Combined experimental and computational investigation into inter-subject variability in cardiac electrophysiology

Oliver J. Britton
St Edmund Hall

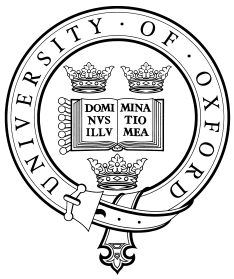

Computational Cardiovascular Science Group
Department of Computer Science
University of Oxford

Hilary Term 2015

This thesis is submitted to the Department of Computer Science, University of Oxford, for the degree of Doctor of Philosophy. This thesis is entirely my own work, and, except where otherwise indicated, describes my own research.

Oliver J. Britton
St Edmund Hall

Doctor of Philosophy
Hilary Term 2015

Combined experimental and computational investigation into inter-subject variability in cardiac electrophysiology

Abstract

The underlying causes of variability in the electrical activity of hearts from individuals of the same species are not well understood. Understanding this variability is important to enable prediction of the response of individual hearts to diseases and therapies. Current experimental and computational methods for investigating the behaviour of the heart do not incorporate biological variation between individuals. In experimental studies, experimental results are averaged together to control errors and determine the average behaviour of the studied organism. In computational studies, averaged experimental data is usually used to develop models, and these models therefore represent a 'typical' organism, with all information on variability within the species having been lost.

In this thesis we develop a methodology for modelling variability between individuals of the same species in cardiac cellular electrophysiology, motivated by the inability of traditional computational modelling approaches to capture experimental variability. A first study is conducted using traditional modelling approaches to investigate potentially pro-arrhythmic abnormalities in rabbit Purkinje fibres. A comparison with experimental recordings highlights their wide variability and the inability of existing computer modelling approaches to capture it. This leads to the development of a novel methodology that integrates the variability observed in experimental data with computational modelling and simulation, by building experimentally-calibrated populations of computational models, that collectively span the variability seen in experimental data.

We apply this methodology to construct a population of rabbit Purkinje cell models. We show that our population of models can quantitatively predict the range of responses, not just the average response, to application of the potassium channel blocking drug dofetilide. This demonstrates an important potential application of our methodology, for predicting pro-arrhythmic drug effects in safety pharmacology. We then analyse a data set of experimental recordings from human ventricular tissue preparations, and use this data to develop a population of human ventricular cell models. We apply this population to study how variability between individuals alters the susceptibility of cardiac cells to developing drug-induced repolarisation abnormalities. These abnormalities can increase the chance of fatal arrhythmias, but the mechanisms that determine individual susceptibility are not well-understood.

Publications and Prizes

Below are a list of publications and prizes resulting from the work described in this thesis.

Publications

O. J. Britton, A. Bueno-Orovio, L. Virag, A. Varro and B. Rodriguez: Modulation of susceptibility to repolarisation abnormalities by inter-subject variability in human cardiomyocytes. *In preparation*.

O. J. Britton, A. Bueno-Orovio and B. Rodriguez: Experimentally-calibrated populations of models methodology. *In preparation*.

A. Bueno-Orovio, **O. J. Britton**, A. Musckiewicz, B. Rodriguez: Cardiac modelling chapter, Encyclopedia of Cell Biology. *In press*.

O. J. Britton, A. Bueno-Orovio, L. Virag, A. Varro and B. Rodriguez: Effect of inter-subject variability in determining response to IKr block in human ventricular myocytes. *Computing in Cardiology*, 41, 869-872, 2014.

O. J. Britton, A Bueno-Orovio, K Van Ammel, HR Lu, R Towart, DJ Gallacher and B Rodriguez: Experimentally-calibrated population of models predicts and explains inter-subject variability in cardiac cellular electrophysiology. *Proceedings of the National Academy of Sciences of the United States of America*, 110(23), E2098-105, 2013.

Prizes

NC3Rs Prize 2014, prize winner for the paper: Experimentally-calibrated population of models predicts and explains inter-subject variability in cardiac cellular electrophysiology.

EPSRC PhD Prize, 2014.

EPSRC ICT Pioneers UK Competition 2013, finalist in category 'Transforming Society'.

EPSRC Impact Acceleration Account, 2013.

Microsoft Research Project Award, Systems Biology Doctoral Training Centre, 2011.

Contents

Acknowledgements

First of all, I want to thank my supervisors, Blanca and Alfonso, for all their support and guidance throughout my DPhil. In particular, I want to thank them for pushing me to apply for things I would never have gone for on my own, and for their constant positivity. It makes a big difference to know your supervisors will always look for the good in your work, as well as what can be improved.

I want to thank our experimental collaborators at Janssen Pharmaceutica, and at the University of Szeged for kindly providing us with their data sets. The work in this thesis was built on direct access to raw experimental data. Performing cardiac electrophysiology experiments is difficult, time-consuming work, and without access to raw experimental data, this thesis could never have happened. Therefore I'm very grateful to everyone that has been willing to entrust us with their hard-earned data, in particular to András Varró, for providing us with 15 years of human electrophysiology experiments, and László Virág and Norbert Jost, for their help and hospitality when I visited Szeged.

I'd also like to acknowledge the funding agencies that made this work possible, in particular the Engineering and Physical Sciences Research Council, for funding my DPhil through the System Biology Doctoral Training Centre.

I would like to thank my parents for all their support over the years, and for instilling into me an interest in science and the natural world, without which I would never have arrived here.

Last, but certainly not least, I would like to thank my fiancée, Alex for her love and support throughout my PhD. As she is also finishing her Medicine degree this year I would also like to thank her for putting the process of writing up into perspective, in comparison to becoming a (her words) "proper doctor".

1

Introduction

1.1 Introduction

The heart is a muscular pump, capable of continuous and uninterrupted operation for billions of cycles. Like normal muscles it can relax and contract, but unlike other muscles it cannot truly rest, cramp up or lose its rhythm without placing the organism it is part of in grave danger. Due to its vital function, the heart has been the focus of intensive study. Understanding the electrical activity of the heart, which if disrupted can lead to lethal arrhythmias, has been an active field of investigation for over a century. In particular, the development in the early 1950s of experimental techniques that allowed the electrical activity of individual cardiac cells to be directly recorded greatly increased our understanding of how the behaviours of the different types of voltage-gated ion channels in the heart collectively contributed to the electrical excitation of individual cardiac cells, and of the heart as a whole.

However, death due to arrhythmias is still a major cause of mortality in the developed world. Sudden cardiac death caused by lethal arrhythmias accounts for approximately 25-50 deaths per 100,000 people per year in Europe and North America (Fishman et al. (2010); Goldberger et al. (2011)). It is also a major side effect, leading to the withdrawal of many otherwise beneficial drugs both before and after the drug is approved by regulators (Redfern et al. (2010)). While anti-arrhythmic treatments have been developed, they are often unsuccessful in individ-

ual patients. One potential cause is variability between individuals. The responses of different individuals to cardiac diseases and to therapies, including drug application, are highly variable. However, we currently understand little about the mechanisms governing electrophysiological variability, what effects it can have on the heart, or how to predict the results of treatments, such as drugs, on individuals, as this variability is difficult to study using traditional experimental approaches. Experimentally observed variability in cardiac cellular electrophysiology recordings is typically averaged out, to reduce experimental error and to determine overall trends across a species and cell type.

Over the last 50 years, cardiac modelling has become a key tool for investigating the functioning of the heart and for determining potential causes when this function is impaired. In particular, biophysically detailed models of cardiac cells have been extensively developed, from the first cardiac cell models to recent models incorporating our current knowledge of each ionic current, in human (e.g. O'Hara et al. (2011)) and in other important species and cell types (Corrias et al. (2011)). In that time, computing power has increased exponentially, and simulations that would have been unfeasible years ago are now routine. This has allowed ever more complex tissue simulations to be run, moving from 1D cables and 2D sheets, to full patient-specific heart models generated from medical imaging.

However, over this time, the modelling process, and the interpretation of the cardiac cell models that underlie modelling studies has, in most cases, remained constant. Cardiac cell models are developed using averaged experimental data, ideally from the cell type and species being studied. Often, parts of the model are derived from previous models of different species (Niederer et al. (2009); Bueno-Orovio et al. (2014)) due to both the difficulty of carrying out cardiac electrophysiology experiments and the difficulty of obtaining the hearts necessary for experimentation, particularly in human. The interpretation of a cardiac model is then that it represents the typical, or average behaviour of an isolated cardiac cell of the type being modelled, obtained from a typical, healthy individual of the modelled species. As the experimental data used to de-

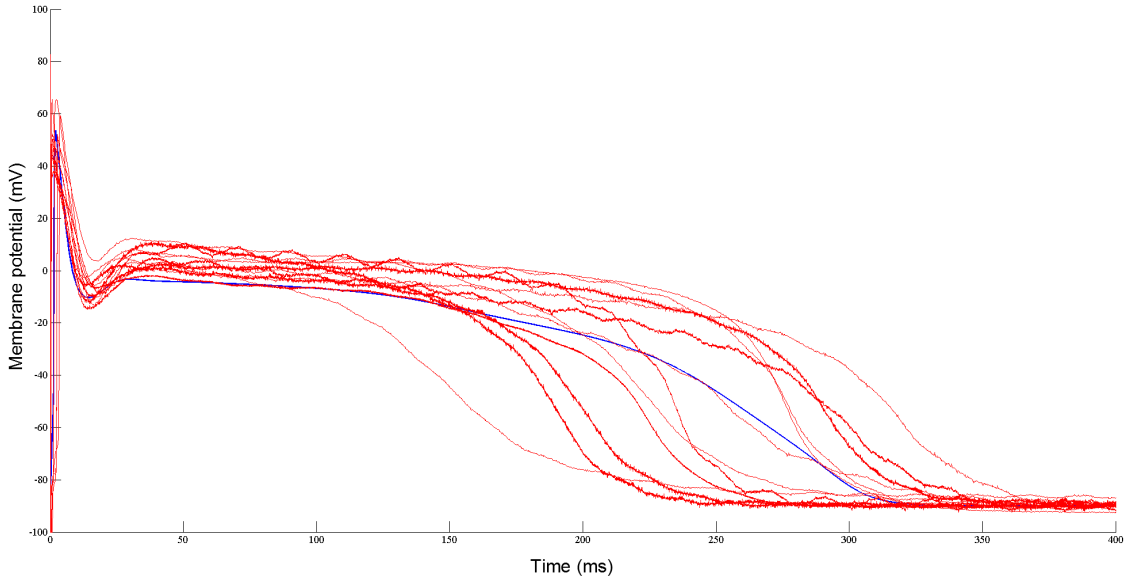

Figure 1.1: Example action potentials from isolated rabbit Purkinje cardiomyocytes from different rabbit hearts (red, n=12), compared to a rabbit Purkinje cell model (blue).

velop the model has been averaged over many cells from many individuals, variability between cells and between individuals is not included in these models. However, as can be seen from comparison to electrophysiological recordings from rabbit and human cardiac cells in Figures 1.1 and 1.2 respectively, the electrical signals these cells produce differ significantly, even under normal conditions. Exposure to drugs or other abnormal conditions can amplify differences between individuals further. As biological systems, and the heart in particular given its vital role, are highly robust to small perturbations, it may take more than one additional factor to amplify the effect of variations between cells or individuals to the point where the difference has an observable, phenotypic effect. Therefore, understanding how variability modulates response to potentially pathological conditions, using a purely experimental approach, is difficult, and using a traditional modelling approach is not possible due to how models are currently developed.

Previous approaches to modelling variability have incorporated variation in underlying biological properties, such as the strengths of individual ionic currents in a cardiac cell (e.g. Romero et al. (2009); Sarkar and Sobie (2011); Sadrieh et al. (2014)), but have not linked modelled variability to observed experimental levels of variability in measures of electrophysiological be-

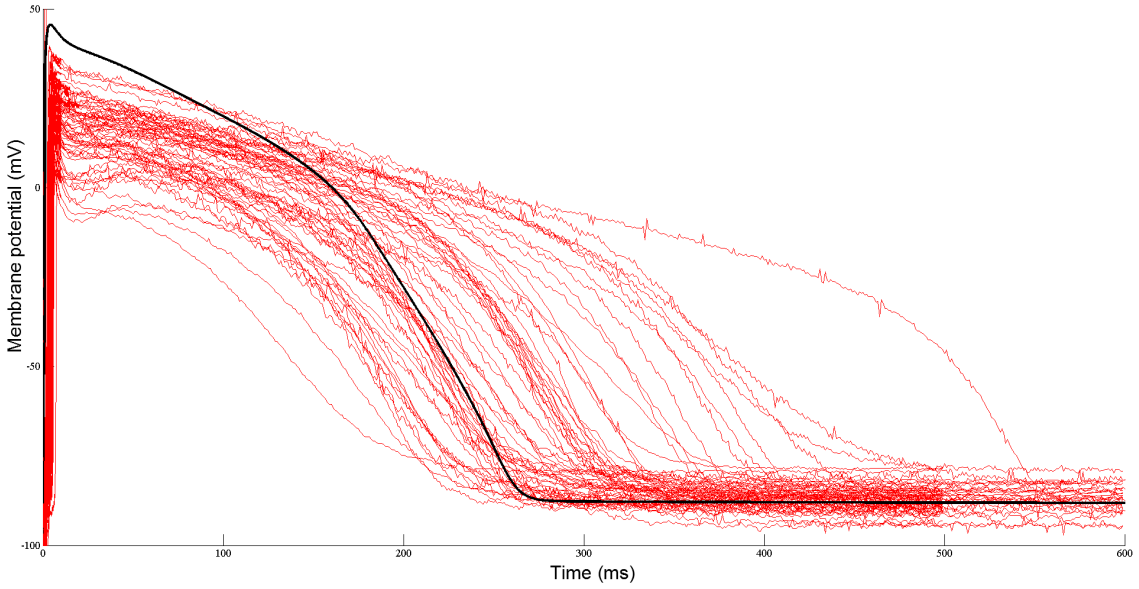

Figure 1.2: Example action potentials from human ventricular cardiomyocytes from different hearts (red, n=62), compared to a human ventricular cell model (black).

haviour. Modelling studies in neuroscience (e.g. Marder and Taylor (2011)) have incorporated inter-individual neuronal variability from experimental recordings, however the methodology used in these studies is not directly applicable to cardiac modelling, due to the low number of preparations from the hearts of different individuals available in typical cardiac electrophysiology experiments, and the high computational complexity of modern cardiac cell models.

The core idea driving this thesis is that integration of non-averaged experimental data with computational modelling can allow us to investigate and understand inter-subject variability in cardiac cellular electrophysiology in ways that traditional modelling or experiment alone cannot. We have therefore developed a framework to integrate experimental variability into cardiac modelling, using experimentally-calibrated populations of models. A population of models consists of many models with different underlying parameter values and therefore different behaviour in simulated experimental conditions, but in which every model's output is within the range of behaviours seen in experiments on different individuals. By using this methodology, we can capture the variation observed in experimental electrophysiology recordings at the level of the whole cell, and recreate it within a population of cell models by varying model param-

eters, such as ionic current conductances, that we hypothesise will vary between cells from different individuals.

In cardiac electrophysiology, as in many physiological fields, studies of human tissue are drastically more difficult to perform than studies of other organisms, due to the difficulty of obtaining human tissue samples for research. As non-failing and non-diseased hearts and other organs are required to study the electrophysiology of healthy people, the most suitable hearts for study are also usually transplant candidates. Therefore, as there is generally a shortage of donor hearts, few human hearts are available for research, and the short length of time this tissue can be kept reasonably healthy limits the number of experiments that can be performed with each heart.

However, computational modelling allows us to test many scenarios without requiring new human cardiac tissue each time, and through doing this we can generate novel hypotheses and predictions, the most promising of which could be tested in experiments using the limited human hearts available for research. This process of using a model to understand human cardiac biology and identify promising targets for further study is the current role of much of the animal experimentation that is carried out. Animal models have been used extensively across the biological sciences as a more easily available proxy for studies on human cells and tissue. However, animal experimentation is expensive, has its own ethical issues that must be satisfied, and provides results that, like modelling, must always be tested against human biology before they can be trusted. Often there are significant differences between human and animal biology (e.g. Jost et al. (2013)). The work in this thesis has potential applications in reducing the need for animal models for experimental studies and industrial uses, such as drug safety testing, by using populations of cardiac cell models, incorporating natural variability, to investigate pro-arrhythmic cellular mechanisms and predict the effects of drugs.

In addition, variability is of particular importance when studying human physiology for biomedical applications, as ideally medical treatment should be provided based on an individual's specific biology, rather than the average human's. While the work presented in this thesis does not

address patient-specific research questions, it is a step towards understanding how to integrate a wide range of varying biological parameters into our existing modelling framework and extract predictions and new hypotheses as to which electrophysiological parameters have significant effects on hearts cells, and in which combinations.

1.2 Thesis goals

The first goal of this thesis is to develop a methodology that can be used to investigate and predict the effects of inter-individual variability in the electrophysiological behaviour of cardiomyocytes. To address this goal, we initially use a traditional modelling approach, a single parameter sensitivity analysis, in the study of delayed after-depolarisation mechanisms in Chapter 4 of this thesis. We use this sensitivity analysis to validate our cardiac cell model by checking that it produces behaviour within the bounds of experimental variability when its parameter values are varied from their baseline values. However, while we find that our model produces delayed after-depolarisations, we find that a standard sensitivity analysis is insufficient to capture the experimental variability we see in control conditions data. The variation in action potential behaviour this sensitivity analysis generates is much smaller than the variation seen across different experiments in our data set. This finding then motivates the development of a framework for studying inter-subject variability in cardiac cellular electrophysiology.

The development of this framework is important because variability is known to have significant effects on a broad range of electrophysiological phenomena, but is not considered in almost all current experimental studies, and computational modelling studies. In this thesis we describe our approach to developing this framework and detail the methodology we have developed - the experimentally-calibrated population of models methodology - based in part on ideas from neuroscience and in part from our own experience of working with the variability inherent in experimental data.

Our methodology integrates the variability observed in experimental data with computational modelling and simulation, by building populations of computational models, that include experimentally observed variability. To build a population, we first generate a large pool of candidate cardiac cell models from an existing baseline model, in which all candidate models have key electrophysiological parameters varied over a wide range, so all models produce different behaviours in simulations. We then simulate the behaviour of each model in conditions that match our experimental data, and discard all models that display behaviours outside the experimental range. The remaining models form a population of models in which all models have significant variation from one another, but are all consistent with experiment and can collectively span the variation seen in experimental data.

The second goal of this thesis is to apply this population of models methodology to investigate the effects of inter-subject variability in cardiac electrophysiology, and to demonstrate that populations of models can be used to perform investigations that could not practically be carried out using standard experimental or computational modelling approaches alone. To achieve these aims we will carry out two studies using populations of models, demonstrating the different applications of our methodology.

In the first study, we will use a population of models to predict the range of effects of the action of a drug, and to determine which underlying ionic currents are important for determining where in this range of responses a particular cell lies. This study will demonstrate the ability of the methodology to make quantitative predictions and validate these predictions against experiment data. This capability is important for many potential applications of cardiac modelling, such as *in silico* prediction of drug effects for safety testing.

In the second study, we will integrate recordings from human heart cells with a computational model developed primarily using data from the same lab as our recordings. We will use the resulting population of models to investigate how variability in magnitudes of underlying ionic currents alters the susceptibility of human cardiomyocytes to developing drug-induced repo-

larisation abnormalities, which can potentially cause arrhythmias at the whole heart level. We will investigate the effects of a range of different drug blocks of different types and different channels to try to understand which combinations of drug blocks and cellular current configurations are particularly susceptible to developing repolarisation abnormalities. This study will demonstrate the use of populations of models to develop new hypotheses that would be difficult to develop using a purely computational or experimental approach alone.

1.3 Outline of thesis

In Chapter 2, we introduce cardiac electrophysiology and the standard experimental techniques used in the field. We describe the basic electrical functioning of a cardiomyocyte and of cardiac tissue, the behaviour of ion channels, and the ionic currents that pass through them. We then describe how these currents collectively determine the whole cell's electrophysiological activity, and generate the cardiac action potential. We move on to describing how the calcium subsystem functions, and describe briefly how calcium release couples electrical excitation with mechanical contraction. We finish this introduction with a review of our current understanding of abnormalities in the repolarisation of cardiomyocytes, their underlying mechanisms and the pro-arrhythmic effects they can have on the heart. We then describe the experimental techniques that have proved themselves vital for probing the electrical activity at the cellular level: microelectrode recordings, voltage clamping, and patch clamping. We finish with a review of the experimental evidence for inter-subject variability in cardiac cellular electrophysiology - the core research topic for this thesis - and provide evidence for its existence, its importance, and our current lack of a predictive understanding of its effects on the heart.

Chapter 3 reviews the current state of the art in computational and mathematical modelling of inter-subject variability in cardiac cellular electrophysiology. We first describe the Hodgkin-Huxley formulation, which is the standard formulation used to model ion channel gating and ionic current flow in cardiac models. We then recap the history of the cardiac cell model, from

Noble's original 1962 model, based on the work of Hodgkin and Huxley, to the latest models that are being used in current research. Following this we describe methods that have been developed for modelling the experimental variability introduced in Chapter 2 and review mathematical and computational techniques for parameter sampling, model simulation, and correlation detection, as these techniques are necessary to construct and analyse the populations of models developed in later chapters. In particular, we cover the Latin hypercube sampling technique for sampling high-dimensional parameter spaces, which is used to create the parameter sets that differentiate models in our populations; and the partial correlation coefficient, which is a statistical technique that allows us to determine correlations between two variables while accounting for the effects of the remaining variables. This is important, given the number of different parameters we vary to create populations of models.

Chapter 4 moves on from our literature review to the first of three simulation studies in this thesis. In this chapter, we describe a study into the generation of delayed after-depolarisations (DADs), in rabbit Purkinje fibres, motivated by the experimental study of Maruyama et al. (2010), which provided evidence that these DADs were caused by calcium overload. In this chapter we use a standard cardiac modelling approach, and construct an appropriate cell model to study DADs in rabbit Purkinje fibres, by combining parts of two existing models. We construct this updated model to include a more detailed calcium sub-system, in order to better capture the calcium overload induced spontaneous calcium release events that we hypothesise to cause these DADs. We show that this model can produce DADs, and we validate its behaviour in control conditions against experimental data. Based on a single parameter sensitivity analysis of key model parameters, we find the model matches the experimental data as well as or better than the original rabbit Purkinje model, but that neither model is capable of capturing the amount of variability seen in the data using the standard sensitivity analysis approach. This chapter builds the case that the standard modelling methodology and tools used in our field are insufficient to capture observed variation.

In Chapter 5 we develop our experimentally-calibrated population of models methodology, and use it to explain the variability seen in recordings from rabbit Purkinje fibres and predict their response to the potassium channel blocking drug dofetilide. We build an experimentally-calibrated population of rabbit Purkinje cell models that spans the variation seen in control conditions microelectrode recordings of rabbit Purkinje fibres at three different pacing frequencies. We then analyse the population and determine which ionic mechanisms are important for determining individual biomarkers of action potential behaviour. Finally, we use our population, developed using data from experiments in control conditions, to predict the effects on action potential duration of four concentrations of the potassium channel blocking anti-arrhythmic drug dofetilide. We find good agreement between experiments and the results from the population, demonstrating the predictive capabilities of our methodology.

In Chapter 6 we move from the rabbit heart to the human heart. We describe the curation of a database of human ventricular microelectrode recordings obtained from our collaboration with the Pharmacology and Pharmacotherapy group at the University of Szeged, and our current progress in converting this database into a fully digital form. We then describe analysis of the database and the range of variation observed within it, as motivation for the simulations studies in Chapter 7 and to demonstrate the high degree of variability observed in electrophysiology experiments on human tissue.

In Chapter 7 we exploit the database we developed in Chapter 6 to investigate how variability alters the susceptibility of human cardiomyocytes to the development of repolarisation abnormalities, following drug application. These abnormalities occur infrequently, and only in some hearts, usually only in conditions far from optimal physiological ones, but in rare cases can translate into arrhythmias. The mechanisms that determine whether an individual will develop these abnormalities are not well understood. In this chapter we aim to determine how variability in the conductances of important ionic currents in the human heart alter susceptibility to these abnormalities in ventricular cardiomyocytes. In this chapter, we apply our methodology, not

to make quantitative predictions, as in Chapter 5, but as a method to generate hypotheses as to how variability across a large number of ionic currents can cause cells that look equally healthy under normal control conditions to exhibit different responses to conditions such as drug block, and therefore demonstrate different levels of pro-arrhythmic susceptibility.

Chapter 8 discusses the process of creating and analysing experimentally-calibrated populations of models in detail, based on our experiences using populations of models in Chapter 5 and 7. We explain the computational and mathematical techniques that we apply in this thesis to create, simulate and analyse the behaviour of a population, and discuss the decisions that need to be taken when designing a simulation study using the methodology.

In Chapter 9 we conclude the thesis with an overview of its major contributions and findings and a discussion of how this work relates to other recent work in our field. Finally, we finish the thesis with a discussion of the limitations of our current results and methodology that we believe could be resolved in further studies, and of particular research questions and areas that were beyond the scope of this thesis, but which could be fruitful grounds for future work.

2

Cardiac electrophysiology and experimental methods

2.1 Introduction

In this chapter, we introduce the core concepts of cardiac cellular electrophysiology. This will provide the biological background necessary for the studies presented in later chapters. We describe the anatomy and function of the heart and its constituent tissue, and the mechanisms behind the electrical activation and generation of action potentials by cardiomyocytes, through the action of voltage-gated ion channels. We explain the importance of the cardiac action potential for the safe and effective functioning of the heart, and describe the calcium sub-system that links the electrical activation of cardiomyocytes with their mechanical contraction, through the use of intracellular calcium concentration as a signalling mechanism. We then describe important abnormalities in the repolarisation of the action potential: early after-depolarisations, delayed after-depolarisations, and alternans. These abnormalities are investigated in this thesis and have been shown to be potentially pro-arrhythmic if they occur in cardiac tissue.

All of the studies presented in this thesis rely on experimental data recorded from cardiac electrophysiology experiments. Experimental data is also required throughout computational cardiac electrophysiology to develop new models, refine existing models, validate results, generate hypotheses, and test predictions made with these models. Therefore, we describe the important

voltage clamp and microelectrode techniques, that are vital for experimental studies in cardiac cellular electrophysiology.

Following this overview of cardiac electrophysiology, we review experimental studies specifically relevant to the main topic of this thesis, inter-subject variability in cardiac cellular electrophysiology. We describe experimental evidence for the existence of many different sources of inter-subject variability in cardiac cellular electrophysiology and demonstrate that many different sources of variability have been found to influence the electrophysiological behaviour of cardiac cells.

Finally, we present studies that examine the differences between human hearts and animal hearts from commonly used animal models. The existence of these differences increases the difficulty of applying discoveries made in studies using animal hearts to human biology. This potential mismatch between experimental animal models and human hearts motivates the use of the human *in silico* cell models used later in this thesis, as these models can be developed using data from human tissue, and used to model human cardiac biology, without the use of animal experiments.

2.2 Cardiac electrophysiology

2.2.1 Anatomy of the heart

The purpose of the heart is to constantly pump and recirculate blood through the body, without pause, to transport oxygen and other important compounds to tissue where they are needed. When the heart beats, it first relaxes, allowing blood to enter two chambers, the left and right atria. The left atrium collects oxygen rich blood from the lungs; the right atrium collects oxygen depleted blood from the rest of the body. The atria contract and two larger chambers with thick, muscular walls, the left and right ventricles, then receive blood from their respective atria. After a delay the ventricles contract and the blood in them is pumped out of the heart. Oxygenated

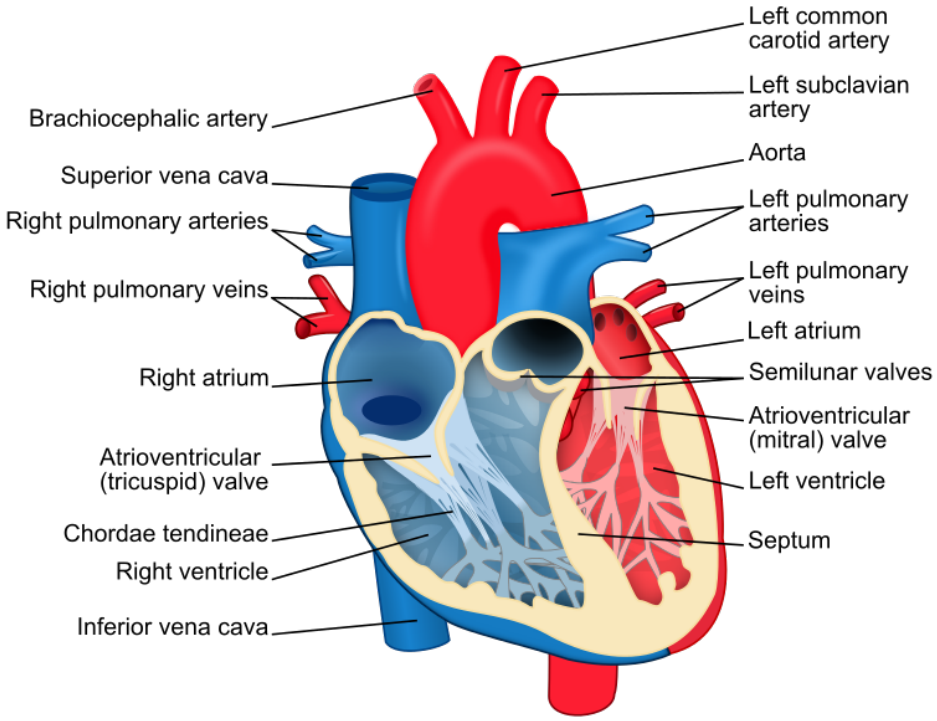

Figure 2.1: Anatomical structure of the heart. The right side of the heart (blue) is responsible for pumping blood to the lungs. The left side of the heart (red) is responsible for pumping blood to the rest of the body. This image is from Wikimedia Commons and is re-used under the Creative Commons Attribution-Share Alike 3.0 Unported license. The original image was created by Wikimedia Commons user ZooFari.

blood from the left ventricle heads out to the rest of the body and de-oxygenated blood from the right ventricle is sent to the lungs. Figure 2.1 shows a diagram of the anatomy of the human heart.

The muscular tissue surrounding the chambers of the heart is called the myocardium, and contracts to provide the pumping force necessary to squeeze blood from the ventricles. The left and right ventricles of the heart are separated from each other by a partition of muscle tissue called the septum. The myocardium is composed primarily of cardiac muscle cells, known as cardiomyocytes. These cells are roughly cylindrical in shape and are typically 50 - 100 μM in length and 10 - 20 μM in diameter. In tissue, they are organised into sheets of cells, and are joined by intercellular connective protein complexes known as gap junctions. These connections allow ions to pass between connected cells and therefore allow electrical impulses to

propagate through cardiac tissue. Gap junctions are primarily located at the end-to-end connections between cells and these strands of connected cells are known as fibres. Due to the increased concentration of gap junctions along fibres, electrical conduction happens preferentially along the fibre direction.

The muscle in the heart is different from skeletal muscle in that it is intrinsically capable of generating and transmitting the electrical impulses that are required to signal it to beat. For these beats to pump blood effectively, the individual muscle cells in the heart must contract and relax in a precise pattern, to maximize the strength of each contraction and the amount of blood pumped. This is accomplished using a regular, repetitive electrical impulse that is generated by a region of the heart called the sinoatrial node, which consists of specialised pacemaker cells that control the rate at which the heart beats. An impulse, in the course of a single heartbeat, traverses the entire heart and triggers the orderly contraction of the cardiomyocytes as it propagates through them. This impulse allows the heart to beat as one organ rather than as many disorganized single cells.

After electrical signals are generated at the sinoatrial node, they pass through the connected synctium of cardiac tissue, regenerated as they go by the action of voltage-gated ion channels. The specific pattern of conduction is governed by the architecture of the myocardium's sheets and fibres, due to preferential conduction along the fibre direction; by the presence of inexcitable tissue that blocks conduction between atria and ventricles; and by the presence of the specialised conduction system, which consists of a network of cardiomyocytes specialised for rapid conduction. As electrical impulses pass through cardiomyocytes, calcium is released from their intracellular stores, which acts as a signal for that cell to initiate contraction. Due to the specific pattern of conduction, this contraction is synchronised with the rest of the myocardium and produced a twisting motion that efficiently pumps blood. The long refractory period of the cardiac action potential, compared to action potentials from spiking excitable cells, such as neurons, prevents premature reactivation of the myocardium before the heart is ready to beat

again. This gives the heart time to rest, and for the atria to refill with blood, before the next beat begins. In an average human lifetime this cycle will happen approximately two billion times, without fail, as any significant break in the operation of the heart would quickly be fatal.

2.2.2 Electrophysiology of a cardiomyocyte

Under physiological conditions with no external electrical signals, cardiomyocytes maintain a negative voltage relative to their environment. However, when sufficiently depolarized, such as by an external change in voltage, ion channels in the cell membrane are activated, altering the balance of currents into the cell and acting to rapidly depolarize the cell further. This triggers the release of calcium ions from a cellular compartment known as the sarcoplasmic reticulum (SR), which raises the bulk cytoplasmic concentration of calcium and signals the myocyte to contract. The ion channels initially responsible for firing this action potential inactivate while others act to repolarize the myocyte back to its resting potential to allow it to fire another action potential during the next heartbeat. The cardiac action potential (first observed by Coraboeuf and Weidmann (1949)) allows the heart to control its own pattern of muscular contraction without external stimuli, as the action potential generated by each cardiomyocyte excites nearby unexcited cardiomyocytes, sustaining the electrical signals that drive the heart.

Ion channel gating

Like all electrically excitable cells, cardiomyocytes have voltage-gated ion channels embedded in their cell membranes. When open, these ion channels allow ions to flow through the otherwise impermeable cell membrane. While a cardiomyocyte is unstimulated and quiescent, most of these ion channels are closed, and the cardiomyocyte maintains a negative membrane potential relative to their surroundings. When an electrical stimulus above a certain threshold is delivered to the cell, it triggers a positive feedback loop, where the small change in voltage from the initial stimulus causes the activation of ion channels that allow further current to flow into the cell. This flow of current depolarises the cell and initiates an action potential. In most electrically

excitable cell types this action potential ends rapidly, and current flowing out of the cell through other ion channel types quickly repolarises the cell. In the heart, the action potential persists for a much longer time, usually several hundred milliseconds in larger mammals such as humans. This longer duration action potential prevents further action potentials from being fired and provides a refractory period that allows the heart to beat and then recover.

The ion channels that control the cardiac action potential regulate the flow of ions, primarily calcium, potassium, and sodium, into and out of cardiomyocytes. They do this using gating mechanisms that are sensitive to the cell's membrane potential, and in some cases to the ionic concentrations around them. When all the gates in an ion channel open, ions can flow through the channel. When one or more gates are closed, ions can no longer get through. There are two main types of gate, activation gates, and inactivation gates. Activation gates are usually closed, but will open in response to a certain stimulus, for example increased membrane potential, and in doing so activate the channel. These gates will stay open until the conditions of their activation are no longer met, when they deactivate and close. Inactivation gates are gates that usually open, but when certain conditions are met, they will inactivate, closing the channel. When these conditions, such as depolarised membrane potential, are no longer met, inactivation gates will recover from inactivation, and open. Usually the timescale in which inactivation gates close should be longer than the timescale for activation, or the conditions for activation should occur significantly earlier in the action potential than the conditions for inactivation, to allow significant current to flow through the channel.

An ion channel usually possesses multiple gating mechanisms, to allow both activation and inactivation. For example, Hodgkin and Huxley (1952) found the sodium channel in the squid giant axon possessed at least two gates: an activation gate that was closed at resting potentials but opened as the membrane potential depolarised, and an inactivation gate that was open at resting potentials, but which closed following membrane depolarisation. As another example, which also illustrates a non-voltage dependent system of gating, the L-type calcium channels

present in cardiomyocytes possess voltage-dependent activation and inactivation gates, but also have an inactivation gate that is calcium-dependent, and will partially inactivate the channel when the intracellular calcium concentration rises. The feedback between the gating mechanisms of these channels and the resulting changes to the cell's membrane potential leads to the complex non-linearity of the behaviour of the cardiac action potential, as a change in any ionic current can alter the membrane potential and therefore the behaviour of other currents.

The cardiac action potential

When an electrically excitable cell, such as a cardiomyocyte, is stimulated above a certain threshold, it is excited and generates a characteristic pattern of membrane potential depolarisation and repolarisation. This pattern is called an action potential, and because it regenerates as it passes through each excitable cell, it allows cells within multicellular organisms to communicate with each other over relatively long distances. In the heart, this communication mechanism allows contraction to be synchronised over the entire heart, despite the fact that a human heart, for example, contains 2 to 3 billion cardiomyocytes.

A cardiac action potential begins when a cardiomyocyte in a quiescent state receives an electrical stimulus of that is sufficient to depolarise the cell above a threshold voltage necessary to activate enough ion channels, usually sodium channels, to continue the depolarisation. From this point, the typical cardiac action potential consists of 4 phases, beginning with phase 0. A diagram of an action potential labelled with these phases is shown in Figure 2.2.

In phase 0, the upstroke, the cardiomyocyte depolarises to its fullest extent. Sodium channels are activated, and the resulting fast sodium current rapidly depolarises the cell, causing a sharp upstroke, as the time scale of this phase of the action potential is much shorter than subsequent phases.

In phase 1, the depolarisation of the cell causes sodium channels to inactivate, and the upstroke ceases. The transient outward potassium current (Ito) causes a downward deflection in the

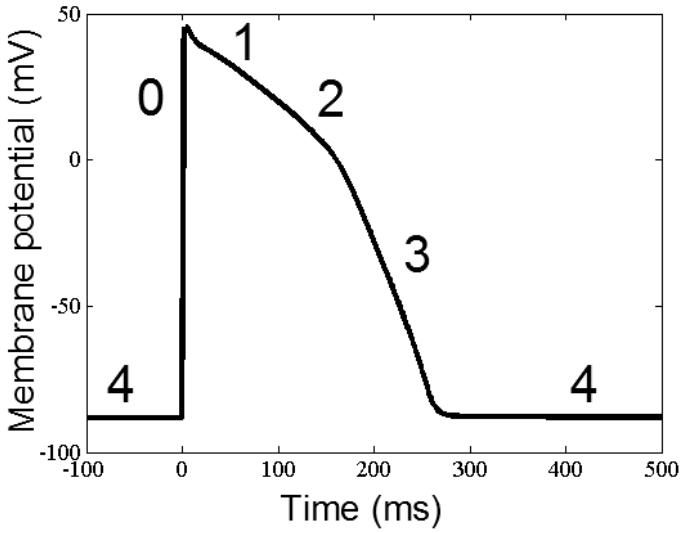

Figure 2.2: Phases of the action potential, starting from the resting membrane potential (phase 4), through the upstroke (phase 0), initial repolarisation (phase 1), plateau (phase 2), repolarisation (phase 3) and then back to phase 4, shown for a human ventricular action potential.

action potential. The changing balance between this outward current (a current flowing out of the cell, repolarising it), and inward currents (currents flowing into the cell, depolarising it), such as the L-type calcium current, that are beginning to activate in this phase can cause the appearance of a notch (Figure 2.3B) that is a characteristic of certain species and cell types, depending on their typical Ito channel densities.

In phase 2, the plateau, the L-type calcium current, which is an inward depolarising current, is fully activated and competes with outward potassium currents. This often results in a small net outward current through the cardiomyocyte, leading to a plateau, where the membrane voltage repolarises slowly for a period. Due to time and voltage dependent inactivation the L-type calcium current eventually falls off and there is reduced opposition to the outward potassium currents, leading to phase 3.

In phase 3, repolarisation, outward potassium currents, in particular the rapid and slow delayed rectifier potassium currents (IKr and IKs respectively), are active and unopposed by significant inward current. Therefore, repolarisation happens more rapidly in this phase compared to phase 2. As membrane potential becomes more negative, IKr and IKs inactivate, preventing runaway

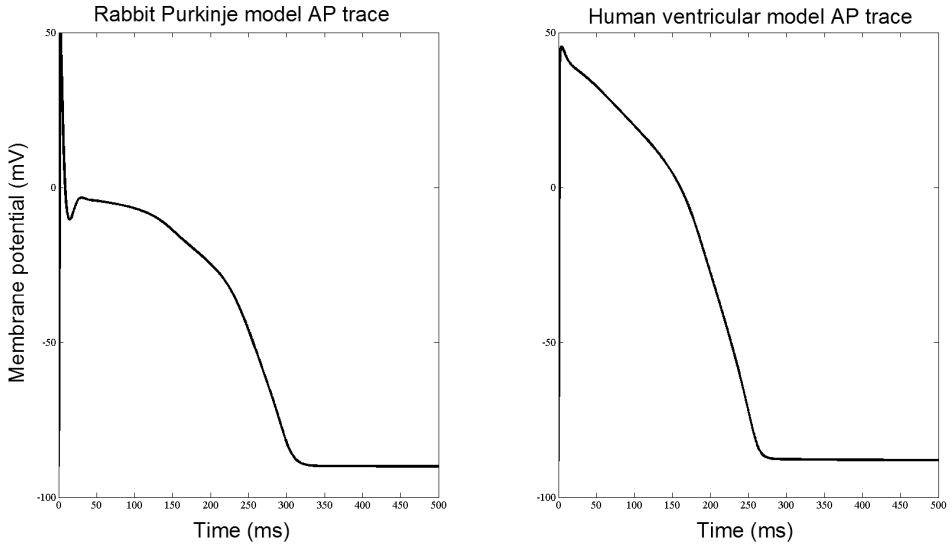

Figure 2.3: Example action potentials from two cardiac cell models, both paced at 1 Hz. Left: Action potential from the rabbit Purkinje cell model developed in Chapter 4 and used in Chapter 5 and in Britton et al. (2013). Right: Action potential from the O'Hara-Virag-Varro-Rudy (ORd) model of a human ventricular cardiomyocyte (O'Hara et al. (2011)), which is used in Chapter 7.

repolarisation. Phase 3 completes when membrane potential reaches a stable resting value and IKr and IKs channels close.

At this point, the action potential has finished, and the strongly negative resting membrane potential (generally in the range -90 to -70 mV) is negative enough for sodium channels to recover from inactivation. In this quiescent phase, phase 4, the cardiomyocyte remains at its resting membrane potential, which is maintained by the inward rectifier potassium current, IK1. Because the sodium channels are closed but recovered from inactivation, a stimulus can now activate the cardiomyocyte again, firing a new action potential.

The key difference between the cardiac action potential and a neuronal action potential is the long duration of the post-upstroke repolarisation, compared to a neuronal spike. In a cardiac action potential the long refractory period caused by the relatively long duration of plateau and repolarisation prevents sodium channels from recovering from inactivation and so prevents the firing of additional action potentials, usually for several hundred milliseconds.

2.2.3 Linking electrophysiology to cardiac function - calcium and conduction

There are two reasons that a cardiac action potential must prevent further action potentials from firing: firstly, the action potential causes calcium release from intracellular stores, and calcium signals the cardiomyocyte to contract; secondly, a single contracting cardiomyocyte is not sufficient to pump blood around the body, the whole heart must pump together as an organised muscle for successful pumping of blood to occur. Therefore, the cardiac action potential is a signal to control and synchronise cardiac muscle, it causes each cardiomyocyte to contract and then holds it in an unexcitable state to reduce the chance of premature contraction. In this section we review the calcium sub-system of a cardiomyocyte, followed by the electrical conduction system of the heart. This conduction system ensures electrical impulses reach different areas of the heart in a pattern that organises the individual contraction of cardiomyocytes into an effective pumping action. Both of these systems are important for the work on DAD formation in rabbit Purkinje fibres presented in Chapter 4.

The calcium sub-system

Calcium is the ion that links electrical activation of a cardiomyocyte with mechanical contraction. It is the key signalling molecule responsible for electrical-contraction coupling in the heart. As calcium is an ion as well as a signalling molecule, and calcium currents play an important role in the action potential, there is also bidirectional coupling between calcium and the action potential. The details of these coupling mechanisms, and the many other roles of calcium in the heart are beyond the scope of this chapter, but have been reviewed by Bers (2008). In this section we describe how calcium is stored, regulated, and released within a cardiomyocyte, during the action potential.

A rise in cytosolic calcium concentration triggers muscular contraction, with the strength of contraction being related to the concentration of calcium in the cytosol. To prevent the cell

from constantly contracting, but to allow it to contract when required, a large amount of the calcium within a cardiomyocyte is held in a storage compartment known as the sarcoplasmic reticulum (SR). In the SR, calcium is taken up from the rest of the cell by the sarco/endoplasmic Ca-ATPase (SERCA), which pumps calcium out of the cytosol and into the SR where it is held. The SR also contains calcium release channels, in particular the ryanodine receptors (RyRs), which are activated by cytosolic calcium. Inward calcium currents, such as the L-type and T-type calcium currents (ICaL and ICaT, respectively) increase the calcium concentration around the RyRs and cause them to open, allowing calcium to flow out of the RyRs , which activates them further. This calcium-induced calcium release allows a smaller amount of calcium influx into the cell to trigger a large calcium release from the SR, signalling contraction. As calcium stores in the SR are depleted, RyRs, which are also sensitive to SR calcium levels, close and calcium release from the SR stops. Calcium remaining in the cytosol is primarily taken back up into the SR by SERCA, and additionally some is exchanged out of the cell by sodium-calcium exchangers. This process of calcium release and reuptake during the action potential produces a characteristic rise and fall of cytosolic calcium that is known as the calcium transient.

Electrical conduction in the heart

We conclude this introduction of the normal functioning of the heart by outlining how electrical activation of individual cardiomyocytes is controlled throughout the whole heart, so that activation proceeds in an ordered fashion. This sequencing of activation is performed by the conduction system of the heart, shown in Figure 2.4. It comprises the sinoatrial node that generates the initial impulse that propagates through the heart; the bulk myocardium; inexcitable areas of tissue that act as conduction blocks to separate different areas of the heart; the atrioventricular node that slows propagation from atria to ventricles; and the specialised conduction system that consists of a network of cardiomyocytes optimised for fast conduction in the ventricles.

The initial impulse that activates the rest of the heart is generated in a region of specialised tissue in the right atrium called the sinoatrial node. This region has the fastest spontaneous

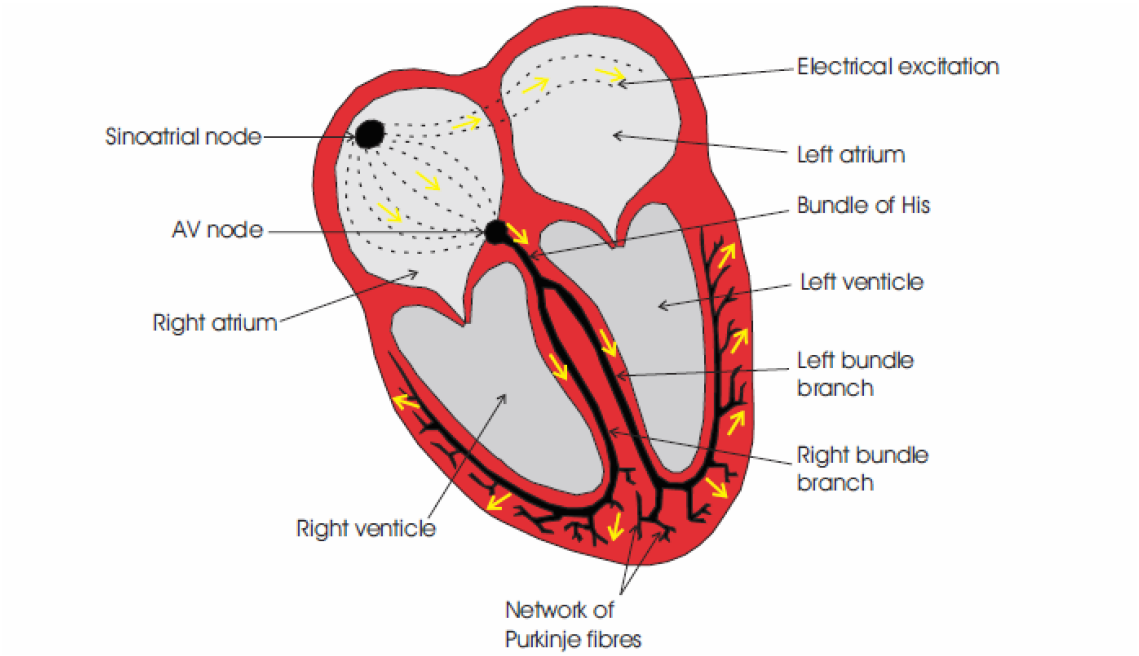

Figure 2.4: Diagram of the pattern of electrical activation and conduction in the heart. Reproduced from Bishop (2008).

depolarisation of any region of the heart and so drives the rest of the heart. While the heart's excitation is self-driven, unlike other muscles which are driven by neural signals from the brain, the sinoatrial node is connected to the brain via the autonomic nervous system, allowing some control over the pacing frequency of the heart. From the sinoatrial node, the propagating impulse excites both atria, causing them to contract and squeeze blood into the ventricles. The wave of excitation cannot pass directly to the ventricles, as almost the entire boundary between the atria and ventricles is made up of inexcitable tissue. The only way for the signal to propagate is through an area called the atrioventricular node, which has some of the slowest conduction times of any cardiac tissue. This causes ventricular excitation and contraction to occur after atrial contraction has finished, which ensures there is a full load of blood within the ventricles to pump out. The ventricles are large and have relatively thick muscular walls. To rapidly activate the entire ventricular tissue from the atrioventricular node, electrical activation passes through a series of fast conduction cardiomyocytes, which are part of the specialised conduction system. First, signals pass through the bundle of His, which then break up into a network of Purkinje

fibres. These are cylindrical fibres that contain the Purkinje cells that transmit electrical signals rapidly throughout the whole ventricles. This causes synchronised contraction throughout each ventricle, pumping blood out of the heart.

2.2.4 Abnormalities in cardiac repolarisation

While a healthy cardiomyocyte usually repolarises following the four phases of the action potential, as described earlier in this chapter, there are several important phenomena that may cause the action potential to deviate from this pattern. These are called repolarisation abnormalities, and have been extensively studied, because they can present a pro-arrhythmic risk if they occur in the living heart. There are three main categories of repolarisation abnormality that occur at the cellular level - early after-depolarisations (EADs), delayed after-depolarisations (DADs), and alternans.

Early after-depolarisations

EADs are depolarisations that occur during the plateau or repolarisation phases of the action potential, as shown in Figure 2.5A. The initial driver of EAD formation is typically an extended plateau or repolarisation phase duration that holds the membrane potential at a level that allows regenerative inward currents, such as ICaL and the sodium-calcium exchange current (INCX), to reactivate (Volders et al. (2000); Weiss et al. (2010)). Regenerative currents are currents that increase their magnitude through their own action. For ICaL this is due to depolarisation of the membrane potential to more positive values. For INCX, increased intracellular calcium increases inward current, because INCX exchanges 3 Na^+ ions for 1 Ca^{2+} ion, resulting in $+e$ of charge entering the cell for every Ca^{2+} ion it exchanges out, where e is the elementary charge. As ICaL brings additional calcium into the cell, which can trigger calcium-induced calcium release from the SR, the regenerative mechanism of INCX is based on the regenerative action of ICaL.

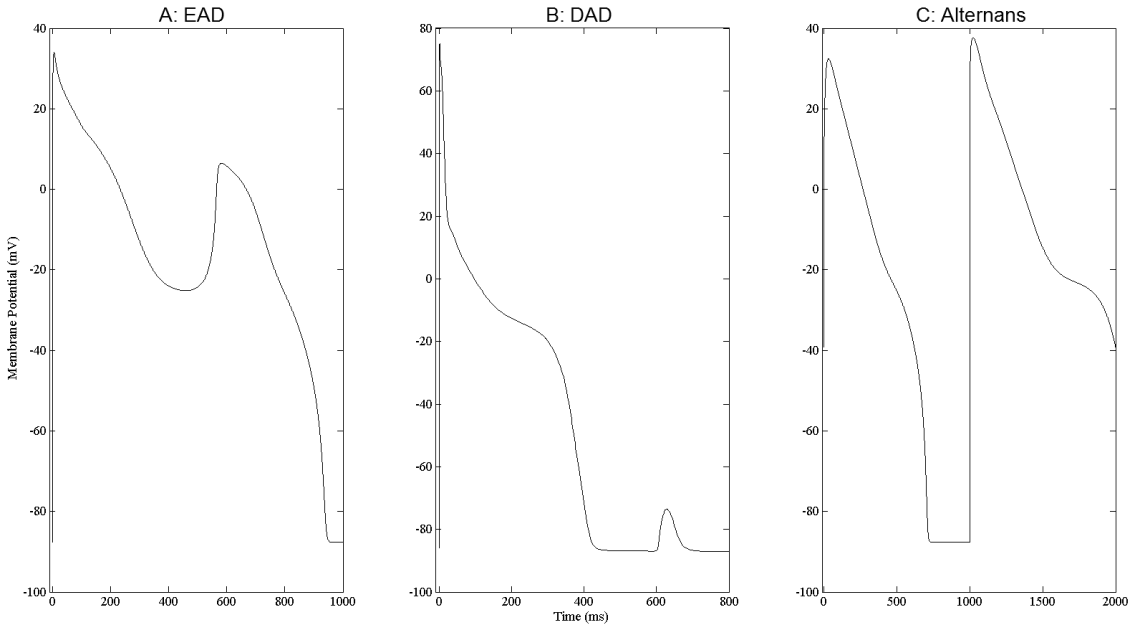

Figure 2.5: Examples of cellular repolarisation abnormalities. A: An early after-depolarisation (EAD) from a variant of the ORd human ventricular cell model, from the study described in Chapter 7. B: A delayed after-depolarisation (DAD) from the rabbit Purkinje cell model used in Chapter 5. C: Alternans from a different variant of the ORd model, from the study described in Chapter 7.

Reactivation of ICaL is traditionally thought of as the most important mechanism for generating the EAD upstroke (January and Riddle (1989)). ICaL usually functions by activating during phases 1 and 2 of the action potential, providing an inward current that sustains the plateau, followed by inactivation to allow repolarisation in phase 3. However, ICaL will recover from inactivation over time. If, when it recovers, repolarisation has not brought the membrane potential down to a sufficiently negative voltage (below approximately -30 mV), the activation gate will still be partly open and current will flow through ICaL again. If this causes repolarisation to stop and turn into depolarisation, an EAD occurs. As membrane potential rises, ICaL will inactivate for a second time, which usually ends the EAD. However, if further currents, particularly INa, recover from inactivation during the EAD, they can increase the magnitude of the EAD and potentially generate a new action potential out of sequence. This is called triggered activity, and can be caused by both EADs and DADs of sufficient magnitude.

The extended plateau or slow repolarisation that provides the conditions that allows an EAD

to occur can be caused by either or both of: increased inward current compared to normal; or decreased outward current. Outward current at this stage of the action potential is primarily due to potassium currents such as IKr and IKs, while important inward currents are ICaL, INa and INCX. Delayed inactivation of INa or ICaL can contribute to a lengthened plateau phase, while INCX provides a mechanism for intracellular calcium concentrations to influence EAD formation, as higher intracellular calcium causes a larger inward INCX current, which can prolong the plateau enough for ICaL to reactivate.

INCX has also been implicated as a possible source of the inward current that generates the EAD. If calcium is released spontaneously from the SR, INCX can provide the initial inward current to allow ICaL to recover from inactivation and continue the upstroke of the EAD. Studies supporting both ICaL and INCX driven mechanisms have been performed (Luo and Rudy (1994b); Choi et al. (2002)). The current viewpoint (Weiss et al. (2010)) is that both ICaL and INCX act in synergy to promote EADs, but that reactivation of ICaL is necessary for EAD formation, INCX alone is insufficient.

EADs are pro-arrhythmic, as they can increase heterogeneity of repolarisation in tissue and potentially create areas which are still in their refractory period, due to the EAD, when the next activation wave passes through. In extreme cases they can also generate a new action potential which can propagate through tissue, potentially rendering it unexcitable when the next beat is supposed to occur. This can potentially set up conditions for an arrhythmia to occur.

Delayed after-depolarisations

If an out of sequence depolarisation happens after the action potential has ended, it is referred to as a delayed after-depolarisation (DAD). DADs are depolarisations that occur in phase 4 of the action potential, after full repolarisation has occurred, but before the next electrical signal from the sinoatrial node has reached the cell. A DAD usually manifests itself on a voltage trace as a small depolarising bump after the action potential, as shown in Figure 2.5B. However, if

the magnitude of this depolarisation is sufficiently large, the fast sodium current can activate and fire an out of sequence action potential. This is another example of triggered activity. If this occurs in a significant number of cells in an area of tissue, the tissue may be in a refractory state when the next wave of normal excitation arrives, disrupting the normal activation sequence of the heart and potentially setting up conditions for an arrhythmia to occur.

The mechanisms that cause DADs to form are believed to originate in the calcium sub-system (Bers (2008)). If the SR becomes overloaded with calcium, it is possible for spontaneous emission of calcium from the SR to occur outside of the normal action potential's calcium cycle. If calcium levels in the SR are elevated, increased leakage from the SR can increase calcium levels around RyRs enough to activate them, leading to calcium-induced calcium release. This increase in intracellular calcium leads to a depolarisation of the cell, outside of the normal action potential. It is believed that the sodium-calcium exchange current, INCX, is responsible for this depolarisation (Pogwizd et al. (2001)). By exchanging the excess calcium out of the cell with extracellular sodium, the result is a net inward current, resulting in depolarisation. This process normally occurs when the cell is fully repolarised, which allows time for calcium reuptake into the SR via SERCA. However, there is also evidence that it can occur during repolarisation, leading to an EAD-type deflection in the voltage trace, driven by DAD-type mechanisms (Volders et al. (1997); Choi et al. (2002)). Lone DADs in single cardiomyocytes within tissue do not pose an arrhythmic risk, as the surrounding cells act as current sinks to smooth out the depolarisation. However, if DADs occur synchronously within many cells in a single area of tissue, they can trigger an action potential outside of normal pacing, which can potentially initiate an arrhythmia.

Alternans

As well as both forms of after-depolarisation, alternans are an additional common abnormality that affects cellular repolarisation. Alternans are steady beat-to-beat alternations in the duration of either, or both, the action potential and the calcium transient. A typical alternans pattern

is one short action potential, followed by a long action potential, then another short action potential, and so on, at a constant pacing cycle length, as shown in Figure 2.5C. The general mechanism that causes alternans formation is that by the end of one pacing cycle, the cell has not fully recovered in some way. For example, calcium stores in the SR may not have been fully replenished. On the next beat, the cell is therefore in a different state than it was on the last beat (e.g. smaller calcium stores), and so the action potential and calcium transient are also different. However, if by the end of this beat, the cell has recovered, due to the extra time available, to the state it was at two beats ago, then this two beat cycle is a stable oscillating steady state and can continue.

Alternans can be pro-arrhythmic when they occur in tissue. If alternans occur in tissue, they can be concordant (all parts of the tissue that display alternans have the same pattern, e.g. a long action potential then a short action potential), or discordant (different parts of tissue have alternate patterns e.g. long-short in one region and short-long in another). Discordant alternans pose a greater pro-arrhythmic risk than concordant alternans, as they increase heterogeneity of repolarisation within the tissue. This makes it more likely that some areas of tissue will still be repolarising when the electrical impulse reaches them, blocking activation and setting up potential conditions for an arrhythmia.

While concordant alternans are not a known pro-arrhythmic mechanism themselves, they still mark out a region of heart tissue that is not behaving normally. The occurrence of alternans has been shown to be a biomarker of increased risk of ventricular arrhythmias (Rosenbaum et al. (1994)). While alternans themselves may not increase the chance of an arrhythmia occurring, they are a signal that repolarisation within a particular portion of tissue is not occurring normally.

Source-sink mismatch in cardiac tissue

The three types of repolarisation abnormalities that we have described occur in single cells and

are generated by cellular mechanisms, but their importance for pro-arrhythmic risk is determined by how they affect living cardiac tissue. A full discussion of repolarisation abnormalities in tissue is beyond the scope of this chapter; however it is important to identify the main difference between abnormality occurrence in isolated cardiomyocytes and in tissue. The primary difference between connected cardiac tissue and isolated cardiomyocytes is that in tissue a repolarisation abnormality occurring in a single cardiomyocyte will be smoothed out by the surrounding tissue due to electrotonic effects (passive spreading of charge between connected cells). This source-sink mismatch means that for an abnormality to have a noticeable effect in tissue it must occur simultaneously in many nearby cardiomyocytes. Therefore, conditions that are sufficient to cause repolarisation abnormalities to occur frequently in isolated cardiomyocytes may not produce any abnormal behaviour in tissue, and may require an additional mechanism, or amplification of existing factors, to observe the abnormality in tissue (Pueyo et al. (2011)). The probability of each cardiomyocyte in a region of coupled tissue developing a repolarisation abnormality on a particular beat must be high before there is a significant chance of the abnormality propagating through tissue.

2.3 Experimental techniques

We have given an introduction of the normal functioning of the heart, and of cellular abnormalities in repolarisation that relate to this thesis. In this section we now describe the techniques that have been used extensively in cardiac cellular electrophysiology studies and that are also necessary to gather the data used to develop and validate cardiac cell models. These comprise two main techniques: microelectrode recordings, which are used to record the membrane potential of a cardiomyocyte; and voltage clamping, which can be used to investigate the gating mechanisms of individual ionic currents, or the behaviour of individual ion channels.

Microelectrode recording techniques

Microelectrode recording is the standard experimental technique for recording the action potentials of cardiomyocytes in cardiac electrophysiology. It is a technique to both insert a recording device into a cell and to have a way to apply current to it to stimulate action potential generation. A microelectrode is an electrode that is small enough to be inserted into an individual cell. The development and first use of the microelectrode in cardiac tissue (Draper and Weidmann (1951)) was a significant step forward for cardiac electrophysiology, as it meant that the action potentials of individual cardiomyocytes could be recorded, whereas previously electrical activity had to be inferred from whole body and whole heart recording techniques such as the electrocardiogram (Hoffman (2002)). Recording at the single cell level allowed mechanisms of depolarisation and repolarisation to be studied. Recordings of individual cells within a tissue preparation can also be obtained, to study how tissue effects alter the behaviour of cells within the tissue.

When a microelectrode experiment is being performed, typically one electrode will be inserted into a cell to deliver stimulus current that will depolarise the cell sufficiently to trigger an action potential, while a second electrode will be inserted to measure the cell's membrane potential relative to ground and therefore record the action potential trace. This allows control over the magnitude of the stimulus current, and the pacing rate, which in turn allows steady pacing at different pacing rates and response to changes in pacing rate (restitution) to be studied.

Voltage and patch clamp techniques

Microelectrode experiments allow investigation of the electrophysiology of an entire cell, by recording its membrane potential. To study the ionic currents that collectively make up the action potential, and the behaviour of the individual ion channels through which these current flow, two further experimental techniques are required: the voltage clamp and the patch clamp. Voltage clamping and patch clamping are experimental techniques that are used to interrogate the relationship between a cell's membrane potential and the current that flows through the ion channels embedded in the cell membrane. Voltage clamping was developed after microelec-

trode techniques, and allowed researchers to gain a deeper understanding of the mechanisms controlling individual ionic channels and currents, and feed that knowledge back into their understanding of the action potential. The patch clamp technique (Neher and Sakmann (1976)) refined the voltage clamp technique by allowing the measurement of the current through individual ion channels for the first time.

The principle of voltage clamping is to impale an excitable cell with an electrode that both measures the voltage of the cell and injects current in order to hold the voltage of the cell membrane at a predetermined value. The amount of current needed to hold the membrane potential steady can then be used to calculate the opposing flow of current through ion channels in the membrane. By using protocols that vary the voltage the cell is clamped at, the gating kinetics of different ionic currents can be studied. For example, by holding the membrane potential at a positive membrane potential for a long time, ion channels will open fully, but inactivate. A sudden reduction in membrane potential can then be used to investigate recovery from inactivation, assuming recovery from inactivation occurs on a faster timescale than closing from a fully open state. In a normal cardiomyocyte, there are many ionic currents active at most physiological membrane potentials. Therefore, to isolate an individual current for study, a common method is to perform the same experiment twice, once in control, and once with a drug that selectively blocks the studied current. By subtracting the results of the two experiments away from each other, the contribution of the blocked current can be discovered. However, drugs are not perfectly selective at blocking only a single type of ion channel. Often drugs can have appreciable blocking effects on other ion channels, which can lead to uncertainty in voltage clamp results.

In patch clamping, instead of a traditional electrode, a glass micropipette is used to form a seal with a patch of cell membrane, by applying suction within the pipette once it is pressed against the membrane. Once applied this creates a very high resistance (10-100 gigaohms) seal over the membrane patch. The voltage across the membrane can then be clamped to a particular

value, or particular voltage protocol, and the current that flows across the membrane in response can be measured. This can be done using a variety of experimental conditions and voltage protocols, e.g. to understand the voltage and time dependencies of a particular ion channel. Because a small patch of membrane is isolated by the gigaohm seal, potentially small enough to have a single ion channel embedded in it, patch clamping can be used to study the behaviour of individual ion channels. This is a significant advantage of patch clamping compared to voltage clamping. In cardiac modelling, patch and voltage clamp experiments are important for model development. These experiments generate the data that is used to parametrise the gating mechanisms of the different ionic currents used in cardiac cell models, such as those described in this thesis.

2.4 Inter-subject variability in cardiac cellular electrophysiology

The motivation for this thesis is that variability between individuals modulates cardiac electrophysiological function, demanding the integration of experimental data and computational modelling to address the complexity of a biological system that differs from individual to individual. In this section we review evidence for variability in cellular cardiac electrophysiology between individuals of the same species.

The ionic currents that control the cardiac action potential are primarily controlled by the ion channels through which they flow. Therefore, we expect inter-individual differences in the ion channel configurations of cardiomyocytes to be a primary source of electrophysiological variability. In general, we expect ion channels to be produced with a consistent structure, and therefore consistent functional behaviour across a population of healthy individuals of the same species. However, the density of functional ion channels of a particular type that are present in the membrane of a cell is not expected to be as consistent, and is known to be subject to considerable variation from many sources. Biological systems are usually robust to variation in

protein concentrations, as they have to be due to the many sources of variability they encounter. Substantial variation between cardiomyocytes, and between individuals, exists in ion channel densities in the cell membrane, which correspond to changes in the maximal flow of the ionic currents those channel conduct. Differences between ion channel structures in different individuals also exist, however, this is usually due to a genetic mutation, and in general, unlike natural variability, functional mutations in ion channels are often pathological. Individuals possessing these mutations are not thought of, in terms of the behaviour of their heart, as part of the healthy normal population, and these mutations are rare, occurring only in a small fraction of the population.

Evidence for variation in the properties of ionic currents in the cell membrane of cardiomyocytes comes from a variety of different causes and mechanisms. We focus on factors that include circadian rhythms; alteration of pacing rate; drug application; and the development of diseases that affect the heart.

Natural circadian rhythms have been shown to cause variation in ion channel expression throughout the day. In a study on mice, Jeyaraj et al. (2012) showed that one particular circadian clock dependent protein, *Klf15*, altered expression of the KCh1P2 gene, which produces subunits of the ion channel responsible for carrying the transient outward potassium current, Ito. In mice, this is a key current involved in repolarisation, unlike in humans where that role is performed primarily by IKr. They also found that the QT interval, which is the measure on the electrocardiogram that is generally linked to action potential duration, varied throughout the day. While this study was performed in mice, there is a known trend in humans for sudden cardiac death to exhibit diurnal variation, with a peak in deaths occurring during morning hours, and a secondary peak occurring in the evening.

Sustained changes in pacing rate have also been shown to alter channel expression. Tsuji et al. (2006) performed 3 week long experiments on rabbits in which they were exposed to tachypacing (pacing at faster than normal rates) and bradypacing (slower than normal rates). They then

investigated the effects on the delayed-rectifier potassium currents, IKs and IKr. IKs was found to be reduced in both tachypaced and bradypaced cases, while IKr was decreased in the bradypaced case. This remodelling was found to promote the development of ventricular arrhythmias, particularly in the bradypaced case. In Qi et al. (2008), studies on dogs revealed that mRNA expression in isolated cardiomyocytes for channels carrying the L-type calcium current were reduced by approximately 50% after 24 hours of exposure to an increased pacing rate of 3 Hz. In this case the authors were able to find a potential mechanism, increased build-up of calcium in the cell resulting from the rapid pacing, that could cause cells to downregulate expression of ICaL channel genes.

Sustained ion channel block can cause cardiomyocytes to alter their ion channel distributions. However, the mechanisms that cause these alterations are not well understood. Xiao et al. (2008) reported that prolonged exposure to the drug dofetilide, which selectively blocks IKr, caused canine ventricular myocytes to upregulate the production of channels that carry the IKs current, which has a similar role to IKr in repolarisation and is thought of as the primary mechanism behind the concept of "repolarisation reserve" (Roden (1998)), which is the concept that while IKr is the primary current involved in repolarisation, cardiomyocytes possess a variable reserve of other currents, including IKs, that are capable of carrying out repolarisation if IKr is inhibited. Le Bouter et al. (2004) demonstrated that mice exposed for 6 weeks to the anti-arrhythmic drug amiodarone, which blocks multiple ion channels, exhibited dose-dependent altered expression profiles of a large number of genes that encode cardiac ion channel subunits. Sodium, potassium and calcium channel subunits were downregulated, as was the sodium-calcium exchanger. Some potassium channel subunits were also upregulated. Some, but not all of these changes were reflected in altered current densities obtained from subsequent patch clamp recordings.

Many diseases are known to cause the heart to remodel its distributions of ion channels in some way. An example of this is the study by Borlak and Thum (2003), in which they measured the expression of a large number of genes encoding ion channel proteins in explanted human hearts

from patients suffering from ischemic and dilated cardiomyopathy. In these hearts they found numerous changes in ion channel gene expression. Transcripts of sodium and L-type calcium channels were reduced to 30-50% of control. Slow delayed-rectifier potassium channel genes (carrying the IKs current), were increased by 1.6 times in left ventricular tissue, and 4 times in right ventricular tissue, while rapid delayed-rectifier channel genes for the IKr current were unchanged in left ventricles and increased by 2 times in right ventricular tissue relative to control. While the study did not measure the alteration of action potential behaviour these changes in expression caused, it is likely they significantly altered the electrophysiological profile of cardiomyocytes in these hearts.

We see from these studies that ion channel density, and therefore ionic current conductances can vary considerably due to a number of factors that could be present simultaneously in a cardiomyocyte. There are many different factors that can alter the conductances of ionic currents, as well as other properties of cardiac cells, from modification of the expression of ion channel mRNA, to changes during the process of embedding functional channels in the membrane. These are not the only changes that can cause electrophysiological variability between cardiac cells from different individuals. However, these changes that affect ionic conductances can have a significant effect on every heart due to the importance of ionic current strengths for determining the properties of the action potential, and act through mechanisms that can affect all individuals, unlike, for example, inherited mutations. The link between changes in transcript expression and ionic current function, and the post-transcriptional processes that could alter ionic current function (e.g. regulation by microRNA, or transport of channels to the membrane) are not well understood as of now (Nattel et al. (2010)). Also, the level of variation that could be considered 'baseline', across individuals from the same species is another important topic that is difficult to study experimentally and has yet to be conclusively addressed. However, we do know that this variation exists, and that it can have a significant effect on the behaviour cardiomyocytes and the chances of arrhythmias developing in the heart.

2.5 Evidence of differences between human and animal experiments

The purpose of a vast amount of biological and biomedical research is to improve healthcare outcomes in humans. However, much of this research is carried out on non-human species, due to the ethical implications of experiments and clinical trials performed on humans, and the difficulty of obtaining human tissue for study. Therefore, there is the possibility that discoveries made in non-humans do not transfer over to human biology, and also that important facets of human biology are not being discovered because they are not present in other species. In this section we review recent experimental studies in cardiac electrophysiology where differences between human and animal hearts have been found, to motivate the use of computational models of human cardiac electrophysiology, as used in Chapter 7 of this thesis.

In Jost et al. (2013), it was shown that the balance of important currents for repolarisation in canine, and in human, differ significantly. In studies on right ventricular papillary muscle, IKr was found to be larger in human, while IKs and IK1 were larger in dog. Selective IKr block lengthened action potential duration at 90% repolarisation (APD90) by 3-fold more than in dog, while selective block of IK1 and IKs increased APD90 more in dog than human. Using the concept of repolarisation reserve (Roden (1998)), which states that the amount of APD prolongation caused by block of IKr is inversely related to the amount of 'backup' repolarisation currents (IKs and IK1) available to the cell, we see from these results that human repolarisation reserve is lower compared to dogs. This therefore suggests that if the findings of experiments using IKr blockers performed in dog are translated to humans, they are likely to underestimate the effect of IKr block.

Lu et al. (2001) studied the effects of dofetilide, a selective IKr blocker, and quinidine, an INa blocker that also blocks IKr, IKs, ICaL, ITo and INaL, in Purkinje fibres from rabbits, guinea pigs, dogs, pigs, goats, and sheep. As an example of the variability they found across species,

they saw changes in APD90 from 25 minutes exposure to dofetilide, compared to control, at 1 Hz pacing, range from a high of 83% in rabbit, to a low of 18% in pig. With the application of the less selective channel blocker quinidine, paced at 0.2 Hz, changes in APD90 ranged from an increase of 124% in rabbit to a decrease of 39% in sheep. The study also found that EADs occurred during infusion of either drug at 0.2 Hz in rabbit, but not in any other species. While this study did not include human tissue, there exist significant differences in the balance of ionic currents of cardiomyocytes from different species, which usually result in quantitative differences in response to drugs between species, and that can result in qualitative differences in some cases, e.g. whether a drug prolongs or shortens of APD90, or whether EADs form. Overall, we see significant differences between the cellular electrophysiology of humans, and of other large mammals that are often used as animal models. Addressing the differences between experimental animal models and humans is an area where computational models can be used to directly model human electrophysiology, and maximise the value of scarce experimental data from human hearts.

2.6 Conclusions

In this chapter we begun by outlining the function and structure of the heart, introduced the electrophysiology of the cardiomyocytes that perform the heart's key pumping function, and described the key experimental techniques relevant to this thesis. We then provided evidence that variability in ion channel densities in cardiomyocytes from different individuals is pervasive and can come from many sources. We also described studies of the differences between human and animal cardiomyocytes, to illustrate the limitations of animal models for human cardiac research. Our aim in this last section was to motivate a role for cardiac modelling to bridge the gap between understanding the typical or average behaviour of cardiomyocytes from a particular species, and understanding the range of different behaviours cardiomyocytes from different individuals can produce, and what are the underlying mechanisms that drive this variability, by

using computational cardiac models of the species being studied.

The focus of the next chapter is on the history and the current state of the art in computational modelling in cardiac electrophysiology. To develop our scientific understanding of any complicated system, we need to build models of it. A good model allows us to simplify a complex series of interacting parts, by removing, simplifying, or abstracting detail, to allow us to determine which parts and which interactions are crucial for a particular aspect of the system's behaviour. All scientists use models of some kind in their research, whether they are animal models, mathematical and computational models, or theoretical models developed within a scientist's mind from their knowledge of the system they are studying. By design, all models are simplified, imperfect representative instruments, that can be used to investigate the organism, organ, cell, protein, etc. that is being modelled. However, given the evidence in this chapter, there is no guarantee that an experimental study performed on an animal model is a superior method for answering a given research question than using a computational model of the species the study aims to understand, which is usually humans. Variability, in particular, is difficult to address with experimental studies alone, as data must be averaged from preparations from a number of individuals to reduce experimental error and increase confidence in results. Computational modelling in cardiac cellular electrophysiology is a mature and extensive field, and in the next chapter we describe the historical development of models in the field and in particular the latest models for species and cell types relevant to this thesis, as well as reviewing important techniques for parameter sampling and analysis of model output that will be needed for the modelling of inter-subject variability in the studies presented in later chapters.

3

Computational modelling in cardiac cellular electrophysiology

3.1 Introduction

In the previous chapter we introduced the biological and experimental background for the work presented in this thesis. In this chapter, we introduce and review the topics of computational modelling in cardiac cellular electrophysiology and methods for modelling inter-subject variability. We begin with an explanation of the Hodgkin-Huxley formulation for modelling ionic currents, upon which most cardiac cell models are based. Following this we provide an overview of the history and evolution of cardiac cell models. We then move to the current literature on modelling cardiac cellular electrophysiology, and describe important contemporary cardiac models that are relevant to this thesis. Finally, we review methods for modelling inter-subject variability, as well as related mathematical methods for performing the parameter sampling that is often required for these variability modelling methodologies, computational methods involved for simulating model behaviour, and methods for analysing the results of simulation studies that model variability.

3.2 Cardiac cellular electrophysiology models

3.2.1 The Hodgkin-Huxley formulation of ionic current behaviour

In the last of a landmark series of papers Hodgkin and Huxley (1952) showed that their mathematical model of the ionic currents of the isolated squid giant axon could recreate many of the axon's key electrical properties. This was the first mathematical model of an action potential, but it was of a neuronal action potential rather than a cardiac action potential. The original Hodgkin-Huxley model contained three ionic currents, an inward (depolarizing) sodium current, I_{Na}, an outward (repolarizing) potassium current, I_{K} and a small leakage current I_{l} that had chloride as well as other species of ions as its charge carrier. This model introduced their formulation for describing each ionic current.

In the Hodgkin-Huxley model, the cell membrane is treated as a capacitor in parallel with resistors that each represent an ionic current, and the total applied current through the membrane is then given by the equation:

$$I_{\text{tot}} = C_m \frac{dV_m}{dt} + I_{\text{ion}}, \tag{3.1}$$

Where I_{tot} is the total current applied to the membrane, C_m is the membrane's capacitance, V_m is the membrane potential, and I_{ion} is the sum of the currents due to ions flowing through the membrane, with inward currents (positive ions entering the cell) set as positive. We now describe the general structure of the equations that govern the I_{ion} term.

Each of the individual currents that make up the I_{ion} term are determined by calculating the product of three component terms: a conductance term, a term describing channel gating, and a term describing the electrochemical gradient(s) for the ionic species flowing through that channel.

The first term, the conductance term, is a constant. It is the maximal conductance value (the

current per unit potential different that would flow through all channels of that type if they were all open) for that ionic current, and can be thought of as the product of the maximum conductance that could flow through one ion channel of this type and the number of ion channels of that type that are embedded in the cell membrane. It is usually denoted with a capital G, the symbol for conductance, so for example the fast sodium current conductance would be G_{Na}.

The second term describes channel gating, and is the most complex part of modelling current flow through ion channels. For each ionic current there will be a set of equations governing the activation, deactivation, inactivation and recovery from inactivation of the gates for the ion channel type that carries that current. In the Hodgkin-Huxley formulation, these equations are expressed as a system of ordinary differential equations, averaging out the effects of stochastic channel kinetics and instead expressing the activation states of each channel as the mean probability for that given channel type. For example, if a channel contains three activation gates, with open probabilities m_1, m_2, m_3, and one inactivation gate with open probability h, then the open probability of the channel as a whole is $m_1 m_2 m_3 h$. If the 3 activation gates are modelled as being identical and independent of one another, so that the opening or closing of one gate does not alter the behaviour of the others, then the gating term could be simplified to $m^3 h$.

The value of each gating variable is governed by an ordinary differential equation of the form (using the m gate as an example):

$$\frac{dm}{dt} = m_{\text{inf}}(V_m) - \frac{m}{t_m(V_m)}, \tag{3.2}$$

where

$$m_{\text{inf}}(V_m) = \frac{a_m(V_m)}{a_m(V_m) + b_m(V_m)}, \tag{3.3}$$

and

$$t_m(V_m) = \frac{1}{a_m(V_m) + b_m(V_m)}. \tag{3.4}$$

Here, a_m and b_m are voltage-dependent transition rates from closed to open, and open to closed states respectively. Expressions for these rates are determined empirically by fitting to voltage clamp recordings of that current. The third term is the electrochemical driving force, which models the combined effects of diffusion and the electromagnetic force on ions moving across the cell membrane. It consists of the difference between the current membrane potential and the Nernst, or equilibrium potential. Diffusion acts to equalise concentrations of ions across the cell membrane, however if the cell membrane has a potential difference relative to its environment, ions such as sodium, potassium and calcium will be attracted into the cell when the membrane is negatively charged, and will be repelled when the membrane is positively charged. The Nernst potential is the membrane potential required, for the current intracellular and extracellular concentrations of a particular ion, to achieve a zero net flux of that ion through the membrane. It is given by the equation:

$$E_x = \frac{-RT}{zF} \ln(\frac{[x]_i}{[x]_e}), \tag{3.5}$$

where R is the gas constant, T is the temperature in Kelvin, z is the valency of the ion x (e.g. +1 for K^+, +2 for Ca^{2+}), F is the Faraday constant and $[x]_i$ and $[x]_e$ are the intracellular and extracellular concentrations of ion x, respectively. This term, as well as affecting the magnitude of the current, like the other two, also determines the direction current flows in. If V_m passes through the Nernst potential, current flow will reverse. Putting these terms together, using the example of the Hodgkin-Huxley model's sodium current, I_{Na}, (with three independent activation gates and one inactivation gate), we obtain the full sodium current equation:

$$I_{\text{Na}} = G_{\text{Na}} m^3 h (V_m - E_{\text{Na}}). \tag{3.6}$$

By repeating this process for all ionic currents that are to be modelled within a cellular electrophysiology model, and summing them, the I_{ion} term in equation 3.1 can be computed, and for an isolated cardiomyocyte the evolution of V_m over time can be computed by rearranging equation 3.1 and solving:

$$\frac{dV_m}{dt} = \frac{-1}{C_m} I_{\text{ion}}, \tag{3.7}$$

where I_{tot} has been set to 0 in the absence of any applied currents. When a stimulus current is applied to the cell, the equation becomes:

$$\frac{dV_m}{dt} = \frac{-1}{C_m}(I_{\text{ion}} - I_{\text{stim}}), \tag{3.8}$$

Solving the Hodgkin-Huxley model is therefore achieved by solving the system of ODEs corresponding to each of the gating variables (e.g. equation 3.2) and equation 3.8. For modern cardiac models, additional equations relating to intracellular ionic concentrations also need to be solved to track each ion entering and exiting the cell, and in more complex models, diffusing between cellular compartments.

3.2.2 History of cardiac cell models

Cardiac cellular electrophysiology models have, from the very beginning of the field, used the Hodgkin-Huxley formulation to describe the behaviour of ionic currents, although many models now also use the more general Markov model formulation to explicitly model transitions between different gating states. From the earliest models that were very closely based on the original three current Hodgkin-Huxley model, new models have increased in complexity, based on our growing understanding of cardiac cellular electrophysiology, e.g. the discovery of calcium channels. The additions made in each new model have usually been additions of new currents carrying ions such as calcium; adding new gating mechanisms for existing currents; sub-dividing a single current into multiple currents either because of different time scales for the parts of the current (e.g. the fast and late sodium currents), or because different ion channel proteins carry the different components (e.g. slow and rapid delayed-rectifier potassium currents). Also, for improving the modelling of intracellular ionic concentrations, there has been the addition of homeostasis mechanisms, including adding ion transporters (such as the sodium-potassium pump and the sodium-calcium exchanger), and adding additional cellular compartments, particularly the sarcoplasmic reticulum, for calcium handling. Finally, there

have been additions of biochemical mechanisms for signalling, ion channel modification or other purposes, e.g. modelling the action of the Ca^{2+}/calmodulin-dependent protein kinase II, CamKII (Livshitz and Rudy (2007), O'Hara et al. (2011), Heijman et al. (2014)).

To illustrate this process of gradually increasing complexity in both model structure and knowledge of the underlying biology, we will describe some of the most historically important cardiac cell, beginning with the 1960 FitzHugh model (Fitzhugh (1960)) and the 1962 Noble model (Noble (1962)). The FitzHugh model, while not a model of a cardiac cell, showed that the Hodgkin-Huxley model of the fast spiking neuronal action potential could be modified to generate the longer plateaued cardiac action potential. By altering the activation speed and peak conductance of the potassium current I_{K} the model produced action potentials with slow repolarisation and a long plateau phase. However the predicted energetic cost was far too large – too many ions passed across the membrane's electrochemical gradient with each action potential to be consistent with experiment.

The 1962 Noble model of Purkinje fibres built on the recent discovery of the inward-rectifier current (I_{K1}), which is almost fully closed while the cell membrane is depolarised (e.g. during the plateau phase of the action potential), to show that a model consisting of Hodgkin-Huxley formulated currents for I_{Na}, I_{K} and I_{K1} could explain all observed changes in current magnitude during each phase of the action potential. The model succeeded in this and showed that this combination of currents could also explain the energy saving mechanism used during the plateau phase that could not be explained with the FitzHugh model. However, it did not incorporate a slower inward calcium current as calcium channels had yet to be discovered. Instead the sodium current took the roles of both its initial excitatory inward role and the slower inward role of the calcium current.

The first model of a ventricular action potential (as opposed to a Purkinje fibre action potential) was reported by Beeler and Reuter (Beeler and Reuter (1977)). Using voltage clamp data from multicellular preparations, they constructed a system of equations using the Hodgkin-Huxley

formulation that described two inward currents: a sodium current I_{Na} and a slower inward calcium current I_S, which had at that point been discovered, and two outward potassium currents: I_{K1} which was time-independent and I_{X1} which was time-dependent. I_{X1} and I_S controlled repolarisation through time-dependent decrease of I_S and increase of I_{X1} during the plateau phase.

The next major advance in cardiac cellular modelling was the addition of ion exchangers and pumps that could manipulate the concentrations of sodium, potassium and calcium within the cell. These were essential to the study of several important disease states such as ischemia, that alter the expression of these transporters, and therefore alter the balance of ionic concentrations within the cell. To model the transporter mechanism of one ionic species required the addition of transporters for all the important species (usually calcium, sodium, and potassium) for a consistent model, particularly as two of the key transporters, the sodium-potassium pump and the sodium-calcium exchanger transported two species at once. Therefore there was a sudden step-change in the number of components needed in a modern cardiac cell model. The 1985 DiFrancesco-Noble model of Purkinje fibres (DiFrancesco and Noble (1985)) brought all of these processes together along with intracellular calcium release from the sarcoplasmic reticulum. This took modelling in cardiac electrophysiology beyond models of the action potential alone, by incorporating sub-cellular processes involved in generating the action potential and by relating electrical excitation to mechanical contraction through the activity of the calcium sub-system.

Over the last fifty years, not only have cardiac cell models increased in their complexity and ability to recreate and predict an increasingly diverse range of electrophysiological phenomena, but the availability of new experimental techniques have also increased the types of electrophysiological data that can be acquired. The first Luo-Rudy model (Luo and Rudy (1991)) was a reformulation of existing ventricular AP models to include up to date single-channel experimental results for the major ionic currents. Previous ventricular models such as the Beeler-Reuter

model predated patch clamping and single cell isolation techniques that allowed recordings from single myocytes as opposed to more complex tissue preparations. The model specifically updated I_{Na}, I_{K} and I_{K1}, and added a plateau potassium current I_{Kp}. As an example of the type of reformulation carried out, I_{Na} had its slow and fast inactivation gates supplemented by a reformulation of the fast activation process, which in the Beeler Reuter model had used the original formulation from the Hodgkin-Huxley model.

Following up on this model, the 1994 dynamic Luo-Rudy model Luo and Rudy (1994a,b) incorporated the same processes of ion regulation and concentration change that had been modelled in the DiFrancesco-Noble model and also incorporated more recent experimental findings. In particular, the L-type calcium current I_{CaL} was added to replace the slow inward current I_{Si} and both voltage and calcium gating mechanisms for I_{CaL} were included.

Today, there are over 40 published cardiac cell models held in the Physiome CellML cardiac cell model repository (http://www.cellml.org/) covering many different tissue types and species. Rather than trying to create an all-in-one model of electrophysiology, the emphasis in model development is now to develop or modify models to answer specific scientific problems, for example the ten Tusscher and Panfilov 2006 model ten Tusscher and Panfilov (2006) was developed from an earlier model specifically to investigate potential mechanistic causes of ventricular fibrillation in human tissue.

3.2.3 Contemporary cell models

The work described in this thesis focuses on modelling rabbit Purkinje fibres and human ventricular myocytes. Here, we review some of the most up-to-date models for each of these preparations.

Rabbit Purkinje cell models

Few mathematical models of rabbit Purkinje fibres exist in the literature. There are several re-

cent Purkinje models from other species available including the 2009 Aslanidi model (Aslanidi et al. (2009)) and the 2011 Pan-Rudy model (Li and Rudy (2011)) for canine. The only recent two rabbit Purkinje models are the 2010 Aslanidi model (Aslanidi et al. (2010)) and the 2011 Corrias-Giles-Rodriguez (CGR) model (Corrias et al. (2011)). Both contain descriptions of the standard known currents in rabbit Purkinje fibres and model intracellular calcium dynamics.

The Aslanidi rabbit model is part of a series of rabbit AP models covering Purkinje fibres and ventricular myocytes. These models were all developed by modifying an existing ventricular myocyte model by Shannon et al. (2004). The model was developed, along with the ventricular models, to study action potential heterogeneity at the junction between Purkinje fibres and ventricular tissue.

The CGR model (shown schematically in Figure 3.1) was developed and validated using results from the literature on isolated rabbit Purkinje fibres, when such data was available, and from the literature on Purkinje fibres from other species when not. The model was shown to be capable of producing pro-arrhythmic behaviour, such as early after-depolarisations (EADs), that was consistent with experiment under appropriate simulated conditions, and has been validated in single cell and 1D fibre simulations against results from the literature. We initially chose to use this model for the work presented in Chapter 4 due to its extensive validation, particularly in pro-arrhythmic conditions, and its development from the ground up as a specific rabbit Purkinje fibre model.

Human ventricular cell models

For modelling human ventricular cells, a number of potentially useful models have been developed in the last 10 years. These include the ten Tusscher and Panfilov 2004 and 2006 models (ten Tusscher et al. (2004); ten Tusscher and Panfilov (2006)), the Grandi model (Grandi et al. (2010)), the Carro model (Carro et al. (2011)) and the O'Hara-Virag-Varro-Rudy (ORd) model (O'Hara et al. (2011)). These are biophysically detailed models, in that biophysical processes

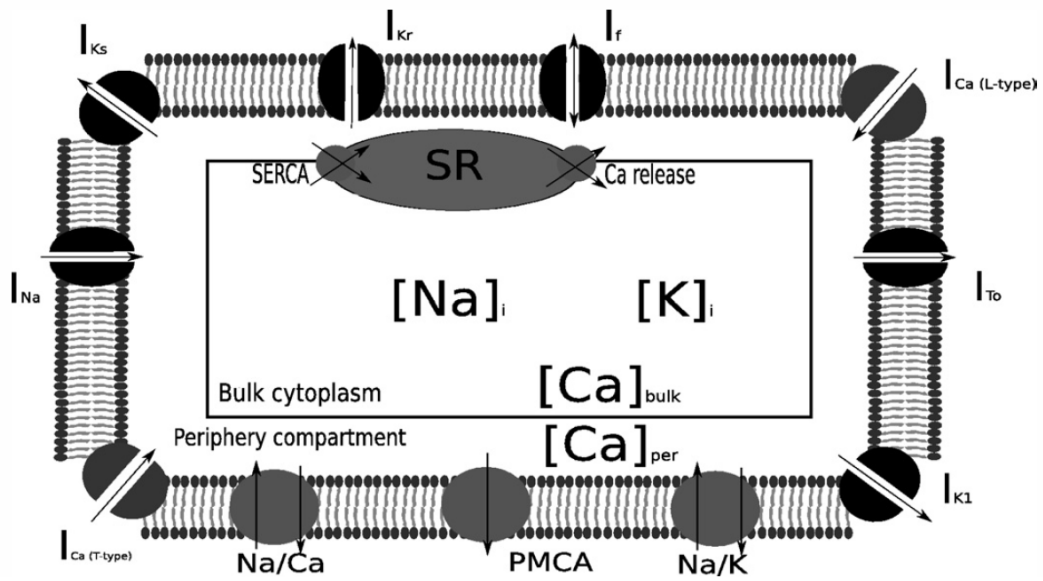

Figure 3.1: Schematic of the CGR model from Corrias et al. (2011) showing the ionic currents and intracellular compartments included in the model. The modelled currents are: I_{Na}, the sodium current; I_{CaL} and I_{CaT}, the L- and T-type calcium currents; I_{To}, the transient outward potassium current; I_{Kr} and I_{Ks}, the rapid and slow delayed rectifier potassium currents; I_{K1}, the inward rectifier potassium current; I_f, the funny current; I_{NaCa}, the sodium-calcium exchange current; I_{pmCa}, the calcium pump current and I_{NaK}, the sodium-potassium pump current. Intracellular ionic behaviour is represented by cytoplasmic concentrations of calcium, sodium and potassium as well as modelling of intracellular calcium dynamics through calcium uptake into the sarcoplasmic reticulum by SERCA, calcium induced calcium release from the sarcoplasmic reticulum and separate tracking and diffusion between the peripheral calcium concentration close to the cell membrane and the bulk cytoplasmic calcium concentration.

such as ion transport across the membrane by ion channels and intracellular calcium handling are described by equations that represent individual ionic currents and fluxes. Another type of modelling approach is the use of phenomenological models (e.g. Bueno-Orovio et al. (2008)), that reproduce the electrophysiological behaviour of cardiac cells without detailed modelling of the underlying biophysical processes. These models require fewer equations and parameters and are usually quicker to compute, making them particularly useful for tissue simulations. However, they are not suitable for connecting mechanisms at the level of individual ionic currents with whole cell electrophysiological behaviour, as these ionic mechanisms are not modelled explicitly.

Modern biophysically detailed human ventricular cell models generally share a number of bio-

physical components, including ionic currents and cellular compartments. Ionic currents that are usually included in human ventricular models are: I_{Na}, the sodium current, sometimes divided into fast and late components; I_{CaL}, the L-type calcium current; I_{to}, the transient outward potassium current; I_{Kr} and I_{Ks}, the rapid and slow delayed rectifier potassium currents; I_{K1}, the inward rectifier potassium current; I_{NaCa}, the sodium-calcium exchange current, and I_{NaK}, the sodium-potassium pump current. Usually these models contain at least three compartments. First is the bulk cytoplasm, encompassing the bulk of the cell and the majority of the cell membrane, where most ionic currents enter or exit the cell and where intracellular sodium, calcium and potassium ionic concentrations are modelled. Secondly, a cytoplasmic subspace representing the space near the T-tubules through which the L-type calcium current flows. Finally, there will be one or more compartments comprising the sarcoplasmic reticulum, with modelled uptake of calcium from the bulk cytoplasm by SERCA and release into the subspace compartment by calcium-induced calcium release through ryanodine receptors. Other currents, biochemical signalling processes and compartmentalisations exist, but whether these are included differ from model to model. The components described here are included in all of the biophysically detailed human ventricular cell models included in this review.

The ten Tusscher and Panfilov 2006 (TP06) model was developed from the previous 2004 human ventricular model by ten Tusscher et al. (2004), specifically to study alternans and wave breakup in the context of investigating the mechanisms that may cause ventricular fibrillation. The model was designed to be efficiently simulated in tissue. However, some aspects of the model have been shown to be non-physiological, particularly its predictions of intracellular calcium concentrations, and an exaggerated I_{Ks} current, probably due to a large value for the current's conductance.

The Grandi model was developed from a previous rabbit ventricular model by Shannon et al. (2004) to study adaptation and calcium transient behaviour in human ventricular myocytes, with the ionic currents refitted to human data to give species-specific behaviour. The model captures

rate-dependence in the effects of potassium channel block on action potential duration (APD). The model also predicts that intracellular sodium accumulation is the main mechanism of APD adaptation (the shortening of steady state APD following changes in pacing rate), due to the changes in I_{NaCa} and I_{NaK} it causes.

The Carro model adapted the Grandi model to study arrhythmias by reformulating I_{CaL} and I_{K1} along with changes of the conductances G_{Na} and G_{NaK}, based on data from humans. These changes were made due to the previous model's limitations with respect to recreating the dynamic response of the APD to changes in pacing rate and the S1S2 APD restitution curve. This is the curve formed by prematurely triggering an action potential at different diastolic intervals (the times between the repolarisation of one action potential and the triggering of the next) and plotting the diastolic interval against the resulting APD. Carro et al.'s adaptations to the Grandi model brought these behaviours in range with the literature and their model was able to predict pro-arrhythmic behaviour in single cell (alternans) and in tissue (conduction block in a 1D fibre) during hyperkalaemia (high extracellular potassium concentration), which can occur in ischemic hearts (hearts that have suffered damage due to lack of blood supply to a region of tissue).

The ORd model (Figure 3.2) was developed from human ventricular data obtained from experiments carried out by a single research group and focuses on capturing the steady state rate-dependence and restitution properties of human ventricular myocytes. Notably, equations governing the L-type calcium current have been reformulated. In addition to the two voltage-gated inactivation gates, that are also included in the Carro and TP06 models, a third, calcium-dependent inactivation gate was included, based on newly available data. Additionally, the model includes a late component to the sodium current, unlike the other models, which contributes to the dependence of APD on pacing rate and to APD restitution. Both the ORd and Carro models use a sensitivity analysis of the kind used in Romero et al. (2009) to study the relative importance of individual model parameters in determining different features of model

output.

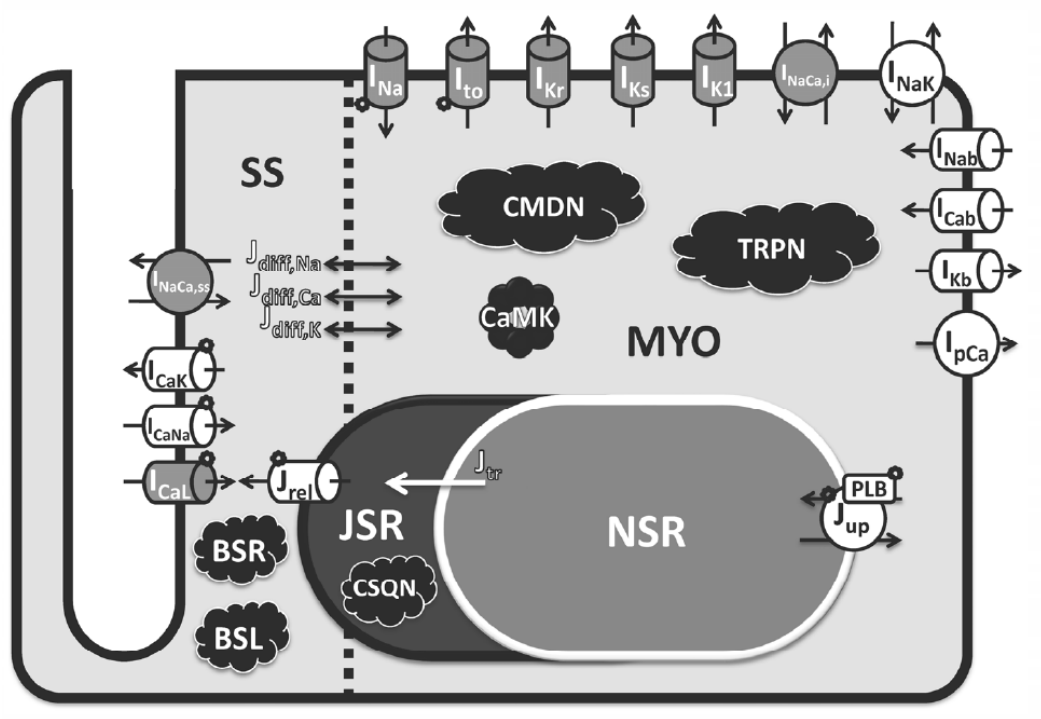

Figure 3.2: Schematic of the ORd model from O'Hara et al. (2011) showing the ionic currents and intracellular compartments included in the model. The model is divided into four compartments - two compartments for the cell itself, representing the bulk cytoplasm and the subspace near the T-tubules and two compartments for the sarcoplasmic reticulum (SR) - the junctional SR and the network SR. Currents that flow through the bulk cytoplasm in the model are: I_{Na}, the fast sodium current; I_{NaL}, the late sodium current; I_{to}, the transient outward potassium current; I_{Kr} and I_{Ks}, the rapid and slow delayed rectifier potassium currents; I_{K1}, the inward rectifier potassium current; I_{Nab}, I_{Cab} and I_{Kb}, the background currents; 80% of I_{NaCa}, the sodium-calcium exchange current; I_{pCa}, the sarcolemmal calcium pump current and I_{NaK}, the sodium-potassium pump current. Currents that flow through the T-tubule subspace area of the membrane are: I_{CaL}, the L-type calcium current and 20% of I_{NaCa}. Intracellular calcium dynamics are also modelled: calcium is taken up into the network SR by SERCA, diffuses into the junctional SR where it is released by ryanodine receptors and can diffuse between the bulk and subspace compartments. Diffusion of sodium, potassium and calcium ions between the bulk and subspace cytoplasm is also modelled.

3.3 Modelling approaches for variability in cardiac electrophysiology

As described in the previous chapter, there is substantial evidence suggesting that conductances of major ionic currents in cardiomyocytes can vary considerably between individuals. However, there appears to be little information in the literature or systematic studies of the magnitude or distribution of inter-subject variability, in conductances, or other properties of ionic currents, e.g. ion channel kinetics. Generally, variability in experimental data is averaged out by taking the mean over samples from multiple individuals and variability is then expressed as part of the error on mean values of measured quantities. Gaborit et al. (2007) performed a study quantifying differences in the expression patterns of a large number of genes encoding ion channel subunits across different regions of human tissue, and include the standard deviation of their results across their sample of 15 individuals. Many experimental papers (e.g. Szentadrassy et al. (2005); Jost et al. (1998)) provide standard deviations on the peak values of different measured ionic currents. However, these studies do not provide a direct way to estimate inter-subject variability in ionic current properties. This is because the distribution of the variation is not included and other sources of variation, such as measurement error and damage to cells during the isolation process, are combined.

In a traditional cardiac cell model, such as those described earlier in this review, any given set of simulated conditions yields a single set of model outputs. These are usually taken to represent the typical behaviour of a cardiac cell of the studied tissue type and species, as models are usually parameterised from mean values taken from experiments. Therefore, they cannot be used as they are for studies of inter-subject variability. In order to adapt these models to investigate variability, modellers have utilised two main methodologies to incorporate the effects of variability into an existing modelling framework, such as a system of ODEs with fixed parameter values. These methodologies are sensitivity analysis based methods, and population of models based methods.

Sensitivity analysis based methods are those where one or more parameters are varied around an existing parameter set (most often the original published parameter set for the model). The response of the model's output in terms of relevant electrophysiological quantities, such as action potential duration and amplitude, relative to the change in parameter values, is quantified to give a measure of the sensitivity of the model to changes in each parameter. In cardiac electrophysiology, most studies of variability have used this type of approach.

Romero et al. (2009) used the now common method of performing a single parameter sensitivity analysis to determine the impact of ionic variability within a model, in this case the TP06 human ventricular cell model described earlier in this chapter. They varied a set of conductances and time constants in the model, one at a time at $\pm 15\%$ and $\pm 30\%$ change from their original value. These values are based on the standard deviations of peak conductances that have been recorded from patch clamp experiments on ionic currents. They then quantified the change in important preclinical biomarkers of arrhythmic risk to determine the effects of variability and the mechanisms causing it, as well as to validate the model by comparing the range of each biomarker from the sensitivity analysis against published experimental ranges.

In a series of papers (Sobie (2009); Sarkar and Sobie (2010, 2011)) Sarkar and Sobie describe their method of performing multivariate regression analyses to investigate and quantify the effects of variability on cardiac cell models. In this approach multiple model parameters are varied at once to create an ensemble of models, which is then simulated. Rather than varying at fixed values, a log-normal distribution was used to generate parameter sets, centred on the original parameter set of the model being used. The log-normal distribution has a higher probability of selecting parameter values close to the centre of the distribution (the original parameter set) and the probability falls off rapidly at the ends of the sampled range, reducing the probability of sampling extreme values. The behaviour of models that used these different parameter sets was analysed using multivariate linear regression analysis, to create a linear model that could relate changes of parameter values (e.g. conductances) to changes of output (e.g. action potential

duration, peak upstroke velocity).

This method was applied in Sarkar and Sobie (2010) to test the hypothesis that cardiac model parameters, while not able to be constrained using the shape of the AP alone (multiple sets of parameters are capable of reproducing the same AP in control conditions), could be constrained by measuring a combination of AP and calcium transient biomarkers. By inverting the matrix of regression coefficients used to determine the sensitivity of each output to each parameter, the authors were also able to determine which of the tested outputs had the most influence in determining model parameters. By using these coefficients to determine the parameter set of the baseline model they used prior to parameter variation, they were able to predict the values of 12 of the 16 parameters considered in the study with good agreement with the baseline model values. The authors also showed they could accurately predict changes to 5 out of 7 parameters altered in the HRd model in Shannon et al. (2005), to create a model of heart failure in canine ventricular myocytes. Overall, this study demonstrates that if enough non-redundant outputs, that are sensitive to a broad range of different components of a cardiac cell model, are considered, a particular set of model outputs can highly constrain model parameters. The key requirement is that the model is required to produce outputs that closely match a specific set of values. This is a key difference between individual or experiment-specific modelling, where parameters can be highly constrained if enough outputs are considered because the model must match an exact target, and the population-specific modelling described later, where the range of allowed behaviours may allow a wide range of parameter values to be consistent with observed variability across the population.

The multivariate regression methodology was subsequently used in Sarkar and Sobie (2011), to quantify how variability influenced drug-induced APD prolongation when IKr was blocked. Multiple different ventricular cell models were used to build and rank a consensus list of parameters that were important for determining repolarisation reserve, considering conductance parameters, ion channel time constants and voltage dependencies. The study found that APD

in control conditions did not correlate with APD prolongation following IKr block. Therefore, APD prior to drug application was not predictive of whether prolongation following drug block would be pro-arrhythmic, or not. This study indicates a role for computational modelling in determining drug effects in cardiomyocytes. Models allow easy access to underlying parameters, such as ionic conductances, something that is difficult to achieve with current experimental techniques, and so can be used to identify possible mechanisms for the changes seen experimentally at the action potential level.

Walmsley et al. (2013) also used the multivariate regression approach to construct and analyse two populations, of failing and non-failing human ventricular cardiomyocytes. The non-failing population was constructed by sampling from uniform distributions of conductances varying $\pm 30\%$ from the baseline ORd model, while the failing population used mRNA expression data to alter these distributions by upregulating (sample from 0% - +60% of baseline) or downregulate (-60% - 0% of baseline) conductances that showed expression differences in failing compared to non-failing mRNA data. Two of the main findings of this study were that the mRNA changes were sufficient to recreate the reported effects of heart failure on action potential and calcium transient properties, and that alternans behaviour in the failing population was due to low G_{Kr} values, while in the non-failing population it was due to low SERCA conductance, and high G_{CaL}.

The second methodology that has been used for modelling inter-subject variability is the population of models methodology. The version of this methodology that is used in this thesis is described in more detail in Chapter 4 but we summarise it here. To create a population of models, a subset of the parameters in the model are selected to be varied based on which parameters are known or hypothesised to vary significantly between individuals. Many parameter sets are generated using a random sampling method (such as Latin Hypercube Sampling, described later) to vary the chosen parameters. These parameter sets are then inserted into an existing model to create an initial large pool of candidate models with the same underlying equations

but with selected parameters varying widely from model to model. The output of these models is then simulated and compared to the distribution of results seen in experimental data. From here, only candidate models that have produced outputs that are entirely within the bounds of variation seen in available experimental data are accepted into the population, and models that are not consistent with experimental data are discarded. This calibration step is the main difference between this method and the methods employed by Romero *et al.*, and Sarkar and Sobie. The properties of the ensemble of models that make up the population can then be investigated using a variety of methods.

We have developed and used this population of models approach in this thesis to model inter-subject variability. Population based studies have previously been used in the field of neuroscience, particularly by Marder, Prinz and others (Prinz et al. (2003, 2004); Taylor et al. (2009); Marder and Taylor (2011)). Marder *et al.* constructed databases of neuronal models that had been selected from a large number of models with randomly generated parameters based on their ability to produce simulated electrophysiological properties that were within 2 standard deviations of the mean of those properties for experiments carried out on real neurons. They were able to search this database to find neuron models that best represented given real neuronal profiles and have used their approach to show that identical profiles can be produced by highly varied sets of ion channel conductances.

Recently, other cardiac modelling studies have used the population of models approach to incorporate experimentally observed variability. In Sanchez et al. (2014) a similar methodology to the our methodology described in Chapters 4 and 6 was used to investigate atrial fibrillation in humans, by developing populations of models that mimicked the variability seen recordings of isolated human atrial cardiomyocytes from patients who displayed either a) sinus rhythm (SR) or b) chronic atrial fibrillation (cAF). Three different atrial models were used, and for each a sinus rhythm and a cAF population was constructed. The populations were largely successful in mimicking observed variability with relatively small ($\pm$30%) variation of baseline model con-

ductances, although the different models each had different aspects of AP variability that they were better at capturing than the others. The differences in conductance properties found between SR and cAF populations was found to be in agreement with remodelling of ionic currents observed in experimental studies.

In Dangerfield et al. (2015), under review, the population of models approach is combined with modelling stochastic beat-to-beat variability in canine cardiomyocytes, to investigate how inter-subject variability in ionic conductances modulates biomarkers of beat-to-beat variability. The magnitude of this beat-to-beat variability has been shown to be itself an indicator of pro-arrhythmic risk. The goal of the study was to better understand how stochasticity in individual currents contributes to the total beat-to-beat variability in a cell, while also incorporating inter-subject variability in current conductances.

These studies indicate some of the different ways populations of models can be used to address research questions while incorporating experiment variability, with the exact methodology used being dependent on the question being asked and the experimental data that is available.

3.4 Methods for parameter sampling

In order to capture variability in a population of models, we need an initial sample of randomly generated parameter sets, which are used to generate a pool of candidate models for a population. Therefore, we need to use a random sampling method to generate this initial sample. There are many different methods for sampling parameter spaces, of which some have been used in previous studies of variability. These methods generally fall into two categories: parameter sweeping schemes that sample systematically at fixed points of the parameter space, and Monte Carlo methods that sample using statistical methods, by selecting parameter sets randomly from probability distributions over the parameters that are being varied.

Parameter sweeping schemes include the local sampling performed by Romero et al. (2009), and

also form part of the method of fractional factorial design (Peachey et al. (2008)), which is used to sweep wide ranges of parameter space. In this method parameters are sampled at set values, either by varying them from an original starting point or by effectively laying a grid of points on to a region of parameter space and sampling systematically at each point. In fractional factorial design only a subset of the total number of points are sampled, in full factorial design all points are sampled. These parameter sweeps are used either in experiments or in simulation studies to find the effects of varying parameters. The main drawback of the method is that the number of samples that are made increases exponentially as the number of parameters is increased and as the resolution of the grid increases, which makes parameter sweeps most useful for cases where only a small number of parameters need to be varied over a small number of values.

Monte Carlo methods encompass any sampling method that samples from a probability distribution function in order to generate parameter sets. This includes the method of sampling performed by Sobie *et al.* (Sobie (2009)) where a log-normal distribution centred around the original parameter set of the model is used. In this case samples are selected randomly from the distribution to create as many parameter sets as are required. The distribution can be varied to alter the sampled space and include information from experiments on the distribution of parameter values, if available, or set as a uniform distribution over a biologically plausible range if no such information is available.

Another Monte Carlo sampling method that can be used to generate parameter sets is Latin hypercube sampling (LHS) (McKay et al. (1979)). In this method the range of values to be sampled for each parameter is partitioned into N regions (N is defined by the user) and N samples are taken such that for each parameter each region has been sampled once and only once. For example, for a 2-dimensional space with both parameters divided into N equally sized regions, a Latin Hypercube Sample would take samples so that each of the N rows and columns created by the partition had one sample taken from them. This sampling method has the advantage of sampling each parameter evenly (unlike standard Monte Carlo sampling) and allows

sampling across a potentially wide range for each parameter. This means that good coverage is always ensured on each individual parameter, to a given resolution. However, the parameter space is not completely characterised as only a subset of possible combinations of parameter values are sampled. In exchange for this, the number of samples needed for a Latin Hypercube Sample is independent of the number of parameters sampled, and therefore including a parameter that has no effect on model output does not incur a computational cost. This makes it a useful method for sampling high-dimensional parameter spaces where the relative importance of each parameter in determining system output are not yet known, and where complete characterisation of the parameter space is not required. It is for these reasons we use LHS to generate the parameter samples for the populations of models-based studies presented in Chapter 6 and Chapter 8.

3.5 Simulating the behaviour of cardiomyocytes using cardiac cell models

For the development of the populations of models described in this thesis, the behaviour of thousands of cardiac cell models must be simulated. Following the creation of the population, each additional simulation on the population will usually require hundreds of simulations to be performed. It is therefore important that the solvers we use to solve the system of ODEs that make up each cardiac cell model are as efficient and reliable as possible. This section describes the problem of solving cardiac cell models and the solver we use in this thesis, (CVODE), and why we use it.

Simulation requirements and pitfalls

To perform the simulations required to develop and analyse a population of models, it is important that cardiac cell models are able to be solved efficiently. Performing the calibration process typically requires simulating thousands of different cell models, each for thousands of pacing

cycles. Due to the nature of an action potential, with its rapid upstroke, solving the system of ordinary differential equations (ODEs) that makes up a cardiac cell model is a stiff problem - the timescales over which the system evolves during the upstroke are much shorter than the plateau and repolarisation phases of the action potential. Therefore, an ODE solver with a fixed time step is not appropriate for solving cardiac cell models - it will either lose accuracy on the upstroke, or behave inefficiently during repolarisation. Solvers with adaptive time steps, that can update the time step during the simulation to match the timescale of the current stage of the simulation, have been found to be ideal for solving cardiac models. In this thesis, the CVODE adaptive ODE solver has been used for all simulations, and it is described in the next section.

An additional pitfall in cardiac simulations is the discontinuous nature of the stimulus current in most cardiac models. Usually the stimulus current is controlled using an *if* statement that switches it on at the beginning of each pacing cycle in the simulation. This gives the stimulus current the appearance of a step function. As the stimulus duration is usually short compared to the pacing cycle length (typical stimulus durations are 0.5 ms up to 2 ms), if the simulation is ran continuously with an adaptive solver, the timestep will usually be long at the end of one pacing cycle, as the cell will usually have fully repolarised, so if the simulation continues running it is possible for the stimulus to be completely skipped during the next timestep. Therefore, it is important to stop and restart the solver at the beginning of each pacing cycle, to make sure the stimulus current fires every cycle.

Solving a cardiac cell model using the CVODE adaptive solver

One solution to solving a stiff set of ODEs such as a cardiac cell model is to use an adaptive timestep solver, so that the solver timestep can be automatically varied as needed throughout the simulation. For this reason, we use the open-source CVODE library, which are part of the larger SUNDIALS library (Hindmarsh et al. (2005)), and is implemented within the CHASTE open-source computational biology software package (Pitt-Francis et al. (2009)). CVODE is an adaptive timestep solver, which has been extensively developed and tested. Additionally, in a

recent benchmarking test, CVODE was identified as the best of the ODE solvers implemented within CHASTE for simulations of individual cardiac cells (Cooper et al. (2014)).

Dealing with uncertain initial conditions

Normal cardiac cell models are usually supplied with a set of initial conditions. These represent the conditions once the model's behaviour has been simulated for a long enough time for the model to enter a steady cycle of repeated pacing. As each model we are simulating for a population of models has different parameter values from the others, these supplied initial conditions will not represent a steady state for them. Therefore, we simulate, first of all, a relatively long period of quiescence for each model (no stimulus current applied), as this is computationally cheap and allows state variables in each model to relax towards a steady state. We then allow a significant amount of simulation time for the actual simulation protocol (in this thesis, in all simulations models underwent 1000 seconds of simulated quiescence followed by 1000 seconds of simulated pacing), again to allow models to reach a steady state. Further work could be done to automate this search for a steady state, e.g. by tracking differences in state variables between subsequent beats. This would be particularly useful if larger populations needed to be used and computational cost became a more important issue than it is now.

3.6 Biomarkers for quantifying cardiac model output

The choice of biomarkers used to determine which models are consistent with experiments has a large effect on the characteristics of an experimentally-calibrated population of models. We will describe the standard biomarkers of the cardiac AP that we use in later chapters, followed by a discussion of additional less generally applicable biomarkers that we have also used in later chapters to quantify particular features of certain AP types. These biomarkers are also represented in Figure 3.3.

The standard biomarkers of the cardiac AP that are used in throughout this thesis are:

Peak membrane potential (Vm Peak) - The peak value of the membrane potential following stimulus.

Maximum upstroke velocity (dVm/dt Max) - The maximum value of the change in membrane potential with respect to time during the upstroke of an AP. This biomarker can be used as a cell-level indicator of conduction velocity in tissue. Low upstroke velocities correspond to lower conduction velocities, and vice versa.

Action potential duration at xx% of repolarisation (APDxx) - The first point since the stimulus where membrane voltage reaches xx% of full repolarisation, measured from the peak membrane voltage to the resting membrane potential. In this thesis we used APD40, APD50, and APD90. APD90 is the most commonly used biomarker of the cardiac AP, as it provides a measure of the length of the refractory period before a new AP can fire, and because both particularly long and particularly short values of APD90, and its ECG level equivalent, the QT interval, have been shown to be predictors of pro-arrhythmic drug effects.

Triangulation (Tri xx- yy) - The difference between APDxx and APDyy. Tri 90-40 is a commonly used measure of triangulation, and describes whether the action potential is more triangular (short plateau relative to total APD90, therefore a large value of Tri 90-40), or more square (long plateau, therefore short Tri 90-40).

Resting Membrane Potential (RMP) - The steady value of the membrane potential when the cell is fully repolarised and quiescent.

We have also developed three additional biomarkers to measure other properties of the cardiac AP. These are:

Peak membrane time (Vm Time) - In the case where a cell has a very low sodium current conductance, inward calcium currents can eventually generate an upstroke in response to a stimulus current, although much more slowly than the sodium current can normally. To measure this, and exclude this behaviour from our populations when it is not observed in the data sets

being used, we use VmTime to measure the duration from initial stimulus to the peak of the upstroke.

Dome peak - Certain species and tissue types display a spike and dome configuration of AP (a characteristic example of this AP type is the rabbit Purkinje AP shown previously in Figure 2.3), where following the rapid partial repolarisation in phase 1, there is a second, smaller and slower depolarising upstroke, generally attributed to the changing balance between inward sodium and L-type calcium currents, and the transient outward potassium current Ito. To quantify this dome, we developed a biomarker called dome peak that measures firstly, whether the AP has a secondary dome, and if it does the peak membrane potential of that dome.

Plateau duration - The existence of a spike and dome can make calculating intermediate values of APD, such as APD40 or APD50, more difficult for certain cell types, as the membrane potential may cross the threshold of repolarisation both before and after the dome. Therefore, to measure the duration of the plateau prior to repolarisation, we developed the plateau duration biomarker, which measures the duration from the beginning of the AP to the point during the plateau at which dVm/dt falls below a user-defined negative value (excluding the depolarisation during phase 1, directly after the upstroke). It is intended as a rough measure of when repolarising potassium currents begin to dominate the inward currents that sustain the AP plateau.

3.7 Methods for model analysis

Many methods exist for analysing relationships between model inputs (such as parameter values) and model outputs (such as biomarkers of action potential behaviour, e.g. action potential duration or peak membrane potential). These methods are used for models where the exact mapping between input and output is unknown and cannot be found using analytical methods. This is the case for cardiac cell models due to their nonlinearity and complexity. Here, we review the use of two varieties of methods that have been used in the studies of variability described

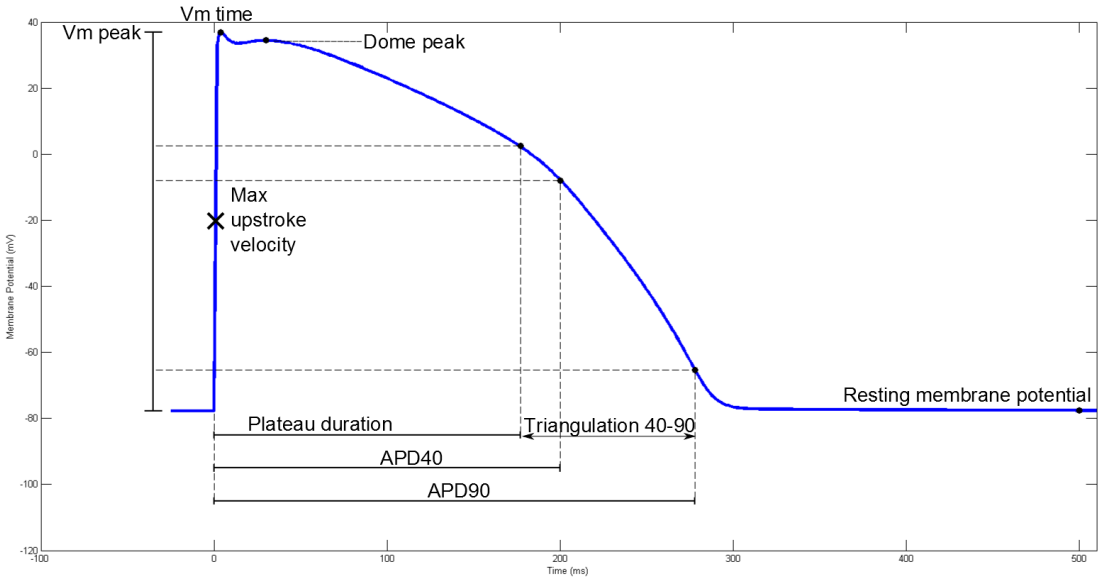

Figure 3.3: Representation of each of the biomarkers used in this thesis to analyse the action potential.

previously: sensitivity analysis and regression analysis.

The aim of a sensitivity analysis is to quantify how changes in key parameter values alter model output. In a local sensitivity analysis, e.g. the kind performed in Corrias et al. (2011); Romero et al. (2009), parameters are varied one at a time and the sensitivity of model outputs to each parameter are measured by the fractional change of that output relative to its original value. The most sensitive parameters in a model are those that cause a larger fractional change in output for a given fractional change in parameter value. Sensitivity is calculated using the formula:

$$S_{ij} = \frac{O_{i+} - O_{i-}}{P_{j+} - P_{j-}}, \tag{3.9}$$

where S_{ij} is the sensitivity of an output i to variation in parameter j, $O_{i+/-}$ are the values of the output i when the parameter j is increased (+) or decreased (-) and $P_{j+/-}$ are the fraction the parameter was altered by for that simulation (for $\pm 30\%$ variation these would be 1.3 and 0.7). To allow comparison between sensitivities of different outputs, each sensitivity value is

then normalised by dividing by the largest absolute sensitivity value for that output, so that each sensitivity is dimensionless and scaled between -1 and +1.

Regression analyses are a general class of techniques used to find correlations in mathematical models between the inputs (e.g. parameter sets for cardiac cell models) and outputs (e.g. biomarkers calculated from simulating models using each parameter set). Linear regression techniques have been used to analyse the outputs of cardiac cell models that have had their parameter sets generated using a Monte Carlo sampling process to vary many parameters at once (e.g. Sarkar and Sobie (2010)). In these cases regression analysis has been used to identify linear correlations between an output of the model and one or more input parameters by finding the linear model of the following form:

$$y = a + \sum_{i=1}^{n} c_i p_i, \tag{3.10}$$

where y is a model output, a and c_1 to c_n are constants that are determined by the regression process and p_1 to p_n are the chosen input parameters. A correlation coefficient (often referred to as R^2) describes how well a given linear regression model fits the variation in outputs to variation in inputs. For biological models where outputs often depend nonlinearly on inputs, regression models other than the linear model may be useful. Although cardiac models are nonlinear, the relationships between parameter values and outputs of cardiac models are often approximately linear across a wide range of physiological parameter values, due in part to the negative feedback present in the voltage dependency of most ionic currents (e.g. the sodium current, when activated, depolarises the cell membrane, inactivating itself), which prevents runaway positive feedback.

A review by Marino et al. (2008) discusses other measures of correlation in the literature and their potential uses. Of particular interest for our purposes are the partial rank correlation coefficient (PRCC) and partial rank correlation coefficient (PCC), which the review identifies as

particularly good measures for capturing monotonic relationships between outputs and inputs, and the eFast method which is identified as a good measure if trends are both nonlinear and non-monotonic.

The PRCC is a measure of the correlation between rank-transformed parameter sets and rank-transformed output values after the linear effects of the remaining parameters on the output have been discounted. Rank-transforming is the process of mapping a series of n values, x_i where $i = 1$ to n onto the series of numbers 1 to n, where the 1 is given to the x_i with the lowest value, the 2 to the x_i with the second lowest value, etc. PRCC is identified by Marino *et al.* as a "robust sensitivity measure for nonlinear relationships between [inputs and output] as long as little to no correlation exists between the inputs". This makes it a potentially useful correlation measure for our purposes, based on the sampling nature of LHS.

To determine correlations between the properties of individual ionic currents and properties of the whole action potential, we use the PCC method in this thesis. We chose to use partial correlation over other correlation measures because partial correlation controls for the effects of one or more additional variables when looking for correlations between two quantities, which is important given that our models are generated by varying multiple parameters simultaneously. We also evaluated the PRCC method, however the results obtained with both methods have been similar, and therefore we chose to use the simpler method (PCC). Partial correlation is a method to find correlations between two variables, after accounting for the linear effects of one or more additional variables (Marino et al., 2008). The PCC between variables x and y, given the set of N additional variables z_i , is found by first calculating linear regression models of x and y against z_i :

$$\hat{x} = c_0 + \sum_{i=1}^{N} c_i z_i \text{ and } \hat{y} = b_0 + \sum_{i=1}^{N} b_i z_i. \tag{3.11}$$

The partial correlation coefficient between x and y is then defined as the correlation coefficient

between the residuals $r_x = x - \hat{x}$ and $y_x = y - \hat{y}$:

$$PCC(x, y, z_i) = \frac{\text{Cov}(r_x, r_y)}{\text{Var}(r_x)\text{Var}(r_y)}. \tag{3.12}$$

The extended Fourier amplitude sensitivity test (eFast) (Saltelli et al. (1999)) is a method for determining what fraction of variance in model output is due to each of the varied inputs. The method requires generation of a series of parameter sets that vary each parameter throughout the series at a different frequency. The propagation of these different frequencies into the output can be quantified using Fourier analysis techniques. This then allows the relative importance of each parameter in determining model output to be quantified. The eFast method has the advantages of being able to quantify higher order sensitivities (such as the sensitivity of outputs to input parameters raised to higher powers and products of the different inputs) and to be able to detect non-monotonic correlations. However, eFast requires parameter sets to be generated using its own methods to ensure that across parameter sets each parameter is varied at a different specific frequency, which may be incompatible with our existing methods for parameter set generation. This is because the process we use to generate parameter sets includes a stage where parameter sets that produce model output that is inconsistent with experimental data are discarded. In the eFast method it is assumed that all parameter sets in the sampled range will give valid model behaviour.

3.8 Modelling drug-ion channel interactions

Modelling drug-ion channel interactions is an important part of cardiac modelling, as the prediction of drug effects on the action potential is an important potential application for cardiac modelling. Many different models of the effects of drug binding to ion channels exist with varying levels of complexity. For our purposes, we use the single-pore block model of drug activity described in detail in Brennan et al. (2009).

The single-pore model

The single-pore model of drug block is one of the simpler models of drug block, but this is also one of its advantages. As it is simpler, it requires less data to parameterise the model for a given drug than more complication formulations, such as Markov models. The single-pore model describes the fraction of an ionic current that is blocked, B, as a function of the drug's concentration, $[C]$. The function takes the form of a Hill function, which when plotted appears as a sigmoidal curve (Figure 3.4 gives an example of this using data from application of dofetilide). To parameterise the model for a specific drug and specific ionic current, only two parameters are needed. The first is the IC50 of the drug, which is the concentration at which the drug blocks 50% of the ionic current. The second is the Hill coefficient, h, which is a measure of the cooperativity of drug binding. This term defines how much the binding of other molecules of the same drug help other molecules of the drug bind to the same channel. The larger the Hill coefficient, the closer the Hill function resembles a step function, rather than a smooth curve.

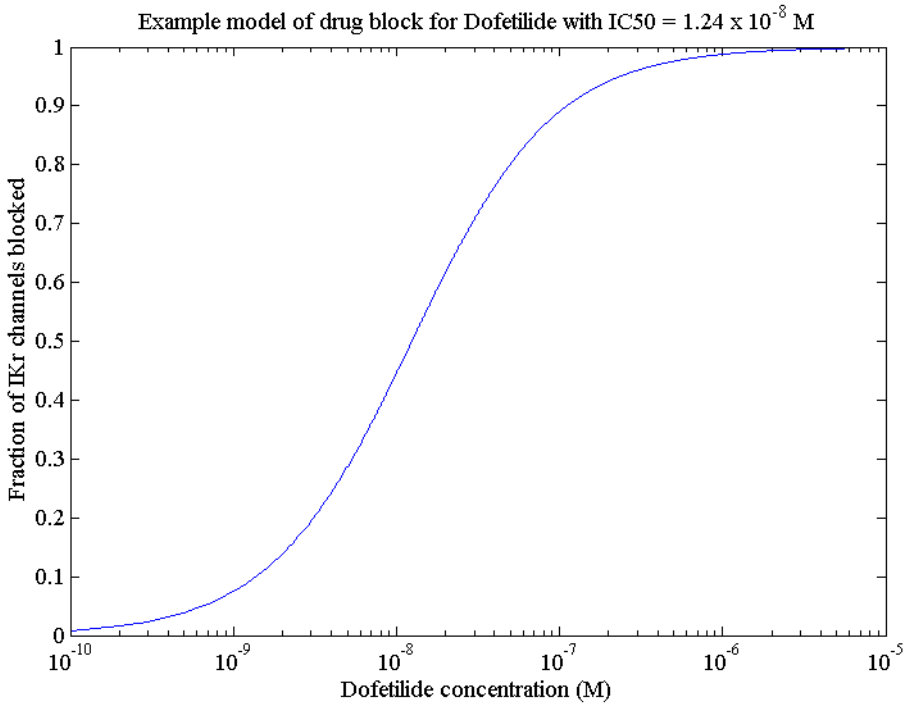

Figure 3.4: Concentration-response curve for dofetilide's effect on IKr in rabbit Purkinje cells, using the single pore drug block model. The model parameters are IC50 = 0.0124 , h = 1.

With these parameters estimated from data of the drug's activity at multiple concentrations, the equation for the single pore model is then:

$$B = 1 - \frac{1}{1 + (\frac{[C]}{IC50})^h}. \tag{3.13}$$

3.9 Conclusions

In this chapter, we have reviewed the Hodgkin-Huxley formulation for modelling ionic currents, upon which most cardiac cell models are constructed, important historical cardiac models, and recent current models of importance for this thesis. We then turned to the main topic of this thesis, inter-subject variability in cardiac cellular electrophysiology, and described different methods that have been used to model it, as well as of the recent studies that have used these methods, to show the variety of research questions that can be addressed when biological variability is incorporated into cardiac modelling.

In Chapter 4, the first results chapter of this thesis, we present a study into the mechanisms of delayed after-depolarisations (DADs) in rabbit Purkinje fibres. These DADs can be pro-arrhythmic and are believed to occur due to spontaneous emission of calcium from the sarcoplasmic reticulum. In this study, we develop a hybrid model from an existing rabbit Purkinje cell model and the more detailed calcium sub-system of a second model, to create a model that could be used to investigate DAD generation through the calcium sub-system. The results of this study motivate our interest in inter-subject variability, as we find that the models we use cannot capture the full range of observed variability across a variety of biomarkers in rabbit Purkinje fibres, following a standard sensitivity analysis of individual parameters.

4

Modelling the mechanisms underlying delayed after-depolarisations in rabbit Purkinje cells

4.1 Introduction

In the previous chapter we reviewed the history and recent literature for cardiac cell models relevant to this thesis, and also reviewed previously developed methods that are important for modelling inter-subject variability, such as parameter sampling and correlation detection techniques.

In this chapter we describe the development and validation of a model of a rabbit Purkinje cell that can be used to simulate delayed after-depolarisations (DADs) using experimentally verified protocols. We demonstrate the model can generate DADs by simulating existing experimental protocols and we attempt to validate the model using both previously published simulation data and experimental data from rabbit Purkinje fibres obtained from our collaborators. This validation reveals that the range of variability seen across our experimental data is too wide to be captured with the standard cardiac cell models we use in this chapter, which motivates the development of the experimentally-calibrated population of models methodology used in later chapters.

4.1.1 Delayed after-depolarisation formation in Purkinje fibres due to calcium loading

The natural excitability of cardiomyocytes allows them to regenerate and sustain the electrical signals that drive the heart. However, cardiomyocytes cannot distinguish between a signal that originated from the sinoatrial node or another source of depolarization, such as an increased ionic current or an external electric shock. When the heart is beating normally, such signals can prematurely or incompletely depolarize the heart, disrupting its natural rhythm. This can cause the heart to enter an arrhythmic state where cardiac muscle tissue contracts and relaxes in a chaotic and ineffective way. The heart's ability to pump blood can be severely reduced, which can lead to cardiac arrest and death if a normal rhythm is not restored. A common and often effective treatment for life-threatening arrhythmia is defibrillation. A strong electric shock is passed through the body to rapidly polarize the entire heart. Ideally, this resets the cardiac tissue to a state that can resume normal beating at the next signal from the pacemaker.

However, what appears to be a successful defibrillation that stops the cardiac arrhythmia in the patient is often followed by post-shock refibrillation, where the heart spontaneously re-enters an arrhythmic state (van Alem et al. (2003)). The mechanisms that induce a post-shock arrhythmia are not fully understood. However, Maruyama et al. (2010) investigated the mechanisms of post-shock arrhythmia in excised rabbit hearts following simulated ventricular tachycardia, an arrhythmic condition where the heart beats regularly but abnormally fast. They found that following the cessation of the tachycardia by means of a defibrillation shock, the hearts could, in certain conditions, spontaneously depolarize from their resting potential following the end of stimulation. These DADs would in some circumstances trigger a new action potential outside of the heart's normal rhythm, which in a living organism could return the heart to an arrhythmic state.

Their investigations linked post-shock arrhythmia with a known mechanism (Bers (2002)) for the generation of DADs: spontaneous emission of calcium from the sarcoplasmic reticulum

(SR). Calcium loading - an increase in intracellular calcium concentration - has been shown to occur during tachycardia (Maruyama et al. (2010)) and if sufficiently raised could cause further calcium to be spontaneously released from the SR when the tachycardia ceased as SR calcium release channels are calcium activated. When released into the bulk of the cell the calcium would then be free to be exchanged out of the cell by sodium-calcium exchanger channels, which exchange three sodium ions (total charge +3e, where e is the elementary charge) inwards for one calcium ion (total charge +2e) outwards creating a net positive inward current. This will depolarize the cell and if the magnitude of the depolarization is sufficient can trigger an action potential. As well as a mechanism, Maruyama et al. found evidence to suggest that Purkinje fibres were particularly susceptible to DADs and could be the tissue type responsible for triggering further arrhythmic activity in the rest of the heart.

The aim of this chapter is to use computational modelling to investigate the mechanisms that cause DADs to occur in rabbit Purkinje fibres, building on the findings of Maruyama et al. The mathematical modelling of cardiac electrophysiology is a mature field and there are large bodies of work for both single cell and tissue modelling that we could draw on to begin our investigations. However there are also a wide variety of different species and tissue types that have been studied, which reduced the amount of previous work that was applicable to modelling DADs in rabbit Purkinje cells. Therefore, the first step in this study was to identify a suitable model of a rabbit Purkinje cell, that was also suitable for studying DADs.

4.2 Methods

To model single Purkinje cells we used an ODE based compartment modelling approach. The cell is considered to be a collection of multiple discrete compartments that can be connected to each other and an external medium by ion channels through otherwise impermeable membranes. The model describes how ions flow between the compartments and between the outer compartment(s) of the cell and the extracellular medium. These currents can be used to compute

the resulting changes in the cell's membrane potential and its internal ionic concentrations. The external medium is assumed to have fixed ionic concentrations. External voltage is set constant but can be altered during a simulation to simulate an external stimulus, such as normal pacing of the heart or a defibrillation shock. For each compartment each ionic concentration can change over time as ions enter and leave, but within a compartment the concentration of each species is uniform, the only spatial factors considered in the model are in the choice of compartments used and the specification of the volumes of each compartment.

This compartment based approach allows us to model important effects of the cell's internal organization, such as the use of the sarcoplasmic reticulum to store calcium and the inability of ions to leave or enter the cell except through the cell's periphery, without using a full continuous spatial model that would be difficult to validate against existing data and would be too computationally expensive to use in more complex multi-cellular simulations.

The states of individual ion channels (e.g. active/inactive) in the model are also abstracted, and averaged over all ion channels of that type, by using the Hodgkin-Huxley formulation of ion channel behaviour which was previously described in Chapter 3.

For the model to accurately simulate a Purkinje cell, appropriate model equations and parameter values must be determined to describe the behaviour of each ion channel type, as well as for whole cell properties such as the membrane potential. Ideally channel properties are determined from experimental data on a channel-by-channel basis by fitting to experimental data, such as voltage clamp recordings (as described in Chapter 2), for each particular type of ion channel from the species in question. In practice such data is not usually available for every ion channel used in a reasonably complex model even for the most commonly modelled organisms, so other methods such as taking data from the equivalent channels in other species or fitting to less specific biomarkers such as the action potential shape or duration are commonly used to fill in unknown parameters.

For this study we began by using an existing rabbit Purkinje cell model by Corrias et al. (2011), the Corrias-Giles-Rodriguez (CGR) model. This recently developed model uses three compartments to model the cell, one for the bulk interior of the cytoplasm, one for the peripheral region of the cell that is in contact with the cell membrane ion channels and one for the sarcoplasmic reticulum. The ionic concentrations and ion channel currents are determined by a system of twenty two ODEs. All of the experimental data available in the current literature on rabbit Purkinje cells was used to determine the model's parameter values, and validate the model using a combination of a sensitivity analysis and comparison to experimental action potential recordings, taken from both normal physiological conditions and after a variety of drug interventions.

We initially chose to use this model because it was a well verified model that was less complex than others available, particularly in the number of compartments used, and it had been shown that the model could generate early after-depolarizations (EADs), which are similar conceptually to DADs but occur during the plateau phase of the action potential, while the membrane voltage is still repolarizing. The model had not, however, been shown to be able to generate DADs, but we were not able to find any rabbit Purkinje model in the literature that had already been demonstrated to display DADs.

After implementing the model in Matlab we tried to generate DADs using the same protocol as used by Maruyama et al. Their protocol calls for fifteen minutes of constant pacing at a given pacing cycle length (usually between 300 ms and 1000 ms) then a cessation of pacing. If DADs are generated the first DAD is expected to occur within approximately ten seconds of the end of pacing. Under physiological conditions and also increased calcium load conditions (increased extracellular calcium concentration) we were not able to get the model to produce DADs by trial and error experimentation.

Fink et al. (2011) have demonstrated empirically that there is a link between whether a cardiac cell model can produce DADs and whether the calcium subsystem of that model, defined as

a reduction of the model to just the equations dealing with intracellular calcium flux plus the equations describing the sodium-calcium exchanger channel, can demonstrate sustained steady-state oscillations. Using this result we could reduce the problem of determining whether the full model could demonstrate DADs to a problem of determining whether a much simpler subsystem could display oscillations. A common tool in analysing dynamical systems for particular types of steady state behaviour, such as oscillation, is bifurcation analysis. This is a computational method of steadily changing a parameter value or variable in a dynamical system and mapping the steady state(s) that result at each fixed value of that parameter. Therefore, we performed a bifurcation analysis on the reduced calcium subsystem of the CGR model. High concentrations of intracellular calcium are known to be a cause of DADs (Maruyama et al. (2010)). The only method of transporting calcium in or out of the cell in the reduced model is the sodium-calcium exchanger. Therefore, we chose intracellular sodium as the bifurcation parameter to vary. This parameter was chosen because an increase in the value of intracellular sodium will cause the equilibrium current from the sodium-calcium exchanger to increase - more sodium will be exchanged out of the cell in exchange for more calcium. As we fix the value of intracellular sodium to stay constant, the effect of this at sodium concentrations slightly higher than the physiologically normal value is to increase the total calcium in the cell. At very high sodium concentrations total calcium in the cell falls again to counteract the highly depolarizing effect of the highly increased concentrations of positive ions in the cell. Therefore varying intracellular sodium gives access to a wide range of calcium loads.

Starting from a single steady state at physiological sodium, we increased sodium by approximately an order of magnitude and plotted the results on a bifurcation diagram as shown in Figure 4.1. Calcium levels rise and then fall off again (in order to retain a stable membrane potential) but the only available solution to the model at any sodium concentration is a stable steady state. We found two qualitatively different types of stable steady state in the CGR model, a static equilibrium at lower calcium concentrations where all intracellular calcium channels

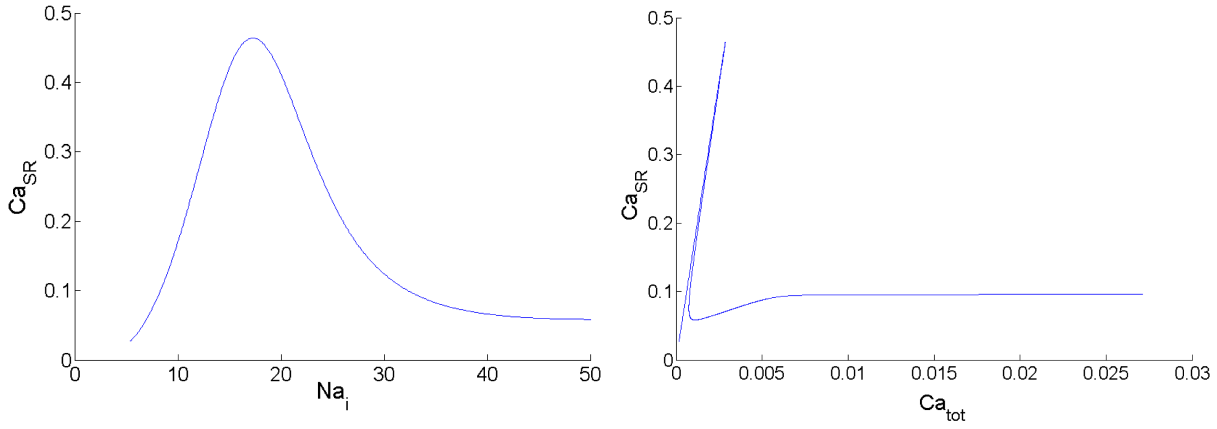

Figure 4.1: Left: Bifurcation diagram showing behaviour of the steady state solution of the SR calcium concentration in the CGR model calcium subsystem, as intracellular sodium is increased. Only stable steady states are observed with no possible oscillatory solutions. Right: A plot showing the same data but with total intracellular calcium on the x-axis. This plot shows that over multiple orders of magnitude difference in total intracellular calcium the CGR model's calcium subsystem did not display oscillatory behaviour.

were always closed and the fluxes between compartments were effectively zero, and a dynamic equilibrium at higher calcium concentrations where the SR release channels were constantly active and calcium cycled round the three compartments endlessly with no effect. From this analysis, we concluded the CGR model cannot demonstrate DADs without significant modification. However, Fink et al.'s findings suggested that if we found a Purkinje cell model that displayed DADs, with a calcium subsystem that could oscillate, we could adapt the CGR model to use this subsystem instead of its own, so that this new combined model would be capable of generating DADs. By reproducing the results of the verification of the original CGR model with this new model we could then have a reliable model for investigating DADs in rabbit Purkinje cells.

As we could not find any rabbit Purkinje models that were reported to display DADs, we instead looked for models of Purkinje cells in other species, in particular the Pan-Rudy model of canine Purkinje cell model (Li and Rudy (2011)). This model has been shown to develop DADs under conditions of increased sensitivity of the SR release channels to calcium.

The CGR model's original calcium subsystem is essentially a 3-component circuit. Calcium

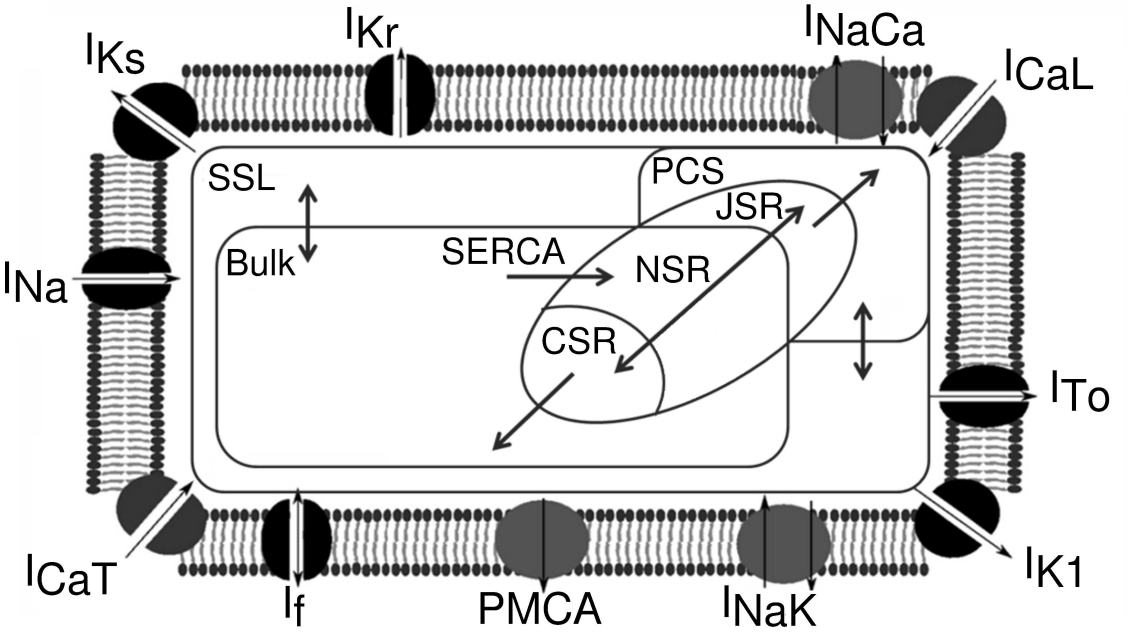

Figure 4.2: Schematic for the new combined model. Arrows through the cell membrane represent ionic currents, while arrows within the cell represent intracellular calcium currents.

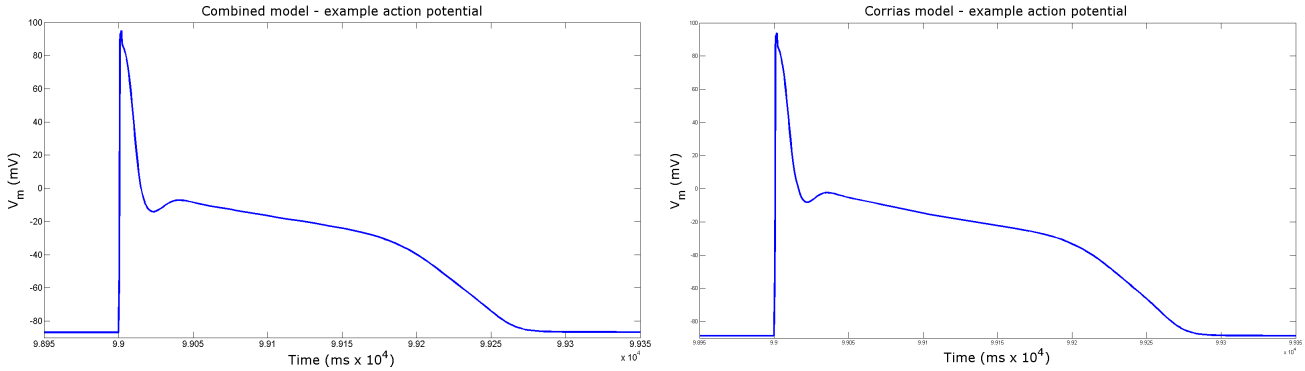

Figure 4.3: Example action potentials from the combined (left) and Corrias (right) models under physiological conditions and pacing at a cycle length of 1000ms.

is stored in the sarcoplasmic reticulum at a much higher concentration than in the other two compartments, the cell bulk cytoplasm and peripheral cytoplasm. It is loaded into the SR from the bulk cytoplasm by SERCA, an ATP-ase that pumps calcium into the SR. Calcium is released into the peripheral cytoplasm compartment, from the SR, by Ryanodine Receptors (RyRs), which are calcium sensitive calcium-release channels. Due to the concentration gradient a small amount of calcium is constantly released from the SR. If the amount of calcium in the cell is

unusually high, this can be enough to activate the RyRs, fully opening them and allowing a burst of calcium to be released from the SR. This calcium can then exit the cell through membrane calcium channels such as the sodium-calcium exchanger (which depolarizes the cell and can cause DADs) or by diffusing into the bulk of the cell where it can be taken back up into the SR.

In the Pan-Rudy model the calcium dynamics are more complex than in the CGR model. The periphery of the cell is divided into two compartments, the sub-sarcolemma (SSL) which contains most of the volume and non-calcium channels in the periphery and the peripheral coupling subspace (PCS), which is the space the SR emits calcium into and also contains the majority of channels responsible for calcium transport across the cell membrane.

The SR is divided into three compartments, the network SR which takes calcium up by SERCA, the junctional SR which can release calcium into the cell periphery and the corbular SR which can release calcium into the bulk of the cell, an effect that is not included in the CGR model.

This increased granularity in the compartment structure allows for more complex calcium dynamics than the CGR model was capable of. As SR calcium release channels are calcium activated on the cytoplasm side of the channel, the release of calcium into the PCS, a smaller volume than the peripheral region of the CGR model, will cause a larger change in concentration and make it easier for spontaneous calcium release from the SR to occur. Also, the presence of release channels into the bulk cytoplasm allow for a secondary feedback effect where calcium released into the PCS can diffuse into the bulk cytoplasm and open further channels, triggering another burst of calcium. This effect has been observed experimentally in canine studies (Hess and Wier (1984)) and there is evidence that these channels exist in rabbit Purkinje cells and though not activated by normal pacing (Cordeiro et al. (2001)), they can be activated during calcium overload.

However, there is evidence that the calcium compartmentalisation used in the Pan-Rudy model and in particular the presence of calcium release channels into the bulk cytoplasm as well as

the periphery reflects rabbit Purkinje cell biology better than the CGR model does ((Cordeiro et al. (2001)). Additionally, several ion channels in the CGR model have parameter values that originate from canine studies, and the action potential traces of canine and rabbit Purkinje cells are more similar than those of rabbit Purkinje cells and other rabbit cardiac cell types. Therefore, we decided to integrate the two models, creating a new model that would potentially be able to generate DADs.

We verified the Pan-Rudy model was capable of DAD generation by replicating the published results of the model, using the C++ model code supplied on the authors' website with the modifications from normal physiological parameters values they used to produce DADs. This produced DADs following the end of pacing. We then implemented a new 'combined' model by replacing the equations and parameter values governing intracellular calcium dynamics and the sodium-calcium exchanger in the CGR model with those from the Pan-Rudy model. This new model was of greater complexity than the CGR model (containing 29 ODEs due to the larger number of compartments and ionic currents between them) and it was hoped the increased complexity of the intracellular calcium dynamics would allow the new model to display DADs while still retaining the behaviour of the CGR model under normal physiological conditions. A schematic showing the currents and compartments in this combined model and an example action potential compared to an example action potential from the CGR model are shown in Figure 4.2 and Figure 4.3 respectively.

4.2.1 The updated CGR model

The updated CGR model contains the following major currents: I_{NaF} and I_{NaL}, the fast and late components of the sodium current; I_{CaL} and I_{CaT}, the L-type and T-type calcium currents; I_{K1}, the inward rectifier potassium current; I_{ToFast} and I_{ToSust}, the fast and sustained components of the transient outward potassium current; I_{Kr} and I_{Ks}, the rapid and slow components of the delayed rectifier potassium current; I_{f}, the funny current; I_{NaCa}, the sodium-calcium exchange current,

and I_{NaK}, the sodium-potassium pump current. An additional current, the stimulus current I_{stim} is included and represents external electrical stimulus of the cell to trigger excitation. This current can be applied at different rates to simulate different rates of pacing and investigate rate-dependent behaviour. Different pacing rates elicit different behaviours from the model due to the dynamics of the time and voltage dependent activation and inactivation gates that are modelled for appropriate ionic currents. The modified intracellular calcium sub-system tracks intracellular calcium concentrations in six separate compartments: the bulk cytoplasm, which represents the interior of the cell and the majority of its volume; the sub-sarcolemma (SSL), which represents the majority of the peripheral volume of the cell where the majority of non-calcium channels are located; the peripheral coupling subspace (PCS), which represents the remainder of the cell periphery where the majority of calcium carrying channels are located and where calcium emission from the sarcoplasmic reticulum (SR) occurs; and the junctional (JSR), network (NSR) and corbular (CSR) compartments of the SR, where calcium is stored. The network SR is where calcium is taken up into the SR by SERCA, the junctional SR can release calcium into the cell periphery and the corbular SR can release calcium into the bulk volume of the cell.

We adopted the calcium sub-system and I_{NaCa} formulations used in the Pan-Rudy model (all other ionic membrane currents used the CGR model formulation). The equations for the relevant processes incorporated into our model are given in the supplementary material for Li and Rudy (2011). Specifically, the equations from the sections on the Sodium-Calcium Exchanger and SR Ca^{2+} fluxes, as well as the equations describing the ionic concentrations for $[Ca^{2+}]_{\mathrm{PCS}}$, $[Ca^{2+}]_{\mathrm{SSL}}$, $[Ca^{2+}]_{\mathrm{i}}$, $[Ca^{2+}]_{\mathrm{JSR}}$, $[Ca^{2+}]_{\mathrm{NSR}}$ and $[Ca^{2+}]_{\mathrm{CSR}}$ and the calcium/calmodulin dependent protein kinase (CAMKII) from the Pan-Rudy model were used. Additionally, we used the Pan-Rudy model's parameter values for the fractions of the cell volume taken up by each compartment, although the total volume of the cell was taken to be the published value in the CGR model.

4.3 Results

4.3.1 Validation

The development of this model required heavy alteration of the CGR model to enable it to generate DADs, therefore it was necessary to validate the model under normal physiological conditions to test whether it could correctly simulate normal rabbit Purkinje cell behaviour.

To validate the model, we first performed a sensitivity analysis of the key parameters of the model and compared the results to those published by Corrias et al. of an identical analysis of their model. This was to gain confidence that the changes to the model did not affect the behaviour of the model under normal physiological conditions and that under these conditions the model would behave similarly to the CGR model, which had been fully verified. Corrias et al.'s sensitivity analysis compared the values of six standard electrophysiological biomarkers when key parameter values in the model were individually increased and decreased by 30% from their baseline values. The value of $\pm 30\%$ represents a rough estimate of the natural variation between healthy organisms of the same species.

The biomarkers used were: Action Potential Duration at 90% repolarization (APD90); Triangulation 90-70; Resting Membrane Potential (RMP); Peak Membrane Potential; Maximum Upstroke Velocity; and Dynamic Restitution - the maximum rate of change of APD90 as the pacing cycle length is increased.

These biomarkers allow the quantitative characterization of an action potential and can be used to give an overview of how the action potential changes in response to changes in parameter values. They also provide a way to compare simulation results to experimental data.

The sensitivity, S, of each biomarker to changes in each parameter was calculated using equation 3.9. In general a sensitivity analysis can show which parameter values are particularly influential and how stable the model is to small changes. However, our main use of the analysis

was to compare to the sensitivity analysis of Corrias et al. to determine whether the addition of the new calcium subsystem had altered the normal behaviour of the model significantly.

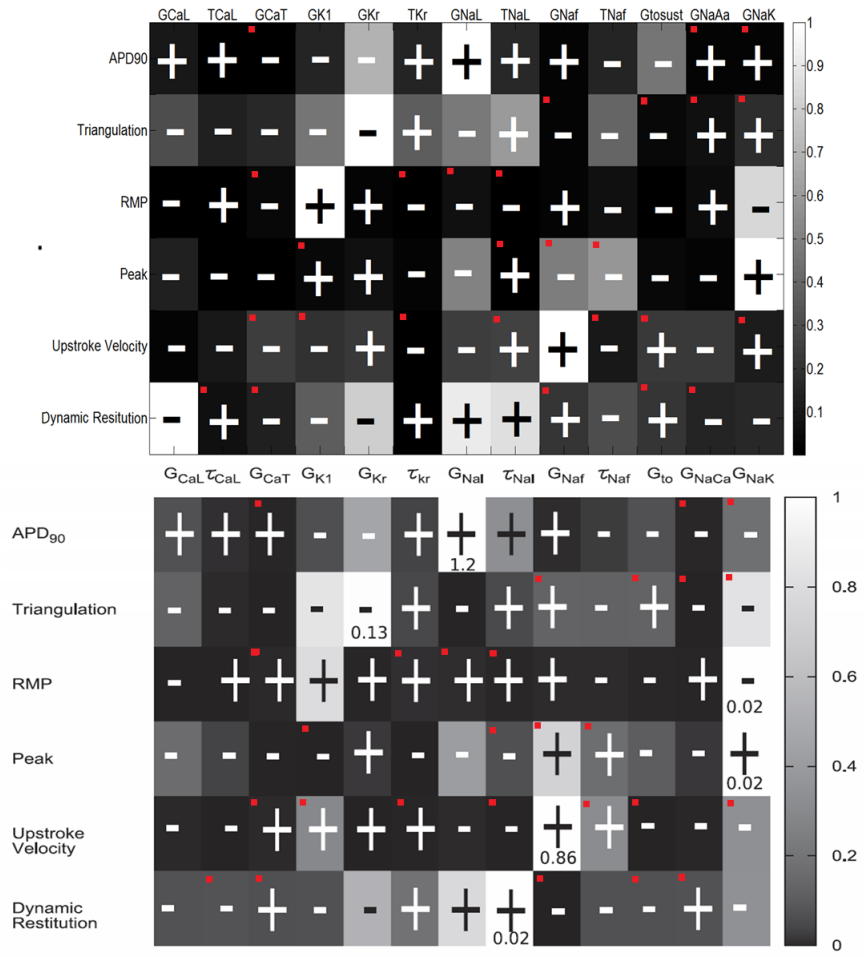

Figure 4.4: Comparison of sensitivity analyses of the combined model (top) and CGR model (bottom, from Corrias et al. (2011)). Sensitivities are normalised so that the largest sensitivity value for each biomarker (positive or negative) is given a value of one. Plus and minus signs indicate whether an increase in the parameter value increased (plus) or decreased (minus) the value of the biomarker. Red dots indicate biomarker/parameter pairs that differ in sign between the two models.

Figure 4.4 shows that the normalized sensitivities of both models were similar across many biomarkers, including the majority of the biomarker/parameter pairs with the highest sensitivities. The parameters that each biomarker was most sensitive to were either unchanged or varied between two parameters of similar sensitivity, except for the maximum gradient of the resti-

tution curve (APD90 against pacing cycle length). This biomarker was far more sensitive to L-type calcium conductance, possibly due to the altered calcium dynamics of the model. 27 out of 78 parameter-biomarker pairings displayed qualitatively different behaviour to the CGR model (e.g. decreasing a biomarker's value when the parameter was increased instead of increasing it) but most of these pairings had very low sensitivities indicating that the value of the parameter was not important in determining the value of the biomarker.

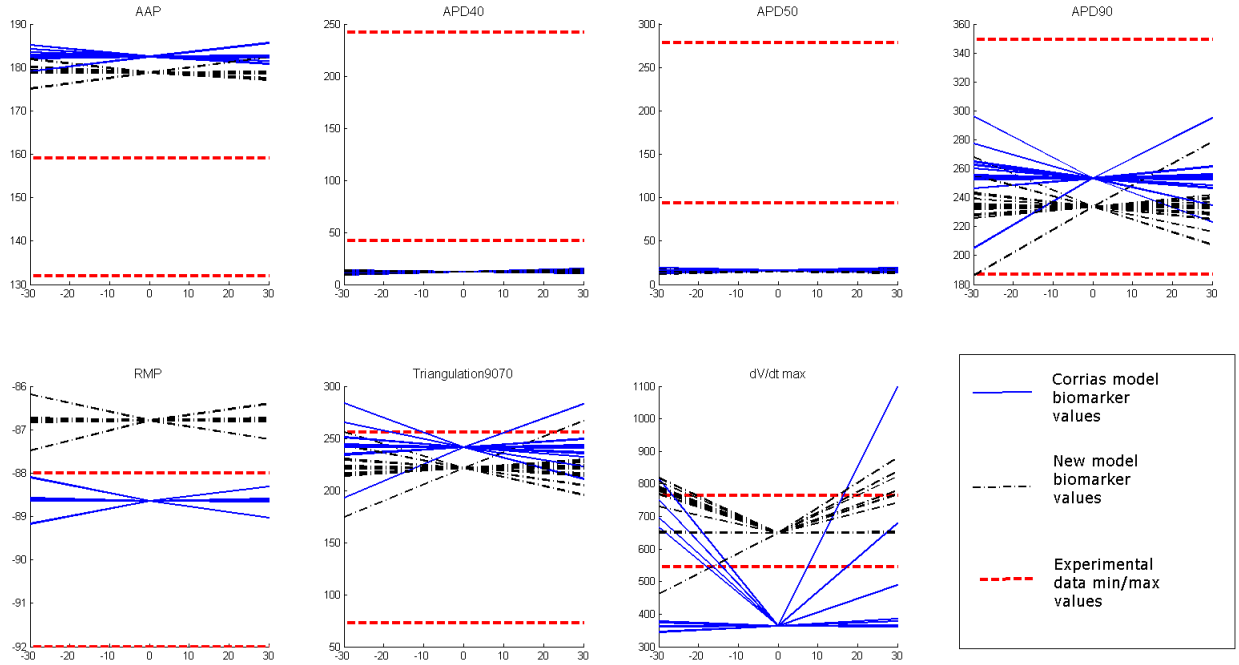

Figure 4.5: Comparison of model variability due to parameter variation and variability between individual rabbit hearts. For each biomarker a selection of important parameters (channel conductances and time constants) were varied $\pm 30\%$ in the Corrias (blue solid lines) and combined (black dot dashed lines) models so that results of displayed for each biomarker/parameter pair at baseline parameter value, baseline plus thirty percent and baseline minus thirty percent. These values are compared against the minimum and maximum values of each biomarker measured in seven rabbit hearts (red dashed lines) to see whether the variation from adjusting parameters fall within the bounds of natural variation.

In general, we believe this data should provide confidence in the new model as the most important parameter-biomarker relationships in the CGR model have been retained in the combined model. The behaviour of the CGR model under normal conditions has been well validated and our intention in creating the combined model was only to alter the CGR model's behaviour in

pharmacological or pathological situations known to increase the likelihood of DADs.

The next step in validating the model was to compare the output of the new model to experimental data. From a collaborator, we obtained biomarker data calculated from experiments on dissected Purkinje fibres from 7 rabbit hearts. These biomarkers were similar to those used by Corrias et al., that have already been described. The biomarkers were: Amplitude of Action Potential (AAP) - the difference between resting potential and the peak of the action potential; APD40; APD50; APD90; RMP; Triangulation $90-40$ and Maximum Upstroke Velocity. Of particular interest to us was the massive variability these biomarkers displayed between hearts. While the AAP, RMP and upstroke velocities were similar across all seven hearts, APD biomarkers varied tremendously. APD40 in particular varied from a recorded minimum of 42ms in one heart to 242ms in another under the same experimental conditions at 1000 ms cycle length.

Using this data we could go beyond the validation performed by Corrias et al. and directly validate the model against experimental data. To accomplish this we performed a sensitivity analysis, with $\pm 30\%$ variation to account for estimated variation between different hearts, and then determined whether the biomarkers output by the combined model fell within the bounds of natural variation observed in the experimental data. This allows us to evaluate not just whether our chosen parameter set can simulate an 'average' Purkinje action potential but whether the model still gives realistic results over a range of its parameter space. The functions of real biological systems must be robust against the natural variation between individuals and our model should reflect this.

Figure 4.5 shows the results of this analysis, plotted with the results of the same analysis applied to the CGR model. It is clear that for some of the biomarkers, particularly AAP, APD40 and APD50 our model output is different from the experimental data. However, the analysis with the base CGR model instead of our combined model also provides results well outside of the spread of the data. AAP measures peak voltage and APD40 and APD50 measure the duration of the

early part of the action potential. This suggests that both models are not accurately simulating the beginning of the action potential and that the initial peak of the action potential is at too high a voltage but decays too rapidly, as model AAP is consistently too high and APD40 and APD50 too low. A major component of the early action potential is the transient outward current. This current produces the characteristic notch in the rapid repolarization phase of the Purkinje cell action potential, following its initial peak. This current combines the effects of three currents: two are potassium currents, one calcium independent and the other calcium dependent, and the third is a calcium activated chloride current (Cordeiro et al. (1998)). Chloride dynamics are not modelled in the CGR or Pan-Rudy models. It is therefore possible that ignoring the effects of this current gives an unrealistic repolarization profile. If true it would be especially important to implement this current as it is calcium activated and therefore would be particularly active during the high calcium conditions where we expect to find DADs.

However, the combined model displays good agreement with the data for the total duration of the action potential (APD90), better agreement for upstroke velocity (how fast the initial depolarization of the membrane occurs) and triangulation than the CGR model. The good results for APD90 and triangulation suggest the model describes the later stages of the action potential reasonably well. Resting membrane potential results are not within the bounds of the data, but only by a maximum of 2 mV in the worst case, so it is likely only a small change to the model will be needed to adjust this.

Overall these results show that while the combined model does not accurately recreate the entire rabbit Purkinje action potential, it equals or beats the performance of the original CGR model over most of the biomarkers. The triangulation and upstroke velocity results fit the experimental data noticeably better for the combined model. Resting membrane potential is the only biomarker model where the CGR model unambiguously fits the data better than the new model, but the difference between models for this biomarker is minor. Also, the experimental data was obtained from multicellular Purkinje fibres, rather than the individual cells both models aim to

model, although we do not believe this is the main reason for the model to disagree with the data.

4.3.2 Generation of DADs

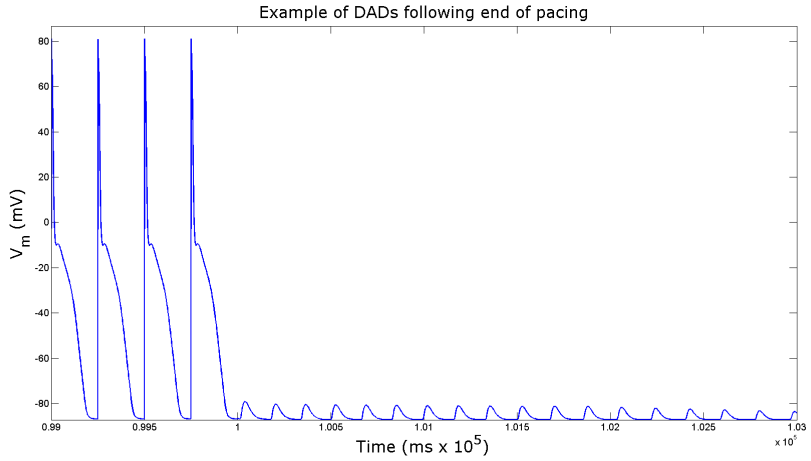

Figure 4.6: Example of DAD generation following the end of pacing at 250ms cycle length. L-type calcium channel conductance was increased 2-fold and extracellular calcium was increased 8-fold from standard physiological values to simulate additional calcium loading. The DADs gradually lose amplitude and decay away over a period of roughly 10 seconds.

Maruyama et al. report that they observed DADs in rabbit hearts following rapid pacing to simulate ventricular tachycardia. The percentage of hearts in which DADs were observed increased as pacing cycle length decreased. We simulated their experimental protocols for DAD generation (pace at a set cycle length for 15 minutes then stop pacing) at a variety of cycle lengths between 200 ms and 1000 ms and with varying concentrations of extracellular calcium and calcium channel conductance to further increase calcium loading. At long pacing cycle lengths and physiological conditions DADs do not occur, either in the model or in experiment (Maruyama et al. (2010)). Quicker pacing and increased calcium load increases the chances of DADs occurring. In their experiments, Maruyama et al. used isoprotenerol, which is commonly used to treat abnormally slow heart rates (bradycardia), to increase the susceptibility of rabbit hearts to DADs. We simulated this by increasing L-type calcium channel conductance

and extracellular calcium concentration to increase calcium load (Faber and Rudy (2007)).

This resulted in the development of DADs, an example of which is shown in Figure 4.6. However, as of yet we have not found conditions that produce DADs of sufficient amplitude to trigger a full action potential after the end of pacing. We have primarily tried varying parameters related to calcium dynamics - extracellular calcium concentrations and calcium channel conductances to adjust calcium load, as well as the gating of SR calcium release channels to increase the magnitude and likelihood of spontaneous calcium release events.

4.4 Conclusions

We have combined two verified Purkinje cell models, the CGR and Pan-Rudy models, to create a model that under physiological conditions behaves similarly to the CGR model and that can generate DADs under conditions known to amplify the chance of DADs in tissue. We have validated the model by replicating the results of a sensitivity analysis of the CGR model on the combined model, and by comparing the variation in the model's output when parameter values are varied to the natural variation found in the experimental data set we have access to. The sensitivity analysis showed that the behaviour of the model is similar to the CGR model and that those parameters that most affected the output of the CGR model have the same role in the new model. The comparison to experimental data showed the new model fit the data better than the CGR model. However, neither model displayed good agreement during the early repolarization phase of the action potential.

Due to this lack of agreement, further investigations into understanding the variability seen in the experimental data were performed. The resulting study, which introduces our experimentally-calibrated population of models methodology, is described in the next chapter.

5

Experimentally calibrated population of models predicts and explains inter-subject variability in cardiac cellular electrophysiology

The work presented in this chapter is derived from the publication: 'Experimentally calibrated population of models predicts and explains intersubject variability in cardiac cellular electrophysiology' by Britton et al., Proceedings of the National Academy of Sciences of the United States of America, 2013.

5.1 Introduction

At the end of Chapter 4 we described how the variability seen in action potential biomarkers, derived from experimental preparations from the Purkinje fibres of multiple rabbits was far larger than the ranges on biomarkers derived from a sensitivity analysis of either the original CGR rabbit Purkinje cell model or the combined CGR-PRd model we developed.

This work led to our interest in developing a new methodology for modelling cardiac cellular electrophysiology that could incorporate the variability we were seeing in the experimental data, and move beyond fitting models to biomarkers that had been averaged across an entire data set.

From this point, we investigated an approach that had been used in neuroscience, particularly by the Marder group (e.g. Marder and Taylor (2011)) to model variability in the properties of coupled neural circuits. The core idea of this approach was to develop a group of models that collectively spanned the variation seen in experimental data by generating a large pool of candidate models and discarding all models except for those that were fully in range of the experimental data, as determined by a group of metrics measured from the experiments and from simulations performed using each candidate model.

In this chapter we tightly couple experimental measurements and mathematical modelling to construct and calibrate a population of cardiac electrophysiology cell models representative of physiological variability, which we then use to investigate the causes of experimentally-measured variability in physiological conditions and following drug response. Our research builds on previous studies (Romero et al. (2009); Sarkar et al. (2012); Davies et al. (2012)) showing the importance of mathematical methods such as model populations and sensitivity analysis in investigating the ionic determinants of inter-subject variability in biological properties.

Here we describe the construction and calibration of a population of cell models, which is able to represent the variability exhibited in specific experimental recordings under physiological conditions and to predict inter-subject variability in response to potassium channel block. We base our investigations on rabbit Purkinje electrophysiology, due to the importance of Purkinje fibres in lethal arrhythmias (Maruyama et al. (2010)) and in drug testing in preclinical safety pharmacology (EMA (2005)). We hypothesize that inter-subject variability in experimentally-measured APs is primarily caused by quantitative differences in the properties of ionic currents, rather than by qualitative differences in the biophysical processes underlying the currents. We specifically show that the calibrated cell model population quantitatively predicts the prolongation of AP duration (APD) caused by exposure to four concentrations of dofetilide, a blocker of the rapid component of the delayed rectifier potassium current (I_{Kr}).

5.2 Methods

5.2.1 Experimental data set

Our data set consisted of micro-electrode recordings of isolated Purkinje fibre preparations obtained as described in Lu et al. (2005), from 12 different Purkinje fibres paced at three pacing frequencies (2, 1 and 0.2 Hz). In the experiments, preparations were paced at 1 Hz for 60 minutes to stabilize them and then paced at 1 Hz over four intervals of fifteen minutes each. At the beginning of all intervals except the first (control) interval, increasing concentrations of either an active testing compound (dofetilide, at concentrations of 0.001, 0.01, 0.05 and 0.1 μM, n=6 Purkinje fibres) or vehicle (H_2O) were added. Following these intervals, the preparations were paced for 5 minutes at 0.2 Hz, followed by pacing for 5 minutes at 2 Hz, while still perfused at the last concentration. All biomarker values used for the calibration process were determined from vehicle studies (only H_2O applied to preparation during pacing).

5.2.2 Rabbit Purkinje cell model

The model used in this study is the modified version of the CGR model (Corrias et al. (2011)), adapted as described in Chapter 4 to use the more detailed intracellular calcium handling system from the Pan-Rudy Purkinje fibre model (Li and Rudy (2011)). Figure 4.2 has shown a schematic of the model in the previous chapter. We made two additional changes to this model to make its baseline results better match experimental data. First, the extracellular potassium concentration $[K]_o$ was altered from 5.4 mM to 4.0 mM to reflect experimental conditions. Second, the formulation of the inactivation gate time constant for the fast sodium current was changed from a constant 2.0 ms to the voltage sensitive equation: $\tau_{\text{NaF}_{\text{inact}}} = 0.08 + \frac{2}{1+e^{(V_m+30)/10}}$ to obtain a peak voltage within experimental range.

5.2.3 Construction of the population of rabbit Purkinje models

To begin constructing the population of models we generated 10,000 parameter sets using Latin hypercube sampling (LHS) as described in Chapter 3. Each parameter set initially contained 11 parameters, 8 channel conductances for these currents: fast sodium, late sodium, L-type calcium, rapid delayed rectifier potassium, slow delayed rectifier potassium, inward rectifier potassium and the fast and sustained components of the transient outward potassium current; and 3 channel time constants for: fast sodium, late sodium and L-type calcium. These parameters were chosen as they have the strongest influence on biomarker values, based on a sensitivity analysis conducted on the CGR model, in line with results shown in Corrias et al. (2011). The parameter sets generated by LHS were used to replace the 11 relevant parameter values in the base model to create 10,000 different versions of the model with the same equations but varied parameter values. Due to its importance in AP rate-dependence we varied the sodium-potassium pump conductance at five values from one tenth to twice its initial value.

5.2.4 Biomarkers

We used six biomarkers to quantify the major features of the rabbit Purkinje AP. Four of these were biomarkers commonly used in cardiac electrophysiology: Peak Upstroke Velocity (dV/dt Max), Peak Membrane Potential (Vm Peak), Action Potential Duration at 90 percent repolarization (APD_{90}) and Resting Membrane Potential (RMP). Due to the characteristic spike and dome configuration of the rabbit Purkinje AP, we used two additional biomarkers: Dome Peak and Plateau Duration. All biomarkers used were previously described in Chapter 3. For Plateau Duration we used -350 mV/s as the threshold depolarisation rate for the end of the plateau as we found this gave us a good estimation of the duration of the AP up to and including the plateau phase but excluding the majority of repolarization. Figure 5.2 illustrates the calculation of each biomarker using an example action potential, from one of the models in the calibrated population.

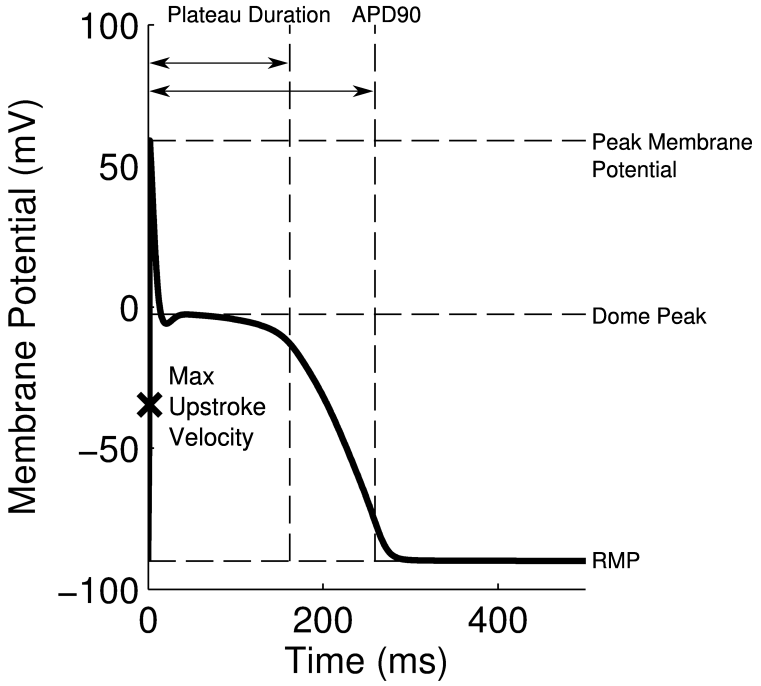

Figure 5.1: Representation of each biomarker measured in this study, calculated from a simulation at 1 Hz using a model from the population of models. The maximum upstroke velocity was calculated as the maximum value of the gradient of the membrane potential against time recorded before the point where the peak membrane potential occurs. Reproduced from Britton et al. (2013).

5.3 Results

Construction and calibration of the model population

We generated a large initial population of 10,000 models with randomly varied parameter sets. This initial population was calibrated to retain only those models that were fully consistent with the experimentally observed ranges of six biomarkers at frequencies of 2, 1 and 0.2 Hz. The calibration process reduced the population to 213 accepted models. Figure 5.3 shows the time course of different APs obtained experimentally (n=12, red traces), all models considered in the initial sample (n=10,000, black traces), and those accepted into the population due to being in range with experiments (n=213, blue traces).

Figure 5.4 further illustrates the calibration process and depicts the biomarker values obtained from each of the 10,000 models during simulated pacing at 1 Hz. We show values from models

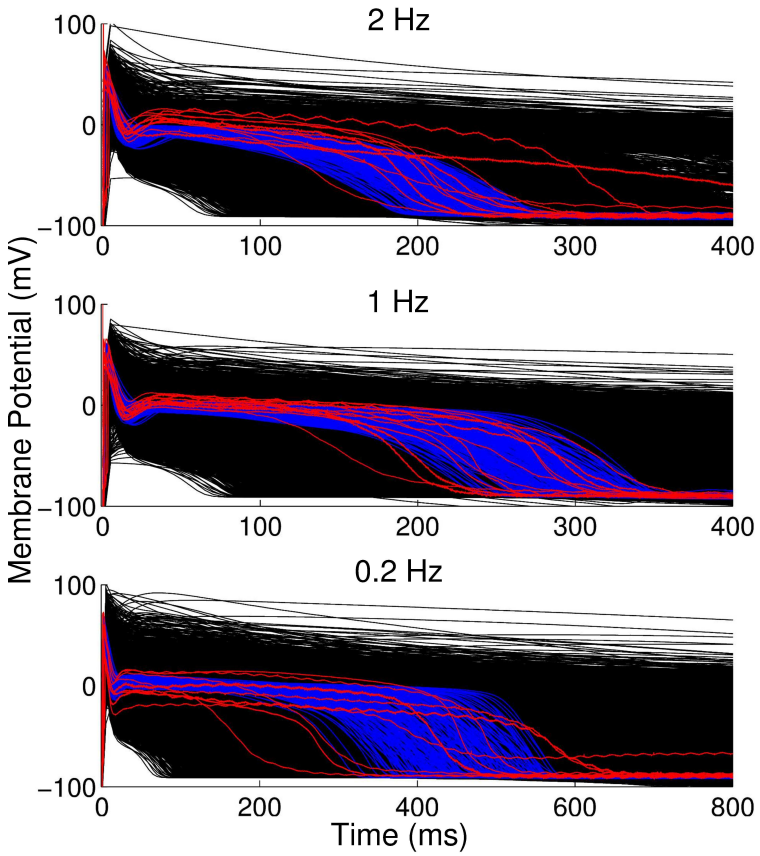

Figure 5.2: Action potentials obtained from experimental recordings (red, n=12), simulations using the models found to be within experimental range (blue, n=213) and all models considered (black, n=10,000), at 0.2, 1, and 2 Hz pacing frequencies. Plots extend to 400 ms for 2 and 1 Hz and to 800 ms for 0.2 Hz. Each experimental trace shows a representative action potential from experiments on isolated female rabbit Purkinje fibres. Reproduced from Britton et al. (2013).

in the calibrated population as white dots, values from models rejected from the population as black dots and the experimental ranges for each biomarker as grey lines. To visualize the distribution of models across the range of allowed biomarker values, we plot the histograms of the distribution of values of each biomarker at 1 Hz across the population, as shown in Figure 5.5. We find that our calibrated population of models yields biomarker values covering the majority of the experimental range for each biomarker.

Ionic properties do not exhibit specific correlations within the model population

As many ionic currents are known to act together in different phases of the AP, we investigated whether there were correlations between parameters values in the models finally accepted into

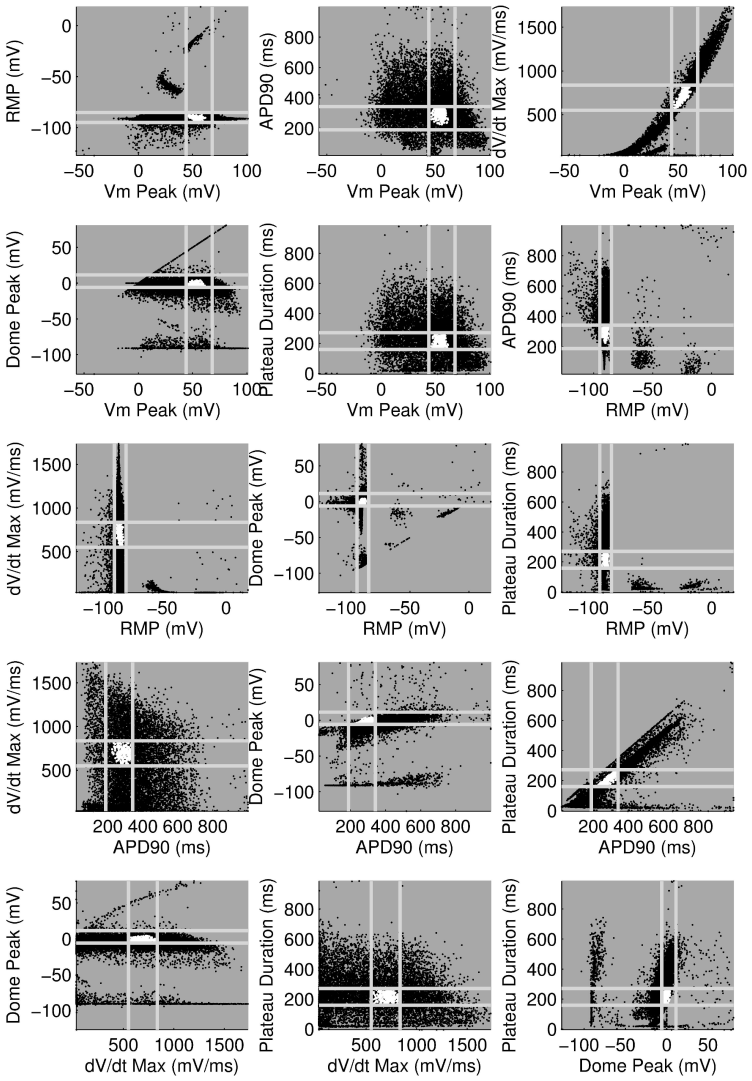

Figure 5.3: Scatter plots showing biomarker values for all models when stimulated at 1 Hz pacing frequency. Light grey lines indicate experimental min/max ranges for each biomarker. White dots correspond to biomarker values for models accepted into the population and therefore within experimental range, black dots correspond to rejected models outside experimental range for at least one biomarker at one or more pacing frequencies. Each panel shows results for a pair of biomarkers. Reproduced from Britton et al. (2013).

the population. The parameter sets of the initial 10,000 models were randomly generated and uncorrelated, so any correlations we found would be due to the calibration process. Figure 5.6 illustrates the distribution of parameter values for the 213 models accepted into the population. These results show that the majority of accepted parameter values span close to the entire range of sampled values (up to $\pm 100\%$ of their values from the original parameter set of the base

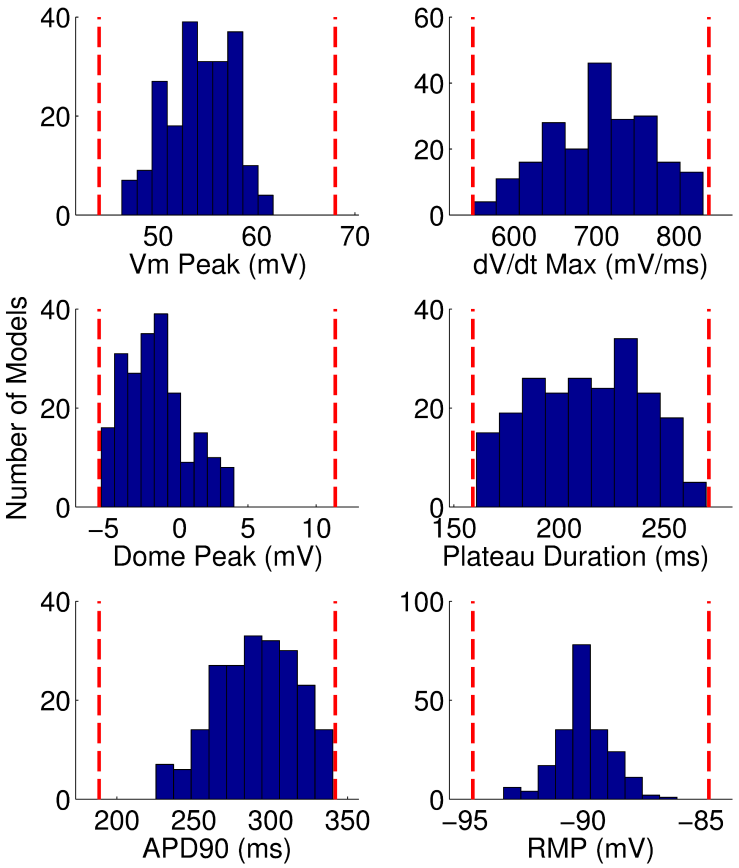

Figure 5.4: Histograms of the distribution of biomarker values across the population of models for 1 Hz pacing. Dashed lines indicate the experimental range used to calibrate the population of models for each biomarker at this pacing frequency. Reproduced from Britton et al. (2013).

model). This is with the exception of G_{NaF} (the conductance of the fast sodium current), whose allowed values are within a narrow subset of the sampled range. This could be due to the fast sodium current's role in determining both the velocity and peak value of the AP upstroke. We also find that the parameter values of models accepted in the calibrated population do not exhibit any obvious pair-wise correlations with other parameters. For most parameters (excluding G_{NaF}), the values of these parameters that were found in accepted models were spread across at least 83% of the total sampled range. For G_{NaF} the spread was 34% of the sampled range. We do find that for some parameters the distribution of their values across the calibrated population of models is non-uniform. Specifically, parameter values for the parameters G_{CaL}, G_{Kr}, G_{K1} and G_{ToSus} are more often in the top half of the sampled range, while for τ_{NaL} parameter values are

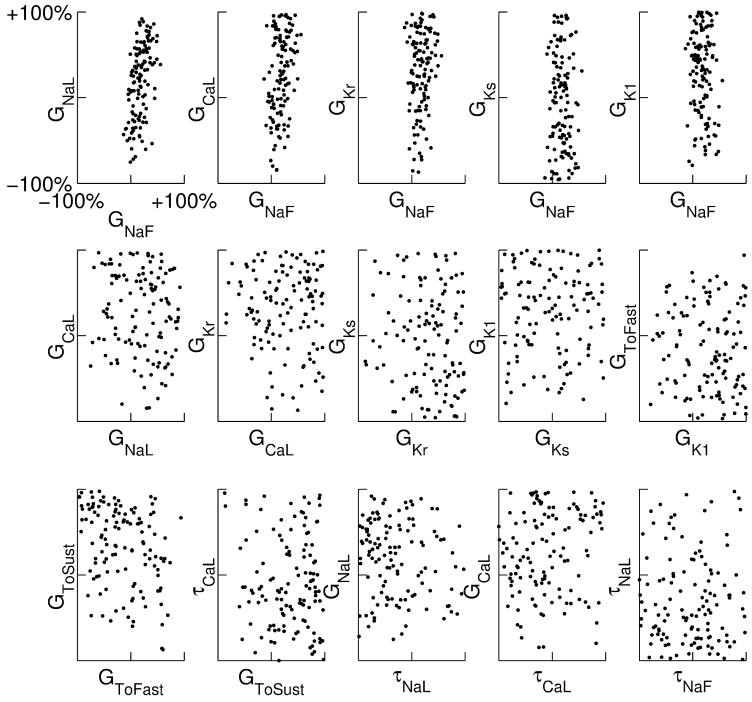

Figure 5.5: Scatter plots illustrating the distribution of ionic properties for accepted models in the population. Each panel shows results for a pair of ionic properties (including G_{NaF}, G_{NaL}, G_{CaL}, G_{Kr}, G_{Ks}, G_{K1}, G_{ToFast}, G_{ToSust}, τ_{CaL}, τ_{NaF}, τ_{NaL}). The scale in all graphs includes $\pm 100\%$ variation with respect to the original value. A representative sample of possible pairings is shown. Reproduced from Britton et al. (2013).

more often in the bottom half of the range. The remaining parameters appear to be distributed without bias across the whole of the covered range. Overall, we find that for almost any parameter value within our sampled range there is a parameter set that includes it and that will produce a valid model. With the exception of the fast sodium current's role in initial depolarization, no current appears to have a unique and irreplaceable role in creating the AP.

We wanted to identify significant correlations between parameter and biomarker values while controlling for the effects of the remaining parameters. Therefore we used partial correlation, which identifies correlations between variables after taking into account the contributions of one or more additional variables (Marino et al. (2008), see Chapter 3 for details). We took each of the parameters that were varied during the construction of the population of models and looked for correlations between each model parameter and any of the biomarkers used. The results of

this analysis at each pacing frequency are shown in Figure 5.7. For each biomarker multiple parameters show significant partial correlation. G_{NaF} correlates strongly and positively with peak membrane potential and peak upstroke velocity, biomarkers that quantify the initial upstroke of the AP. G_{Kr} has strong negative correlations with plateau duration and APD_{90}, both measures of AP duration. G_{K1} correlates primarily with resting membrane potential. The conductances for important plateau phase currents, G_{NaL}, G_{CaL}, G_{NaK} and G_{ToSust} all have significant correlations with most of the measured biomarkers at all pacing frequencies. This is consistent with our findings that a broad range of parameter values can produce models that are consistent with our data, as multiple parameters influence each measured biomarker. Individual parameter values are still important for determining the exact balance of currents, and therefore the specific AP properties of each model.

The model population quantitatively predicts concentration-dependent APD prolongation caused by four concentrations of dofetilide

Following the calibration and analysis of the model population, we evaluated whether the rabbit Purkinje model population could be used to predict electrophysiological response to drug block and to investigate the underlying mechanisms that determine this response for individual preparations. The predictive capacity of the calibrated model population was evaluated using an independent dataset not used for model calibration. Simulations and experiments were independently conducted for dofetilide at concentrations of 0.001, 0.01, 0.05, and 0.1 μM, using identical protocols as described in Methods. Figure 5.8 shows example APs simulated for control (blue traces) and following block of the rapid delayed rectifier potassium current (I_{Kr}) caused by application of a 0.01 μM concentration of dofetilide (red traces). I_{Kr} block caused by dofetilide induces both APD prolongation and increased APD variability, in agreement with previous studies (Pueyo et al. (2011)). Figure 5.9A shows ranges of simulated ΔAPD values (ΔAPD = APD_{90} with I_{Kr} inhibition $-$ APD_{90} under control conditions) obtained using the models in the calibrated population, with experimental values from five preparations shown as

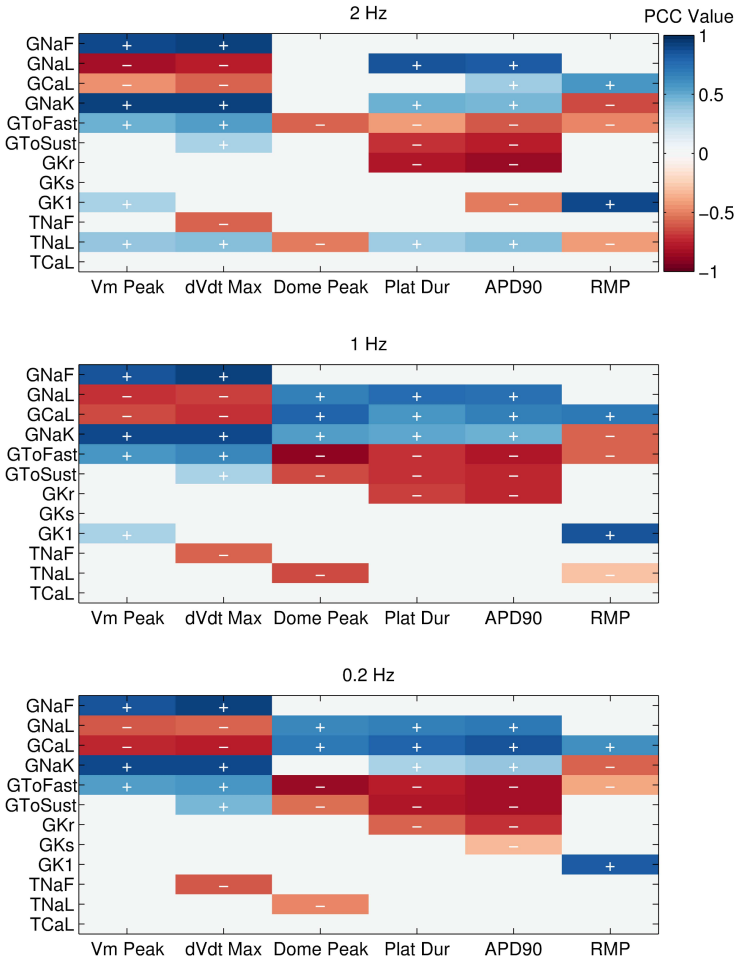

Figure 5.6: Correlation plots showing significant partial correlation coefficients (PCCs) between each parameter that was varied in the population and each biomarker. Coefficient values are represented using the included color bar. For each parameter-biomarker pair, the effects on the biomarker due to the unselected parameters are removed as part of the partial correlation method. PCCs are shown for each frequency used in our simulations (2, 1 and 0.2 Hz). Parameter-biomarker pairs with higher coefficient values displayed stronger partial correlation with each other, while pairs with a coefficient of zero did not show statistically significant partial correlation ($p < 10^{-5}$). $+$ and $-$ symbols indicate whether correlation was positive or negative. Reproduced from Britton et al. (2013).

dots. The sixth dofetilide preparation in our dataset is excluded from comparison. This is because this experiment displayed much higher APD values at all concentrations (APD_{90} of 1851 ms at 1 Hz pacing at maximum concentration; other five experiments 414 ms $\pm$75 ms at the same concentration). The predicted range of ΔAPD caused by dofetilide fully covers the range

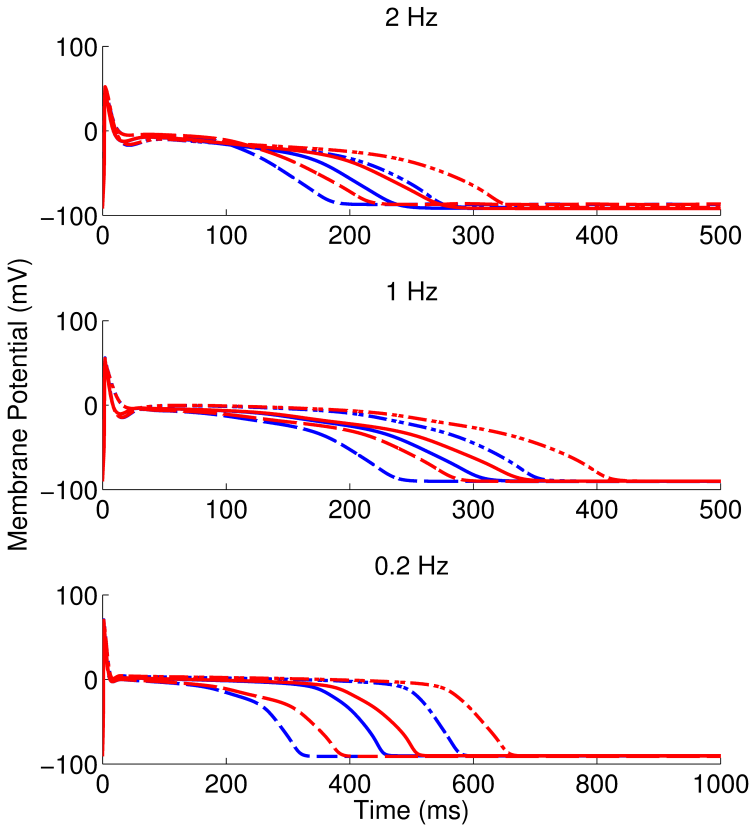

Figure 5.7: Simulated action potential traces obtained for 3 representative models accepted in the population in control conditions (blue) and following application of 0.01 μM concentration of dofetilide (red) at 2, 1 and 0.2 Hz pacing frequencies. This is the concentration closest to the experimentally determined IC50 (therapeutic dose) for dofetilide (0.0124 μM). Plots extend to 500 ms for 2 and 1 Hz and 1000 ms for 0.2 Hz. Line style indicates which of the control and dofetilide traces correspond to each model. Reproduced from Britton et al. (2013).

of the experimental data for each of the four concentrations.

However, for the two higher concentrations the lower end of the predicted range of ΔAPD is significantly less than the smallest values of ΔAPD seen in the data. This could be because the larger number of models relative to experiments gives the models fuller coverage of the range of possible prolongation values than the experiments. In order to further investigate this point, we compared the variability in ΔAPD values by analysing the ranges of ΔAPD seen in sub-populations of five models sampled from the total population of models, thereby matching the number of models to the number of experiments in our data set. To perform this comparison, 100,000 random samples of five models were made and the range of ΔAPD values for each

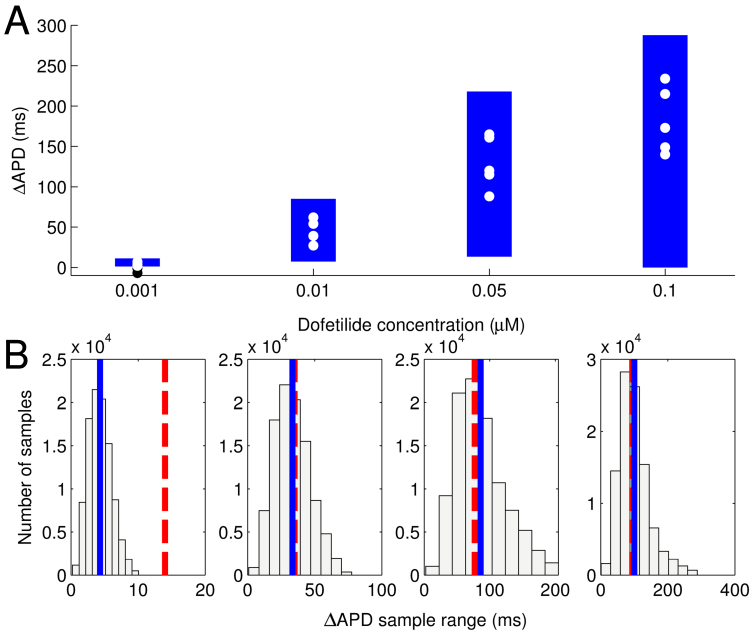

Figure 5.8: A: Ranges of APD_{90} prolongation (ΔAPD) caused by four concentrations of dofetilide using the models in the calibrated population. Dots indicate values of ΔAPD independently obtained in 5 experiments using rabbit Purkinje fibre preparations. B: Histograms of dofetilide-induced ΔAPD range across sets of 5 models randomly sampled from the calibrated population. 100,000 different sets of 5 models were used. The range of ΔAPD was calculated as: maximum value of ΔAPD $-$ minimum value of ΔAPD, for each set of 5 models. For each dofetilide concentration, the mean value of the ΔAPD range across the 100,000 samples of 5 models is shown by a solid blue line, the ΔAPD range from our experimental data is shown by the dashed red line. Reproduced from Britton et al. (2013).

concentration of dofetilide in each sub-population was computed. Figure 5.9B shows the distribution and mean value of these ΔAPD ranges from the models compared to the ΔAPD range seen in the experimental data. These results show that the mean range of ΔAPD values seen in the sub-population samples agrees well with experimental recordings at the three higher drug concentrations. At the lowest concentration, simulations slightly deviate from experiments, but this is mostly due to the lack of effect of the drug at this low concentration. This means that some experiments have negative ΔAPD values due to other sources of variability. Overall, these results suggest that the large number of models in the population, relative to the number of experiments, could explain the difference between predicted and experimental ΔAPD ranges. Repeating the sampling process several times with different sets of 100,000 random five model

samples results in similar mean values and histograms, indicating our results are independent of the particular samples chosen.

Baseline I_{Kr} conductance is the main determinant of APD prolongation caused by dofetilide

We wanted to understand how differences in the underlying ionic properties of rabbit Purkinje cells from different individual rabbits could affect their AP response to I_{Kr} block. To investigate this we used partial correlation coefficients to quantify correlations between the parameter values and ΔAPD values of each model in the population, as shown in Figure 5.10A. We found that at all pacing frequencies there was a strong positive correlation between G_{Kr} and ΔAPD. This G_{Kr}/ΔAPD correlation obtained with our experimentally-calibrated model population is consistent with results shown in the study by Sarkar and Sobie (2011). Rabbit Purkinje cells with a larger G_{Kr} are more dependent on the I_{Kr} current for repolarization, and so will have a greater increase in APD_{90} following I_{Kr} block than cells with a smaller G_{Kr}. Other parameters with a significant level of correlation with ΔAPD caused by dofetilide include the sustained transient outward potassium conductance G_{ToSust} and the inward rectifier potassium conductance G_{K1}. The L-type calcium conductance G_{CaL} and late sodium time constant τ_{NaL} are correlated with ΔAPD at the two higher pacing frequencies (2 Hz and 1 Hz), while G_{Ks} shows significant correlation at 0.2 Hz only. We find that G_{CaL} is positively correlated with APD_{90} but negatively correlated with ΔAPD while G_{Kr} is negatively correlated with APD_{90} but positively correlated with ΔAPD, which is consistent with the study by Sarkar and Sobie (2011). There is also no observed correlation between control values of APD_{90} and the amount of APD prolongation following block, as demonstrated in Figure 5.10B, in agreement with previous clinical and computational studies (Sarkar and Sobie (2011); Kannankeril et al. (2011)).

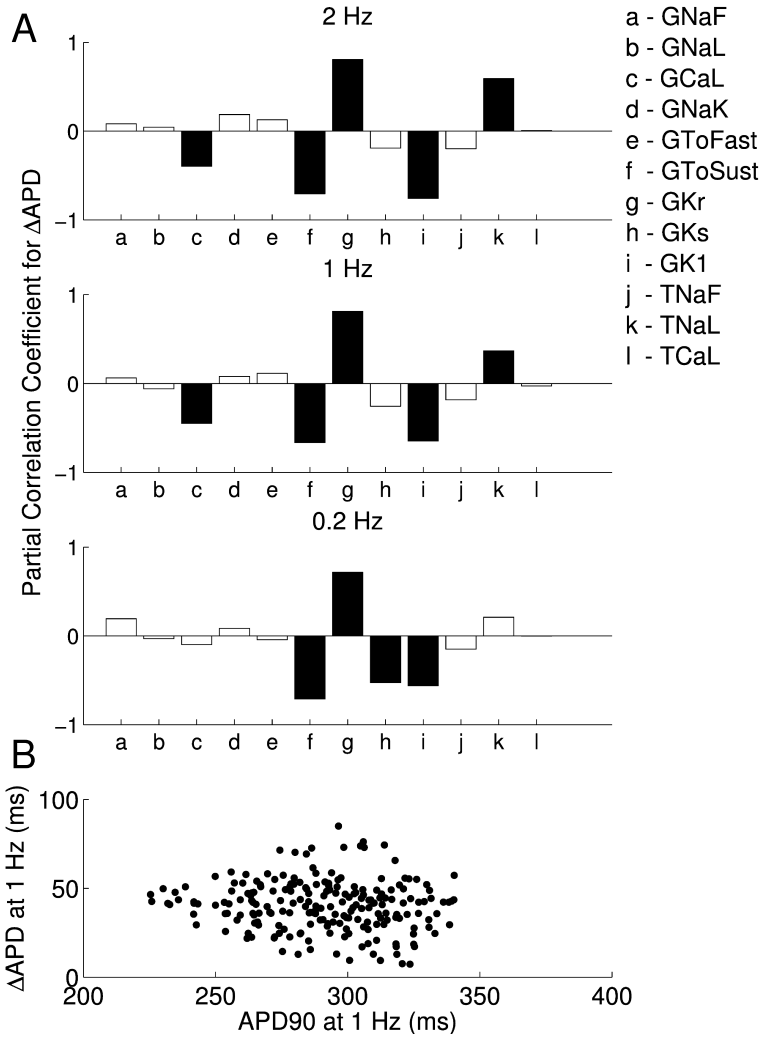

Figure 5.9: A: Partial correlation coefficients for APD prolongation (ΔAPD) caused by I_{Kr} block from a 0.01 μM dofetilide concentration, at each of the three pacing frequencies. ΔAPD was correlated against each of the 12 parameters that were varied to create the population of models, each time controlling for the other 11 parameters as part of the partial correlation process. Three models with outlying values of ΔAPD at 0.2 Hz (ΔAPD = 318, 364 and 395 ms, compared to the rest of the model population's sample mean of 69 ms $\pm$ 26 ms) were excluded from the analysis as they dominate the other models when calculating the partial correlation coefficients at that frequency. Solid bars denote significant correlations with $p < 10^{-5}$, empty bars indicate correlations with $p > 10^{-5}$. B: Scatter plot of control APD_{90} values of each accepted model at 1 Hz against ΔAPD due to I_{Kr} block from 0.01 μM concentration of dofetilide. Reproduced from Britton et al. (2013).

5.4 Discussion

In this study we have built a population of cardiac cell models that reproduces and predicts the variability exhibited in AP measurements from rabbit Purkinje fibres under physiological conditions and following potassium channel block. We calibrated a large number of models derived from randomly generated parameter sets against the range of variability observed in experimental AP recordings, and discarded those models with AP behaviour outside of the experimental range. This produced a population of models with a wide range of underlying ionic current properties that all produced realistic electrophysiological output in simulated physiological conditions. We analysed the variation in underlying parameters and established links between variation in the underlying ionic currents and variation in properties of the AP. We have demonstrated that our model population quantitatively predicts the range of variability in APD prolongation measured experimentally following block of the rapid delayed rectifier potassium current by four concentrations of dofetilide.

Previous modelling studies of variability in cardiac cellular electrophysiology have focused on variability in a single current (Romero et al. (2009)), sensitivity analyses that finely sample the local parameter space close to the original parameter set of the model (Sarkar et al. (2012)), and on replicating AP traces from individual cells (Davies et al. (2012)). In contrast, we have developed an efficient methodology that can be used to simulate the range of AP variability seen in a data set, while varying the underlying parameter sets across a wide range of values, comparatively far from the model's original parameter set. In neuroscience, modelling studies have been carried out that use a similar methodology as ours to capture the full variability of a data set in a population of models (Marder and Taylor (2011); Prinz et al. (2003, 2004); Taylor et al. (2009)). However, to our knowledge these populations have not been used to predict the behaviour of an independent data set and link that behaviour to underlying ionic mechanisms. Grashow *et al.* have performed experimental studies of the effects of variability on two-cell neuronal circuits to investigate how variability affects the way these circuits behave (Grashow

et al. (2009, 2010)). By controlling the values of two conductances they show that similar circuit behaviour can be produced in circuits with different intrinsic membrane properties. They found that the responses of two-cell circuits to two neuromodulatory drugs were generally reliable across a wide range of controllable parameter values, despite variability in the underlying circuits. However, for some circuits, certain parameter sets within their sampled parameter space behaved qualitatively differently to the majority. This is similar to our findings that a wide range of parameter combinations can produce very similar types of behaviour.

Our methodology aims to incorporate the variability between individuals of the same species into traditional models of biological systems, such as the electrophysiological activity of a cardiac cell. We do not look at properties of isolated models in the population or attempt to classify single models as models of particular individuals. Instead, we look at the behaviour of the whole population, particularly how variation in underlying parameters is related to variation in biomarkers, in this case the AP. All of the models in our population have been tested and shown to be within the observed range of AP variability. However, different combinations of ionic parameters produce different behaviours within that range, and also determine the response to non-physiological conditions such as drug-induced block of ionic currents. The ability of the population of models to link underlying mechanisms with variation in both physiological and pathological conditions is a powerful feature of the methodology that we hope can be further exploited in future studies.

We have found that a wide range of different combinations of ionic parameter values can produce model behaviours that are within the bounds of experimental variability. One question that arises from this result is whether the size of this range is due to the relatively limited set of conditions we use to calibrate the population of models, compared to the number of possible conditions a real cardiac cell could experience. Other studies (Davies et al. (2012); Syed et al. (2005); Sarkar and Sobie (2010); Zaniboni (2011)) suggest that in cases where a specific set of model outputs are required, the allowed parameter range for producing them can be highly con-

strained, as long as enough non-redundant outputs are considered. Examples of these outputs could be the mean values of different electrophysiological properties, or of the same property under a range of experimental conditions, such as different pacing frequencies, with each value derived from averaging over many experiments. Our work, along with that of Marder *et al.* (e.g. Prinz et al. (2004)) suggests that in situations where a model must reproduce a class of behaviour (such as a realistic rabbit Purkinje AP in control conditions at 1 Hz pacing) with flexibility on the exact values of the measured outputs, a wide range of parameter sets can produce behaviour within the required range. This is consistent with the idea that underlying conductances can vary considerably and still produce a viable AP, but that the exact values of those conductances determine the exact properties of the AP.

However, while the wide range of allowed parameter values could be a characteristic of the biological system (as in Grashow *et al.*'s work), part of this effect could be due to other factors. To better represent physiological variation in ionic properties, the population may require additional constraints, such as using a wider variety of experimental conditions for the calibration process (e.g. including drug block experiments), and additional biomarkers that probe other important electrophysiological properties beyond the steady state AP, such as intracellular calcium behaviour or repolarization dynamics (Zaniboni (2011)).

A further important benefit of modelling the effects of variability is that we are able to make quantitative predictions of the effect of an intervention such as drug application, based on the range of responses we observe across the population of models. Our study of dofetilide-induced APD prolongation is an example of this, which can be extended to other pharmacological interventions or disease conditions. We found that the range of APD prolongation across the population of models is consistent with experimental data at multiple drug concentrations that were not used to calibrate the population of models. Traditional cell models using a single parameter set can only make qualitative predictions in such cases, e.g. predicting that APD prolongation would increase as drug concentration increased. Using a population of models

allows quantitative prediction of the range of responses to an intervention to be made, and these predictions can be tested experimentally as shown here.

Another potential application for the population of models approach is to generate 'typical' models to summarize the behaviour of an experimental data set. In this study, all models in the population of models are viewed as equal. However, for some applications it may be useful to determine which models in the population best represent typical or averaged experimental behaviour. This could be achieved by classifying or ranking the models to determine which produce behaviour close to mean experimental behaviour and which better represent the behaviour of outlier experiments. Determining which model(s) in the population would be best used for these purposes is another possible way the population of models methodology could be exploited in future work.

The results in this study are based on a data set from a relatively small number of individuals, as is often the case in cardiac electrophysiology, and a single drug block experiment. This small sample size and lack of multiple non-control condition experiments limits our ability to draw statistical conclusions from our work, and to test the predictive power of our population of models in multiple scenarios. Further studies could focus on applying the methodology to ensure the predictive capacity of the population of models for a range of drug block and disease conditions (e.g. as in Walmsley et al. (2013)). The flexibility of the approach we propose ensures its application in other areas of biology to improve our understanding of variability in biological systems.

5.5 Conclusions

The results from this chapter were developed using data from rabbit cardiomyocytes. In the next two chapters we move from animal models to humans. In Chapter 6 we describe the variability present in a data set of human ventricular cardiomyocyte recordings, that will then be used in

Chapter 7 to develop a population of human cardiac cell models incorporating this variability. As electrophysiological data from human hearts is scarce, computational modelling of human cardiomyocytes is particularly important, as models of human cardiac cells can both be reused indefinitely for new studies without the need for new human heart tissue, and can incorporate the human-specific features of our biology that are not captured by experimental animal models.

6

Experimental database of human ventricular microelectrode recordings

6.1 Introduction

In Chapter 5 we used a population of models to model the effects of inter-subject variability on rabbit Purkinje cells and used this population to predict the range of responses to dofetilide, an I_{Kr} blocking drug. Understanding the electrophysiological response of animal model species, such as rabbit, to drugs is important because tissue and cells from these animals are frequently used both in research as a model for understanding the behaviour of human hearts and in safety pharmacology, to test the safety of new drugs without risking human lives. However, the ultimate model for human cardiac biology is a human heart, either within a living patient in the case of clinical trials, or tissue from a donor heart for electrophysiology studies.

In this chapter we move from studying data from experimental animal models to studying data from human hearts. We will describe the extraction and analysis of a data set of microelectrode recordings taken from experiments using human ventricular tissue preparations. Obtaining data directly from experiments on human hearts is challenging, as only hearts that are not suitable for transplant, or that do not have a suitable candidate for transplantation at the time the heart is available, can be used for research. At the same time, hearts that are badly damaged or failing are not good candidates for research into the behaviour of the non-failing human heart.

Therefore, experimental studies of human cardiac electrophysiology are rare, and until recently, cardiac modelling has also been limited by lack of the data needed to develop human cardiac cell models.

However, as described in Chapter 3, there are now a number of accepted, well-validated models of human cardiac cells. In particular, the O'Hara-Virag-Varro-Rudy (ORd) model of the human ventricular myocyte (O'Hara et al. (2011)) was developed primarily using data from non-failing human hearts, obtained by Prof. András Varró's group at the University of Szeged. This is a major advance in model development, as most cardiac models are derived using data from a variety of sources in the literature, usually including data from species other than the species being modelled (for example, Niederer et al. (2009); Bueno-Orovio et al. (2014) describes the reuse of a formulation of the sodium-potassium pump current across cardiac cells models of multiple species). For human cardiac models in particular, it is important that species-specific electrophysiology features are captured in the model, as these features are what cause predictions made using animal models to be inapplicable to human biology. Jost et al. (2013) showed that the average balances of I_{Kr} and I_{Ks} current magnitudes in dog (a common animal model for drug safety testing), were significantly different to that in human, with dogs having smaller I_{Kr} and larger compensatory I_{Ks}, leading to predictions of less APD prolongation in dog models when I_{Kr} was blocked, compared to the same level of block in humans. Therefore, there are potential applications for computational models of human cardiomyocytes that incorporate inter-individual variability, to account for both species-specific effects and to potentially reduce our reliance on animal experiments for research on human cardiac electrophysiology.

Through our collaboration with the Varró group, we obtained their data set of human ventricular microelectrode recordings, obtained over a period of 15 years from small tissue samples of right ventricular endocardium (from both papillary muscle and trabeculae), prepared from non-failing human hearts, from a wide range of ages and from both males and females.

In this chapter we first explain the general features of the data set and how the experiments in

it were performed. We then describe the methods we used to extract the database into a fully computerised database that could be used for further work. Using this database, we compute action potential (AP) biomarker values for each of the available control conditions experiments, quantify the distributions of these biomarkers to understand the variability in AP behaviour present in these recordings, and extract calibration ranges for each biomarker that can be used to develop populations of models. Finally, we analyse available drug experiments to help us design the study of drug effects on human cardiomyocytes that will be described in Chapter 7.

The work in this chapter will pave the way for the next chapter, in which we use the calibration ranges derived from this data set to develop a population of human ventricular cell models. We will use what we learn in this chapter from the experiments with drug to application to design a study using the population on investigating how inter-subject variability affects the susceptibility of cardiomyocytes to developing drug-induced repolarisation abnormalities.

6.2 Methods

6.2.1 Data set features

This data set contains data from 15 years of experiments on non-failing human heart tissue. Hearts are obtained by the Szeged group from organ donors in situations where it is not possible for the heart to be used for transplant.

The recordings we have analysed are obtained from preparations prepared from papillary and trabecular tissue obtained from the right ventricles of undiseased human donor hearts. To obtain these preparations, donor hearts are first explanted and kept cold ($4-6\,^{\circ}\mathrm{C}$) while perfused with a cardioplegic solution to prevent cell death, for 2 to 4 hours. The heart is then dissected, and papillary and trabecular tissue is cut from the right ventricle and mounted in a tissue chamber where it is perfused in oxygenated solution warmed to $37\,^{\circ}\mathrm{C}$ (further details are available in Jost et al. (2005)).

After an hour of perfusion to allow the tissue to equilibrate, the tissue is paced using bipolar electrodes and the membrane potential is recorded using a glass microelectrode. These recordings are then stored in a proprietary format using APES recording software (Hugo Sachs Elektronik, March-Hugstetten).

The complete data set contains recordings of the preparations under control conditions, and under a wide array of different drug applications, both single drug applications and also experiments applying multiple drugs together. Each individual recording consists of 10 subsequent action potentials. All of the recordings used in this thesis and described in this chapter were obtained under steady 1 Hz pacing. During an experiment, a new recording was typically taken every 5-10 minutes. To investigate the effects of a drug, the drug is added to the perfusion solution and superfused (constantly run across the preparation) for 40 to 60 minutes. Measurements are then made at short intervals, once the preparation has stabilised. A preparation is counted as stabilised when APD90 varied by less than 10 ms between subsequent recordings, usually spaced 5 minutes apart during this period.

The total dataset contained information from 159 different hearts, with an age range of 12 to 68. The microelectrode recordings were stored in a proprietary digital format, while details on experimental timings, conditions, drug applications, heart donor age and gender, and tissue type (e.g. papillary or trabeculae) were recorded in paper log books. Therefore the full data set we obtained comprised the digital recordings, and copies of the log books, which could be cross referenced by the dates of each experiment.

6.2.2 Data set preparation

There were two main challenges in converting the data into a form that could easily be manipulated as a whole, in a fully computerised format. The first was that the recording software stored the data in a proprietary, non-plain text format, and so could not be automatically read or extracted into a different format. Instead, each voltage trace had to be loaded into

the software, then exported to a plain text file through the relevant option in the software's graphical user interface. We partially automated this process by writing scripts using the Autohotkey (www.autohotkey.com) macro scripting language, which allowed the extraction of voltage traces with reduced user input.

The second challenge was annotating the extracted traces using information provided in the paper copies of the lab books. For a given experiment, information on timings, drug application, and tissue type were interpreted from the lab books and input into a plain text database file that linked the information in the lab books with the information in the trace files. This allowed us to search the database for control traces only, or for a particular drug, and to group traces that belonged to the same experiment.

For some experiments, it was difficult to extract all the information as it was not always clear which microelectrode recordings corresponded to which lab book entries. Currently we have extracted most of the unambiguous experiments, but further experiments could be extracted in the future. Once this had been accomplished, we used the database to develop a human ventricular population of models. The construction of this population of models is described at the beginning of Chapter 7. At this point, we have not fully annotated the database, and our current database of control recordings comprises 75 preparations from 47 hearts. Figure 6.1 shows examples of action potentials from the database, paced at 1 Hz in control conditions. We see a variety of qualitative differences in overall action potential shape as well as quantitative differences in features such duration and peak amplitude. This is in contrast to our previous study on rabbit Purkinje cells in Chapter 5, where all cells in the study displayed a spike and dome configuration when paced.

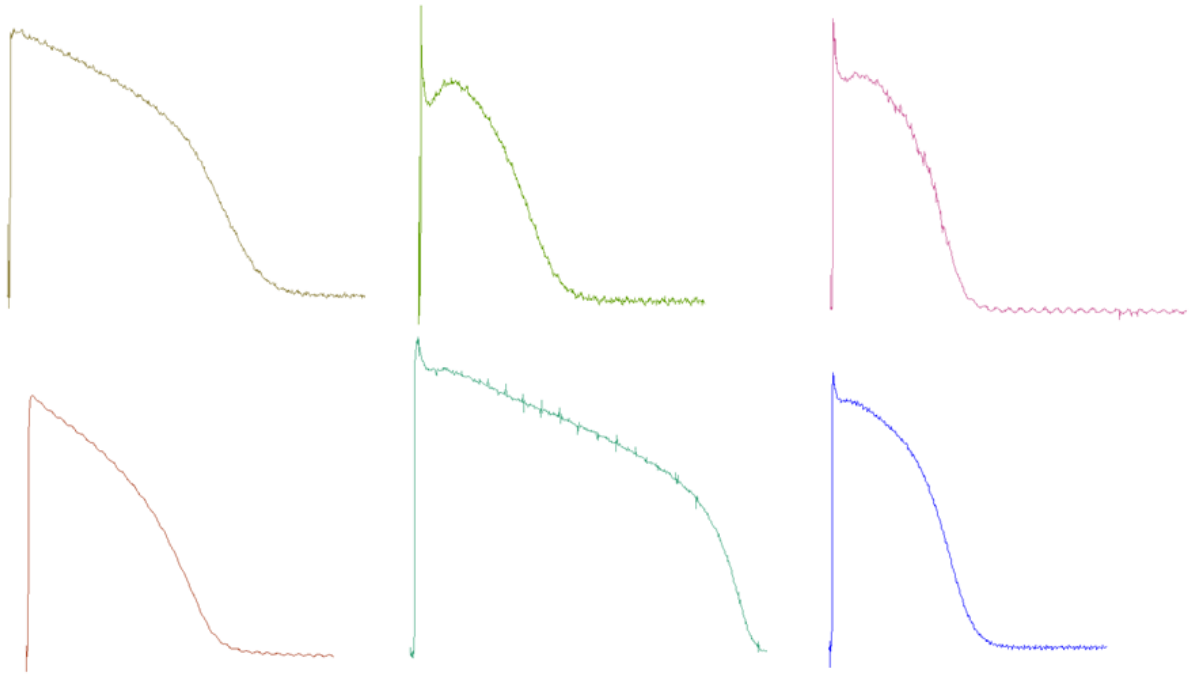

Figure 6.1: Representative action potentials in human ventricular tissue from different donors, displaying differences in action potential shape.

6.3 Data analysis

6.3.1 Calculation of calibration ranges

Once we had extracted a substantial number of AP recordings into a form we could use, our next goal was to summarise and quantify the results of each experiment using AP biomarkers, so that we could analyse the level of variability seen across these different hearts, and generate biomarker ranges that could be used to develop populations of models. In this section we describe this process.

We chose 8 biomarkers to extract from the database: peak membrane potential, time-to-peak, peak upstroke velocity, APD40, APD50, APD90, triangulation 90-40 (APD90 - APD40), and resting membrane potential.

To obtain biomarker values from the recordings, we first excluded all experiments with less than 3 separate recording files, as these experiments would have been terminated early e.g. due

to a damaged preparation. Then, from the remaining experiments, we extracted the traces in the database that were marked as either being under control conditions or as being recorded after a washout but before the addition of a new drug. For each experiment, we took the final control trace, which was usually the last trace recorded before a drug was added for the non-control portion of the experiment, and calculated biomarker values for that trace. We extracted biomarkers in this way for two reasons. First, a key purpose of the control portion of each microelectrode experiment is to stabilise the preparation. Typically, control recordings consisting of 10 consecutive action potentials were taken at regular intervals (e.g. every 5 minutes) until the mean APD90 values of 2 subsequent recordings differed by less than 10 ms. At this point the preparation is relatively stable and the next part of the experiment, which is usually drug application, is begun. Therefore, the most representative traces of the stable, steady behaviour of a given preparation should be the final recorded traces. Secondly, by extracting biomarkers this way we avoid averaging over multiple traces, which can give unrepresentative biomarker values if the early traces in an experiment differ significantly from the later stabilised traces. For the last step before calculating calibration ranges, the data was examined visually, and traces that were obvious and significant outliers compared to the rest of the experiments (e.g. with an APD90 100 ms longer than any other experiment in the data set) were excluded. Finally, to calculate the biomarker ranges we took the minimum and maximum values of each biomarker seen across all of the remaining experiments in the dataset. These values form the calibration ranges used in Chapter 7 to filter out unsuitable candidate models when we construct a human ventricular population of models. These calibration ranges are shown in Table 6.1.

6.3.2 Distribution of control conditions AP biomarkers

After we had obtained calibration ranges, our next aim was to summarise the distributions of the AP biomarkers across the dataset, to determine how they were distributed, and whether there were correlations between them. Histograms of biomarker values in our current control condi-

tions data set are shown in Figure 6.2. The means and standard deviations of biomarker values from the extracted data are summarised in Table 6.2, along with the coefficient of variation (CV) for each biomarker, which is the ratio of the standard deviation and mean and provides a measure of how broadly distributed a set of data is. We find that most biomarkers have moderate CVs around 0.25. This indicates a moderate spread of values about the mean. Three biomarkers have CVs that are significantly different from this - maximum upstroke velocity (1.05), time-to-peak (0.4) and resting membrane potential (0.04). For maximum upstroke velocity, the CV is large, and over 1, indicating a highly spread distribution. The largest values of this biomarker that we see in the data set are extremely high, at over 2,000 mV/ms. We believe this is a recording artefact, not a feature of these cells, and based on this we excluded this biomarker from being used to develop the population in Chapter 8. To quantify the speed of the upstroke, we instead use the time-to-peak biomarker, which measures the time from stimulus to peak of upstroke. This is an important characteristic of the AP to measure because low fast sodium current conductance can be compensated by high levels of L-type calcium current conductance to generate an action potential with normal peak membrane potential but extremely long upstroke time. In tissue this would also result in a low conduction velocity. This type of action potential (which does not occur in the experimental recordings) can be screened out of the population by its low maximum upstroke velocity or by its long time-to-peak, compared to a normal AP driven by the fast sodium current. We see a greater CV for time-to-peak (0.4) than for other biomarkers, but as the CV is still much less than 1, the distribution of this biomarker is far less spread than for peak upstroke velocity. For resting membrane potential, CV is extremely low (0.04), demonstrating the low variability in this biomarker, probably due to the heavy influence of the external medium, in particular the extracellular potassium concentration, in determining the equilibrium potential of the cell.

We then looked to see whether there was correlation between biomarker values. Scatter plots showing each pair of biomarkers are shown in Figure 6.3. Peak membrane voltage, maximum

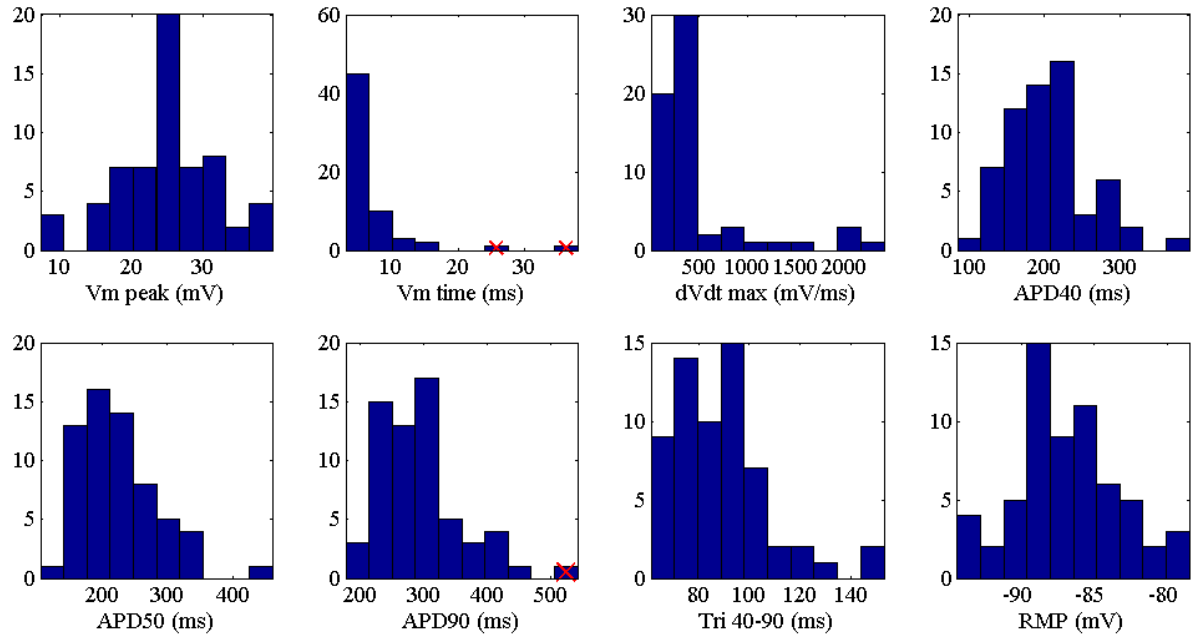

Figure 6.2: Histograms of biomarker values under control conditions at 1 Hz pacing. Three outlier experiments that were excluded from being used to calculate calibration ranges are shown with crosses for the biomarkers for which they were excluded (2 for extended time-to-peak, 1 for long APD90). The number of outlying peak upstroke velocity values, which is assumed to due to processing of the microelectrode recordings, also lead to that biomarker being excluded from use as a calibration biomarker.

	Mean and (standard deviation)	Coefficient of variation
Vm Peak (mV)	24.7 (6.8)	0.28
Vm Time (ms)	5.8 (2.3)	0.40
dV/dt max (V/s)	489.6 (516.5)	1.05
APD40 (ms)	201.2 (51.1)	0.25
APD50 (ms)	223.9 (54.5)	0.24
APD90 (ms)	289.3 (59.3)	0.21
Tri 90-40 (ms)	88.0 (17.0)	0.19
RMP (mV)	-86.9 (3.6)	0.04

Table 6.1: Human ventricular AP biomarker statistics and ranges.

upstroke velocity, time-to-peak, and resting membrane potential were not correlated with any other biomarkers. As expected, APD40, APD50 and APD90 were strongly positively correlated with each other. Triangulation 40-90 was weakly positively correlated with the three APD measures.

Overall, we find that each biomarker has a peaked distribution across the data, often with a long tail of high values for biomarkers measured in units of time or voltage gradient, possibly because these biomarkers are bounded by a minimum value of 0. We also find that biomarkers are not correlated with one another, except for measures of APD, which have a strong correlation with one another, as expected. This suggests that our selection of biomarkers are not redundant with one another, and that most biomarkers, except for the different APD measures, are giving us unique information about the properties of the AP.

6.3.3 Variability of APD in response to drugs

After characterising the variability present in the data set under control conditions, we performed a preliminary study of the drug block experiments we had available. This was to understand how variable the AP response of human cardiac cells to drugs was, and to aid us in designing simulation studies of drug effects, using a population of models calibrated with the ranges we had extracted from the control conditions part of the data set.

We began by quantifying the effects of dofetilide, the same I_{Kr} blocking drug used in Chapter 5, on APD90. We chose dofetilide because there were a large number of experiments using it in the data set, its effect as an I_{Kr} blocker is well known, and because we had successfully predicted its effects in rabbit Purkinje study in Chapter 6. We analysed experiments on 16 preparations where dofetilide was applied at a concentration of 50 nM, which is approximately 2-4 times the reported IC50 of the drug, corresponding to a block of the I_{Kr} current of between 60-90% (e.g. an IC50 of 12 nM was reported by Snyders and Chaudhary (1996) from Xenopus oocytes expressing the hERG gene, which is responsible for encoding the ion channel through which

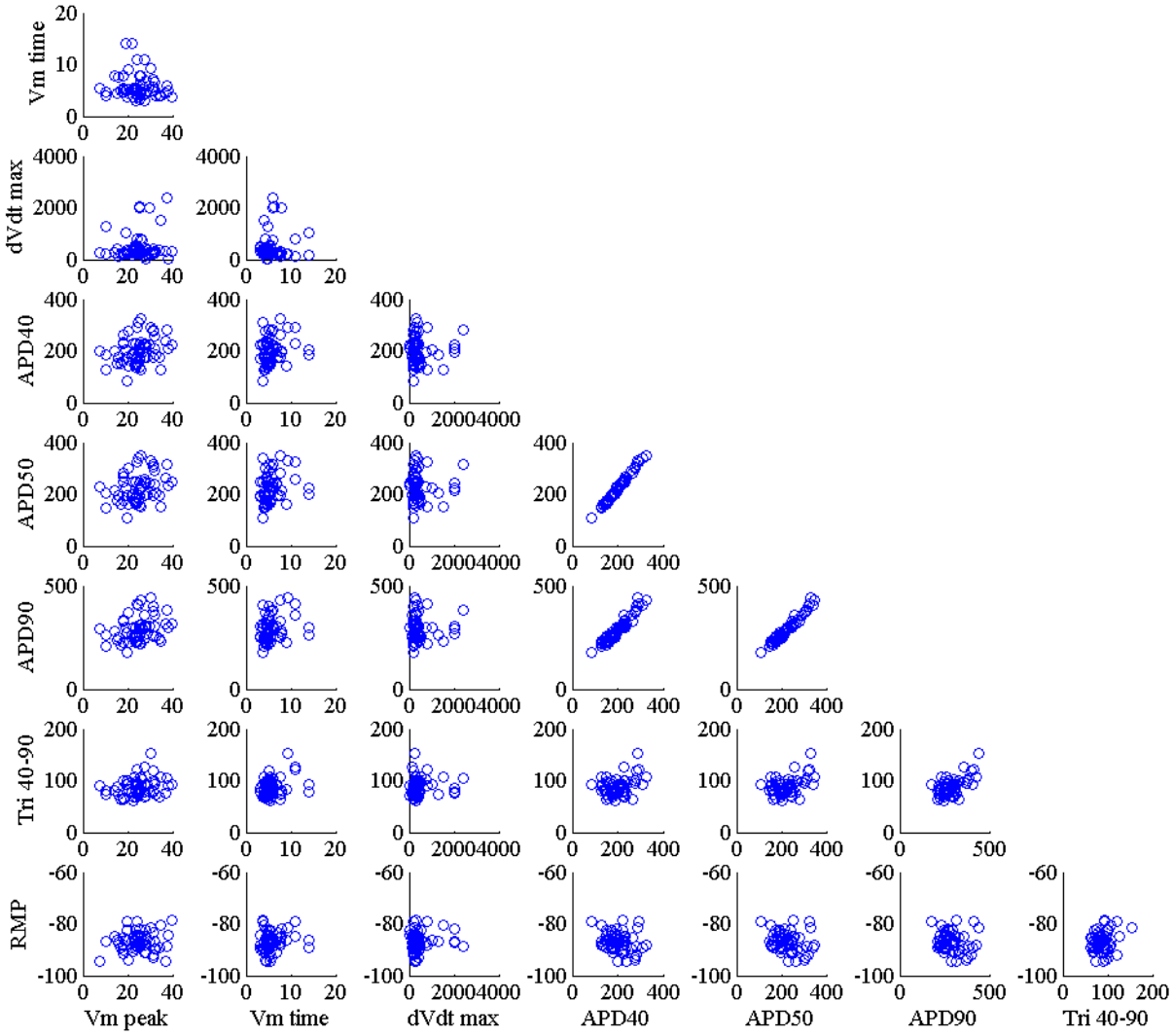

Figure 6.3: Scatter plots of each possible pair of biomarkers for control conditions experiments at 1 Hz pacing. Clear correlations can be seen between different APD measures, but not between any other biomarkers. Maximum upstroke velocity (dVdt max) was excluded from further analysis due to the presence of a number of extremely high values that are believed to be recording artifacts.

I_{Kr} flows in humans).

Effect of dofetilide over time

Unlike the study in Chapter 5, we had no defined equilibration period after the drug was first applied, so we initially looked at how APD90 changed over time after dofetilide was first applied to determine how long it took for the preparation's APD90 to stabilise again at a new steady value. APD90 values across 16 different experiments, for a dofetilide concentration of 50 nM, are shown in Figure 6.4. We see significant variability both in the total amount of prolongation experienced, and the time to reach a stable level of prolongation. APD90 rises gradually over 60-80 minutes for some preparations, and rises rapidly in the first 20-30 minutes for others. Therefore, if we use these drug experiments in the future, to generate calibration ranges or compare to predictions, we should check on an experiment by experiment basis that the AP biomarkers being used have stabilised by the end of the recorded experiment. Otherwise, because for our investigations we are usually interested in the effects of drugs in a steady state, rather than their effects over time, the change in biomarker values caused by the drug could be underestimated.

The amount APD90 was prolonged by dofetilide was highly variable - mean control APD90 (for just the preparations used in these dofetilide experiments, n=16) was 318 $\pm$ 59 ms, mean APD90 following dofetilide application was 475 $\pm$ 86 ms, and mean APD90 prolongation was 156 $\pm$ 68 ms, with a lowest value of 49 ms and a highest value of 286 ms. Control APD was uncorrelated with APD prolongation, as shown in Figure 6.5, which is consistent with our previous work in Chapter 6 and other studies (Kannankeril et al. (2011); Sarkar and Sobie (2011)).

Range of APD prolongation by dofetilide and HMR-1556 at multiple concentrations

Figure 6.6 shows the change in APD90 for experiments using the two drugs in our currently extracted portion of the database that have at least five experiments available at the same con-

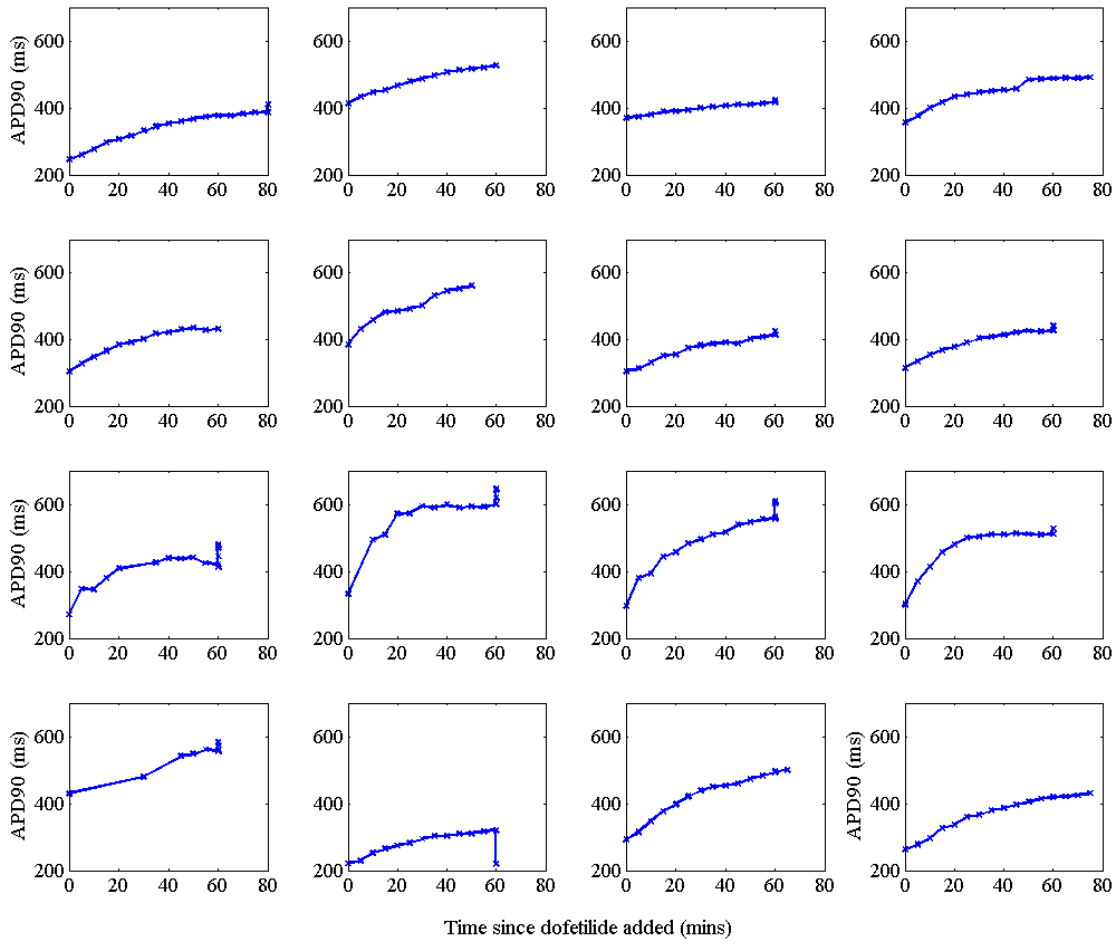

Figure 6.4: APD90 recorded during superfusion of 50 nM dofetilide on different 16 tissue preparations, from initial application to up to 80 minutes of superfusion.

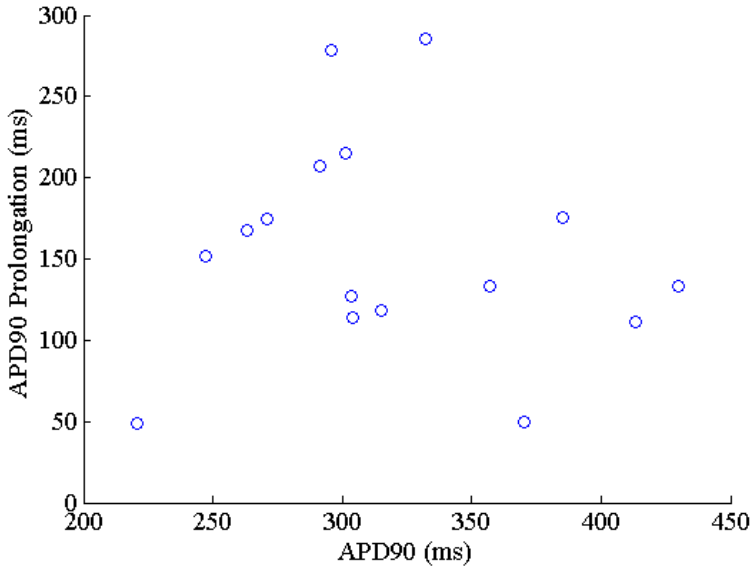

Figure 6.5: APD90 in control conditions plotted against prolongation of APD90 following application of 50 nM concentration of dofetilide, for 16 different experiments. Control and dofetilide APD90 values were calculated using their values at the latest recorded time under each set of conditions (minimum 50 minutes since first application for dofetilide). No clear correlation can be seen between APD90 in control conditions and the amount APD prolongation.

centration of the drug. These are drugs are: dofetilide, which in human, as in rabbit, selectively blocks I_{Kr} , and HMR-1556, which selectively blocks I_{Ks} .

We can clearly see the effect increased number of experiments have on increasing the range of variability by comparing the 50 nM concentrations of dofetilide, for which there are the most (16) experiments, against the two lower (10 and 30 nM) and two higher concentrations (100 nM, 1 μM), for which there are 3 experiments for each concentration. The range of prolongation we see at 50 nM spans the combined range of the experiments on the other four concentrations, due to 4 outlier experiments, 2 with very low levels of prolongation and 2 with very high levels of prolongation. However, there is still a trend of increasing average APD prolongation as dofetilide concentration increases, as we would expect.

For HMR-1556, which blocks I_{Ks} with a reported IC50 of 120 nM (Gögelein et al. (2000)), we see that despite the fact that I_{Ks} block is associated with a small degree of APD prolongation in humans (Jost et al. (2005)), the data, even at the higher 1 μM dose, includes both experi-

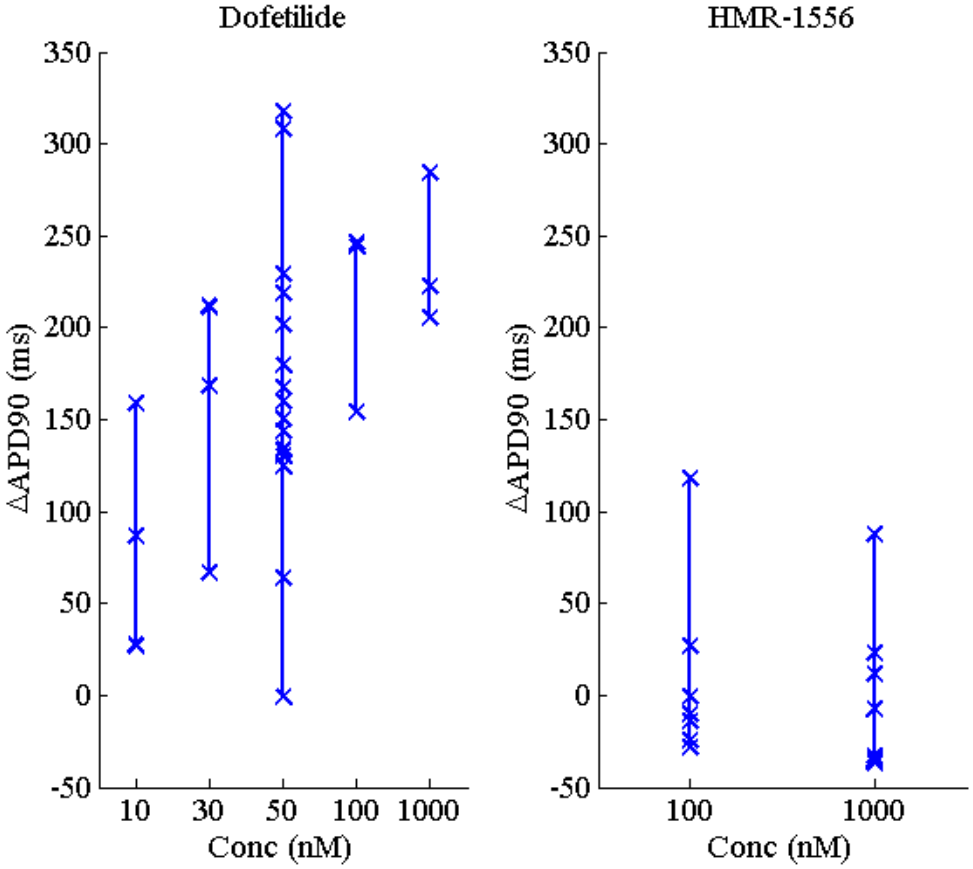

Figure 6.6: APD prolongation caused by different concentrations of dofetilide and HMR-1556. Crosses show APD prolongation from individual experiment, while lines show the total range of prolongation seen at a particular concentration across currently extracted data.

ments where a small amount of APD shortening occurred, and where APD prolongation was significant (>100 ms for one preparation). These effects could be a combination of experimental artifacts and stochastic variability in APD. However, they could also be due to intrinsic variability between different preparations.

Therefore, even a well-understood and selective drug with a small average effect can cause a significantly different response in outlying preparations, and potentially in outlying individuals, compared to its typical effect. We do not currently understand what differentiates cardiac cells that produce a response to a drug that is close to the mean response, and cells that produce outlying behaviours that could be significantly more pro-arrhythmic (e.g. higher APD90 prolongation). However, in the next chapter of this thesis, we will use our population of models methodology to investigate what the potential mechanisms that underlie these differences in AP response could be.

6.4 Conclusions

In this chapter, we analysed a database of microelectrode recordings from human ventricular tissue preparations, in control conditions and under drug block. We developed tools to extract the data set into a database of AP traces we could calculate AP biomarker values from. We used the biomarker values from the control conditions experiments we had extracted to generate a set of calibration ranges, which can be used to develop experimentally-calibrated population of human cell models.

We then characterised the distribution of AP biomarkers across the data set in control conditions. Overall we found that all biomarkers had peaked distributions, with even distributions either side of the mean for measures of membrane potential (Vm Peak, RMP) and lopsided distributions for measures of time that were bounded at 0 (Vm Time, APD, Triangulation). Biomarkers were uncorrelated with each other, except for measures of APD, which were posi-

tively correlated with each other as we would expect.

Finally, we looked at how dofetilide and HMR-1556, two selective potassium channel blocking drugs, affected APD90. These drug experiments illustrated the challenges of using experimentally-calibrated populations of models to quantitatively predict drug effects.

The first challenge is that without large sample sizes (typically not available in cardiac electrophysiology) it is difficult to differentiate between outlier results that are outliers due to non-physiological factors (e.g. a damaged preparation) and outliers that are due to inherent biological mechanisms that we want to understand and investigate with our models.

The second challenge is validating quantitative predictions of drug effects without well-specified concentration-response curves and derived IC50 values, as small changes in IC50, for drug concentrations close to the IC50, can have a large effect on predicted block amount. IC50 values obtained from the literature can vary widely. For example, Polak et al. (2009) collated the results of a large number of studies that measured IC50s for ion channel blockade of the hERG channel (I_{Kr} in humans). Their study showed that measured IC50 values in the literature can vary considerably between different studies performed under small variations in experimental conditions, and this leads to a corresponding uncertainty in the block effect a given drug concentration should be modelled as. In Chapter 6, we had direct experimental characterisation of the IC50 of dofetilide on I_{Kr} provided to us by our collaborators. This IC50 was calculated from experiments carried out in the same lab that performed the microelectrode experiment thats we used to develop our population of models and validate the population's predictions. This gave us confidence in the IC50 value and in our model predictions of APD response to dofetilide. These challenges make it difficult to predict quantitative ranges of drugs effects on human cardiomyocytes using the currently available data we have described in this chapter

In the next chapter, based on the data we have analysed and the calibration ranges we have developed in this chapter, we construct a population of human ventricular cell models. We

allow this population to cover a wide range of different possible cell models, by allowing parameter values to vary widely, as in Chapter 5, and we then use this population to investigate which ionic current conductances are important for determining susceptibility to drug-induced repolarisation abnormalities, such as alternans and EADs. In particular, we investigate which conductances, and what ranges of conductance values differentiate outlying models in the population, that display highly pro-arrhythmic reactions to drug block under a wide range of different block conditions, from the majority of models that produce less extreme responses.

7

Investigation into modulation of susceptibility to repolarisation abnormalities by inter-subject variability in human cardiomyocytes

7.1 Introduction

In the previous chapter, we described the extraction of a data set of human ventricular microelectrode recordings into a database that we then used to calculate action potential biomarker values and calibration ranges, with the intention of using them to develop an experimentally-calibrated human population of models. We then performed an analysis of the variability present across recordings from different hearts, in control conditions and in response to drug application, and found that in both control and drug application, there were significant outlying experiments that produced biomarker values that were far from the mean behaviour across the data set. The factors that could differentiate these outliers from preparations that produced behaviour close to the mean behaviour of the data set are currently not well-understood. This is primarily due to our lack of understanding of the mechanisms that govern inter-individual variability in cardiac electrophysiology.

In this chapter, we use the calibration ranges extracted in the last chapter to develop a human population of human cell models, and use this population to investigate how inter-subject vari-

ability can alter the susceptibility of human ventricular cardiomyocytes to repolarisation abnormalities. Abnormalities in cardiac repolarisation at the cellular level can lead to arrhythmias at the whole heart level. These unwanted abnormalities, including such phenomena as EADs and alternans, can be accidentally induced by therapies such as drug application, but their occurrence is rare and difficult to predict. A wide range of ionic mechanisms are known to contribute to the development of these abnormalities. These include reduced repolarisation reserve (Roden (1998)), L-type calcium current reactivation (January and Riddle (1989)), and changes in intracellular concentrations, driven by external changes or by a reduction in the sodium-calcium exchange current or sodium-potassium pump current (Weiss et al. (2010); Bueno-Orovio et al. (2014)). While each of these individual mechanisms have been extensively studied, understanding the interactions between these mechanisms and what contribution they make towards generating pro-arrhythmic abnormalities is challenging due to the substantial variability that exists between individual hearts.

Variability modulates the ionic current conductances of cardiomyocytes from different individuals. Cardiomyocytes have the capacity to alter the distributions of sarcolemmal ion channels in response to external stimuli (Nattel et al. (2010)), altering the conductances of affected currents. Changes in cardiac ion channel expression levels have been observed as part of circadian rhythms (Jeyaraj et al. (2012)); as a response to exposure to drugs (Xiao et al. (2008)); to sustained change in pacing rate (Qi et al. (2008)); to arrhythmias (Nattel et al. (2001, 2007)); and to disease (Nass et al. (2008); Michael et al. (2009)). Regulation of mRNA expression (Nattel et al. (2010)), and further regulation of mRNA by miRNA (Kim (2013)) are two methods cardiomyocytes use to regulate their complement of ion channels in response to persistent change in external conditions, but overall the underlying causes and effects of variability on sarcolemmal current conductances are not yet understood. This variation in the strengths of different ionic currents allows cardiomyocytes to adapt to changing conditions, but it also unpredictably affects the outcome of therapies such as drug application, which rely heavily on modulating

ionic current conductances.

The unpredictable response of the heart to drug therapies, in particular to block of IKr, lead to the hypothesis that differing levels of repolarisation reserve (Roden (1998)), a measure of the combined strength of available potassium currents active in phase 3 of the action potential, lead to differing individual responses to drug block. This hypothesis has been supported by experimental evidence for the role of IKs (Jost et al. (2005); Xiao et al. (2008)) as a backup current to IKr, and by computational work. Sarkar and Sobie demonstrated (Sarkar and Sobie (2011)) how modulation in the properties of many ionic currents, not just the repolarising potassium currents, can affect the level of APD prolongation seen in response to IKr block. However, to our knowledge no study has investigated how inter-subject variability modulates the generation of pro-arrhythmic repolarisation abnormalities such as EADs and alternans (Roden and Abraham (2011)).

In this chapter, we investigate how inter-subject variability in sarcolemmal current conductances modulates susceptibility to repolarisation abnormalities in human ventricular cardiomyocytes. In Chapter 5 we developed a modelling methodology for studying inter-subject variability, by building experimentally-calibrated populations of computational cardiac cell models, that combine the variation observed in experimental data with the ability to directly access underlying electrophysiological parameters that computational modelling offers. To understand which sarcolemmal current conductances confer susceptibility to repolarisation abnormalities, we apply our methodology to develop a population of human ventricular cells models using the data we analysed in Chapter 6. We assume that variation in sarcolemmal conductances, e.g. caused by variation in the number of ion channels in the cell membrane, drives variability between individuals at the level of the cellular action potential, while ion channel structure is largely conserved across individuals, leading to conserved ionic current kinetics, and therefore restricted variation across our population to the conductances of important ionic currents. We investigate how variability at the level of individual ionic currents leads to differences in the susceptibility of cell

models to developing repolarisation abnormalities in response to a diverse range of ionic current blockades and other pro-arrhythmic conditions. Analysis of the cell models in the population that are highly susceptible to repolarisation abnormalities following ionic current blockade reveals predictions for which combinations of ionic conductances are important for determining whether repolarisation abnormalities occur. We find that IKr block and uninhibited ICaL are required for repolarisation abnormalities, which in this study encompass alternans and early afterdepolarisations, to occur. However, for a cell model to be highly susceptible to these abnormalities, relative to the rest of the population, we find that it must also have a naturally low value one or more of the conductances of INaK, INCX, and IKr.

7.2 Methods

7.2.1 Experimental data acquisition and recording

The experimental data used in this study was obtained from microelectrode recordings of small tissue preparations from non-failing human right ventricular endocardium. Details of the preparation process and recording equipment can be found in Chapter 6 and in Jost et al. (2005).

Human right ventricular trabeculae and papillary tissue preparations of < 2 mm in diameter were used to generate the recordings used in this study. These preparations were dissected from non-failing human hearts, perfused and paced at 1 Hz. Action potential recordings were acquired from these preparations using conventional microelectrode techniques.

7.2.2 The ORd model

For this study, we used the O'Hara-Virag-Varro-Rudy (ORd) model of the human ventricular cardiomyocyte, in its default endocardial configuration, as our baseline cell model.

The model is divided into four compartments - two compartments for the cell itself, representing the bulk cytoplasm and the subspace near the T-tubules, and two compartments for the

sarcoplasmic reticulum (SR) - the junctional SR and the network SR. Currents that flow through the bulk cytoplasm in the model are: INa, the fast sodium current; INaL, the late sodium current; Ito, the transient outward potassium current; IKr and IKs, the rapid and slow delayed rectifier potassium currents; IK1, the inward rectifier potassium current; INab, ICab and IKb, the background currents; 80% of INCX, the sodium-calcium exchange current; IpCa, the sarcolemmal calcium pump current and INaK, the sodium-potassium pump current. Currents that flow through the T-tubule subspace area of the membrane are: ICaL, the L-type calcium current and 20% of INCX. Intracellular calcium handling is also modelled: calcium is taken up into the network SR by SERCA, diffuses into the junctional SR where it is released by ryanodine receptors and can diffuse between the bulk and subspace compartments. Diffusion of sodium, potassium and calcium ions between the bulk and subspace cytoplasm is also modelled.

7.2.3 Model alterations to match experimental preparations

As the experimental data used in this study comes from small tissue samples, rather than single cells, we adopted the biphasic stimulus protocol suggested by Livshitz and Rudy (2009), in order to simulate the electrotonic interactions between coupled myocytes. In their biphasic protocol, after the standard inward square wave of current injection, there is an outward square wave covering the period between the end of the inward stimulus and the beginning of the next stimulus. The amplitude of this outward component is set so that the net injection of stimulus current into the cell, per stimulus, is 0. This reflects a key electrophysiological difference between isolated cardiomyocytes and small tissue preparations - in the latter the charge injected by the stimulus current can flow into the surrounding tissue. By using a biphasic stimulus we aim to incorporate the current sink property of cardiac tissue into our cellular models.

The formula for the biphasic stimulus current, I_{st}, is:

$$\text{if:} t <= \text{stimDur}, I_{st} = \text{amp}, \tag{7.1}$$

$$\text{if:} t > \text{stimDur}, I_{st} = \frac{-\text{amp}}{PCL - \text{stimDur}}. \tag{7.2}$$

Where t is the time measured from the beginning of the current pacing cycle, amp is the stimulus amplitude, stimDur is the duration of the initial inward stimulus, and PCL is the pacing cycle length. For this study, amp $= -80\text{AF}^{-1}$ and stimDur $= 0.5$ms (the default values from the ORd model).

Additionally, we altered the behaviour of the h gate of the fast sodium current in order to bring the peak membrane potential down to the range seen in our experimental data, as the baseline ORd model has a higher peak membrane potential than the highest value seen across our set of recordings. The initial formulation of the h gate and phosphorylated h gate was:

$$h_{ss} = \frac{1.0}{1 + e^{\frac{V_m + 82.90}{6.086}}}, \tag{7.3}$$

$$h_{ssp} = \frac{1.0}{1 + e^{\frac{V_m + 89.1}{6.086}}}, \tag{7.4}$$

where V_m is the membrane potential, h_{ss} is the steady state value of the h gate, and h_{ssp} is the steady state value of the phosphorylated h gate.

Our formulation is:

$$h_{ss} = \frac{1.0}{1 + e^{\frac{V_m + 78.4893}{6.2248}}}, \tag{7.5}$$

$$h_{ssp} = \frac{1.0}{1 + e^{\frac{V_m + 84.689}{6.2248}}}. \tag{7.6}$$

7.2.4 Creation of candidate models

To construct the population of models used in this study, we first generated 10,000 parameter sets using Latin hypercube sampling (LHS) as described in Chapter 3. Each parameter set con-

tained 9 conductance scaling values, for the 9 key sarcolemmal currents in the ORd model that were varied in our study, based on our assumption that these conductances are highly variable due to both intracellular factors and response to external stimuli. The currents that we varied were: the fast sodium current; the late sodium current; the L-type calcium current; the transient outward potassium current; the rapid delayed rectifier potassium current, the slow delayed rectifier potassium current; the inward rectifier potassium current; the sodium-calcium exchange current; and the sodium-potassium pump current. The conductances for each of these currents were scaled by the relevant scaling value in each parameter set to create a pool of 10,000 different candidate models sharing the same equations but with different conductances.

7.2.5 Parameter sampling using the Latin hypercube sampling method

As in Chapter 5, we used Latin hypercube sampling to generate the candidate models for our study. We chose the relatively wide sampling range of 0 to 2 times the baseline parameter value because we wanted to allow models with a wide variety of underlying ionic current configurations to potentially be accepted into the population if they passed the filtering process. An extreme value close to 0 represents almost complete inhibition or lack of expression of the current in the cell. This can occur due to a genetic mutation that leads to loss of function for the channel carrying that current, or due to diseases that induce channel expression remodelling, e.g. Farid et al. (2011). Conductance values at the high end of the sample range can represent stimulation of channel activity under physiological conditions, e.g. beta adrenergic stimulation, or could reflect remodelling that significantly upregulates a particular channel type.

7.2.6 Filtering process used to determine which models were accepted into the population of models

Biomarkers

We used seven biomarkers of action potential behaviour, to determine whether a model pro-

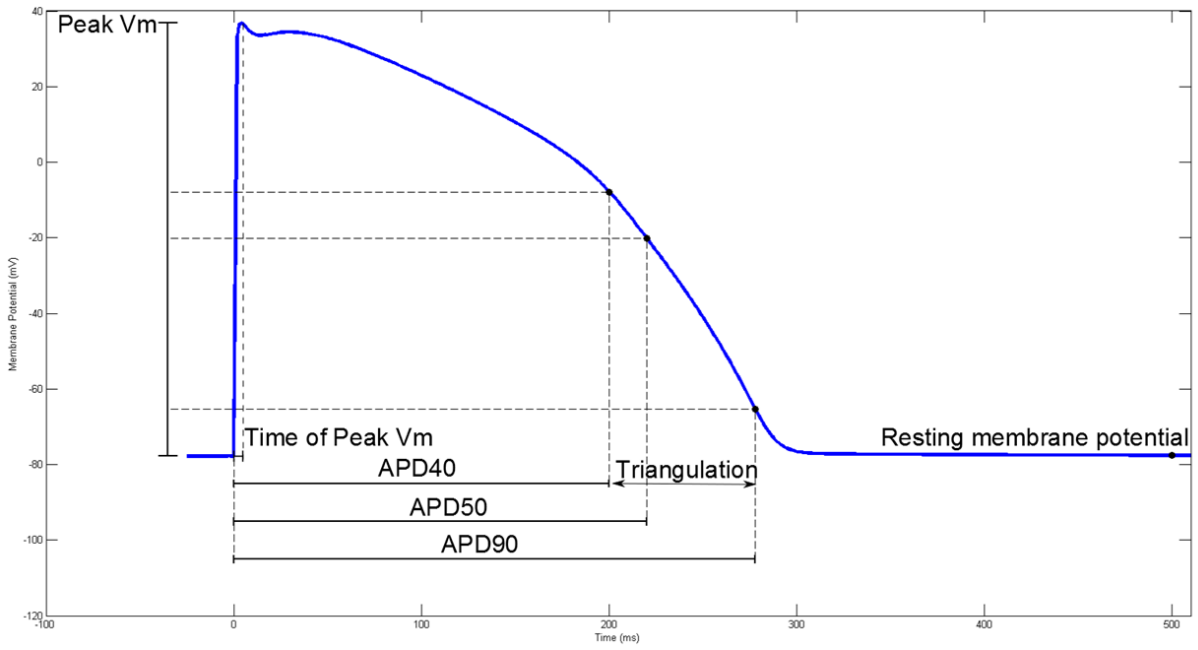

Figure 7.1: Representation of each of the biomarkers used as filters in this study. The trace was obtained from a model in the population used in this study, from a simulation of 1 Hz pacing in control conditions.

duced electrophysiological behaviour that was consistent with our experimental data. For each biomarker, experimental ranges were calculated by the minimum and maximum values, as seen across our dataset at 1 Hz control conditions pacing, after excluding clear outliers. These values were generated for each experiment by taking the value of each biomarker in the final recorded trace of the control portion of each experiment. The biomarkers we used in this study were: peak membrane potential (Vm Peak); peak membrane time (Vm Time); action potential duration at 40%/50%/90% repolarisation (APD40/50/90); Triangulation 90-40; and resting membrane potential (RMP). Figure 7.1 illustrates each biomarker and its position in the action potential.

Alternans

Additionally, the final 2 simulated beats of each model, paced at 1 Hz, were checked for alternans. If APD90 differed by 5 ms or more between these 2 beats, the model was rejected from the population. This criterion was chosen to ensure no models displayed repolarisation

abnormalities under control conditions at a moderate pacing rate, prior to any channel block.

To generate the population of models, we filtered the candidate group of 10,000 models using the above filters, with biomarker values obtained from control from our experimental data set. Performing this filtering process led to a total of 568 models of the initial 10,000 being accepted and these models formed the population of models used in this study. Each of these models had a different set of conductances, but all were consistent with the range of experimental variability observed in our data.

7.2.7 Software and computational methods

Simulations were carried out on a 4-core desktop running a Linux operating system. The CVODE adaptive time step ODE solver library was used to solve the model equations, running within CHASTE (Pitt-Francis et al. (2009)), an open source computational biology software package. Data analysis and analysis of simulation results were carried out in MATLAB (MathsWorks Inc., Natick, MA).

The final two pacing cycles of each simulation on each model were saved and used to determine biomarker values for that simulation and model, as well as further analysis such as abnormality detection.

7.2.8 Detection of repolarisation abnormalities

We developed algorithms to detect 2 classes of repolarisation abnormality in this study: alternans and EADs.

Alternans detection was done by calculating APD90 from the final two pacing cycles of a simulation, and taking the difference between them. If the absolute difference $|\text{APD90}_n - \text{APD90}_{n-1}|$ between the last two beats in the pacing train was greater than or equal to 5 ms, the model was classed as displaying alternans.

EAD detection was performed by analysing the voltage-time gradient of the final two pacing cycles of a simulation. If, for either pacing cycle, a positive gradient of greater than 0.02 mV/ms was detected in the portion of the trace that occurred more than 100 ms after the initial upstroke occurred (as determined by the Vm Time biomarker), that model was classified as displaying EADs. We used the Vm Time + 100 ms criteria in order to avoid models with either delayed initial upstroke, or spike and dome configurations from being misclassified as displaying EADs.

7.3 Results

7.3.1 Properties of the population of human ventricular cell models

Voltage traces from each model in the population, representative experimental traces, and the trace from the ORd baseline model are shown in Figure 7.2. The population of models spans the range of variation seen in the experimental traces. The ORd baseline model has a slightly higher peak membrane potential (45.6 mV) than the highest values seen in our data (39.6 mV), but otherwise would be a viable model if it was included in our population.

Figure 7.3 displays how biomarker values from individual models in the population (white dots) and individual experiments (red crosses) span the experimentally-determined range. Across the population, most biomarkers have good coverage of the experimental range and overlap with biomarker values from the experimental data. The distributions of each biomarker across the population of models are shown in Figure 7.4.

The distribution of ionic conductances within the population of models is shown in Figure 7.5. Most of the parameters span the full sampled range (0 to 2 times the ORd model's baseline value for that conductance). However, GNa, GCaL and GKr are limited to a subset of the sampled range by the calibration process. GNa is confined to the smallest range, 92% of the models in the population have GNa values that are clustered between 0.2 and 1 (conductances are given as fractions of the baseline ORd model's value for that conductance). GCaL values are densely

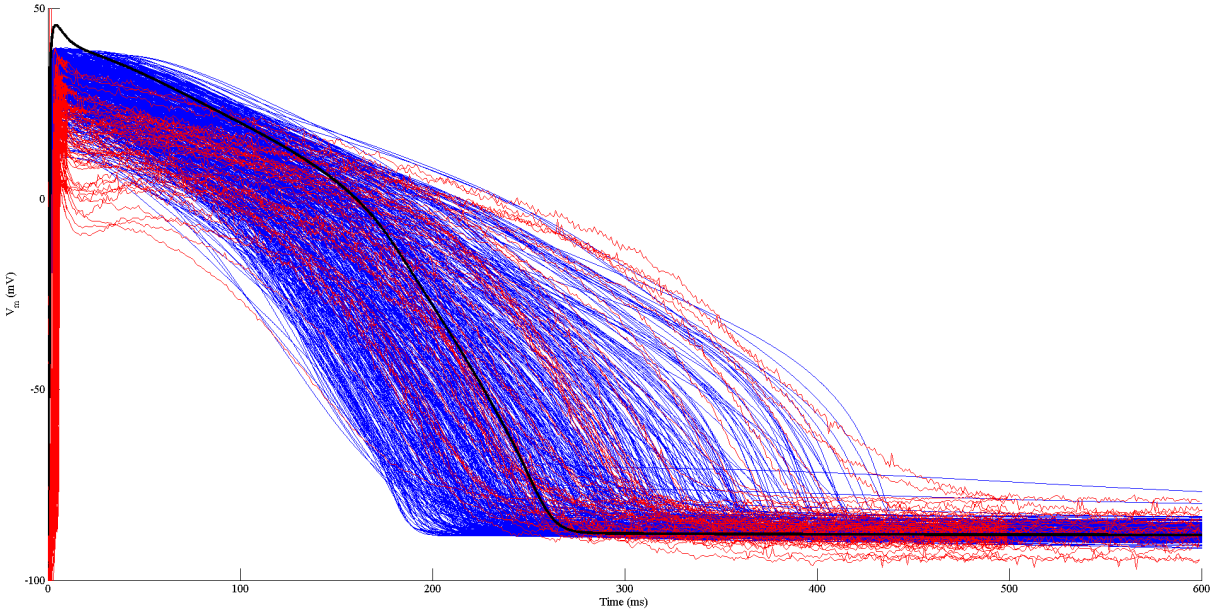

Figure 7.2: Action potentials obtained from experimental recordings (red; n= 59, 3 outliers excluded), simulations using the models found to be within the experimental range (blue; n = 568), and the baseline ORd model (black), at 1 Hz pacing.

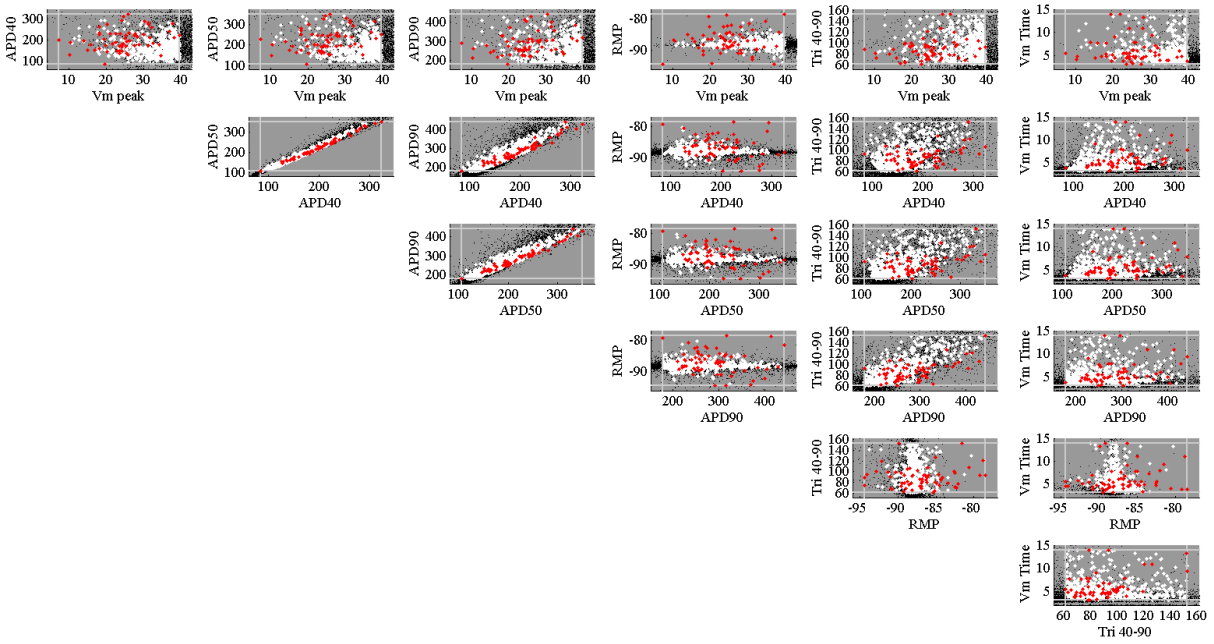

Figure 7.3: Scatter plots showing biomarker values for models accepted into the population of models (white dots), models rejected from the population (black dots), experiments (red dots) and calibration ranges for each biomarker (grey lines). Each plot shows results for a pair of biomarkers.

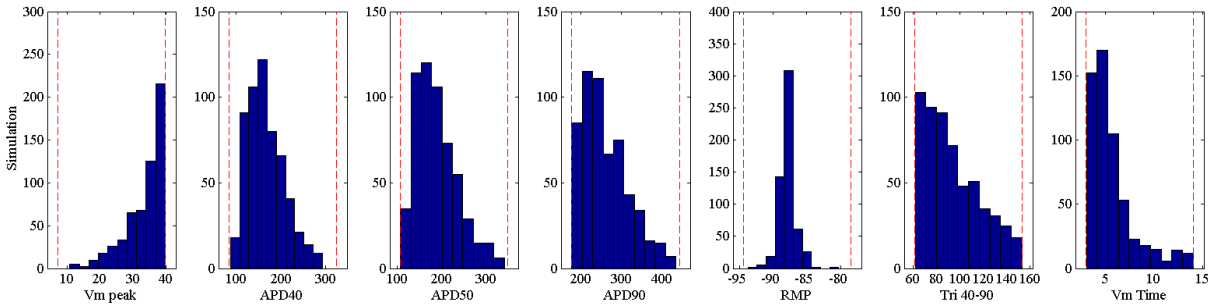

Figure 7.4: Histograms showing distribution of each biomarker across the population of models. Dashed lines indicate the experimental range used to determine whether each model is accepted into the population.

distributed between 0 and 1 (81% of population), with few models having higher GCaL values. Low values of GKr, below 0.13, are not present in the population, but the distribution of GKr values spans the rest of the sampled range, indicating that a certain minimum amount of IKr is necessary in the cell for successful repolarisation under normal conditions.

Certain pairs of conductances display moderate to weak correlations with one another, which also constrains the observed parameter distribution of the population. We used partial correlation coefficients (described in Chapter 3) to give a measure of correlation between parameters after accounting for the effects of the other varied parameters. We found moderate negative correlation between GNa and PNaK (-0.50), and between GKr and GK1 (-0.41). There was weak positive correlations between GNa and GCaL (0.27), GNa and GNCX(0.16), GKr and GNaL (0.16), and GKr and GNCX (0.15). All correlations had $p < (0.05/36)$, which was set as the significance limit because we tested for correlation between the 36 possible unique pairs of the 9 varied parameters.

We see that most conductances are not correlated with one another and a wide range of conductance profiles give behaviour consistent with experiment. This demonstrates that underlying a normal action potential, there can be a wide variety of different balances of ionic currents generating it, with potentially very different responses to changing conditions. However, there are two significant, moderately strong negative correlations within the population. The first corre-

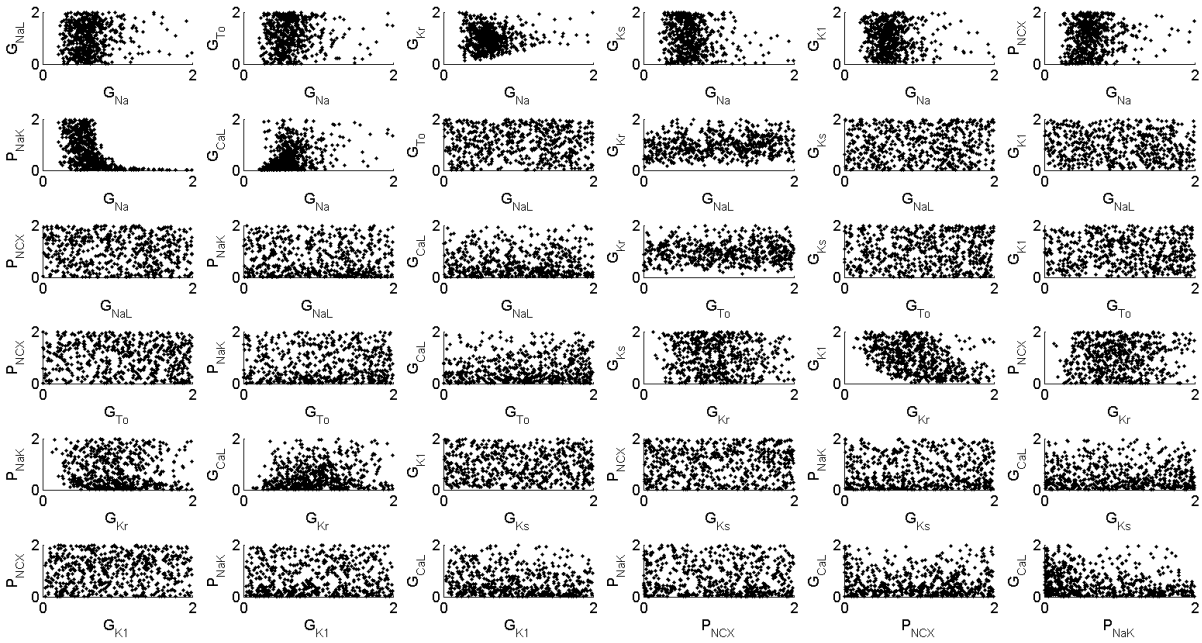

Figure 7.5: Scatter plots showing conductance scaling values for models accepted into the population of models. Each plot shows values for a pair of conductances. The scale of each plot is the sampled range for those 2 conductances: 0 to 2 times the baseline value of those conductances in the ORd baseline model.

lation, between GKr and GK1, likely reflects the need to have a certain amount of repolarisation reserve in a viable cardiomyocyte, as both the rapid delayed rectifier potassium current (IKr) and the inward rectifier potassium current (IK1) are currents that are important for repolarisation. If one of these currents is particularly small, the other must be large enough to compensate. The correlation between GNa and PNaK is primarily due to a group of models in the population with very low sodium-potassium pump current (INaK) and high fast sodium current (INa). Low INaK prevents the cell from pumping excess sodium out of the cell, which then accumulates. This can decrease the electrochemical gradient that causes sodium to flow into the cell through sodium channels. Therefore, models with inhibited sodium-potassium pump currents appear to need increased fast sodium current relative to the majority of the population in order to produce a physiological action potential in control conditions.

7.3.2 Classification of repolarisation abnormalities

In this study we investigated how variability in the sarcolemmal conductances of human ventricular cardiomyocytes affected their ability to successfully repolarise when one or more ionic current were inhibited. In order to investigate repolarisation, we defined two main categories of repolarisation abnormality that we aimed to detect in our population - alternans and afterdepolarisations (see Methods for details). Figure 7.6 shows an example of each of these repolarisation abnormalities.

7.3.3 Revealing susceptibility to repolarisation abnormalities using a systematic study of multichannel block

We performed a simulation study systematically investigating the effects of two-current combinations of different ionic current blocks at a variety of blocking levels. We chose to investigate the following ionic currents: the rapid delayed rectifier current (IKr), the L-type calcium current (ICaL), the slow delayed rectifier current (IKs), and the inward rectifier current (IK1), due to their known roles in repolarisation.

We simulated the effects on the population of models of each possible 2 current combination of these 4 currents, and for each combination simulated the effects of 4 levels of current block: 25%, 50%, 75% and 90% block. We simulated the effects of each possible combination of current and block level. Therefore, with 6 possible current pairings, and 16 pairings of block level, we ran 96 simulations on our population of 568 models. We then analysed these simulations to determine a) the effect on repolarisation of each pair of channel blocks, and b) which underlying ionic parameters determined whether a given model was susceptible to repolarisation abnormalities under a range of different ionic current blocks.

The number of models in the population that generated abnormalities, for each of the current and concentration combinations we simulated, is shown in Figure 7.7. We found that IKr block

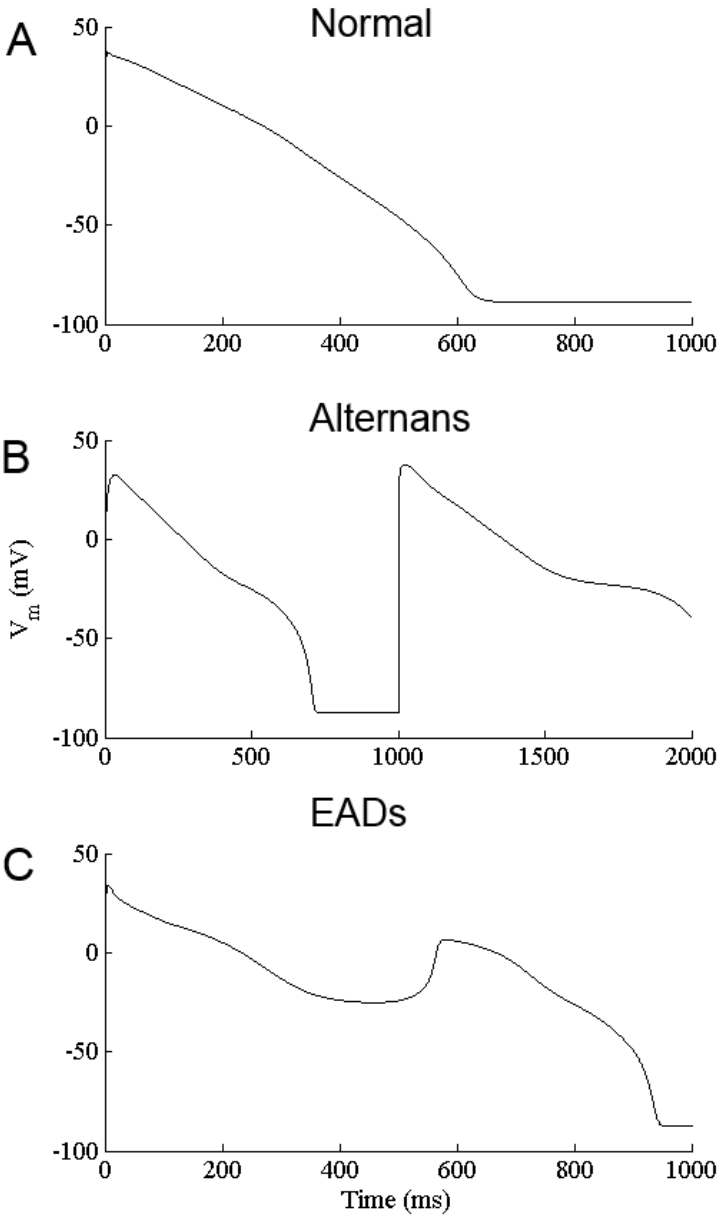

Figure 7.6: Example AP traces of the different repolarisation types: no repolarisation abnormalities (top), alternans (middle, final 2 beats of simulation shown), and EADs (bottom).

was the primary cause of abnormalities. Without some degree of IKr block, no abnormalities were observed across the population. Block of IK1 and IKs acted to augment IKr block, and increased the number of models that produced abnormalities, but were not sufficient to produce abnormalities without IKr block. ICaL block attenuated the effect of IKr block, reducing the number of abnormalities seen in the population. When IKr was 75% blocked, 50% block of ICaL was sufficient to abolish all afterdepolarisations and abolish alternans in all but one model. For 90% IKr block, 90% ICaL block was required to achieve the same effect. In both cases though, even 25% block of ICaL was enough to significantly reduce the total number of abnormal models in the population, from 23 to 6 for 75% IKr block, and from 108 to 39 for 90% IKr block. In general, when the population was exposed to both IKr and ICaL block, few models produced abnormalities.

Because ICaL block and IKr block had opposing effects on the generation of repolarisation abnormalities, we looked at how APD prolongation, another important pro-arrhythmic effect of channel blockade, was affected during combined block of ICaL and IKr. The distributions of APD prolongation observed across the population for the different combinations of ICaL/IKr block are shown in Figure 7.8, excluding the models in the population that displayed abnormalities, as afterdepolarisations make it difficult to calculate a meaningful APD90 from a voltage trace.

We found that IKr block, as expected, strongly increased APD prolongation as block level increased. We also found that variability in the amount of APD prolongation seen across the population increased as IKr block level increased. ICaL block, however, had only a small negative effect on APD prolongation. Unlike its effect on repolarisation abnormality occurrence, ICaL does not negate the prolongation caused by IKr block. Mean APD prolongation ranged from 18 ms at 90% ICaL block and 25% IKr block, up to a maximum of 338 ms at 25% ICaL block and 90% IKr block.

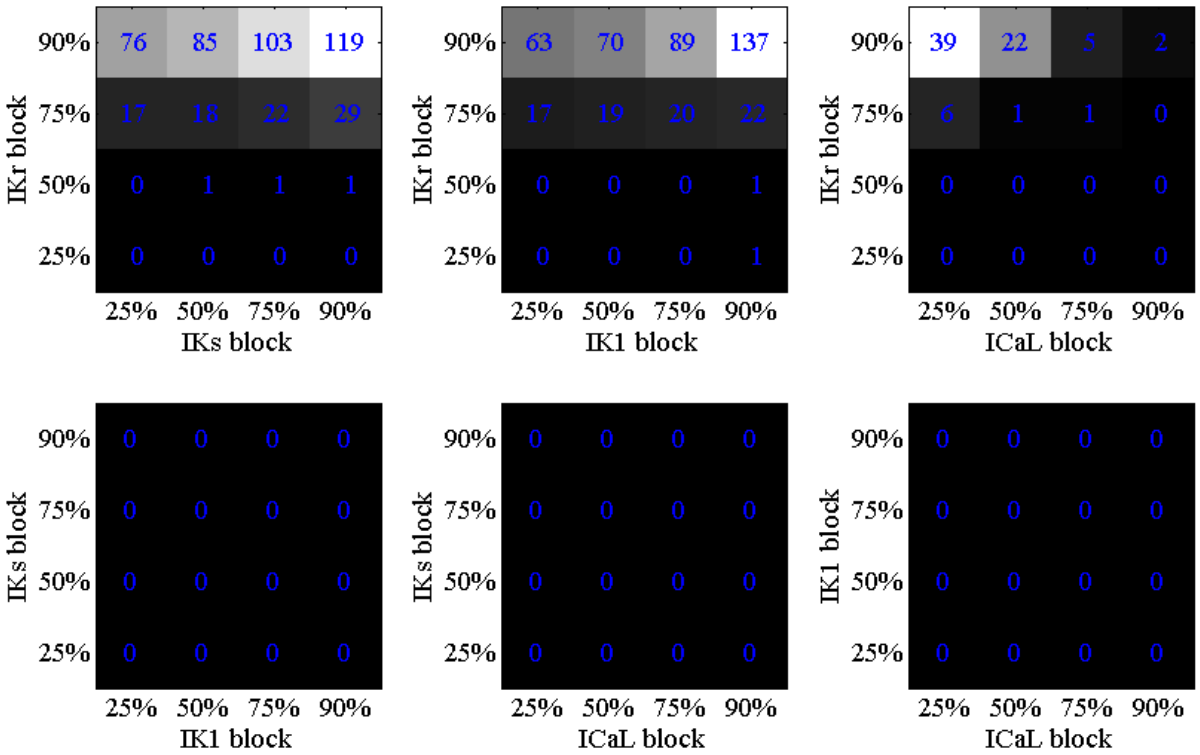

Figure 7.7: Incidence of repolarisation abnormalities across the population of models for each double channel block simulation carried out in this study. Each large square represents one of the 6 possible pairings of the 4 channel blocks investigated: IKr, IKs, IK1 and ICaL. Each of the squares within a large square represents a particular combination of block amounts for those two currents. Numbers in each square display the number of models (out of the 568 models in the population) that displayed repolarisation abnormalities in that simulation.

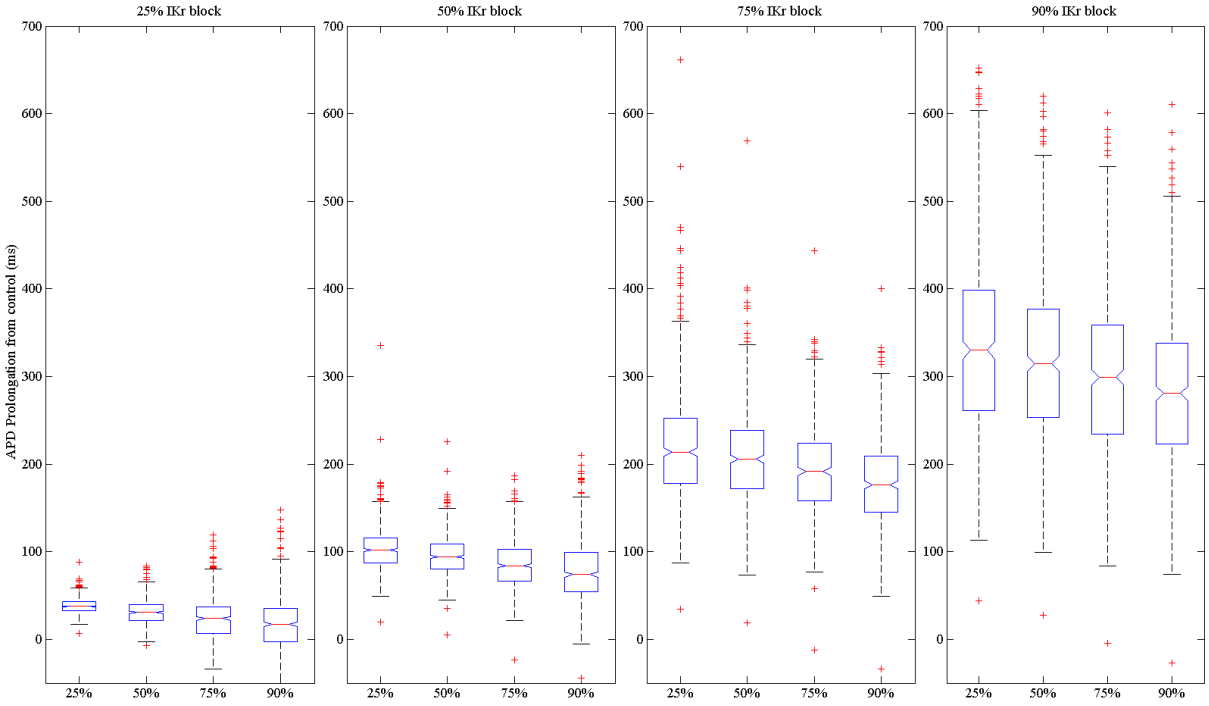

Figure 7.8: APD prolongation of the population as a whole in response to combined ICaL/IKr block. Each panel displays results from a particular level of IKr block, with each boxplot within a panel summarising results for increasing ICaL block. Each boxplot shows the median, quartiles, and outliers of the population's change in APD90 between control and a particular current block scenario. Models that displayed repolarisation abnormalities were excluded from these plots.

7.3.4 High L-type calcium current and low sodium-potassium pump current indicate particular susceptibility to repolarisation abnormalities

The second goal of this multichannel block study was to determine which combinations of ionic current strengths distinguished models that were susceptible to drug-induced repolarisation abnormalities from the models in the population that did not display abnormalities. Therefore, after simulating the effects of multiple combinations of ionic current blocks at varying strengths, we investigated whether there were particular conductance values or conductance value combinations that lead to increased susceptibility to repolarisation abnormalities.

To do this, we scored each model by the total number of simulations they showed abnormalities in. We ran 96 simulations, each on the whole population of models. 29 of these simulations caused one or more models in the population to develop abnormalities. The largest number of simulations that a particular model developed abnormalities in was 22. No abnormalities were seen in the simulations where IKr was not blocked by at least 50%.

Based on these scores, we classed models into 3 categories - those that showed no susceptibility to abnormalities in the multichannel block study (no abnormalities detected for that model in any of the simulations), those that showed some susceptibility (abnormalities detected in 1 to 9 of the simulations), and those that showed susceptibility to abnormalities in a wide range of conditions (abnormalities detected in 10 or more simulations). Figure 7.9 shows the conductances of models in the population, colour coded using this scheme. GCaL and PNaK appear to be the key discriminants between models that are highly susceptible to abnormalities and those that are not, as shown in more detail in Figure 7.10. Models with high GCaL and low PNaK make up the majority of highly susceptible models. We also see that there is no clear difference between models that were entirely unsusceptible to abnormalities and those that were in the intermediate category. Both of these sets of models have overlapping conductance distributions. The roles of the L-type calcium current and sodium-potassium pump current are consistent with previous

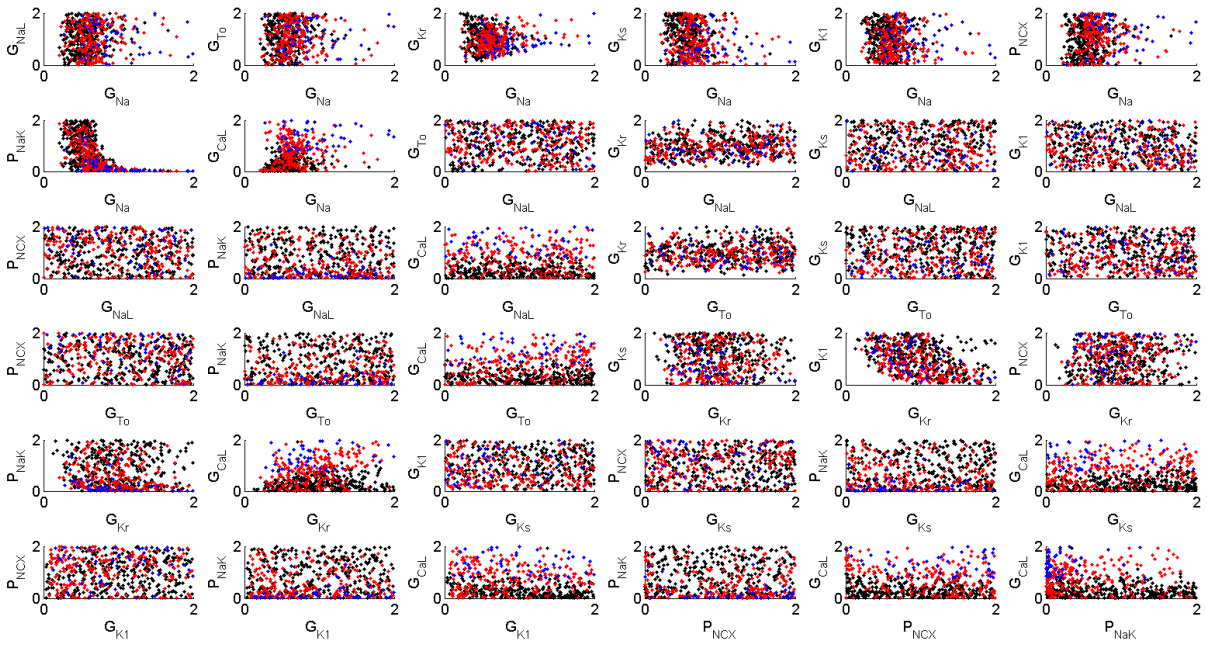

Figure 7.9: Conductance plots showing differences between models that are susceptible to repolarisation abnormalities and those that are not for all possible pairs of conductances varied across the population. Black dots show conductance scaling factors for models that developed repolarisation abnormalities in none of the multichannel block simulations, red dots show models that developed abnormalities in between 1 to 9 simulations and blue dots show models that developed abnormalities in 10 or more simulations.

findings. Reactivation of the L-type calcium current is the primary mechanism for EAD generation (Weiss et al. (2010)), while inhibition of the sodium-potassium pump is known to occur in a number of pro-arrhythmic disease conditions (Bueno-Orovio et al. (2014)).

We then checked to see whether the susceptibility of models could be distinguished prior to drug application by their control APD90 values. In Figure 7.11 we see no clear distinction between models that are highly susceptible to repolarisation abnormalities and those that are not, based on their APD90 values from control conditions pacing. The median APD90 value for high susceptible models is 293 ms compared to 244 ms for the rest of the population, but the variability of APD90 across both sets of models is too large for this difference to be used predictively.

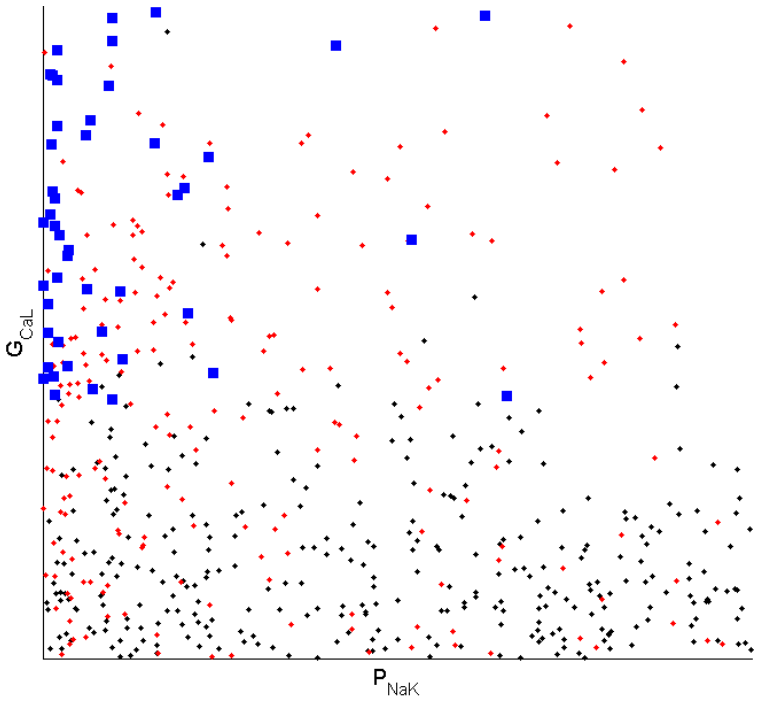

Figure 7.10: L-type calcium conductance against sodium-potassium pump permeability in the population, showing differences between models that are susceptible to repolarisation abnormalities and those that are not. Black dots show conductance scaling factors for models that developed repolarisation abnormalities in none of the multichannel block simulations, red dots show models that developed abnormalities in between 1 to 9 simulations and blue dots show models that developed abnormalities in 10 or more simulations.

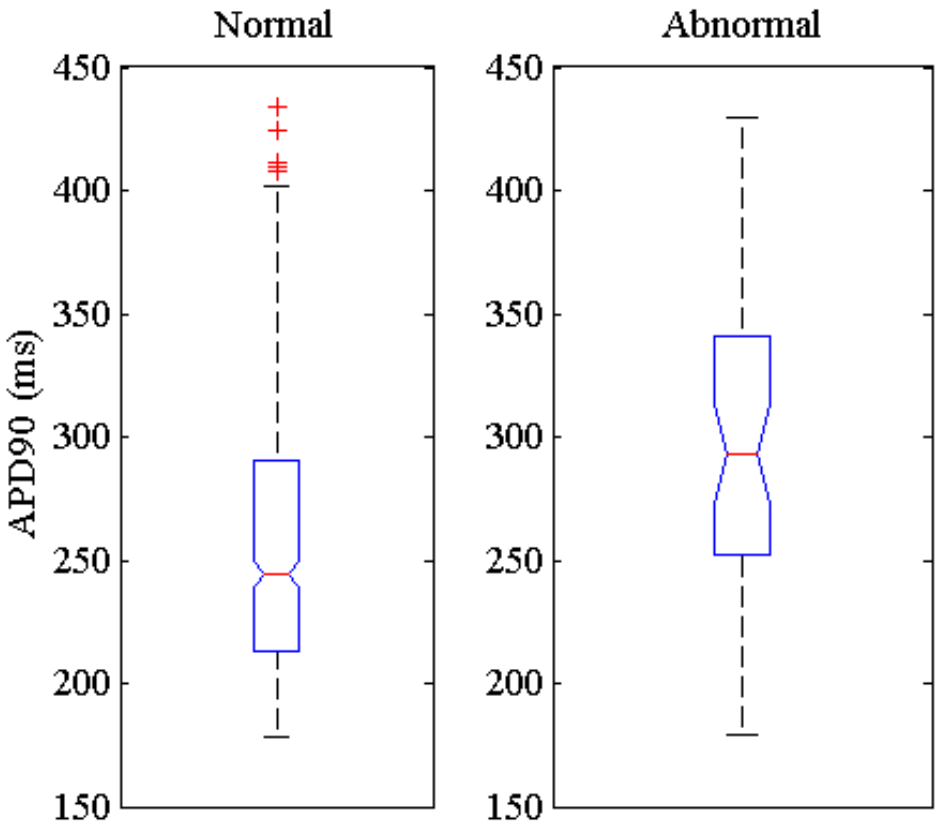

Figure 7.11: Boxplots showing the distributions of APD90 for the 46 models showing repolarisation abnormalities in 10 or more of the multichannel block simulations (right), and the other 522 models in the population (left).

7.3.5 Multiple ionic mechanisms are responsible for drug-induced repolarisation abnormalities

For the majority of models in the population that displayed abnormalities under a large number of the simulated drug block conditions, GNaK was scaled between 0 and 0.5 times its baseline value, suggesting that severely inhibited INaK was the primary mechanism leading to repolarisation abnormalities. Analysis of intracellular ionic concentrations across the population showed that when INaK was inhibited, it strongly increased the intracellular sodium concentration and also decreased the intracellular potassium concentration. An increased sodium concentration leads to increased calcium loading, as the sodium-calcium exchanger will exchange less sodium into the cell, resulting in less calcium leaving the cell. In combination with ICaL, this calcium loading can induce repolarisation abnormalities.

We can see in Figure 7.12 that while most of the highly susceptible models possessed extremely low sodium-potassium pump permeabilities, 4 out of the 46 highly susceptible models had PNaK scaling values greater than 0.5, which indicated they had a functioning INaK. Therefore, for these models we looked for one or more secondary mechanisms that were responsible for these models' high susceptibility to block-induced repolarisation abnormalities. For 3 of the 4 models with uncompromised INaK, GNCX was extremely low. These 3 models had GNCX scaling factors of 0.2, 0.06, and 0.01. Systolic and diastolic intracellular calcium levels were highly elevated in these models, and this lead to increased L-type calcium current and reactivation. The remaining model had functioning exchange currents (GNCX and PNaK scaling factors both above 0.5) but decreased IKr, with a GKr scaling factor of 0.37. For this model, susceptibility to abnormalities appeared to be caused by decreased repolarisation reserve. Abnormalities occurred when IKr and another repolarising potassium channel, either IKs or IK1, were both blocked, and when IKr alone was blocked at a high level (90%). In this case, delayed repolarisation due to decreased outward current caused ICaL to recover and reactivate, triggering a secondary depolarisation.

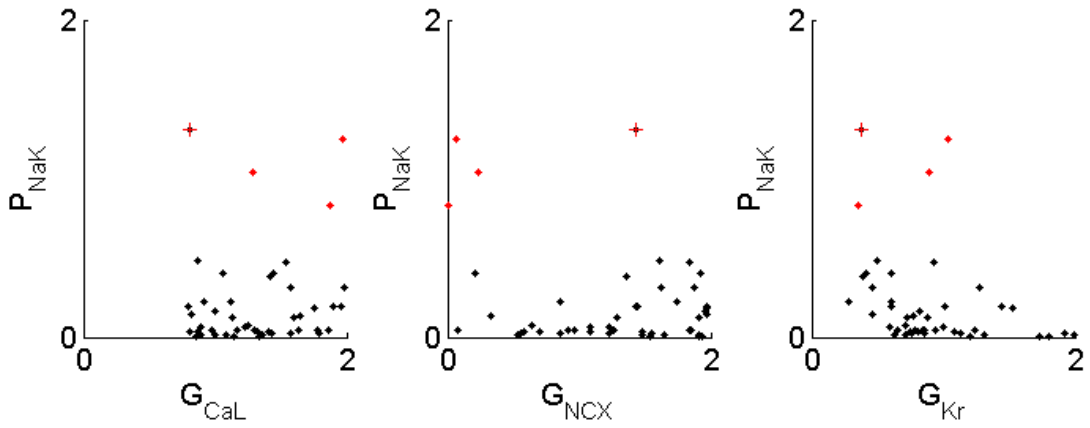

Figure 7.12: Values for selected conductances of the 46 models showing repolarisation abnormalities in 10 or more of the multichannel block simulations. The 4 models with PNaK scaling factor > 0.5 are highlighted in red. Three of these models have high inhibited INCX (GNCX scaling factor < 0.5, red dots), while the remaining highlighted model has GKr scaling factor < 0.5 (red cross).

Overall, highly susceptible models all possessed a functional L-type calcium current with an intermediate or greater conductance value. This appears necessary for a model to be highly susceptible to repolarisation abnormalities under the range of conditions tested in this simulation study. Additionally, all highly susceptible models possessed at least one of three ionic mechanisms underlying abnormalities: compromised INaK; compromised INCX; or compromised repolarisation reserve composed primarily of IKr but also IKs and IK1. Models required at least one of these mechanisms to be highly susceptible to abnormalities. The end cause of abnormalities is indicated to be a combination of ICaL reactivation, increased ICaL magnitude preventing repolarisation, and decreased repolarisation current delaying repolarisation. In almost all cases, block of ICaL was successful at limiting repolarisation abnormalities. The few cases where it was less successful (abnormalities caused by 90% IKr blocked were not abolished even at 75% or 90% ICaL block) were exclusively in models with GNaK scaling factor < 0.05, underlining the important role INaK inhibition played in the generation of repolarisation abnormalities in this study.

7.3.6 Effects of hypokalemia and rapid pacing on repolarisation

Several methods of inducing afterdepolarisations in isolated cardiomyocytes are known. In particular, hypokalemia (reduced extracellular potassium concentration) and calcium loading are known to induce EADs (Weiss et al. (2010)). Calcium loading is also known to increase the likelihood of DADs (Maruyama et al. (2010)). Hypokalemia is of additional interest due to the interaction between potassium levels and the sodium-potassium pump, which appears to be a key determinant of whether abnormalities occur in a given model in our population of models.

To investigate the effects of reduced extracellular potassium, we lowered its concentration across the population of models, from 5.4 mM to 4.0 mM. Under standard pacing at 1 Hz, no abnormalities were detected across the population of models. Mild hypokalemia alone was not sufficient to generate repolarisation abnormalities. We then repeated the simulations with additionally blocked IKr at levels of 25%, 50%, 75% and 90% block. We found a small increase in the number of abnormal models, relative to blocking IKr at control levels of extracellular potassium. These results are displayed in Table 7.1.

Our second investigation into increasing susceptibility to afterdepolarisations was to use fast pacing, in order to place each model in a state of increased calcium load, followed by an immediate decrease of the pacing rate at the end of the simulation. Calcium loading is known to be pro-arrhythmic and increases the likelihood of afterdepolarisation generation. We paced each model in the population for 1000 seconds at a pacing cycle length (PCL) of 400 ms, then for the final two beats of the simulation only, we increased the PCLto 1000 ms.

Fast pacing increased intracellular calcium concentrations across the population by an average factor of 2.4. 296 out of 568 models saw an average increase in calcium concentration of 50% or more compared to pacing at 1000 ms PCL.

Analysing the final two beats of each simulation, paced at a 1000 ms PCL following fast pacing, showed no development of afterdepolarisations across the population under conditions of no

Block level of IKr	Number of alternans models (out of 568)	Number of models with afterdepolarisations (out of 568)	Total number of abnormal models (out of 568)
Control $[K^+]_o(5.4\text{mM})$			
0%	0	0	0
25%	0	0	0
50%	0	0	0
75%	19	21	23
90%	59	101	108
Decreased $[K^+]_o(4.0\text{mM})$			
0%	0	0	0
25%	1	0	1
50%	5	5	6
75%	35	33	39
90%	86	121	136

Table 7.1: Effect of extracellular potassium on occurrence of repolarisation abnormalities in the population, following IKr block.

current inhibition. We did not look for alternans in this case, as all models were adapting to the sudden change in pacing frequency and so beat-to-beat APD90 was changing across all models due to restitution effects, regardless of the individual parameters of each model.

We then simulated the same protocol, additionally blocking IKr at levels of 25%, 50%, 75% and 90% inhibition of current. In this case, we found an increase in afterdepolarisation prevalence compared to IKr block alone. For IKr inhibition in combination with the calcium loading protocol, afterdepolarisation occurrence during these final two beats increased compared to IKr inhibition during steady 1 Hz pacing. At 75% block afterdepolarisation occurrence across the population increase from 4% to 14% of models, and at 90% block from 18% to 30%. The results from these simulations are displayed in Figure 7.13 and Table 7.2.

7.4 Discussion

Understanding how inter-subject variability modulates susceptibility to repolarisation abnormalities is important for determining whether an individual could be susceptible to ventricular

Block level of IKr	Number of models with afterdepolarisations (out of 568)
0%	0
25%	2
50%	17
75%	82
90%	171

Table 7.2: Combined effect of IKr block and 2.5 Hz pacing followed by sudden decrease of the pacing frequency to 1 Hz on repolarisation in the population. Alternans are not counted as an abnormality in this case due to restitution effects from the sudden change of pacing rate.

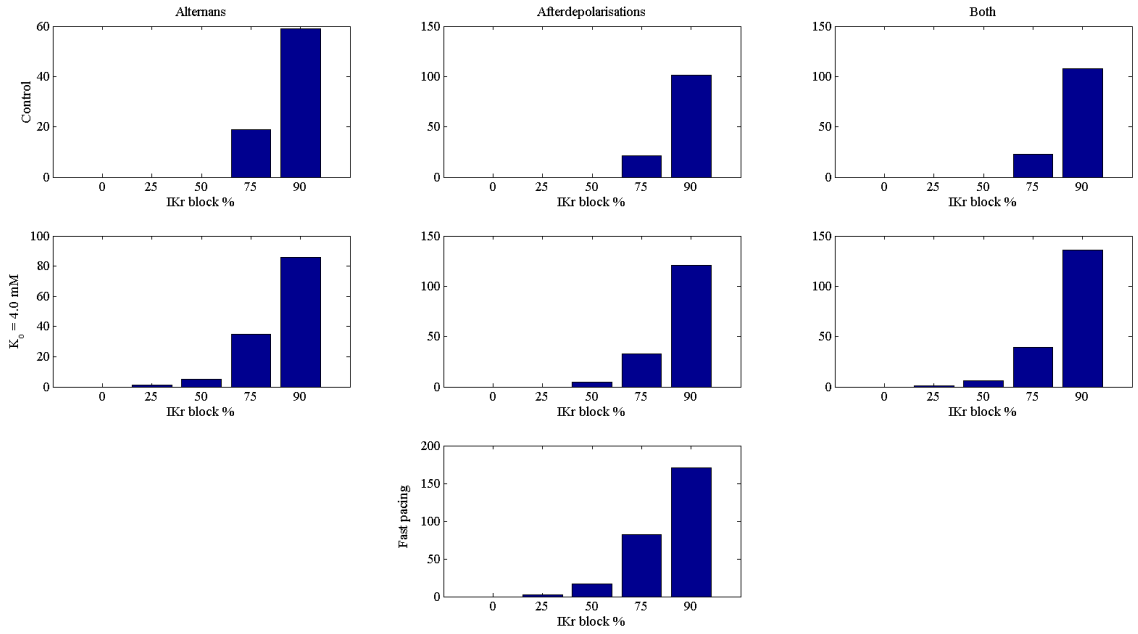

Figure 7.13: Histograms showing incidence of alternans, afterdepolarisations, and both abnormalities combined across the population at difference levels of IKr block. Top: Under control conditions ($[K]_o$ = 5.4 mM, 1 Hz pacing). Middle: Reduced extracellular potassium concentration (4 mM). Bottom: Rapid pacing (2.5 Hz) to increase calcium loading, followed by sudden decrease to 1 Hz. Alternans are not counted as an abnormality in this case due to restitution effects from the sudden change of pacing rate.

arrhythmias. In this chapter we present a framework for understanding the role that variability in sarcolemmal current conductances plays in determining whether drug-induced repolarisation abnormalities occur in human ventricular cardiomyocytes over a variety of conditions. Our results show that block of IKr, and uninhibited ICaL, are necessary for repolarisation abnormalities to occur. In addition, we have identified three different mechanisms that can increase susceptibility to abnormalities over a wide range of conditions: low sodium-potassium pump current permeability, low sodium-calcium exchange current permeability, and low IKr conductance.

Previous studies have investigated the role of variability in determining the effects of specific diseases, such as long QT syndrome (Sadrieh et al. (2014)), or specific drug blocks, including the work of Sarkar and Sobie in quantifying the role of repolarisation reserve in determining response to IKr block (Sarkar and Sobie (2011)), and our previous work in Chapter 5. Recently, Vandersickel et al. (2014) investigated mechanisms of EADs in human tissue using parameter sweeps modifying ICaL, IKr, INCX and IKs. However, to our knowledge, ours is the first study to investigate how inter-subject variability modulates susceptibility to repolarisation abnormalities in human by varying all significant sarcolemmal current conductances simultaneously, and to use experimental data to ensure all cell models used in the study are within the range of experimentally observed variation, while allowing conductances to cover a wide range of values. Therefore, with our approach, rather than preselecting which sarcolemmal currents we believe will be important for abnormality generation, we can instead use our population of models methodology to develop predictions as to which conductances are the key determinants of repolarisation abnormality occurence in response to current block. As with the quantification of the concept of repolarisation reserve performed by Sarkar and Sobie, we have developed an initial framework for understanding of how variation in conductances determines not just variability in important action potential biomarkers such as APD, but susceptibility to pro-arrhythmic phenomena, in this case repolarisation abnormalities.

We constructed a population of human ventricular myocyte models in which all models displayed normal action potentials consistent with experiment in control conditions, with important action potential biomarkers such as APD90 within physiological range, but across the population there were large differences in models' responses to current block and other pro-arrhythmic conditions. This indicates the difficulty of predicting drug-induced susceptibility to repolarisation abnormalities prior to the application of the drug. We see that a wide variety of conductance profiles produced viable control action potentials (Figure 7.2), far from the original conductances of the baseline ORd model (Figure 7.5). Given the wide range of conductance altering conditions the heart has been shown to successfully cope with, as well as the low penetrance of long QT syndromes (Priori et al. (1999)), this is not surprising, and is consistent with results from other studies using the same (Walmsley et al. (2013); Britton et al. (2013); Sanchez et al. (2014)) and other (Sarkar and Sobie (2010); Sadrieh et al. (2014)) approaches, as well as with population-based studies performed in neuroscience (Marder and Taylor (2011)). The wide range of viable conductance configurations that produces functional action potentials under control conditions pacing mean that the range of action potentials produced by normal and abnormal cardiomyocytes under control conditions are overlapping. Therefore, it is difficult to distinguish between these two groups from control action potentials alone.

The first main finding of this study is that for cells to be highly susceptible to repolarisation abnormalities, they must have highly inhibited IKr, and an uninhibited ICaL with moderate or higher GCaL. Both these conditions were required for cells to display abnormalities. No cells displayed abnormalities without IKr block, while moderate ICaL block was sufficient to abolish abnormalities in the majority of models, even at the largest magnitude of IKr block, 90%. These findings are consistent with what is known about the roles of these currents in EAD generation. A low IKr prolongs APD, allowing ICaL to reactivate, while the magnitude of ICaL has been found to be a predictor of arrhythmia susceptibility (Sims et al. (2008)). If ICaL is large enough, reactivation during a prolonged action potential can produce enough inward current to

reverse repolarisation, leading to EAD generation. In the case of alternans, calcium dynamics, and the formation of calcium alternans are believed to be the primary driving force behind APD alternans (Merchant and Armoundas (2012)). Many different interacting mechanisms can potentially generate calcium alternans, which can then lead to action potential alternans through the action of INCX. These action potential alternans are known to be pro-arrhythmic in tissue (Weiss et al. (2011)). While we have not modelled variability in the intracellular calcium-subsystem, we have varied the conductances for the L-type calcium current and sodium-calcium exchange current, which couple calcium alternans and AP alternans, and affect intracellular calcium concentrations.

While IKr inhibition and ICaL availability were sufficient for repolarisation abnormalities to occur in the strongest drug block scenarios (e.g. 90% IKr block combined with block of another potassium current), analysis of cell models that displayed abnormalities in 10 or more of the multichannel block simulations revealed that there was a third mechanism acting to destabilise repolarisation. This mechanism was most commonly extremely low GNaK, and less commonly low GNCX, or low GKr. The roles of INaK and INCX in repolarisation abnormality generation are less well understood than the roles of IKr and ICaL. However, they are known to be highly important both for their contribution to repolarisation and for their roles in maintaining ionic homeostasis, due to the large number of ions they transport across the cell membrane compared to the charge they transport. INaK is known to be inhibited in a number of disease conditions (Bueno-Orovio et al. (2014)), including ischemia and heart failure. INCX has been a target of recent studies investigating the effects of INCX blockers as a therapy to reduce the incidence of alternans (Kormos et al. (2014)) and torsades de pointes in types 2 and 3 of LQT syndrome (Milberg et al. (2008)). Our results suggest that extreme inhibition of INCX could potentially cause repolarisation abnormalities, rather than reduce their incidence. However, only 3 models out of the 46 that displayed high susceptibility had low INCX, without low INaK as well, so such occurrences were uncommon. We found only 1 highly susceptible model without low INaK or

INCX, and this model had low IKr. However, unlike the rest of the current conductances except GNa, there were no models in the population with GKr values below a threshold of 0.13 times the baseline conductance in the ORd model. Above that value, there was a wide range of GKr values in the highly susceptible set of cell models. Overall, this suggests that while higher levels of IKr block increase occurrence of repolarisation abnormalities, low levels of GKr are not necessarily a sign of increased susceptibility, as under control conditions the low baseline will be counterbalanced by other repolarising currents, and will respond less severely to IKr block due to the smaller magnitude of the reduction in outward current caused by applying the same level of block to a small current. In previous work we have also shown that APD90 has a negative correlation with GKr, (Britton et al. (2013)) so unlike other currents, it may be possible to estimate GKr from action potentials recorded during normal pacing.

The rationale for developing a framework for understanding the contributions and interactions of variable ionic currents is that variability between the hearts of different individuals comes not just from a single source, but from many sources. Variability is introduced from intrinsic sources: e.g. from underlying genetics, the mechanisms that create and traffic ion channels to the membrane, and the progression of circadian rhythms (Jeyaraj et al. (2012)). Adding to this, there are changes to the heart caused by aging, by disease (Borlak and Thum (2003); Farid et al. (2011)), and from the remodelling that is performed by the heart to react to changing conditions such as pacing rate (Tsuji et al. (2006); Qi et al. (2008)). There is also variability introduced as the heart responds to therapies, such as anti-arrhythmic drugs (Le Bouter et al. (2004); Xiao et al. (2008)), and so by this point the result of any intervention can itself be highly unpredictable. Therefore, we believe it is important to develop a general framework for understanding which currents are important, and in which combinations, for determining the likelihood of pro-arrhythmic phenomena developing in a given heart, in response to a drug or other therapy. Understanding the effects of each source of variability individually is important, but as any one source of variability in the heart will be interacting with other variable mechanisms to create an

individual-specific balance of ionic currents, it is also important that we build an understanding of what general ionic conditions determine susceptibility to pro-arrhythmic phenomena.

In this chapter, we have investigated the effects of varying the conductances of important sarcolemmal currents, and held other important biological parameters such as ion channel kinetics fixed. We assume that ion channel structure will generally be conserved across individuals, leading to similar kinetics, but that ion channel number will vary significantly in cardiomyocytes from different individuals, resulting in variable conductance values. We focus on sarcolemmal channel conductances as a source of variability because of the wide array of conductance modulating effects that are known to affect cardiomyocytes and because conductance alteration through block is the primary mechanism through which many important drugs act on the heart. We have shown that variation in sarcolemmal conductances alone is enough to produce drug-induced repolarisation abnormalities in models with normal control APs and APDs. However, ion channel kinetics may also vary significantly between individuals. Future work could explore the effects of variation in channel kinetics and how it might interact with changes in conductances. This could be particularly important in the case of recovery from inactivation of the L-type calcium current, due to its importance in determining window current, and EAD generation. Changes in kinetics could also be important for internal calcium channels such as the ryanodine receptors and SR Ca2+-ATP-ase (SERCA), due to the influence of calcium release dynamics on determining EADs formation (Weiss et al. (2010)), and as they are potential mechanisms for alternans generation (Weiss et al. (2011)). Incorporating variation in the kinetics of ion channels that can facilitate repolarisation abnormality occurrence would be expected to increase occurrence of those abnormalities on top of what we have observed in our current population of models. It would be interesting to understand in which cases variation in conductances and kinetics can both act in to produce equivalent effects (e.g. larger currents at key points in the action potential), and in which cases they produce qualitatively different effects, that are not possible otherwise.

7.5 Conclusions

In this chapter and in Chapter 5, we have described two studies using the experimentally-calibrated population of models methodology developed in this thesis. In each case we have described the methods used for that particular study. However, we have not yet addressed the overall process of creating and analysing populations of models, or how to design simulation studies that use this methodology.

In the next chapter, we will describe the population of models methodology upon which most of the work in this thesis has been based, in detail, and explain each of the steps involved in the creation and analysis of a population. We also give our current understanding of the various decisions that need to be made when designing a study using this methodology and discuss the trade-offs that will need to be considered in future modelling studies when using experimentally-calibrated populations of models.

8

Methodological challenges in the design, use and analysis of experimentally-calibrated populations of models

8.1 Introduction

In the previous chapters we presented two studies in which we used our experimentally-calibrated populations of models methodology to model inter-subject variability in cardiac cellular electrophysiology. In these chapters we have described the uses of populations of models, and the specific methods we used to create and analyse each population, but not the underlying process for creating them and analysing them, or the reasons for each choice we made in designing each study. There are a number of decisions that need to be made when using the methodology, such as choosing which parameters to vary, and how many models to include in the initial sample. To make these decisions, multiple factors need to be considered, including the goals of the study, the experimental data and models that are being used, and the available computing power.

In this chapter we address these considerations and explain our current thinking for each step of the process of constructing and analysing a population of models. In most cases, there are no definite rules for each of these steps, but we identify important considerations and trade-offs that must be made when designing a study. We will also cover methods for analysing

simulation results from the many different models within a population, in order to understand the mechanisms that differentiate the behaviours of different models within the population.

8.2 Populations of models

The focus of this thesis is the development and use of the population of models methodology to incorporate experimentally observed variability into the existing cardiac modelling framework, in order to understand how this variability affects the response of cardiac cells to pacing rate, drug application and changes in extracellular ionic concentrations. In this section we describe in detail the process for developing populations of models, and how we analyse them to explain and predict the effects of variability on cardiomyocytes.

The population of models framework extends cardiac modelling beyond the use of a single model, representing the typical behaviour of a cardiomyocyte, to instead use an ensemble of models, all of which have different parameter values from one another, leading to different behaviours for each model. We vary only the parameters that we hypothesise will vary significantly between individuals, and have a significant effect when varied, such as the conductances of ionic currents. We integrate experimentally observed variability into this ensemble of models by discarding all models within an initial candidate pool of models that produce behaviour outside the range observed in available experimental data. The models that are not discarded constitute a population of models, which is a group of models that share a common baseline model, but have varied underlying parameters, and all of which produce different behaviours that are still within the range of variation observed in available experimental data. The development of the population of models methodology, and the construction and analysis of populations of models for rabbit Purkinje cardiomyocytes and human ventricular cardiomyocytes forms the core of the work presented in this thesis. The overall goal of these studies is to improve our understanding of how variability between individuals alters the electrophysiological response of cardiac cells to drug application and other potentially pro-arrhythmic phenomena, and to

identify which biological parameters, e.g. particular ionic current conductances, are important for determining this response.

8.2.1 Creation of a population of models

To create a population of models, the basic process is to: obtain experimental data and select a matching baseline model; select parameters in the baseline model to vary; perform a Latin hypercube sample (LHS) ((McKay et al. (1979)) to generate a large number of parameter sets that can be inserted into the baseline model to create a large pool of candidate models; simulate the behaviour of each model in conditions analogous to the experimental data; extract biomarkers from the data and from each simulation for comparison; discard all models with any biomarker outside the range of values observed, for that biomarker, in the experimental data; and finally, determine which models have not been discarded - these form the population of models. We will now describe each step in more detail.

The initial choice of which data and what baseline model to use is driven by the overall goal of the study being performed, and the availability of both model and data for the target species and cell type being studied. For the model to reflect the experimental data, it may be necessary to iterate the population creation process, altering the baseline model or trying a new model, in order to find one that can produce good agreement with experimental data for a range of different parameter sets. If the baseline model, without variation, produces behaviour that is outside the range of experimental data for multiple biomarkers, it may not be a good candidate for being used to generate a population without modification. A sensitivity analysis could be used to identify the components within the model that have the most significant effects on the biomarkers that are causing model rejection, and if possible, those parts of the model could then be reformulated to better fit the experimental data. Additionally, although not performed in this thesis, if multiple appropriate baseline models are available, multiple populations could be generated using the different models, and results and predictions of each population could be

compared, to separate consensus results from results that are specific to a single baseline model, as performed, for example, in Sarkar and Sobie (2011), and in Sanchez et al. (2014).

Selecting the parameters to vary in the baseline model defines some important assumptions of the study the population is used in. Many, or most of the parameters in a typical biophysically detailed model such as a cardiac cell model can be expected to vary between individual organisms, as well as within the same individual over time, however only a small subset of the parameters in a model should generally be varied, so that the analysis of the population does not become unmanageably complicated and so that the rejection rate of models in manageable in terms of computational costs. As we use a parameter sampling method (LHS) that does not scale with the number of varied parameters, there are no hard limits on how many parameters should be varied. However, there are a number of considerations that should be taken into account when selecting parameters to vary, and the range over which to vary them.

The choice of parameters varied should be driven by a the hypothesis of the study. A parameter should ideally only be varied if an argument, based on the aims of the study, can be made as to why it should be varied. This is partly because, while many parameters within a model of a biological system will exhibit variability in the real system, different biological parameters vary through different mechanisms. For example, while both ionic current conductances and kinetics vary between individuals, conductances vary primarily due to variation in the number of ion channels in the cell membrane, but kinetics vary primarily due to changes in channel structure. Genetic mutations that alter channel kinetics and functionality are generally considered pathological, and differentiate individuals from the range of the population that is considered as healthy. Therefore, a population created by varying channel kinetics would have a different biological interpretation from a population created by varying only conductances, which are thought to vary significantly between healthy individuals.

A sensitivity analysis can be useful for determining which parameters are important to vary and for justifying the choice of varied parameters. They are particularly useful when working with

unfamiliar models, or cell types, where it is not clear which parameters are important for the study and which have little effect. A sensitivity analysis can be used to rapidly determine what effect small variations of individual parameters have on important model outputs, and so can identify which parameters have the largest effects on model behaviour for a given parameter set. A typical sensitivity analysis (e.g. as used in Corrias et al. (2011); Romero et al. (2009) and in Chapter 4), would individually vary a number of parameters that are of interest by +/- 15%, 30% or a similar fraction of their initial value in the baseline model. From simulations with these parameter sets the change in model outputs (e.g. biomarkers such as APD90) is used to calculate the sensitivity of each biomarker output to variation in each parameter using equation 3.9, as described in Chapter 3. Using these results, the sensitivities of each output and each parameter can then be compared to determine which parameters have the most significant effects on model outputs. These results can then be used to motivate the choice of which parameters to vary in a subsequent population of models study.

After determining which parameters will be varied for a population of models, the next choice is to determine the range over which to sample parameter values. This range can be wide or tight, depending on the goals of the study, as both choices have advantages and disadvantages. The wider the range, the more likely models are to produce extreme or abnormal behaviour when simulated in conditions other than those used to create the population (e.g. simulations of drug block), although this can still occur with relatively tight sampling ranges. We currently do not know how much individual ionic current conductances generally vary between individuals (Sarkar et al. (2012)) although it has been shown in isolated neurons that conductances from neurons from different individuals that show similar patterns of activity can have very different conductance profiles (Swensen and Bean (2005)). For other important ionic parameters such as time constants and voltage shifts, we have very little information about how and whether they vary between individuals, except through specific mutations that alter ion channel structure.

In Chapter 2, we provided evidence of how mRNA expression of genes that code for ion channel

for proteins can vary by large amounts, from almost complete downregulation up to increases of at least four-fold compared to baseline (Borlak and Thum (2003)) in the most extreme cases of remodelling such as heart failure. In less extreme cases, such as the effects of circadian rhythms, expression levels could still vary significantly. For example, circadian rhythms in mice were found to alter expression of an important Ito sub-unit by approximately $\pm 40\%$ from the midpoint over a 24 hour cycle (Jeyaraj et al. (2012)). As the different effects that can individually cause variation in expression are not mutually exclusive, it could be expected that different causes of variability could compound with each other to increase the total range of possible variation in conductances. Also, mRNA expression levels do not exactly map onto protein expression levels for a variety of reasons (e.g. post-transcription regulation, or buffering through rate-limiting steps in the chain of post-transcriptional processes that translate mRNA to functional ion channels (Nattel et al. (2010)). Additionally, other potential sources of variation in post-transcriptional processes (e.g. miRNA expression) could affect ionic conductances. These combined factors make it difficult to quantify from available data how much the ”true” variability in conductances might be across a population of individuals, or what the distributions of conductances might look like. Additionally, the number of overlapping sources of variability and different mechanisms through which they act would make it very difficult to design and perform an experimental study to determine these distributions in animal models, and even less feasible in humans given the lack of tissue available for experiments, and the highly heterogeneous nature of any human population, e.g. in terms of lifestyle, age, and genetics. Therefore, a certain amount of informed guesswork is currently necessary when estimating parameter ranges for cardiac action potential (AP) models.

Ranges for parameter sampling can be chosen according to the aims of a particular study and the assumptions made about what a particular population represents. Wider parameter ranges allow for more extreme parameter values and therefore more extreme model behaviours. Also, the physiological assumptions made when increasing ranges for sampling towards infinity are

different to those made by increasing the range towards zero. For ionic current conductances, increasing towards infinity could represent increased expression or activity of that current, as might occur in compensation for block of another current, or due to beta-adrenergic stimulation. Increasing the range towards zero could represent decreased expression of an ion channel, but very low values could also represent mutations that cause loss of function of a channel, meaning no current flows through it, or diseases that impair channel function.

For studies of non-diseased, healthy cardiomyocytes, the level of variation seen in the literature and the results of previous modelling studies suggest that a variation of approximately $\pm 30\%$ in conductance values (from the value of the parameter in the baseline model) might be a moderate estimate on the level of variability, while $\pm 50\%$ would allow substantial variability. For studies that are interested in extreme behaviours, particularly including conditions where one or more types of ion channel are almost completely inhibited or not present in the cell, $\pm 100\%$ variation could be used.

In the two population studies presented in this thesis, this was the range that we used, for two reasons. Firstly, to allow us to explore a wide range of potential models, including models with severely impaired ionic currents, which was particularly important for the repolarisation abnormality study in Chapter 7. This level of variation is of particular importance in studying pro-arrhythmic effects such as repolarisation abnormalities, as is performed in Chapter 7, as for these to occur in a cell usually requires significant deviation from the averaged conductance values found in baseline cell models. Secondly, this range sampled evenly from parameter values that were lower and that were higher than the baseline value. However, even sampling could also be achieved with uneven ranges by using a non-uniform parameter distribution when calculating Latin hypercube samples, such as a log-normal distribution. This could be useful for studies of the effects of channel compensation or stimulation by the autonomic nervous system, where conductances can be significantly increased by factors of four or more compared to average conductance values.

For properties relating to ion channel kinetics, such as time constants and voltage-shifts, there is even less information about the level of variability present across individuals, either human or animal model species, and so the amount these parameters can vary between healthy individuals is an open question.

Although there is little information currently available on the distributions of ion channel parameters in cardiomyocytes, statistical techniques have been developed that could potentially allow for parameter distributions to be approximated using experimentally-calibrated populations of models and experimental data. Approximate Bayesian Computation (ABC) is one of these techniques and allows approximate parameter distributions to be inferred from data. To do this, randomly generated parameter distributions (which are generated based on a prior estimate of the parameter distributions) are used to compute summary statistics. The randomly generated distributions are then accepted or rejected based on the distance between their summary statistics and the values of the summary statistics calculated from the experimental data. The accepted distributions are then combined to compute an approximation of the underlying distribution of the data.

We could potentially apply ABC in cardiac modelling, using experimentally-calibrated populations of models. Summary statistics could be calculated from distributions of biomarker values observed in experimental data (such as the data shown in Figure 8.2), and populations of models could be created using different randomly generated underlying parameter distributions, and after the standard calibration process, each population could then be simulated, to generate their own distributions of biomarker values. Populations with similar distributions of biomarker values to the data could then be accepted and collectively used to estimate an approximate parameter distribution for the data set.

ABC could be particular useful for analysing data from different experimental sub-populations (e.g. recordings from cardiomyocytes from healthy vs. diseased hearts) and inferring approximate parameter distributions for each group. If we assume these parameter distributions are

realistic approximations of the real distributions, they could potentially be used to develop stratified populations of models for different groups, that represented both the distributions of biomarkers, and estimates for the distributions of each varied parameter. These populations could potentially be used for *in silico* drug testing or similar applications, to rank the risks of different drugs causing pro-arrhythmic effect in these groups, based on the percentage of models in each population that produced a pro-arrhythmic response to simulated drug application. This is type of ranked risk assessment is not currently possible with our existing methodology, because while we ensure that all models in a population are within the experimental range, we do not calibrate the population to match experimental distributions of biomarkers within that range, therefore the fraction of models displaying a behaviour within a population is not currently predictive.

The estimated parameter distributions generated by ABC could also be used to understand which regions of parameter space, for a given model, are more likely to generate viable models that pass the calibration procedure, which could be useful if we needed to create very large populations of models while minimising computational expense.

Once parameters and sampling ranges are chosen, the final choice before generating the initial sample is to determine how large it will be. The number of models to use for the initial sample is dependent on three main factors: computing power and time available, given the design of the study; the strictness of the filters being applied; the choice of parameters varied; and the goals of the analysis of the population. Larger samples will take more time to simulate, and will create larger final populations that will also require more time to simulate. Stricter filters (e.g. experimental data from many different experimental protocols, such as different pacing rates) would decrease the number of models that are suitable for inclusion, and so would require a large initial pool. Studies of the behaviour of the population over a large number of different conditions that might require simulating each model in the population hundreds of times would want to limit the size of the initial pool. One method for estimating the size

of the sample to use is to perform an initial test run using a sample of around 1,000 models, to get an estimate of the fraction of candidate models that will be accepted for the study, and then scale up the sample size to reach the size of final population required, perhaps 200 - 500 models for smaller population that is to be simulated many times over, or thousands of models if the purpose of the study is to find statistical trends in the population in a small number of simulated conditions. In this thesis we typically generated 10,000 models for the initial sample, which resulted in populations of between 200 - 500 models, which gave us a good balance between providing coverage of the range of behaviours seen in experiment, while not being too expensive to compute a large number of follow up simulations using the population. As a benchmark, using the O'Hara-Rudy baseline model of the human ventricular cardiomyocyte (a relatively complex cardiac cell model), simulating the behaviour of 10,000 models using the simulation protocol and ODE solver described later in this chapter took approximately 8 hours on a quad-core desktop computer.

There is currently no set rule for determining if a newly created population of models is large enough for the purposes of the study it is to be used in. However, visualising the coverage of the population in parameter space, using scatter plots of two parameter subspaces of the sampled parameter space, can give an indication of whether there are gaps or sparsely covered areas in the occupied parts of the parameter space, i.e. areas that could where there could be viable models that would be accepted into the population, but which have not been sampled sufficiently for these models to be found. If areas like this are found, this indicates a larger population should be constructed to increase confidence that there is adequate coverage of the parameter space. Alternatively, if the scatter plots show good coverage of models across all of the regions of parameter space that contain models that have been accepted into the population, then this increases confidence that the population is sufficiently large.

In addition, the size of the population should be larger than the number of experiments used to create it, and the number of experiments used to validate each model prediction. This is

because the aim of the population is to capture as much of the experimental range of variability seen across the data set as possible, and to explore a large number of possible variant models, that are still consistent with experiment. With a small population in comparison to the data set, it is likely that there will be experiments displaying behaviour that is not represented in the population even if the baseline model is capable of producing these behaviours. In this case, the population of models will not fully mimic the range of variation seen across the data set, only part of it. Additionally, on a practical note, in cardiac electrophysiology simulations are almost always quicker and cheaper to run than experiments, particularly the highly parallelisable simulations used in this methodology.

Building populations of models requires the generation of a large numbers of parameter sets for the initial population, sampled from a high-dimensional parameter space. Sampling every possible combination of parameter values in the space, for all but the lowest resolutions, is computationally infeasible given the complexity of most cardiac cell models. Therefore, we use the LHS method, which generates parameter sets over a large number of parameters efficiently and without bias, as described in Chapter 3. To use the LHS method, we specify an upper and lower bound on the range of values to sample each parameter from and subdivide that range into N intervals. N parameter sets are then chosen randomly but with the constraint that each parameter set can only contain parameter values from intervals that have not been used in any other parameter set. The number of samples taken (N) is specified by the user and so does not scale with the number of parameters sampled. Therefore, a large number of parameters can be varied in total, allowing a more complex parameter space to be explored. In the studies reported in this thesis, parameters that are varied are sampled over a range of $\pm 100\%$ the published value of that parameter in the original baseline model being used. The published values of the parameters that we vary in these studies represent mean values taken from the literature. These values typically have a reported standard error on the mean of much less than the actual mean value, and this has been incorporated into previous studies of variability (e.g. Romero et al.

(2009)). However, this error represents uncertainty in the mean value, not the total range of variation observed in experiments. Therefore, we vary parameters over a larger range than has been used previously, and this range is chosen to be large so that we can produce a wide range of different action potential behaviours in the initial pool of sampled models.

When the initial sample of parameter set has been generated, using the LHS technique, or another method for random sampling of parameter space, the next step is to simulate each model in conditions equivalent to the experimental data that is available, using the protocols described in Chapter 3, so that each model can be compared against experimental data in the calibration process, which is the process of filtering out models which display behaviour that is not consistent with experiment. A model, in this case, is the equations from the baseline cell model, with one of the parameter sets from the sample used to replace the original values of those parameters.

8.2.2 Determining the final population - calibration

To determine the final population, we perform a process called calibration, where we discard models that output values for any of the filters (such as any of the action potential biomarkers described in Chapter 3) that are outside the range of values seen in experiments. This creates a population of models where each model has different underlying parameters, but all are within the range of observed variability for each of the filters chosen in the previous step. To do this, for each filter, each candidate model undergoes a simple test: if the value of the filter biomarker is greater than or equal to the minimum value of the biomarker seen in available experimental data, and less than or equal to the maximum value, the model is not rejected, otherwise it is rejected as a candidate for the population. Therefore, the final population is only those models that were in range for all filters. This also means that any existing population can be used to generate new, more selective populations by adding more filters, as the effect of each filter on the population is independent of any others. This can be achieved both by including different

filters under the same experimental conditions, and by using the same filters under multiple sets of experimental conditions, if the appropriate experimental data is available. This is done in Chapter 5, where calibration is performed with the same set of 7 biomarkers, but over 3 different pacing rates, for a total 21 different filters.

Currently we filter using all measured biomarkers simultaneously, to create one maximally constrained population. As each filter is independent of the others, we could also apply each filter separately, and in different combinations with the others, to generate less restrictive sub-populations. One reason for doing this is to determine whether there are substantial differences in the number of models rejected by different filters, or combinations of filters.

If a filter rejects few models, then this tells us that the parameters we have chosen to vary have little effect on the value of that filter, and that it may be controlled by other parameters we are not varying. If the filter is physiologically important, this could lead us to perform a regression analysis over a wide range of model parameters to determine which parameters do control that filter, and that may need to be varied in the next iteration of a population of models. If a filter rejects far more models than the average across all filters, this tells us that this filter is heavily constraining the parameters we are varying, and is the driving force behind the overall distribution of parameters in a population. If this is a physiologically important filter, this could suggest possible ways to manipulate this filter, using drugs or other interventions that alter the parameters it constrains. If it is not physiologically important, it may be useful to redesign the study so that the filter does not have overwhelming control over which models are accepting into a population of models. If all filters reject roughly equivalent numbers of models, without major overlap (which could be visualised using a Venn diagram) then we can conclude that all filters are constraining the population, without significant redundancy.

Before calculating the experimental range, it may also be necessary to remove experiments from the data set, if they are extreme outliers for one or more filters, and it is believed this is not due to biological variability but instead to an experimental issue such as a damaged

preparation, or a dislodged microelectrode impalement. For smaller data sets, this must be done using intuition and experience, as with few data points it is difficult to tell where the boundary at which reasonable experimental variation ends is. With large data sets, there is the possibility of refining the way experimental ranges are determined. For example, Prinz et al. (2004) used limits of 2 standard deviations from the mean, instead of the minimum and maximum values excluding outliers that we use, to set ranges on their filters for constructing populations of neuronal models. Their data set contained experiments on 99 different lobster preparations, which is larger than most data sets from cardiac preparations. The advantage of this method is that it removes outliers without the need to manually decide which preparations are extreme outliers (e.g. due to damage to the preparation), and which are valid experiments producing output values at the high or low end of the natural range. This process could also be performed on larger cardiac electrophysiology data sets if the experimental biomarker distributions in these data sets could be fit to statistical distributions, as discussed later in this chapter.

8.3 Analysis of a population of models

Analysis of a population of models presents a number of challenges that differ from those posed by analysis the output of a single model, or several entirely different models. Under the population of models methodology there is no favoured parameter set, all parameter sets within the population are equally valid as all produce output that is consistent with the range seen in data we have access to. Additionally, the underlying distribution of parameters in the population is determined by the filters applied on the outputs of these models. Experimental data for the distributions or ranges of the underlying parameters is usually unavailable and so the parameter distributions of a population of models reflect the selectivity of the filters and data used, rather than experimental measurements of the parameter distributions.

Visualisation

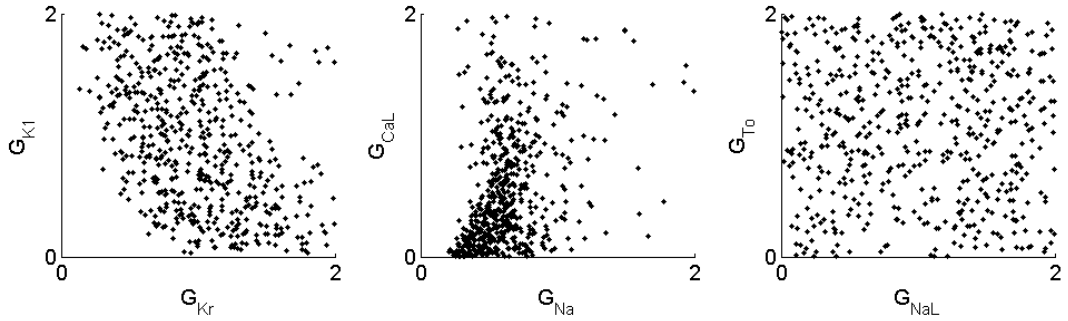

Figure 8.1: Examples of scatter plots showing the relation between two parameters (GKr and GK1) (panel A), constrained coverage of parameter space (panel B), and unconstrained uncorrelated parameters (panel C), from the population of human ventricular cell models developed in Chapter 7.

A first step for understanding the properties of a new population of models is visualisation of the underlying parameters and the biomarkers of the population. The tools we use for this are primarily scatter plots, box plots, and histograms. These plots allow us to pick out correlations between parameter and outputs, and to summarise the distributions of each variable. Direct visualisation of high dimensional spaces is difficult, and while techniques exists to compress high-dimensional spaces into lower-dimensional representations, we have found that for the numbers of parameters we vary (typically 8-12 parameters), the previously mentioned plot types have been the most useful. Box plots and histograms summarise the distribution of a single parameter or output across the population, while scatter plots allow us to see the level of correlation between two variables. These plots are individually easier to interpret than more complex plots and so can be plotted in a grid of small multiples to show all possible variables or pairings at once. Small multiples are grids of plots of the same type with the same scale and axis. For example, we can plot scatter plots of all the possible pairs of parameters in a population, which allows us to immediately see which pairs have a degree of correlation with one another, potentially revealing which parameters can compensate for others, which parameters have no obvious relationship with each other, and how much of the sampled range of parameter space is covered by the models in the population. Examples of these types of scatter plots are shown in Figure 8.1.

The calibration ranges we use are determined from the minimum and maximum values of each biomarker, observed across an entire experimental data set. The other non-extremal experimental biomarker values will be distributed in some way across the calibration range, as will biomarkers for the models in the population. Therefore, it is informative to plot histograms of both experimental and simulated biomarkers so that they can be compared, particularly to determine if the population biomarkers are distributed in a distinctly different way from the experimental biomarkers. If so, this can indicate a mismatch between the baseline model and experiment. An example is shown in Figure 8.2. Here we see that many of the biomarkers for this population follow non-uniform distributions, that peak between the minimum and maximum values of their calibration ranges, as does the experimental data. The distributions for the biomarkers shown in Figure 8.2 that measure time intervals might be approximated by fitting to log-normal distributions, which take real positive values only and could provide a good fit to the data. If a sufficiently good fit with the data could be found, different summary statistics other the minimum and maximum values of biomarkers in the data set could be used to calibrate populations of models.

One biomarker where data and the population of models do not agree is the peak membrane voltage biomarker, VmPeak, for which the bulk of the population of models have values towards the high end of the range, unlike the data. These sort of results can reflect features that are dependent on the baseline model being used (in this case the ORd model, which in its original form has a slightly higher VmPeak than any values seen in this data), and for which the fast sodium current INa was modified in Chapter 7, to improve the agreement between the model and the data. A potential advantage to using biomarker distributions in the calibration process is to reduce these mismatches between model and data, which could increase confidence that a population of models is accurately representing the underlying variability in a data set.

Another useful set of plots are scatter plots of each pair of biomarkers, with both experimental data and model values overlaid on the same plot, as shown in Figure 8.3. These plots compare

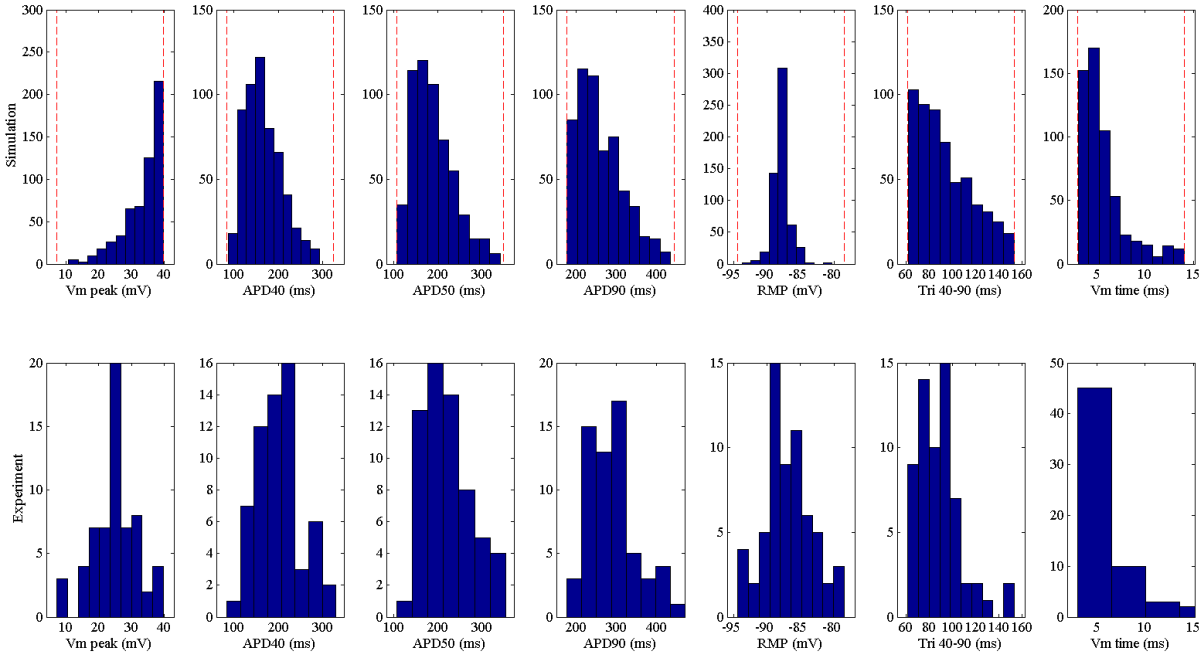

Figure 8.2: Histograms of experimental data and population results for human ventricular cardiomyocytes (from work presented in Chapters 6 and 7). We can see whether models span the whole range of variation for each individual biomarker, and whether the distributions from experiment are roughly preserved across the population, or not. In this example, we see that for some biomarkers, such as APD50, the distributions match well, while we do see a significant difference between data and population for peak membrane voltage (Vm peak).

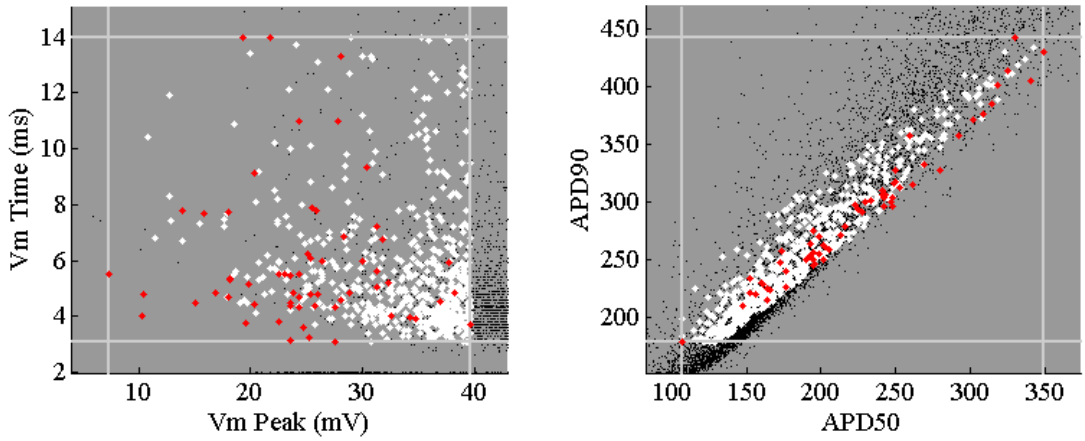

Figure 8.3: Example scatter plots for experimental and model biomarkers, showing the spreads of both and the calibration ranges derived from experiments. Red dots are experimental biomarker values, white dots are biomarker values from models accepted into the population of models, black dots are biomarker values from rejected models. Lines show calibration ranges derived from experiments. Left: Peak membrane potential (Vm Peak) against time-to-peak (Vm Time). In this plot we can see that the population generally preserves the distribution of Vm Time, but has the majority of models at the high end of the experimental range (30-40 mV) for Vm Peak, while the data is more evenly distributed across the experimental range. Right: APD50 against AP950. This plot shows an expected correlation between experimental biomarkers, which is preserved in the population of models.

the spreads of biomarker values for the experimental data, the accepted models in the population, and the rejected models in the population, for each pair of biomarkers. They can also reveal whether correlations between biomarkers that are present in the experiments are also present in the population of models (or vice versa). Finally, these scatter plots provide information about which regions of the experimental data are well-represented by the population and which may contain experiments, but few models. This provides an indication of whether the population sufficiently captures the full range of experimental variability or whether a new iteration of the population with modifications to the baseline model, parameter choices or biomarker choices might improve coverage of the data by the population.

Boxplots are a useful tool for visualising the spread of data that has an unknown underlying distribution, as they are non-parametric - they do not assume the data will fit a specific distribution, but they do summarise the spread of the data. Boxplots display the distribution of a

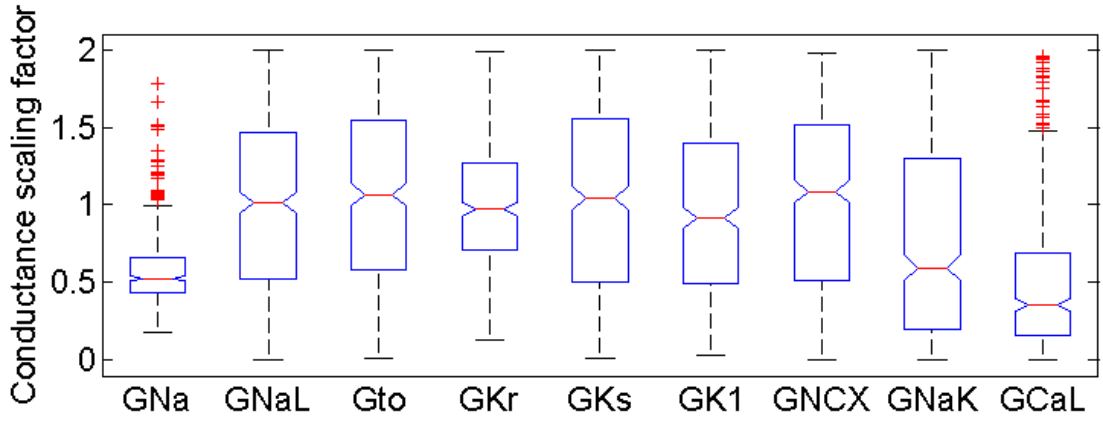

Figure 8.4: Example boxplots of parameter distributions from the population of models developed in Chapter 8. We can see from the boxplot that across the population each individual varied conductance spans the majority of the sampled range. However, ranges for GNa and GCaL are smaller, with a few outlying models with high values of either conductance, indicating that these parameters are more heavily constrained towards lower values, but that there are still some relatively rare parameter combinations with high values of these conductances that produce models with APs that are consistent with experiment. We can also see that no models in the population have GNa or GKr values close to 0, unlike the other parameters, indicating our choice of biomarker filters requires models to have at least a baseline amount of both of these currents to produce a valid AP.

set of values in terms of quartiles and outliers, an example is shown in Figure 8.4. The inner box in a boxplot, shows the range of the inner two quartiles of the data, with the line within the box marking the median. The whiskers on a boxplot can vary in what they display, but typically display the range non-outlying data spans in the outer quartiles. Outliers are defined as values that are more than a user-defined multiple of the inter-quartile range away from the nearest inner quartile (we use a factor of 1.5). The whiskers show the non-outlier range the data occupies, and also display whether the interquartile range is skewed (one whisker longer than the other) or centered (whiskers approximately equal length). Boxplots are useful because they summarise the properties of the normal models population and the outlier models within a population clearly, without assuming they follow a known distribution.

To pick out more complicated multivariate relationships between three or more parameters or biomarkers, machine learning techniques such as principal component analysis could be used

to determine whether these relationships exist within the population. However, due to the limited amount of two-parameter correlations we see in our currently developed populations, we currently do not look for these relationships without a prior reason to believe they might occur.

Prediction and hypothesis generation

Once a population of models is developed and analysis of its biomarker and parameter distributions have been performed, the next step in a study will often be to simulate the behaviour of the population under experimental conditions that were not used to develop the population. The results of these simulations can then be used as predictions. This section will describe how those predictions can be analysed and compared to experimental data, and how population-based simulation studies can be used to go beyond what is currently feasible using experiments, to generate new hypotheses that can then be tested in experiment, but that would be difficult to initially develop using a purely experimental approach or a single computational model.

Comparing simulation results to experiment

Experimental results, for example, the value of APD90 in a particular type of cardiomyocyte, are typically reported as the mean value of the experimental data set $\pm$ the standard error on the mean (SEM) (calculated as the standard deviation of the data divided by the square root of the number of experiment repeats). Generally, a prediction made by a standard cardiac cell model could be considered ”good” if it landed within the mean +/- SEM interval. However, in some situations, for example, when predicting the response to a drug, it is important to predict not just the average effect, but the range of effects that might be seen across a number of cells. In this case, the population of models approach provides the ability to make these kind of predictions.

Unlike in experiments, the underlying parameters that determine the behaviours of models in a population are not likely to be a representative sample of the real distributions of these parameters across individuals. This is because we do not know the distributions of these parameters, and so use the calibration process to mimic natural variability instead. Therefore, while

each model in a population produces behaviour consistent with experiment, the population is not sampled from an experimentally-derived parameter distribution and so the distribution of biomarkers is not a prediction of the distribution in experiment. What can be used as a prediction are the ranges of biomarker values, or the ranges of the change in biomarkers (e.g. the range of APD90 prolongation/shortening in response to a drug, as used in Chapter 5), seen across the population when a set of experimental conditions that have not been used in the calibration process are simulated. This gives a prediction of the range of possible scenarios that could occur, although unlike a probability distribution it does not provide information on how likely different values within the range are to occur. The advantage this offers over standard cardiac cell models is that the range can be compared with ranges obtained in experiments. These ranges can be more informative than a prediction of the average response in cases where outlier responses are important, e.g. for drug safety testing.

Matching the number of experiments with the number of models in a population

A difficulty with using the range of a set of biomarker values, rather than their means and standard deviations, is that they depend only on the most extreme (non-excluded) data points within the population of models or experimental data set. Therefore, as the population size or number of experimental preparations increases, the size of a range can only increase or stay the same. A larger population or data set will generally produce a larger range, up to a limit. This effect means that it is important, given the ease of generating large populations (100+ models), and the difficulty of recording even 10 experiments in one data set in cardiac electrophysiology (which is a motivating factor for using populations of models in this field), to account for mismatches in the number of experiments and the number of models when comparing predictions to data. To adjust for mismatches, we use repeated random sampling of subsets from the more numerous set of values, which should be the population of models, to compare equally-sized sets of values. To perform this process, a random sample of models is taken from the population, without replacement, of size equal to the size of the experimental data set. From this sample, the

quantities that are to be used for prediction are taken and stored. These values can include the maximum and minimum values of important biomarkers, the range those values span, or the range of the change in biomarker value compared to control conditions. This sampling process is repeated a large enough number of times for the mean values of the quantities of interest, taken over all samples, to converge to steady values. The means derived from this resampling process can then be directly compared to the experimental result. An example of this process is shown in Chapter 5 and reproduced here as Figure 8.5.

Simulation studies over multiple experimental conditions using populations of models

Even with a population of hundreds of models, running a single simulation protocol on each model takes a relatively short amount of time. As a benchmark, running 1000 models for 1000 seconds of quiescence followed by 1000 seconds of simulated 1 Hz pacing on a quad core desktop could be expected to take less than an hour. Therefore, an advantage of the methodology is the ability to systematically evaluate the effects of a large number of possible experimental conditions on the variety of different models present in a population. This lets us see how many different models behave under a wide range of different conditions, potentially revealing which parameters are important for affecting model behaviour over a wide range of different experimental conditions and parameter sets, and which parameters or combinations of parameters have significant effects only under specific combinations experimental conditions and parameter values.

We can perform a sweep through several experimental conditions (such as different levels of ionic current block(s), extracellular ionic concentrations, or different pacing rates), to determine trends in how the population responds under a wide variety of different conditions, in particular to changes in two (or more) experimental variables at once, which is often difficult to do experimentally. An example of this is the study of the development of repolarisation abnormalities in response to multiple drug blocks presented in Chapter 7. We were able to determine which parameter values were important for generating repolarisation abnormalities, and which

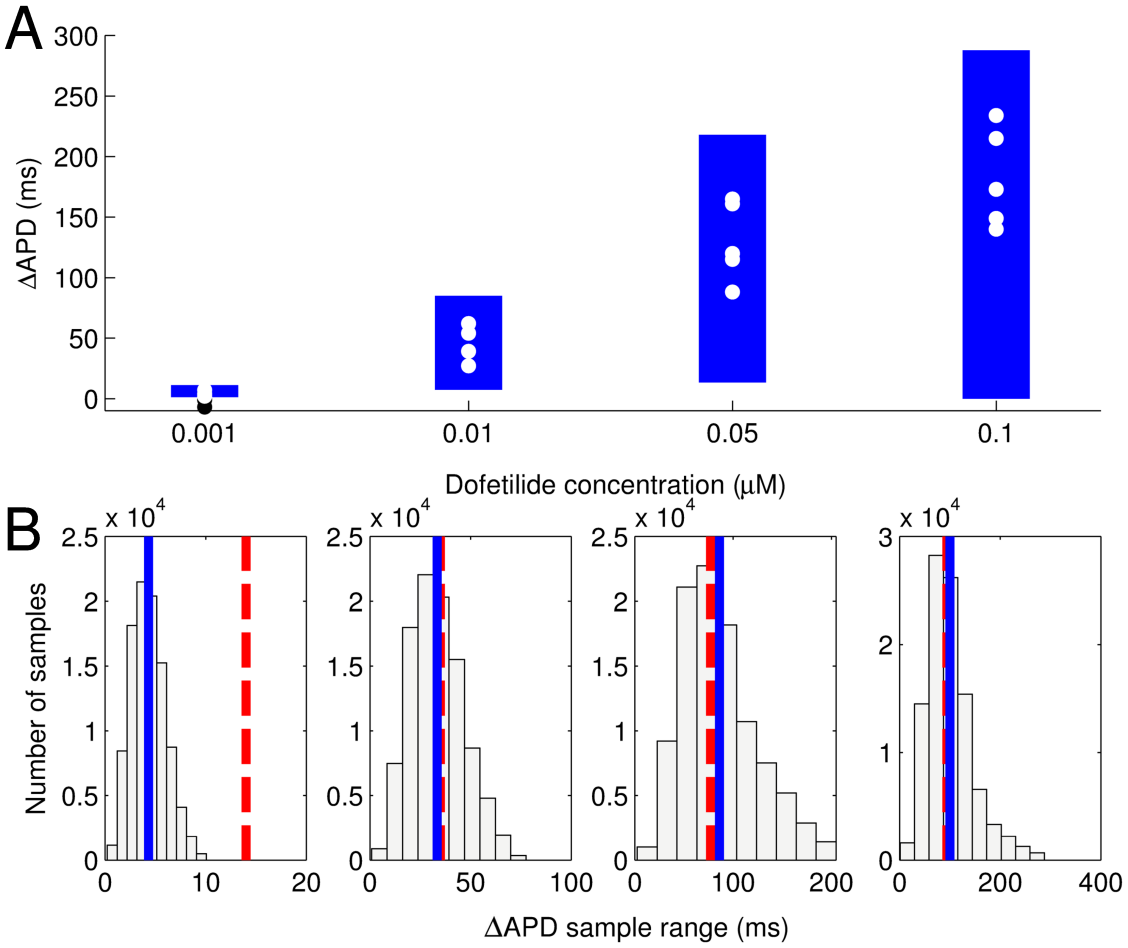

Figure 8.5: Example of matching the number of models in a population to the number of experiments in a data set, in order to compare predictions. In the top panel A, we see bars representing the range of a biomarker, (APD90 with drug applied - APD90 in control conditions), across all of the models in a population of 213 models, for 4 different simulations with differing concentrations of the IKr blocking drug dofetilide applied. Individual experimental results from 5 experiments in equivalent conditions are shown as dots. The population of models' ranges are much larger, but the number of models in the population greatly exceeds the number of experiments. In panel B, we see the results from sampling subsets of 5 models from the population repeatedly (100,000 times). Histograms show the distribution of ranges obtained across all of the sampled subsets. The mean of each of these distributions of the range are shown as blue lines. The range from the experimental data is shown as a dashed red line. Therefore we can compare the range of ΔAPD with the experimental result. Reproduced from Chapter 5 and from Britton et al. (2013).

combinations of ionic current blocks acted to suppress or amplify these effects. These sorts of sweeps comparing behaviours where different conditions are varied, to build up a picture of the effects of varying two or more variables (e.g. blocking two or more ion channels to different degrees), are difficult to perform experimentally. Even using high-throughput automated assays, it is difficult to create experiments to test how, for example, the effects of blocking two different ion channels interact with each other, and how the quantitative level of block of each current affects the response of a cardiomyocyte. However, these dual effects are important, particularly for understanding non-selective drugs that may block two or more channels with similar IC50 values.

The aim for these types of study is to determine how blocks of different currents react in ways that are not apparent from the effects of each individual drug on a cell, e.g. the effects of blocking IKs alone in human are typically very small, however if IKr and IKs are blocked, then the combined effect on APD is significantly larger than blocking IKr alone (Jost et al. (2005)). Other studies have shown that while IKr block is often a marker of pro-arrhythmic behaviour by a drug, certain drugs with significant IKr block, such as ranolazine, have compensatory blocks of other currents (the late sodium current in the case of ranolazine (Antzelevitch et al. (2004))) that have been shown to be able to reduce the pro-arrhythmic effects of the drug (Noble and Noble (2006); Belardinelli et al. (2006)). However, the magnitudes of these currents can also vary between individuals, altering the balances of these currents. Therefore incorporating variability into simulation studies of multi-channel effects could reveal whether variation in these complementary or compensatory currents significantly alters the expected pro- or anti-arrhythmic effects of blocking multiple ionic currents. The study in Chapter 7, and also a recent study by Vandersickel et al. (2014) investigating EAD formation in ventricular tissue, are recent examples of this type of study.

Sub-categorising models

For some studies, understanding the mechanisms underlying the quantitative changes in certain

biomarkers that occur when experimental conditions are varied from control will be the main focus, as in Chapter 5 where we investigate the response of APD90 to different levels of IKr block. For other studies though, such as the study presented in Chapter 7, understanding how changes in conditions lead to qualitative changes in model behaviour (e.g. occurrence of repolarisation abnormalities) may be the focus. In these cases, automatic categorisation of models into different, qualitatively different categories (e.g., whether the model displays a particular abnormality, such as EADs, or not) allows, firstly, the number of models in the population that fall into each category to be compared under different simulation protocols (e.g. control vs. different drugs and drug concentrations). Secondly, the underlying parameters of models in each category can be compared to determine whether models in one category can be distinguished from those in another category by the values of one or more parameters. We can use these differences to inform new hypotheses about the mechanisms that could cause these events in real cells. Techniques that can be used to identify a possible difference between subsets include scatter plots of the different models parameter or output values, boxplots of the different subsets, and analysis of the statistics of each sub-population.

Scatter plots are one technique used to identify differences. Figure 8.6 shows the values of the L-type calcium conductance (GCaL) and sodium-potassium pump permeability (PNaK) for two subsets of models within a population, one of which (red) is susceptible to generating EADs and alternans over a variety of repolarising current blocks, and one of which (black) is less susceptible, as described further in Chapter 7. We see that most, but not all, of the models in red have an extremely low value of the PNaK parameter, compared to the models in black, and that while the majority of black, less susceptible models have low values of GCaL, all of the red, susceptible models have moderate to high GCaL values. Plotting every possible pair of varied parameters this way, allows us to identify which individual parameters, and which combinations of parameters, show marked differences between the subsets of models and whether there exist any correlations between parameters within subsets. We could also search for these differences

by comparing the statistics of the sub-populations, for example by plotting each sub-population in a box plot, and determining the degree to which the sub-populations are separate from one another for the identified parameters or biomarkers for which they differ.

Additionally, if a particular model or small group of particular models are identified as being of particular interest, standard tools for analysing cardiac cell models can be used, for example close examination of state variables to determine how individual currents and intracellular ionic concentrations are behaving throughout the action potential. This type of mechanistic analysis would be particularly useful for determining the mechanisms that produce abnormal or unusual behaviour in particular models within a population. An analysis of an entire population of models can be used to identify which parameters are significantly different between abnormal and normal models. Then, to determine how these parameter values mechanistically cause abnormal behaviour, and to generate a testable hypothesis that can inform future experiments, the ionic currents, compartments and other model components associated with these parameters can be investigated in selected models, using techniques developed in standard cardiac cell modelling. This analysis can reveal the chain of interactions between models components that causes an observed effect. In a population of models, this also be used to determine whether a behaviour observed in the population is caused by the same mechanism across every model in a population displaying that behaviour, or whether multiple different mechanisms are causing the same effect.

Bifurcation analysis, and potentially other techniques from dynamical systems theory, can also be used to further analyse the different dynamical states a model can occupy, over a range of parameter values. Bifurcation analysis was used in Chapter 4 to analyse how calcium storage in the sarcoplasmic reticulum varied over a wide range of different intracellular calcium loads. This type of analysis could be extended across a whole population of models, or a subset of abnormal models, to, for example, investigate the effects of altering the external conditions of a system (such as extracellular ionic concentrations), or the parameter regimes under which

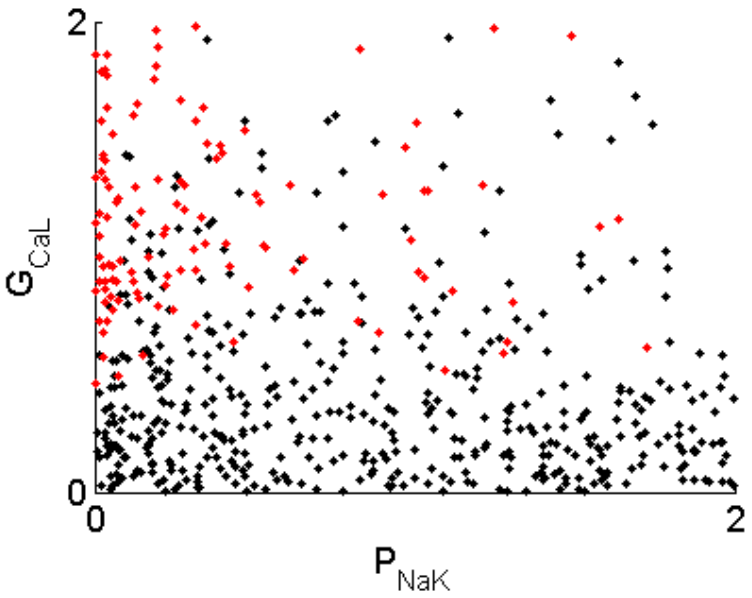

Figure 8.6: Scatter plot showing parameter values for the sodium-potassium pump permeability (PNaK) and L-type calcium current conductance (GCaL) for two subpopulations within a population of models. Red dots represent models with a high susceptibility for developing EADs and alternans in response to a variety of potassium channel blocks, black dots represent models with a low susceptibility. Plots like these can be used to determine whether subsets of a population of models identified through differing outputs (e.g. AP traces) can also be differentiated by their underlying parameter values, pointing to possible mechanisms for their differing outputs. This is useful when models differ qualitatively (e.g. no EADs vs EADs). Figure reproduced from the study in Chapter 7.

different classes of behaviour occur (e.g. fully successful repolarisation or repolarisation abnormalities).

8.4 Conclusions

In this chapter we have presented the experimentally-calibrated population of models methodology, and detailed the process of constructing and analysing a population. For each step we have explained our current understanding of how to balance the various design considerations that are part of this process. However, many aspects of designing population of models-based studies are yet to be well-understood. In many cases the best way to develop a population is through iteration, with knowledge of the behaviour of each population improving the design of the next.

As more studies are performed using populations of models, we will gain understanding in how to tailor study design for different research questions and data sets.

In the next and final chapter we present an overview of the work we have presented in this thesis and its major findings, and we then conclude the thesis with a discussion of the future directions that work building on what has been presented here could take.

9

Conclusions and future directions

9.1 Summary

Disruption of the electrophysiological function of the heart, by drugs, disease or other factors, can cause potentially fatal arrhythmias. These arrhythmias occur rarely, and are difficult to predict in advance. Variability between the hearts of different individuals can modulate the chance of developing both arrhythmias and the electrophysiological abnormalities that can trigger them, but the specific mechanisms through which this variability acts, and how its effects can be predicted in advance, are not well-understood.

Studying this inter-subject variability using current experimental techniques is difficult, as experimental results are typically averaged over preparations from multiple individuals to reduce experimental error and to investigate the typical behaviour of cardiac cells and tissue. Biological data can be highly noisy and difficult to interpret, so this averaging is important, but it also removes the information available in the raw data on inter-subject variability. Cardiac modelling can potentially be used to investigate this variability, but existing cardiac models are developed from averaged experimental data, which does not include information on the variability between different hearts.

In this thesis we have developed a novel framework for modelling inter-subject variability, by

integrating the variability seen in un-averaged experimental data with existing cardiac modelling techniques to create experimentally-calibrated populations of models. We have then applied this methodology to address two problems in cardiac cellular electrophysiology that cannot be addressed without considering the effects of inter-subject variability: predicting the range of responses, not just the average response, of cardiac cells to a drug; and determining the mechanisms that differentiate cells that are highly susceptible to drug-induced repolarisation abnormalities from those that display repolarisation abnormalities either only under extreme levels of block or not at all.

We began in Chapter 2, by introducing important concepts in cardiac electrophysiology. We explained how voltage-gated ion channels conduct the ionic currents that collectively generate cardiac action potentials, and in turn how the propagation of these action potentials through the heart synchronise muscular contraction and allow the heart to beat effectively. We then reviewed our current understanding of repolarisation abnormalities, including EADs, DADs and alternans. Following this we described the microelectrode, voltage clamp and patch clamp techniques that are vital for experimental studies in cardiac electrophysiology. We finished this chapter by reviewing experimental evidence for the importance of inter-subject variability in cardiac cellular electrophysiology.

In Chapter 3, we reviewed computational modelling in cardiac cellular electrophysiology, beginning with the original Hodgkin-Huxley formulation of ionic current flow. We then reviewed a selection of important cardiac cell models, starting with the 1962 Noble model and ending with recently published models that are currently used in research. We then described techniques for sampling parameter spaces, for simulating the behaviour of the models used in this thesis, and for testing for correlations in multidimensional data, which are important for developing and analysing populations of models.

In Chapter 4, we investigated whether calcium overload following rapid pacing could cause DADs in rabbit Purkinje cells. We combined an existing rabbit Purkinje cell model (Corrias

et al. (2011)) with a more detailed calcium sub-system that had been shown to be capable of generating DADs (Li and Rudy (2011)). We demonstrated that this model could produce DADs in simulated conditions equivalent to the experimental conditions reported by Maruyama et al. (2010). To check that our updated model reproduced experimental behaviour at least as well as the original model, we validated both models against control conditions experimental data using a single parameter sensitivity analysis. This analysis showed that the hybrid model reproduced experimental behaviour as well or better than the original model, but that neither model was capable of replicating the significant variability in AP biomarker values seen across our data set. This finding built our initial rationale for using populations of models - that using existing models as is, or with moderate variation in model parameters using a sensitivity analysis - was insufficient to capture the range of biomarker variation seen in experimental recordings.

In Chapter 5 we developed and analysed an experimentally-calibrated population of rabbit Purkinje cell models, and used the population to predict the range of responses to an IKr blocking drug, dofetilide, with a known pro-arrhythmic effect on the action potential. This chapter introduced the use of the experimentally-calibrated populations of models methodology. We developed a population of models, in which all models had varied conductance and time constant parameters from one another, but all of which produced action potential biomarkers during steady state pacing at three pacing rates that were within the range of values observed in experiments on rabbit Purkinje fibres. We determined which ionic parameters were important for influencing the values of each action potential biomarker in control conditions. We then took our population, which was calibrated exclusively with control conditions experimental recordings and predicted the range of APD90 prolongation caused by four concentrations of the IKr blocking drug dofetilide. After matching the number of models and experiments, we found overall good agreement between the predictions of the population and the experimental data.

In Chapter 6 we moved from studying rabbit, an experimental animal model, to studying human cardiac electrophysiology directly. From data provided to us by our collaborators, we devel-

oped and analysed a database of human ventricular action potential recordings, and used this database to calculate a set of calibration ranges that we could use to develop populations of human cardiomyocyte models. We then analysed the distributions of action potential biomarkers in control conditions, and the response of APD90 in drug block experiments using dofetilide and HMR-1556, two selective potassium channel blockers for IKr and IKs respectively. We found substantial variation in biomarker values across both control and drug block experiments, particularly due to outlier preparations with biomarker values far from the mean of the data set, and the majority of other experiments.

The calibration ranges and data analysis performed in Chapter 6 were then used in Chapter 7 to develop a population of human ventricular cell models that we used to investigate how inter-suject variability could modulate the susceptibility of cells to drug-induced repolarisation abnormalities, through variation in sarcolemmal current conductances. We used this population of models to simulate the response to a wide variety of current block levels with different combinations of four currents that are known to be important for repolarisation and repolarisation abnormality generation: IKr, IKs, IK1 and ICaL. For repolarisation abnormalities to occur, we found that IKr must be significantly blocked, and ICaL needs to be uninhibited. Small amounts of ICaL block are sufficient to almost entirely abolish repolarisation abnormalities, for even the highest level of IKr block simulated (90%). For a cell to be highly susceptible to repolarisation abnormalities, meaning they developed them in many different simulated sets of conditions, we find that they must have a pre-existing low conductance value for one or more of the sodium-potassium pump current (INaK), the sodium-calcium exchange current (INCX) and IKr.

In Chapter 8, we provided an in-depth discussion of how experimentally-calibrated populations of models can be created and analysed, depending on the goals of the study they are being used in. We discussed the different decisions and trade-offs that are made when performing a study using this methodology, and our choices of techniques for creating and analysing populations of models. This chapter highlighted the important considerations that need to be made when

designing future studies using the methodology we have introduced in this thesis, based on our experiences with the studies in Chapter 5 and Chapter 7.

9.1.1 Key contributions and main findings

The first major contribution of this thesis is the development of the experimentally-calibrated population of models methodology that we applied in Chapters 5 and 7, to integrate experimentally observed variability with computational modelling. In the study on DAD mechanisms presented in Chapter 4 we demonstrated that standard cardiac modelling methods were insufficient for capturing inter-subject variability in experiments, and so we developed the methodology for using experimentally-calibrated populations of models to address this.

Populations of models have been previously used in neuroscience and in cardiac electrophysiology, but no population used in cardiac electrophysiology prior to this thesis included calibration against experimental data. In neuroscience, the type of calibration process that has been used previously has relied on larger data sets than are typically available in cardiac electrophysiology to compute calibration ranges, and used a grid search of parameter space to generate their initial pool of candidate models, due to the relatively low complexity of the models used and low number of parameters varied. Our methodology introduced the approach of generating calibration ranges that spanned the complete range of biomarker values observed across an experimental data set, and the use of Latin hypercube sampling to sample high-dimensional parameter spaces with fewer samples and without a scaling dependency on the number of parameters, while still sampling values for each parameter evenly across the sampled range.

Our methodology allows us to vary a large number of different parameters, in complex, biophysically detailed models, over a wide range of allowed parameter values. This gives us the ability to evaluate a wide range of possible model behaviours, while still producing a final population of models in which each model behaves in a way that is consistent with experimental data. Therefore we can investigate behaviours that may be rare, and that may be hidden under

normal physiological conditions but which are revealed in conditions such as drug application. These unusual behaviours, such as repolarisation abnormalities, are difficult to study using experiments or computational models alone, and often require extreme experimental or simulated conditions to be applied to cardiomyocytes so that they can be studied, because these behaviours occur rarely and only in a small number of individuals. With a population of models, we can investigate a wide variety of different underlying models and simulate a wide range of different experimental conditions, giving us the advantages of both standard experimental and computational approaches, while counteracting their limitations.

The second major contribution of this thesis is the study of rabbit Purkinje fibres, using a population of models developed using control conditions data from multiple pacing frequencies, presented in Chapter 5. This was the first study in cardiac electrophysiology to use a population of models that had been developed using experimental calibration, to ensure that models were consistent with the range of biomarker variability seen in experiments. The most important contribution of this study was the demonstration that an experimentally-calibrated population of models could predict the range of responses to a drug at multiple concentrations, having only been calibrated with control conditions action potential data. Previously, models of individual animals have been used to predict individual-specific drug block (Davies et al. (2012)), and regression analysis has been used on populations of models to determine which conductances, channel time constants and voltage shifts were most important for determining APD prolongation in response to IKr block (Sarkar and Sobie 2011). However, no study had predicted the range of APD prolongation in response to a drug, while taking into account inter-subject variability. This result suggests our methodology could have applications in safety pharmacology, for predicting drug effects using computational models in a similar way as to how *in vitro* animal testing is currently used in the early stages of preclinical drug safety testing.

The third and final major contribution of this thesis is the creation of a population of human ventricular cell models that reproduce observed AP variability, and the use of this population to

develop hypotheses as to how variability in the conductance values of important ionic currents affect susceptibility to pro-arrhythmic abnormalities during repolarisation, in human cardiomyocytes. This work, presented in Chapter 7, demonstrates the potential for using our methodology to study human cardiac electrophysiology directly, and make use of scarce experimental data from human hearts to construct populations of models that include the range of behaviours seen across a data set.

9.2 Future directions

9.2.1 Inter-subject variability and delayed after-depolarisations

In Chapter 4, we investigated whether we could reproduce the mechanism of DAD generation in rabbit Purkinje fibres proposed by Maruyama et al. (2010) using a computational model. We found that the model we developed could reproduce DADs, but that the range of variability this model produced in control conditions using a standard single-parameter sensitivity analysis was insufficient compared to the variability seen in experiments. This finding motivated us to develop the experimentally-calibrated population of models methodology used through the rest of the thesis. In this thesis, we have not returned to update our study of DADs using this new approach. From our work in Chapter 7, we now have experience in analysing populations of models to investigate repolarisation abnormalities, but in that study, we found that none of our models produced DADs. Therefore, one future direction that would build on the work in this thesis would be to perform a similar study to that used in Chapter 7, using the rabbit Purkinje population of models developed in Chapter 5. However, instead of simulating different drug blocks, we could simulate a variety of conditions thought to increase the susceptibility of cardiomyocytes to DAD development, such as those used by Maruyama et al. (2010). The goal of this study would be to determine whether our population displayed the same overall mechanisms of DAD generation as those reported by Maruyama et al., and to determine how

inter-subject variability altered the susceptibility of rabbit Purkinje cells to developing DADs. In particular, we would be interested in determining whether triggered activity occurred in a subset of models in the population, and if so, what caused triggered activity to occur, as this activity is a possible initiating event for arrhythmias.

9.2.2 Calcium transients and ionic concentrations

In this thesis we have calibrated populations of models exclusively using biomarkers calculated from action potential recordings. Other studies, including those by Sarkar and Sobie (2010) and Walmsley et al. (2013) have also used calcium transient recordings, in additional to action potential recordings, to develop their models. As described in Chapter 2, calcium is a key driver of many physiological processes, and also interacts with the action potential, primarily through the sodium-calcium exchange current and the L-type calcium current. Calcium concentrations in the cytosol can be measured experimentally using optical mapping. Therefore, incorporating calcium recordings would allow us to constrain populations of models through a wider variety of physiological processes. This would be particularly important for studying pro-arrhythmic phenomena that are thought to be mechanistically linked to the calcium sub-system, particularly DADs, so including calcium in the calibration process could be important for the work described in the previous section. Biomarkers of the calcium transient could be used in the same way we have used action potential biomarkers, to filter out candidate models that have calcium concentrations and calcium release dynamics that are outside the range of what we observe experimentally.

9.2.3 Incorporating experimentally-derived distributions of ion channel conductances and kinetics

In this thesis, we have predominantly selected ionic current conductances as the parameters to vary when building populations of models, based on the assumption that variation in the number

or density of ion channels in the cell membrane is the main cause of the inter-individual variability we see in action potential recordings. When sampling these parameters, we have assumed a uniform distribution over a wide range, both due to lack of information on the real ranges conductances span, and to allow us to evaluate a wide range of different electrophysiological behaviours.

However, conductances in individual cells can be measured in voltage clamp experiments, although only after being isolated, which is known to damage the cells, altering the conductance values measured from these experiments. If this issue can be resolved, it is possible that future studies may have access to data that allows the distributions of some or all of the important conductances for a particular species and cell type to be determined. In that case, the sampling process could be modified to include this information by setting the sampled ranges for each conductance to the ranges determined from experiments, to increase confidence that the parameter values in a population of models are realistic. The distribution that is sampled over could also be changed to reflect the distribution found experimentally, however this would most likely mean that more models in the population would display behaviour close to the mean, and fewer models would display extreme or outlying behaviours, which can often be the most scientifically interesting behaviours, and the hardest to study experimentally, so this might be a less useful refinement of the methodology.

Varying conductances based on experimental data could be particularly useful when determining differences between two sub-populations, e.g. healthy individuals and those with a particular disease or mutation that is known to alter ion channel expression, in which case conductances would be expected to vary between the two sub-populations, and the parameter sampling process could incorporate this information. This would be a similar approach to that used by Walmsley et al. (2013) where changes in mRNA expression were used to alter conductances between a population of human ventricular cell models from healthy individuals and a population from individuals with heart disease.

Conductances are not the only parameter governing ionic current behaviour that could vary between individuals. The voltage dependency of ion channels' gating states and the time it takes a channel to adapt to changes in voltage could also potentially vary, through mutations or other mechanisms. If inter-individual variability in these parameters is significant, experimental characterisation of these differences could be incorporated into future studies using our methodology. This would be particularly important for parameters relating to recovery from inactivation of inward currents, such as ICaL and INa, which are known to play a role in determining whether EADs occur. We are not aware of any studies that have characterised the variability present in ion channel kinetics between individuals, but if it is found that there is significant variability in these parameters, that information could be incorporated into future studies using our methodology.

9.2.4 Drug effects on human cardiomyocytes

In Chapter 6 we analysed a database of experiments on human ventricular preparations, with a variety of different drugs applied at different concentrations. Due to a current lack of repeat experiments and characterisation of drug effects (e.g. IC50 values) in the currently extracted database, we have not used these drug experiments further in this thesis. However, with further extraction of experiments in database, we could potentially make use of these data. We could use the range of responses of biomarkers to different drugs to test the predictive capabilities of our human population of models over a wide variety of different conditions. As discussed in Chapter 6, this use of the data set is hampered by a lack of reliable IC50 values, however for concentrations of a drug that are far from the drug's IC50 value this is less of an issue, as inaccuracies in IC50 do not alter the predicted value of current block by as large an amount. Therefore with further extraction of more experiments into the database, we would have a greater range of experiments to choose from, so we could select those that minimise the problem of uncertainty in IC50 values.

We could also potentially use these data in another way, to develop more constrained populations by using the drug experiments to develop non-control calibration ranges. These ranges could be used in a similar way to the calibration ranges at multiple pacing frequencies that were used in Chapter 5. By calibrating in different conditions we apply additional constraints to a population, with the goal of creating a population that more accurately predicts the range of responses to conditions beyond those used to create the population.

9.2.5 Tissue effects

The studies in this thesis have focused on modelling either single cells, or in the case of Chapter 8 used single cell models with a biphasic stimulus to approximate small tissue preparations. However, pro-arrhythmic phenomena such as EADs and DADs, that have been studied here, behave differently in tissue to single cell preparations due to current sink effects from surrounding tissue. Additionally, cardiac arrhythmias occur in tissue, not isolated cells. Therefore, one way to improve our understanding of the effects of inter-subject variability on arrhythmic susceptibility would be to adapt the current population of models methodology to develop tissue-level populations of models. A major challenge that would have to be overcome is the vast increase in computational expense between single cell and tissue simulations, even for relatively simple 1D and 2D simulations. Performing even a single detailed tissue simulation can require supercomputing resources. Performing hundreds or thousands of these simulations for a single study is not currently feasible.

However, even 1D cable simulations are capable of reproducing important tissue-level feature, such as the heterogeneity across the ventricular wall from endocardium to epicardium, which produces behaviours single cell models cannot be used to investigate. The use of Latin hypercube sampling in the existing population of modes methodology, to generate an initial candidate pool of models that spans a wide range of cell configurations but is small enough to be computationally tractable, is an existing trade-off in our methodology between parameter space

coverage and computational cost. A similar trade-off between the detail of tissue simulations, and the numbers of different models and different experimental conditions that are simulated could be found, and then adjusted based on the active research question. This would open up new areas for investigation, such as the role inter-subject variability plays in modulating the effects other forms of heterogeneity present within an individual, such as the previously mentioned heterogeneity across the ventricular wall. It would also allow us to build on our work in Chapter 7 investigating susceptibility to repolarisation abnormalities at the cell level, and relate this to arrhythmic susceptibility at the tissue level, where current sink effects generally require abnormalities to be synchronised across many cells to have an effect.

9.2.6 Non-cardiac applications of experimentally-calibrated populations of models

We have described several areas that future studies using experimentally-calibrated populations of models in cardiac electrophysiology could explore. However, the methodology we have developed is not specific to a particular field, and could be used to study variability in any biological system, where appropriate experimental data and computational models are available.

Therefore, this methodology could be used to investigate the effects of inter-subject variability beyond cardiac electrophysiology. In particular, we believe neurons and pancreatic cells could be good targets to study using experimentally-calibrated populations of model. These are both types of excitable cells, like cardiomyocytes, and in these cases similar types of models and data could be used to investigate how inter-subject variability affects their behaviour and their response to drugs, such as pain-killers, in the case of sensory neurons, and to diseases such as diabetes, in the case of pancreatic cells.

9.3 Conclusions

Variability is an intrinsic part of all biological systems. In cardiac electrophysiology, inter-subject variability is particularly important for determining the response of an individual to therapies, and to disease. However, the mechanisms through which this variability alters the electrophysiological response of an individual's heart are not currently well understood, due to the difficulty of studying variability using standard experimental methods and computational models. Both these approaches rely on averaged data, that captures the typical behaviour of cardiac cells but in doing so removes information about the variability between cells from different hearts.

To study this variability, we developed the experimentally-calibrated population of models methodology presented in this thesis. Initially, this was to address the shortcomings of the standard single-parameter sensitivity analyses used in Chapter 4, where the ranges of biomarker values seen across our data set of isolated rabbit Purkinje cell recordings was far wider than the ranges that our model could produce by varying one parameter at a time. We built on our model development work in Chapter 4, in our first study using an experimentally-calibrated population of models, in Chapter 5. Here, we constructed a population of models, using microelectrode recordings made under control conditions only, at multiple pacing rates. We used the population to predict the range of action potential duration prolongation caused by four concentrations of the IKr blocking drug dofetilide, and validated the population's predictions against data not used to develop the population. We found generally good agreement, particularly at intermediate concentrations near the drug's measured IC50 value, and we were able to determine which of the parameters we had varied across the population were important for determining the amount of prolongation a particular model experienced.

Understanding the behaviour of experimental animal models, such as rabbit, is important, as they are widely used both in research and for testing the safety of new drugs. However, in

these applications animal hearts are used as imperfect models of the human heart, in much the same way computational models are. Ideally, research on human cardiac biology would be carried out using human tissue, but the availability of healthy human hearts in research is extremely low, and until recently this was also reflected in the availability of human cardiac cell models. Building on the availability of well-validated human cardiac cell models and our access to a data set of human cardiac electrophysiology recordings, we first curated a database of human ventricular action potential recordings in Chapter 6, and then used calibration ranges calculated using this database to develop the human population of models used in Chapter 7. We used this population to understand what factors differentiated models that displayed a high susceptibility to drug-induced repolarisation abnormalities, that could potentially cause or increase the likelihood of arrhythmias occurring in tissue, from those that displayed few or no abnormalities. This study demonstrated the ability of the methodology we have developed in this thesis to generate hypotheses that would be difficult to develop using experiments or modelling alone.

To conclude, we hope that the work presented in this thesis provides a valuable contribution to understanding the effects of inter-individual variability in cardiac electrophysiology, and potentially in other fields. We also hope that our work may find applications, particularly in safety pharmacology, in replacing or reducing the use of existing animal assays.

Bibliography

van Alem, A. P., Post, J. and Koster, R. W. (2003) VF recurrence: characteristics and patient outcome in out-of-hospital cardiac arrest. *Resuscitation*, **59**, 181–188.

Antzelevitch, C., Belardinelli, L., Zygmunt, A. C., Burashnikov, A., Di Diego, J. M., Fish, J. M., Cordeiro, J. M. and Thomas, G. (2004) Electrophysiological effects of ranolazine, a novel antianginal agent with antiarrhythmic properties. *Circulation*, **110**, 904–910.

Aslanidi, O. V., Sleiman, R. N., Boyett, M. R., Hancox, J. C. and Zhang, H. (2010) Ionic mechanisms for electrical heterogeneity between rabbit Purkinje fiber and ventricular cells. *Biophys J*, **98**, 2420–31.

Aslanidi, O. V., Stewart, P., Boyett, M. R. and Zhang, H. (2009) Optimal velocity and safety of discontinuous conduction through the heterogeneous purkinje-ventricular junction. *Biophysical Journal*, **97**, 20–39.

Beeler, G. W. and Reuter, H. (1977) Reconstruction of the action potential of ventricular myocardial fibres. *The Journal of Physiology*, **268**, 177–210.

Belardinelli, L., Shryock, J. C. and Fraser, H. (2006) Inhibition of the late sodium current as a potential cardioprotective principle: effects of the late sodium current inhibitor ranolazine. *Heart*, **92**, iv6–iv14.

Bers, D. M. (2002) Calcium and cardiac rhythms: physiological and pathophysiological. *Circ. Res.*, **90**, 14–17.

— (2008) Calcium cycling and signaling in cardiac myocytes. *Annu. Rev. Physiol.*, **70**, 23–49.

Bishop, M. J. (2008) *Optical mapping signal synthesis*. Ph.D. thesis, University of Oxford.

Borlak, J. and Thum, T. (2003) Hallmarks of ion channel gene expression in end-stage heart failure. *The FASEB Journal*, **17**, 1592–1608.

Brennan, T., Fink, M. and Rodriguez, B. (2009) Multiscale modelling of drug-induced effects on cardiac electrophysiological activity. *Eur J Pharm Sci*, **36**, 62–77.

Britton, O. J., Bueno-Orovio, A., Van Ammel, K., Lu, H. R., Towart, R., Gallacher, D. J. and Rodriguez, B. (2013) Experimentally calibrated population of models predicts and explains intersubject variability in cardiac cellular electrophysiology. *Proceedings of the National Academy of Sciences*, **110**, E2098–E2105.

Bueno-Orovio, A., Cherry, E. M. and Fenton, F. H. (2008) Minimal model for human ventricular action potentials in tissue. *Journal of Theoretical Biology*, **253**, 544–560.

Bueno-Orovio, A., Sanchez, C., Pueyo, E. and Rodriguez, B. (2014) Na/k pump regulation of cardiac repolarization: insights from a systems biology approach. *Pfluegers Archiv-European Journal of Physiology*, **466**, 183–193.

Carro, J., Rodriguez, J. F., Laguna, P. and Pueyo, E. (2011) A human ventricular cell model for investigation of cardiac arrhythmias under hyperkalaemic conditions. *Philos Transact A Math Phys Eng Sci*, **369**, 4205–32.

Choi, B.-R., Burton, F. and Salama, G. (2002) Cytosolic ca2+ triggers early afterdepolarizations and torsade de pointes in rabbit hearts with type 2 long qt syndrome. *The Journal of physiology*, **543**, 615–631.

Cooper, J., Spiteri, R. J. and Mirams, G. R. (2014) Cellular cardiac electrophysiology modeling with chaste and cellml. *Frontiers in Physiology*, **5**, 511–.

Coraboeuf, E. and Weidmann, S. (1949) Potentiels de repos et potentiels d'action du muscle cardiaque, mesurés à l'aide d'électrodes intracellulaires. *CR Soc Biol (Paris)*.

Cordeiro, J. M., Bridge, J. H. and Spitzer, K. W. (2001) Early and delayed afterdepolarizations in rabbit heart Purkinje cells viewed by confocal microscopy. *Cell Calcium*, **29**, 289–297.

Cordeiro, J. M., Spitzer, K. W. and Giles, W. R. (1998) Repolarizing K+ currents in rabbit heart Purkinje cells. *J. Physiol. (Lond.)*, **508 (Pt 3)**, 811–823.

Corrias, A., Giles, W. and Rodriguez, B. (2011) Ionic mechanisms of electrophysiological properties and repolarization abnormalities in rabbit Purkinje fibers. *Am J Physiol Heart Circ Physiol*, **300**, H1806–13.

Dangerfield, C., Pueyo, E., Britton, O., Virag, L., Kistamas, K., Szentandrassy, N., Varro, A., Nanasi, P., Burrage, K. and Rodriguez, B. (2015) Experimentally-based computational investigation into beat-to-beat variability in ventricular repolarisation and its response to ionic current inhibition. *Under review*.

Davies, M. R., Mistry, H. B., Hussein, L., Pollard, C. E., Valentin, J. P., Swinton, J. and Abi-Gerges, N. (2012) An in silico canine cardiac midmyocardial action potential duration model as a tool for early drug safety assessment. *Am J Physiol Heart Circ Physiol*, **302**, H1466–80.

DiFrancesco, D. and Noble, D. (1985) A model of cardiac electrical activity incorporating ionic pumps and concentration changes. *Philosophical Transactions of the Royal Society of London B: Biological Sciences*, **307**, 353–398.

Draper, M. H. and Weidmann, S. (1951) Cardiac resting and action potentials recorded with an intracellular electrode. *The Journal of physiology*, **115**, 74–94.

EMA (2005) The European Medicines Agency Safety Pharmacology Studies for Human Pharmaceuticals.

Faber, G. M. and Rudy, Y. (2007) Calsequestrin mutation and catecholaminergic polymorphic ventricular tachycardia: a simulation study of cellular mechanism. *Cardiovasc. Res.*, **75**, 79–88.

Farid, T. A., Nair, K., Masse, S., Azam, M. A., Maguy, A., Lai, P. F., Umapathy, K., Dorian, P., Chauhan, V. and Varro, A. (2011) Role of katp channels in the maintenance of ventricular fibrillation in cardiomyopathic human hearts. *Circulation research*, **109**, 1309–1318.

Fink, M., Noble, P. J. and Noble, D. (2011) Ca2+-induced delayed afterdepolarizations are triggered by dyadic subspace Ca2+ affirming that increasing SERCA reduces aftercontractions. *Am. J. Physiol. Heart Circ. Physiol.*, **301**, H921–935.

Fishman, G. I., Chugh, S. S., DiMarco, J. P., Albert, C. M., Anderson, M. E., Bonow, R. O., Buxton, A. E., Chen, P.-S., Estes, M., Jouven, X. et al. (2010) Sudden cardiac death prediction and prevention report from a national heart, lung, and blood institute and heart rhythm society workshop. *Circulation*, **122**, 2335–2348.

Fitzhugh, R. (1960) Thresholds and plateaus in the hodgkin-huxley nerve equations. *The Journal of General Physiology*, **43**, 867–896.

Gaborit, N., Le Bouter, S., Szuts, V., Varro, A., Escande, D., Nattel, S. and Demolombe, S. (2007) Regional and tissue specific transcript signatures of ion channel genes in the non-diseased human heart. *J Physiol*, **582**, 675–93.

Gögelein, H., Brüggemann, A., Gerlach, U., Brendel, J. and Busch, A. E. (2000) Inhibition of iks channels by hmr 1556. *Naunyn-Schmiedeberg's archives of pharmacology*, **362**, 480–488.

Goldberger, J. J., Buxton, A. E., Cain, M., Costantini, O., Exner, D. V., Knight, B. P., Lloyd-Jones, D., Kadish, A. H., Lee, B., Moss, A. et al. (2011) Risk stratification for arrhythmic sudden cardiac death identifying the roadblocks. *Circulation*, **123**, 2423–2430.

Grandi, E., Pasqualini, F. S. and Bers, D. M. (2010) A novel computational model of the human ventricular action potential and Ca transient. *J Mol Cell Cardiol*, **48**, 112–21.

Grashow, R., Brookings, T. and Marder, E. (2009) Reliable neuromodulation from circuits with variable underlying structure. *Proc Natl Acad Sci U S A*, **106**, 11742–6.

— (2010) Compensation for variable intrinsic neuronal excitability by circuit-synaptic interactions. *J Neurosci*, **30**, 9145–56.

Heijman, J., Voigt, N., Wehrens, X. H. T. and Dobrev, D. (2014) Calcium dysregulation in atrial fibrillation: the role of camkii. *Frontiers in Pharmacology*, **5**, 30–.

Hess, P. and Wier, W. G. (1984) Excitation-contraction coupling in cardiac Purkinje fibers. Effects of caffeine on the intracellular [Ca2+] transient, membrane currents, and contraction. *J. Gen. Physiol.*, **83**, 417–433.

Hindmarsh, A. C., Brown, P. N., Grant, K. E., Lee, S. L., Serban, R., Shumaker, D. E. and Woodward, C. S. (2005) Sundials: Suite of nonlinear and differential/algebraic equation solvers. *ACM Transactions on Mathematical Software (TOMS)*, **31**, 363–396.

Hodgkin, A. L. and Huxley, A. F. (1952) A quantitative description of membrane current and its application to conduction and excitation in nerve. *The Journal of Physiology*, **117**, 500–544.

Hoffman, B. F. (2002) And then came the microelectrode. *Cardiovascular research*, **53**, 1–5.

January, C. T. and Riddle, J. M. (1989) Early afterdepolarizations: mechanism of induction and block. a role for l-type ca2+ current. *Circulation research*, **64**, 977–990.

Jeyaraj, D., Haldar, S. M., Wan, X., McCauley, M. D., Ripperger, J. A., Hu, K., Lu, Y., Eapen, B. L., Sharma, N., Ficker, E., Cutler, M. J., Gulick, J., Sanbe, A., Robbins, J., Demolombe, S., Kondratov, R. V., Shea, S. A., Albrecht, U., Wehrens, X. H., Rosenbaum, D. S. and Jain, M. K. (2012) Circadian rhythms govern cardiac repolarization and arrhythmogenesis. *Nature*, **483**, 96–99.

Jost, N., Virag, L., Bitay, M., Takacs, J., Lengyel, C., Biliczki, P., Nagy, Z., Bogats, G., Lathrop, D., Papp, J. and Varro, A. (2005) Restricting excessive cardiac action potential and qt prolongation a vital role for iks in human ventricular muscle. *Circulation*, **112**, 1392–1399.

Jost, N., Virág, L., Comtois, P., Ördög, B., Szuts, V., Seprényi, G., Bitay, M., Kohajda, Z.,

Koncz, I., Nagy, N. et al. (2013) Ionic mechanisms limiting cardiac repolarization reserve in humans compared to dogs. *The Journal of physiology*, **591**, 4189–4206.

Jost, N., Virg, L., Opincariu, M., Szcsi, J., Andrs, V. and Papp, J. (1998) Delayed rectifier potassium current in undiseased human ventricular myocytes. *Cardiovascular Research*, **40**, 508–515.

Kannankeril, P. J., Norris, K. J., Carter, S. and Roden, D. M. (2011) Factors affecting the degree of QT prolongation with drug challenge in a large cohort of normal volunteers. *Heart Rhythm*, **8**, 1530–4.

Kim, G. H. (2013) Microrna regulation of cardiac conduction and arrhythmias. *Translational Research*, **161**, 381–392.

Kormos, A., Nagy, N., Acsai, K., Váczi, K., Ágoston, S., Pollesello, P., Levijoki, J., Szentandrássy, N., Papp, J. G., Varró, A. et al. (2014) Efficacy of selective ncx inhibition by orm-10103 during simulated ischemia/reperfusion. *European journal of pharmacology*, **740**, 539–551.

Le Bouter, S., El Harchi, A., Marionneau, C., Bellocq, C., Chambellan, A., van Veen, T., Boixel, C., Gavillet, B., Abriel, H. and Le Quang, K. (2004) Long-term amiodarone administration remodels expression of ion channel transcripts in the mouse heart. *Circulation*, **110**, 3028–3035.

Li, P. and Rudy, Y. (2011) A model of canine purkinje cell electrophysiology and Ca(2+) cycling: rate dependence, triggered activity, and comparison to ventricular myocytes. *Circ Res*, **109**, 71–9.

Livshitz, L. and Rudy, Y. (2009) Uniqueness and stability of action potential models during rest, pacing, and conduction using problem-solving environment. *Biophysical journal*, **97**, 1265–1276.

Livshitz, L. M. and Rudy, Y. (2007) Regulation of ca(2+) and electrical alternans in cardiac myocytes: Role of camkii and repolarizing currents. *American journal of physiology. Heart and circulatory physiology*, **292**, H2854–H2866.

Lu, H. R., Mariën, R., Saels, A. and Clerck, F. (2001) Species plays an important role in drug-induced prolongation of action potential duration and early afterdepolarizations in isolated purkinje fibers. *Journal of cardiovascular electrophysiology*, **12**, 93–102.

Lu, H. R., Vlaminckx, E., Van De Water, A. and Gallacher, D. J. (2005) Both beta-adrenergic receptor stimulation and cardiac tissue type have important roles in elucidating the functional effects of I(Ks) channel blockers in vitro. *J Pharmacol Toxicol Methods*, **51**, 81–90.

Luo, C. H. and Rudy, Y. (1991) A model of the ventricular cardiac action potential. depolarization, repolarization, and their interaction. *Circulation Research*, **68**, 1501–1526.

— (1994a) A dynamic model of the cardiac ventricular action potential. i. simulations of ionic currents and concentration changes. *Circulation Research*, **74**, 1071–1096.

— (1994b) A dynamic model of the cardiac ventricular action potential. ii. afterdepolarizations, triggered activity, and potentiation. *Circulation Research*, **74**, 1097–1113.

Marder, E. and Taylor, A. L. (2011) Multiple models to capture the variability in biological neurons and networks. *Nat Neurosci*, **14**, 133–8.

Marino, S., Hogue, I. B., Ray, C. J. and Kirschner, D. E. (2008) A methodology for performing global uncertainty and sensitivity analysis in systems biology. *Journal of theoretical biology*, **254**, 178–196.

Maruyama, M., Joung, B., Tang, L., Shinohara, T., On, Y. K., Han, S., Choi, E. K., Kim, D. H., Shen, M. J., Weiss, J. N., Lin, S. F. and Chen, P. S. (2010) Diastolic intracellular calcium-membrane voltage coupling gain and postshock arrhythmias: role of purkinje fibers and triggered activity. *Circ. Res.*, **106**, 399–408.

McKay, M. D., Beckman, R. J. and Conover, W. J. (1979) A comparison of three methods for selecting values of input variables in the analysis of output from a computer code. *Technometrics*, **21**, pp. 239–245.

Merchant, F. M. and Armoundas, A. A. (2012) Role of substrate and triggers in the genesis of cardiac alternans, from the myocyte to the whole heart implications for therapy. *Circulation*, **125**, 539–549.

Michael, G., Xiao, L., Qi, X.-Y., Dobrev, D. and Nattel, S. (2009) Remodelling of cardiac repolarization: how homeostatic responses can lead to arrhythmogenesis. *Cardiovascular research*, **81**, 491–499.

Milberg, P., Pott, C., Fink, M., Frommeyer, G., Matsuda, T., Baba, A., Osada, N., Breithardt, G., Noble, D. and Eckardt, L. (2008) Inhibition of the na+/ca 2+ exchanger suppresses torsades de pointes in an intact heart model of long qt syndrome-2 and long qt syndrome-3. *Heart Rhythm*, **5**, 1444–1452.

Nass, R. D., Aiba, T., Tomaselli, G. F. and Akar, F. G. (2008) Mechanisms of disease: ion channel remodeling in the failing ventricle. *Nature Clinical Practice Cardiovascular Medicine*, **5**, 196–207.

Nattel, S., Frelin, Y., Gaborit, N., Louault, C. and Demolombe, S. (2010) Ion-channel mrna-expression profiling: Insights into cardiac remodeling and arrhythmic substrates. *Journal of molecular and cellular cardiology*, **48**, 96–105.

Nattel, S., Khairy, P. and Schram, G. (2001) Arrhythmogenic ionic remodeling: adaptive responses with maladaptive consequences. *Trends in cardiovascular medicine*, **11**, 295–301.

Nattel, S., Maguy, A., Le Bouter, S. and Yeh, Y.-H. (2007) Arrhythmogenic ion-channel remodeling in the heart: heart failure, myocardial infarction, and atrial fibrillation. *Physiological reviews*, **87**, 425–456.

Neher, E. and Sakmann, B. (1976) Single-channel currents recorded from membrane of denervated frog muscle fibres. *Nature*, **260**, 799–802.

Niederer, S., Fink, M., Noble, D. and Smith, N. (2009) A meta-analysis of cardiac electrophysiology computational models. *Experimental physiology*, **94**, 486–495.

Noble, D. (1962) A modification of the hodgkin-huxley equations applicable to purkinje fibre action and pacemaker potentials. *The Journal of Physiology*, **160**, 317–352.

Noble, D. and Noble, P. J. (2006) Late sodium current in the pathophysiology of cardiovascular disease: consequences of sodiumcalcium overload. *Heart*, **92**, iv1–iv5.

O'Hara, T., Virag, L., Varro, A. and Rudy, Y. (2011) Simulation of the undiseased human cardiac ventricular action potential: model formulation and experimental validation. *PLoS Comput Biol*, **7**, e1002061.

Peachey, T. C., Diamond, N. T., Abramson, D. A., Sudholt, W., Michailova, A. and Amirriazi, S. (2008) Fractional factorial design for parameter sweep experiments using nimrod/e. *Sci. Program.*, **16**, 217–230.

Pitt-Francis, J., Pathmanathan, P., Bernabeu, M., Bordas, R., Cooper, J., Fletcher, A., Mirams, G., Murray, P., Osbourne, J., Walter, A., Chapman, S., Garny, A., van Leeuwen, I., Maini, P., Rodriguez, B., Waters, S., Whiteley, J., Byrne, H. and Gavaghan, D. (2009) Chaste: a test-driven approach to software development for biological modelling. *Comp Phys Comm*, **180**, 2452–2471.

Pogwizd, S., Schlotthauer, K., Li, L., Yuan, W. and Bers, D. (2001) Sodium-calcium exchange contributes to mechanical dysfunction and triggered arrhythmias in heart failure. *Circ Res*, **88**, 1159–1167.

Polak, S., Winiowska, B. and Brandys, J. (2009) Collation, assessment and analysis of literature

in vitro data on herg receptor blocking potency for subsequent modeling of drugs' cardiotoxic properties. *Journal of Applied Toxicology*, **29**, 183–206.

Prinz, A. A., Billimoria, C. P. and Marder, E. (2003) Alternative to hand-tuning conductance-based models: construction and analysis of databases of model neurons. *J Neurophysiol*, **90**, 3998–4015.

Prinz, A. A., Bucher, D. and Marder, E. (2004) Similar network activity from disparate circuit parameters. *Nat Neurosci*, **7**, 1345–52.

Priori, S. G., Napolitano, C. and Schwartz, P. J. (1999) Low penetrance in the long-qt syndrome clinical impact. *Circulation*, **99**, 529–533.

Pueyo, E., Corrias, A., Virag, L., Jost, N., Szel, T., Varro, A., Szentandrassy, N., Nanasi, P. P., Burrage, K. and Rodriguez, B. (2011) A multiscale investigation of repolarization variability and its role in cardiac arrhythmogenesis. *Biophys J*, **101**, 2892–902.

Qi, X. Y., Yeh, Y.-H., Xiao, L., Burstein, B., Maguy, A., Chartier, D., Villeneuve, L. R., Brundel, B. J., Dobrev, D. and Nattel, S. (2008) Cellular signaling underlying atrial tachycardia remodeling of l-type calcium current. *Circulation research*, **103**, 845–854.

Redfern, W., Ewart, L., Hammond, T., Bialecki, R., Kinter, L., Lindgren, S., Pollard, C., Roberts, R., Rolf, M. and Valentin, J. (2010) Impact and frequency of different toxicities throughout the pharmaceutical life cycle. *The Toxicologist*, **114**, 1081.

Roden, D. M. (1998) Taking the idio out of idiosyncratic: predicting torsades de pointes. *Pacing and Clinical Electrophysiology*, **21**, 1029–1034.

Roden, D. M. and Abraham, R. L. (2011) Refining repolarization reserve. *Heart rhythm: the official journal of the Heart Rhythm Society*, **8**, 1756.

Romero, L., Pueyo, E., Fink, M. and Rodriguez, B. (2009) Impact of ionic current variability

on human ventricular cellular electrophysiology. *Am J Physiol Heart Circ Physiol*, **297**, H1436–45.

Rosenbaum, D. S., Jackson, L. E., Smith, J. M., Garan, H., Ruskin, J. N. and Cohen, R. J. (1994) Electrical alternans and vulnerability to ventricular arrhythmias. *New England Journal of Medicine*, **330**, 235–241.

Sadrieh, A., Domanski, L., Pitt-Francis, J., Mann, S. A., Hodkinson, E. C., Ng, C.-A., Perry, M. D., Taylor, J. A., Gavaghan, D., Subbiah, R. N. et al. (2014) Multiscale cardiac modelling reveals the origins of notched t waves in long qt syndrome type 2. *Nature communications*, **5**.

Saltelli, A., Tarantola, S. and Chan, K.-S. (1999) A quantitative model-independent method for global sensitivity analysis of model output. *Technometrics*, **41**, 39–56.

Sanchez, C., Bueno-Orovio, A., Wettwer, E., Loose, S., Simon, J., Ravens, U., Pueyo, E. and Rodriguez, B. (2014) Inter-subject variability in human atrial action potential in sinus rhythm versus chronic atrial fibrillation. *PLoS ONE*, **9**, e105897–.

Sarkar, A. X., Christini, D. J. and Sobie, E. A. (2012) Exploiting mathematical models to illuminate electrophysiological variability between individuals. *J Physiol*, **590**, 2555–67.

Sarkar, A. X. and Sobie, E. A. (2010) Regression analysis for constraining free parameters in electrophysiological models of cardiac cells. *PLoS Comput Biol*, **6**, e1000914–.

— (2011) Quantification of repolarization reserve to understand interpatient variability in the response to proarrhythmic drugs: A computational analysis. *Heart Rhythm*, **8**, 1749–1755.

Shannon, T. R., Wang, F. and Bers, D. M. (2005) Regulation of cardiac sarcoplasmic reticulum ca release by luminal [ca] and altered gating assessed with a mathematical model. *Biophysical Journal*, **89**, 4096–4110.

Shannon, T. R., Wang, F., Puglisi, J., Weber, C. and Bers, D. M. (2004) A mathematical treat-

ment of integrated ca dynamics within the ventricular myocyte. *Biophysical Journal*, **87**, 3351–3371.

Sims, C., Reisenweber, S., Viswanathan, P. C., Choi, B.-R., Walker, W. H. and Salama, G. (2008) Sex, age, and regional differences in l-type calcium current are important determinants of arrhythmia phenotype in rabbit hearts with drug-induced long qt type 2. *Circulation research*, **102**, e86–e100.

Snyders, D. J. and Chaudhary, A. (1996) High affinity open channel block by dofetilide of herg expressed in a human cell line. *Molecular Pharmacology*, **49**, 949–955.

Sobie, E. A. (2009) Parameter sensitivity analysis in electrophysiological models using multivariable regression. *Biophys J*, **96**, 1264–74.

Swensen, A. M. and Bean, B. P. (2005) Robustness of burst firing in dissociated purkinje neurons with acute or long-term reductions in sodium conductance. *The Journal of neuroscience*, **25**, 3509–3520.

Syed, Z., Vigmond, E., Nattel, S. and Leon, L. J. (2005) Atrial cell action potential parameter fitting using genetic algorithms. *Med Biol Eng Comput*, **43**, 561–71.

Szentadrassy, N., Banyasz, T., Biro, T., Szabo, G., Toth, B. I., Magyar, J., Lazar, J., Varro, A., Kovacs, L. and Nanasi, P. P. (2005) Apico-basal inhomogeneity in distribution of ion channels in canine and human ventricular myocardium. *Cardiovascular Research*, **65**, 851–860.

Taylor, A. L., Goaillard, J. M. and Marder, E. (2009) How multiple conductances determine electrophysiological properties in a multicompartment model. *J Neurosci*, **29**, 5573–86.

Tsuji, Y., Zicha, S., Qi, X.-Y., Kodama, I. and Nattel, S. (2006) Potassium channel subunit remodeling in rabbits exposed to long-term bradycardia or tachycardia discrete arrhythmogenic consequences related to differential delayed-rectifier changes. *Circulation*, **113**, 345–355.

ten Tusscher, K. H., Noble, D., Noble, P. J. and Panfilov, A. V. (2004) A model for human ventricular tissue. *Am J Physiol Heart Circ Physiol*, **286**, H1573–89.

ten Tusscher, K. H. and Panfilov, A. V. (2006) Alternans and spiral breakup in a human ventricular tissue model. *Am J Physiol Heart Circ Physiol*, **291**, H1088–100.

Vandersickel, N., Kazbanov, I. V., Nuitermans, A., Weise, L. D., Pandit, R. and Panfilov, A. V. (2014) A study of early afterdepolarizations in a model for human ventricular tissue. *PLoS ONE*, **9**, e84595–.

Volders, P. G., Kulcsár, A., Vos, M. A., Sipido, K. R., Wellens, H. J., Lazzara, R. and Szabo, B. (1997) Similarities between early and delayed afterdepolarizations induced by isoproterenol in canine ventricular myocytes. *Cardiovascular research*, **34**, 348–359.

Volders, P. G., Vos, M. A., Szabo, B., Sipido, K. R., de Groot, S. M., Gorgels, A. P., Wellens, H. J. and Lazzara, R. (2000) Progress in the understanding of cardiac early afterdepolarizations and torsades de pointes: time to revise current concepts. *Cardiovascular research*, **46**, 376–392.

Walmsley, J., Rodriguez, J. F., Mirams, G. R., Burrage, K., Efimov, I. R. and Rodriguez, B. (2013) mrna expression levels in failing human hearts predict cellular electrophysiological remodeling: A population-based simulation study. *PLoS ONE*, **8**, e56359–.

Weiss, J. N., Garfinkel, A., Karagueuzian, H. S., Chen, P.-S. and Qu, Z. (2010) Early afterdepolarizations and cardiac arrhythmias. *Heart Rhythm*, **7**, 1891–1899.

Weiss, J. N., Nivala, M., Garfinkel, A. and Qu, Z. (2011) Alternans and arrhythmias from cell to heart. *Circulation Research*, **108**, 98–112.

Xiao, L., Xiao, J., Luo, X., Lin, H., Wang, Z. and Nattel, S. (2008) Feedback remodeling of cardiac potassium current expression a novel potential mechanism for control of repolarization reserve. *Circulation*, **118**, 983–992.

Zaniboni, M. (2011) 3D current-voltage-time surfaces unveil critical repolarization differences underlying similar cardiac action potentials: A model study. *Math Biosci*, **233**, 98–110.